Papers presented to the

FOURTEENTH SYMPOSIUM

ON ANTARCTIC METEORITES

6-8, June 1989

NATIONAL INSTITUTE OF POLAR RESEARCH, TOKYO

国立極地研究所

Papers presented to the

FOURTEENTH SYMPOSIUM

ON ANTARCTIC METEORITES

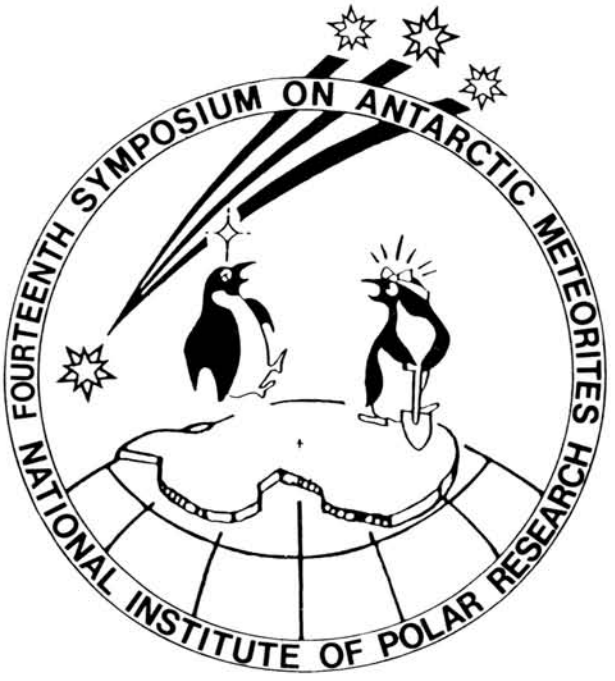

6–8, June 1989

NATIONAL INSTITUTE OF POLAR RESEARCH, TOKYO

国立極地研究所

Tuesday, June 6, 1989

0900 - 1200 Registration — Auditorium (6th Floor)

0930 - 0935 Opening Address — Takao Hoshiai
Director General
National Institute of
Polar Research

* Speaker

Chairmen: Akira Shimoyama and Takaaki Fukuoka

1 0935 - 0950 Yanai K.* and the JARE-29 Asuka Party
The meteorite concentration on the bare ice surface around the Sør Rondane Mountains, Antarctica

2 0950 - 1005 Naraoka H.*, Fujita S. and Yanai K.
Search for dust bands from blue ice fields near the Sør Rondane Mountains, Antarctica

3 1005 - 1025 Fireman E. L.
The uranium-series age of Yamato K-26 ice

4 1025 - 1045 Nishiizumi K.*, Klein J., Fink D., Middleton R, Kohl C. P. and Arnold J. R.
Exposure ages of rocks from the Sør Rondane Mountains, Antarctica

5 1045 - 1100 Takeda H.*, Mori H., Kojima H. and Yanai K.
Second consortium reports of the Yamato-86032 lunar meteorite sample and a mineralogical study

6 1100 - 1115 Fukuoka T.*, Laul J. C. and Schmitt R. A.
Chemistry of Yamato-86032 lunar meteorite

7 1115 - 1135 Wang M. S. and Lipschutz M. E.*
Volatile/mobile trace elements in lunar meteorite Yamato-86032

8 1135 - 1150 Ikeda Y.
Petrological study of the Y-74359 and Y-74360 unique meteorites

1150 - 1250 Lunch Time

Chairmen: Yukio Ikeda and Kosuke Onuma

9 1250 - 1305 Tomeoka K.
Belgica-7904: A new kind of carbonaceous chondrite from Antarctica; mineralogy and petrography

10 1305 - 1320 Matsunami S.*, Nishimura H. and Takeshi H.
Compositional heterogeneity of alteration products in B-7904 chondrite

11 1320 - 1335 Akai J.
Mineralogical evidence of heating events in carbonaceous chondrites, Y-82162 and Y-86720

12 1335 - 1355 Zolensky M.*, Barrett R. and Prinz M.
Mineralogy and petrology of Yamato-86720 and Belgica-7904

13 1355 - 1410 Yamamoto K.* and Nakamura N.
Chemical characteristics and their inference to classification of Yamato-82162 and -86720 meteorites

14 1410 - 1425 Kojima H.* and Yanai K.
Origin of PCP

15 1425 - 1445 Paul R. L. and Lipschutz M. E.*
Consortium report on carbonaceous chondrites from Queen Maud Land, Antarctica: Glimpses of new parents

16 1445 - 1505 Kallemeyn G. W.
A new chondrite grouplet: Allan Hills 85151 and Carlisle Lakes 001

1505 - 1535 Tea Time

17 1535 - 1550 Ebihara M.* and Shinonaga T.
Chemical compositions of some primitive carbonaceous chondrites from Antarctica

18 1550 - 1605 Yamamoto T. and Kozasa T.*
On the relation of carbon and nitrogen contents in carbonaceous chondrites

19 1605 - 1625 Franchi I. A.*, Exley R. A., Gilmour I. and Pillinger C. T.
Stable isotope and abundance measurements of solvent extractable compounds in Murchison

20	1625 - 1640	Shimoyama A.*, Hagishita S. and Harada K. Purines in Antarctic carbonaceous chondrites
21	1640 - 1655	Komiya M.*, Shimoyama A., Naraoka H. and Harada K. TG-MS analysis of insoluble organic matter in Antarctic carbonaceous chondrites
22	1655 - 1710	Murae T.*, Masuda A. and Takahashi T. Studies of carbonaceous residues obtained from carbonaceous chondrites by acid treatments
23	1710 - 1725	Fujita T.*, Tsuchiyama A. and Kitamura M. Homogenization process in pyroxene of ordinary chondrites
24	1725 - 1740	Noguchi T. Variations of compositional changes of pyroxenes and olivine in L chondrites. Evaluation of "petrologic type"
25	1740 - 1800	Sanchez-Rubio G.*, Reyes-Salas A. M. and Nieto A. Allende III: A SEM study of its glassy phases
	1810 - 2000	Reception

Wednesday, June 7, 1989

Chairmen: Ikuo Kushiro and Nobuo Morimoto

26 0900 - 0915 Hiroi T.*, Saito J. and Takeda H.
Mineralogical and spectroscopic studies of primitive achondrites with reference to the S-type asteroids

27 0915 - 0930 Saito J.*, Nakamura T. and Takeda H.
Mineralogical study of the Yamato-8448 ureilite and some thoughts on the origin of ureilite

28 0930 - 0945 Takeda H.*, Saeki K. and Tagai T.
Mineralogy of Yamato-791466 and -791438 achondrites and the evolution of materials in the HED parent body

29 0945 - 1000 Ikeda Y.*, Ebihara M. and Prinz M.
Eucritic enclaves in the Mt. Padbury and Vaca Muerta mesosiderites

30 1000 - 1015 Isobe H.
Densities of experimental reproduced diogenitic pyroxenes and eucritic melts

31 1015 - 1030 Watanabe S. and Kitamura M.*
High dislocation densities of relict minerals in chondrules

32 1030 - 1045 Kitamura M.*, Tsuchiyama A., Watanabe S., Syono Y. and Fukuoka K.
Shock-melting origin of chondrules

33 1045 - 1100 Horii Y.*, Fujii N. and Takeda H.
Mechanical and morphological characterization of shock effects in Antarctic meteorites (II) -Hardness & grain shape analysis of metallic particles-

34 1100 - 1115 Miura Y.* and Hanaura Y.
Plagioclase compositions of Yamato-691 chondrite

35 1115 - 1130 Nagahara H.*, Kushiro I. and Tomeoka K.
Vaporization experiments in the system plagioclase-hydrogen: 2. composition of the gas and residue

36 1130 - 1145 Tsuchiyama A.
Experimental and theoretical studies of solid-gas equilibria and their implication to redox reactions in the nebula

37 1145 - 1200 Uyeda C.*, Okano J. and Tsuchiyama A.
The magnesium isotope abundance of silicates produced from gas-condensation furnace

1200 - 1300 Lunch Time

Chairmen: Akimasa Masuda and Mitsuru Ebihara

38 1300 - 1315 Takahashi K.*, Shimizu H. and Masuda A.
Rb-Sr age of diogenite younger than that of eucrite

39 1315 - 1330 Shinonaga T.*, Ebihara M., Nakahara H., Kondoh A., Honda M., Miyamoto M. and Kojima H.
Alteration of Antarctic meteorites and their anomalous abundances of Halogens

40 1330 - 1345 Yoneda S.*, Mihara H., Nagai H. and Honda M.
Neutron activation analyses for rare earth elements in meteorites and others

41 1345 - 1400 Matsuda H*. and Nakamura N.
Further characterization of fractionated and unfractionated REE and alkali metal abundances in the Allende (CV3) chondrules -part 1-

42 1400 - 1415 Nakamura N*. and Matsuda H.
Further characterization of fractionated and unfractionated REE and alkali metal abundances in the Allende (CV3) chondrules (II)

43 1415 - 1430 Nagai H., Honda M.*, Imamura M., Kobayashi K. and Ohashi H.
Be-10 and Al-26 in metal and stone phases of meteorites

44 1430 - 1445 Nagao K.*, Miura Y. and Koh T.
Noble gas isotopic compositions of nine chondrites from Antarctica

45 1445 - 1500 Kaneoka I.*, Takaoka N. and Yanai K.
40Ar-39Ar age and noble gas isotopes of a clast(H) in a shocked L6 chondrite Y-75097

1500 - 1530 Tea Time

Thursday, June 8, 1989

Chairmen: Nobuo Takaoka and Kunihiko Kigoshi

53 0900 - 0915 Yajima H.* and Matsuda J.
Diffusion of noble gases in diamonds

54 0915 - 0930 Fukunaga K.*, Matsuda J. and Ito K.
Isotopic composition of rare gases in vapour growth diamond

55 0930 - 0945 Suzuki K.* and Matsuda J.
Fractionation of noble gases in the carbon material synthesized by glow-discharge CVD

56 0945 - 1000 Kusaba M.*, Imamura M., Yagi K., Ozima M., Watanabe S. and Hiyagon H.
Detailed measurement of potassium 40 electron capture decay, and the compressional and chemical effect to its decay constant

57 1000 - 1015 Ozima M.*, Azuma S. and Hiyagon H.
244Pu fissiogenic Xe in the mantle

58 1015 - 1030 Matsuda J.*, Murota M. and Nagao K.
Investigation of high 3He/4He ratio in deep-sea sediments

59 1030 - 1045 Misawa K.*, Yamakoshi K., Nogami K., Yamamoto K. and Nakamura N.
Chemical characteristics of magnetic, stony spherules from deep-sea sediments

60 1045 - 1105 Lin W.
Nuclear explosion glasses and tektite

Chairmen: Hitoshi Mizutani and Naoji Sugiura

61 1105 - 1120 Yabushita S.
End-Cretaceous event-Is it due to an encouter with a giant molecular cloud?

62 1120 - 1135 Akai J.* and Kanno T.
Small crater and impactite found in Toyama Prefecture, Japan

63 1135 - 1150 Miyamoto M.
Carbonates in some Antarctic meteorites: Infrared spectroscopy

1150 - 1250 Lunch Time

64 1250 - 1310 Zbik M.
Micromorphometry of several Yamato meteorites

65 1310 - 1325 Hirano T.*, Funaki M., Nagata T., Taguchi I., Hamada H., Usami K. and Hayakawa K.
Observation of Allende and Antarctic meteorites by monochromatic X-ray CT based on synchrotron radiation

66 1325 - 1340 Nagata T.* and Funaki M.
Paleomagnetic intensity studies on carbonaceous chondrites

67 1340 - 1355 Nagai H.*, Momose K. and Funaki M.
Magnetic properties of the alloy mixtures simulated to Y-74115 and DRPA78007

68 1355 - 1415 Danon J.*, Funaki M., Nagata T. and Taguchi I.
Magnetic and mössbauer properties of Cherokee Spring LL6 chondrite

1415 - 1435 Tea Time

Chairman: Noboru Nakamura

-- Special Lecture --

69 1435 - 1535 Lipschutz M. E. (Invited Speaker, Professor, Purdue University)

Title: Comparison between Antarctic and non Antarctic meteorite populations

1535 - 1555 Takeda H.
Coment with reference to Yamato achondrite

Abstract only

Tuesday, June 6, 1989

0900 - 1200 ***Registration, 6th Floor***

0930 - 0935 ***Opening address, Auditorium***

0935 - 1800 ***Symposium, Auditorium***

1810 - 2000 ***Reception, Lecture Room, 2nd Floor***

THE METEORITE CONCENTRATION ON THE BARE ICE SURFACE AROUND THE SØR RONDANE MOUNTAINS, ANTARCTICA

Yanai, K. and the JARE-29 Asuka Party
National Institute of Polar Research, 9-10, Kaga 1-chome, Itabashi-ku, Tokyo 173

Search for Antarctic meteorites have been carried out, over a 2 years period, from January 1988 to January 1989 by the Asuka winter party of the 29th Japanese Antarctic Research Expedition (JARE) 1987-1989.

More than 2000 specimens of meteorite have been found as individuals or fragments on the three major sites of the bare ice surface near the Sør Rondane Mountains (71°-73°S: 21°-29°E), Antarctica.

These recoveries will be established the site as one of major interest to Antarctic researchers, since large total number have been reported only for the Yamato Mountains (72°S: 35°E), Allan Hills (76°40'S: 159°40'E) and the Lewis Cliff Ice Tangue (84°20'; 161°30'E).

Meteorites collected around the Sør Rondane Mountains were designated as Asuka (A) meteorites since Asuka-86 meteorite collections. These recent collections will be named as Asuka-87 and Asuka-88 meteorites. Meteorite types in the Asuka collections will be distributed most range, irons, stony-irons, achondrites, chondrites and carbonaceous chondrites including unique specimens. Preliminary report of the new collections will be carried out after initial processing in the near future.

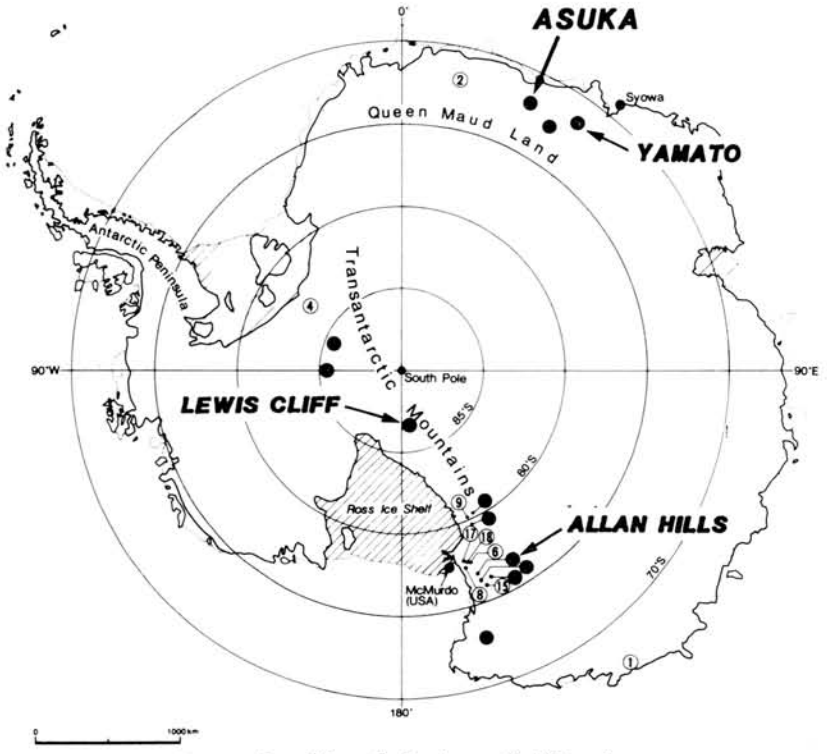

Fig. Localities of the Antarctic Meteorites

2

SEARCH FOR DUST BANDS FROM BLUE ICE FIELDS NEAR THE SØR RONDANE MOUNTAINS, ANTARCTICA

Naraoka,H.[1], Fujita,S.[2] and Yanai,K[3]
1)Department of Chemistry, University of Tsukuba, Tsukuba, Ibaraki 305. 2)Faculty of Engineering, Hokkaido University, Kita-ku, Sapporo 060. 3)National Institute of Polar Research, Itabashi-ku, Tokyo 173.

Past 10 years, dust bands were found from the bare ice fields near the Yamato Mountains, Queen Maud Land, and near the Allan Hills, Victoria Land(1). Dust bands are mainly assigned to volcanic ash. Their origins and formation ages are very interesting in connection with fall ages of Antarctic meteorites.

During the 1988-89, dust bands were observed on the surface of the bare ice fields near the Sør Rondane Mountains by the traverse parties of the 29th Japanese Antarctic Research Expedition. Antarctic meteorites were found on the same or nearby ice fields. Field appearance of dust bands were straight or curve lines, which were 10-30 cm in width and from a few meters to several kilometers in length. The ice containing dust materials were collected in situ by ice hammer etc.. After melting in a bag, dust materials were filtered by a membrane filter, 0.45μm or 0.8μm in porous size. About 100 specimens were obtained, in which they were almost assigned to volcanic ash. A few specimens, however, were associated with the formation of the moraine. These are distinguished easily from the others because they have larger particles.

Preliminary observation by a optical microscope indicated that dust materials were mainly composed of volcanic glass shards. Several types of volcanic ash were observed with respect to the colors and sizes of particles.

(1) Katsushima,T., Nishio,F., Ohmae,H., Ishikawa,M. and Takahashi,S. (1984) Mem.Natl.Inst.Polar Res.,Spec.Issue 34, 174-188.

THE URANIUM-SERIES AGE OF YAMATO K-26 ICE

Fireman, E. L.

Smithsonian Astrophysical Observtory, Cambridge, MA 02138,USA

The ice ablation zone near the Yamato mountains was the first meteorite collecting area discovered in Antarctica (1). The ice ablation area at Allan Hills was the second meteorite collecting area discovered in Antarctica (2). Other ice ablation meteorite collecting areas were also found (2,3). Dust bands are a common feature of Antarctic ablation zones and were visually observed in both the Yamato and Allan Hills ice (4,5). Properties of the dust have been measured (5,6). The particulates consist mainly of volcanic glass shards. On the basis of their chemical compositions, the Yamato glass shards are associated with volcanos in the South Sandwich islands and the Allan Hills shards with volcanos in the McMurdo group(5,6).

In the ablation zones near the margins of the polar ice sheets, deep ice from the interior comes to the surface. This idea has been carried over to the meteorite collecting areas (7). The easy access of this surface ice provides a means of obtaining large samples of ancient ice and is a stimulus for isotopically dating such ice. In order to establish a chronology for this easily accessible ice, an ablation zone with a simple flow regime-free from the complications of folds is required. Where the ice flow has been simple, the dust bands appear as straight lines perpendicular to the direction of the ice flow. The volcanic dust bands provide opportunities for dating the ice by radioactive methods.

Fireman (8,9,10) used a uranium-series method to date tephra banded ice from the Main Allan Hills Icefield. The Allan Hills tephra has approximately 5ppm of uranium with the ^{238}U, ^{234}U, ^{230}Th, and ^{226}Ra in radioactive equilibrium. Dissolved in the clear ice away from the tephra bands, these nuclides are also in radioactive equilibrium but with extremely low concentrations. The nuclides dissolved in the ice surrounding the tephra particles are in radioactive disequilibria caused by small additions of ^{234}U, ^{230}Th, and ^{226}Ra from the tephra to the ice. The disequilibria allow one to obtain $^{226}Ra/^{230}Th$ and $^{226}Ra/^{234}U$ ages for the ice(8,9).

The ^{232}Th in glass shards from the Yamato K-26 dust band(6) is

between 0.06 and 0.11ppm. Approximately 0.02 ppm of uranium is therefore expected in the Yamato K-26 tephra, which is 250 times lower than in Allan Hills tephra. Nevertheless, we attempted to date the K-26 Yamato ice sample, which was graciously supplied by Dr. F. Nishio. Table 1 gives our preliminary results for Yamato K-26 samples together with previous results obtained for Allan Hills 85-1 samples. From these results a $^{226}Ra/^{230}Th$ age of approximately 35 x 10^3 years is obtained for Yamato K-26 ice.

Table 1 Uranium-series nuclide activities in Yamato K-26 and in Allan Hills 85-1 Ice.

Sample	Yamato K-26	Allan Hills 85-1
Dusty Ice (Weight)	1.50 kg	1.63 kg
Dust (g)/ Ice (kg)	0.168	0.210
^{226}Ra (filtered H_2O)*	0.0317±0.0010	0.144±0.004
^{230}Th (filtered H_2O)*	0.0182±0.0008	0.080±0.001
^{234}U (filtered H_2O)*	0.0157±0.0008	0.049±0.001
^{238}U (filtered H_2O)*	0.0137±0.0008	0.031±0.001
$(^{226}Ra-^{238}U)/(^{230}Th-^{238}U)$	4.0±1.0	2.3±0.1
Age of Dusty ice	~35 x 10^3	(100±10) x 10^3
Clear Ice(Weight)	1.78 kg	1.40 kg
Dust (g)/Ice (kg)	0.002	0.002
^{226}Ra (filtered H_2O)*	0.004 ± 0.002	0.014±0.002
^{230}Th (filtered H_2O)*	--------	0.013±0.002
^{234}U (filtered H_2O)*	--------	0.014±0.002
^{238}U (filtered H_2O)*	--------	0.015±0.002

*Activity in dpm kg^{-1} (decays per minute per kg) units.

This work is supported by NSF Grant 8716835

References : (1) Yoshida, M. , Ando, H. , Omoto, K. , Nuruse, R. & Ageta, Y. (1971) Antarctic Record 39, 602. (2) Cassidy, W. A. (1971) Antarctic Journal of the U.S., XII-4, 96. (3) Nagata, T. (1971) Antarctic Journal of the U.S., XII-4, 95, (4) Nishio, F., & Annexstad (1979) Mem. Natl. Inst. Polar Res., 15, 13. (5) Katsushima, T., Nishio, F., Ohmae, H., Ishikawa, M., & Takahashi, S. (1984) Mem. Natl. Inst. Polar Res., 34, 174. (6) Fukuoka T., Arai, F., & Nishio, F. (1987) Bull. Vulcanol. Soc. Japan, 2, 103. (7) Whillans, I. M. & Cassidy, W. A. (1983) Science, 222, 55. (8) Fireman, E. L. (1986) Journ. of Geophys. Res. 91, B4, D539. (9) Fireman, E. L. (1986) Journ. of Geophys. Res. 8393. (10) Fireman, E. L. (1987) Antarctic Journal of the U.S., XXII-5, 75.

EXPOSURE AGES OF ROCKS FROM THE SÖR RONDANE MOUNTAINS, ANTARCTICA

Nishiizumi, K., Klein, J.*, Fink, D.*, Middleton, R.*, Kohl, C. P. and Arnold, J. R.
Department of Chemistry, B-017, University of California, San Diego, La Jolla, CA92093
* Department of Physics, University of Pennsylvania, Philadelphia, PA19104

Exposure ages of Antarctic rocks can contribute a great deal to understanding of the dynamics of the Antarctic ice sheet, in particular to determination of past elevation changes of the ice. Combined with the terrestrial ages of Antarctic meteorites, we can also use rock exposure ages to examine such problems as ages of the ice sheets, direction and rate of ice movement and production of moraines.

When bedrock is exposed above the ice, cosmic ray bombardment produces a variety of nuclides. Recently we demonstrated the feasibility of using ^{10}Be ($t_{1/2}$=1.5My) and ^{26}Al ($t_{1/2}$ =0.7My) produced *in-situ* in terrestrial quartz to trace continental weathering/erosion processes and to determine surface exposure time [1,2]. This paper applies the method to the history of rocks from the Sor Röndane mountains in Antarctica as part of our continuing investigation of the Antarctic continent.

Quartz is an ideal material for these studies. It is present in a wide variety of geologic settings. Its simple composition helps us understand and calculate the nuclear reactions. Its tight crystal structure minimizes possible contamination from "garden variety" ^{10}Be produced in the atmosphere. It has a low Al content which allows measurement of ^{26}Al, and it can be separated from other minerals fairly easily.

To apply this method production rates and, in particular, the production ratio of these two nuclides must be well known. Recently the values were experimentally determined using glacially polished granite from the Sierra Nevada [3]. The production rate of ^{10}Be is 6.1 atom/g SiO_2 year at sea level (geomagnetic latitude >50°). The production rate of ^{26}Al is 37 atom/g SiO_2 year. The production ratio of ^{26}Al to ^{10}Be production is 6.0 [3] . The production rates increase with increasing altitude due to the decrease in atmospheric shielding. At 3 km altitude the production is more than a factor of ten greater than at sea level. The production rates also change with latitude due to the higher cut-off energy toward the equator.

These production rates are extremely low. Fortunately the present detection limit for both ^{10}Be and ^{26}Al by AMS (accelerator mass spectrometry) is also low, about 10^6 atoms. This allows meaningful measurements of ^{10}Be and ^{26}Al in 15 g of quartz exposed for 10,000 years at sea level.

The concentration of each nuclide increases with exposure time exactly as for meteorites but interpretation of results is complicated by the erosion experienced by most terrestrial rocks. The nuclide concentration in most terrestrial samples is, in fact, controlled by the erosion rate. For the simple case of a constant erosion rate (ε), the steady state nuclide concentration (C) is given by the following equation.

$$C = P_0 / (\lambda + \rho\varepsilon / \Lambda)$$

Since the production rate (P_0), the decay constant of the nuclide (λ), the density of rock (ρ), and the absorption mean-free-path (Λ) are known, the erosion rate can be calculated from the nuclide concentration assuming continuous exposure.

However, nature is not always so simple, especially in Antarctica. Sometimes a thick ice sheet covered the rock and cosmic ray production stopped. Then glaciation suddenly eroded the old exposed surface. Although a simple erosion model can't be applied to many samples, the combination of erosion and exposure time can constrain the surface history of rocks.

A series of rock samples was collected by H. Kojima and K. Moriwaki (NIPR) from the Sor Röndane mountains (72° S, 25° E). We report here results on 8 of those samples. The sampling locations are shown in Figure 1 and the ^{10}Be and ^{26}Al measured values are given in Table 1. AMS was performed at the University of Pennsylvania's Tandem van de Graaff. Table 2 presents the exposure ages and erosion rates calculated using the production rates discussed above and correcting for altitude and latitude effects. The errors on the calculated exposure ages do not include an error of approximately 10% for the production rate calculations.

The outstanding features of Table 2 are the long exposure ages and correspondingly low erosion rates for many of the samples. Five of the samples have exposure ages over 1 My and erosion rates of only a few x 10^{-5} cm/year; calculations made separatly for the two nuclides are in agreement. These findings are consistent with observations from other parts of Antarctica; i.e. Allan Hills and Tillite glacier [4], and they are in marked contrast to results from other continents. Erosion rates for rocks from more temperate continents are in the range 10^{-3} - 10^{-4} cm/year; these rocks would never develop the high (saturated) concentrations of ^{10}Be and ^{26}Al seen in Antarctica.

Some conclusions can be drawn about the individual sampling sites although in several cases there are more samples to be measured. TAC- 7 is from near the peak of the Menipa Mountain 800 m higher than the

Mefjellbreen. Field observations show weathered bedrock and indicate a possibility of the local glacier covering the location sampled fairly recently [5]. However the results in Table 2 indicate a continuous exposure of over 1 My for this sample. The erosion rate for this sample is quite low in spite of the weathered appearance of the surrounding rock. TAC-8 is from the opposite side of the local glacier; it was taken from the SE facing slope of Menipa, ~200 m higher than Mefjellbreen. The low $^{26}Al/^{10}Be$ ratio for this sample compared to the concentrations the individual nuclides indicates a complex history and is consistent with the location sampled which is closer to the ice surface. TAC-9 was taken from the S side of the E wall of Birger Bergersenfjellet 3 m above the surface of the Byrdbreen. The 36,000 year exposure age measured for this sample is short compared to other samples in the area, as expected. The low $^{26}Al/^{10}Be$ ratios compared to the nuclide concentrations may be due to a complex history of exposure and reburial in the ice. TAC-10 is from the E slope of Sörhaugen. It was taken from a pegmatite dike cutting approximately vertically through the rock mass. A series of 5 samples were taken from different altitudes, we report on one of them taken 25 m down from the highest. Continuous exposure over the last 1 My or more with low erosion rate, $2x10^{-5}$ cm/y, is indicated for this sample. TAC-11 was collected from near the peak of the local rock mass, elevation above the ice is not yet known for this sample but the $^{26}Al/^{10}Be$ ratio indicates a simple exposure history with a $6x10^{-5}$ cm/y erosion rate. TAC-12,13, and 14 are from the crests of the highest ridges on the Mefjell Mountain. The surface of the ice locally is at least a few hundred meters lower than the lowest sample. The minimum exposure ages are 1.5 to 1.8 My. They are similar for all samples once the measured values are corrected for altitude, which varies almost 900 m. ^{26}Al is nearly saturated in these samples as is shown by the $^{26}Al/^{10}Be$ ratio of ~ 3. This mountain mass has not been covered by ice within the last 1.5-2.0 My. In general the presently exposed mountains in the Sor Röndane area have been ice free for at least 1 My, and the ice thickness has not been substantially greater in the same time period. The erosion rates for all these samples are also very similar, suggesting a common mechanism, and no dependence on the direction the surface faces.

Meteorites have been collected near the Sör Rondane mountains but have not yet been received for study. We intend to measure terrestrial ages for these objects which will help define the history of the ice in this region of Antarctica as we have done for the Allan Hills. The Yamato mountains are another region which needs further study. Exposure age/erosion rate determinations of well selected rock samples from this area could be combined with existing meteorite data to clarify the local history of the ice and the meteorite accumulation mechanisms.

The author wishes to thank H. Kojima and K. Moriwaki for sample collection. This work was supported by NSF Grant ERA 86-17994 and NASA Grant NAG 9-33 .

References

[1] Lal, D. and Arnold, J. R. (1985) *Proc. Indian Acad. Sci. (Earth Planet. Sci.), 94*, 1-5.
[2] Nishiizumi, K., Lal, D., Klein, J., Middleton, R. and Arnold, J. R. (1986) *Nature, 319*, 134-136.
[3] Nishiizumi, K., Winterer, E. L., Kohl, C. P., Klein, J., Middleton, R., Lal, D. and Arnold, J. R. (1989) *J. Geophys. Res.* (in press)
[4] Nishiizumi, K. (1988) (abstract) *Workshop on Antarctic Meteorite Stranding Surfaces, (Lunar Planet. Inst., Houston)* (in press).
[5] Kojima, H. (1986) personal communication

TABLE 1. RESULTS OF ^{10}Be AND ^{26}Al IN SÖR RONDANE MOUNTAIN SAMPLES

ID	NAME	Altitude (m)	^{10}Be (10^6 atom/g SiO_2)	^{26}Al (10^6 atom/g SiO_2)	$^{26}Al/^{10}Be$
TAC- 7	860118-01	2,100	34.47 ± 0.86	132.7 ± 8.0	3.85 ± 0.25
TAC- 8	860119-02	1,460	3.14 ± 0.09	15.92 ± 0.80	5.07 ± 0.29
TAC- 9	860128-01B	1,410	0.846 ± 0.029	3.43 ± 0.23	4.06 ± 0.30
TAC-10	A860116-03-3	1,350	20.94 ± 0.61	81.45 ± 4.07	3.89 ± 0.23
TAC-11	A860118-02B	1,800	15.77 ± 0.60	70.12 ± 3.50	4.45 ± 0.28
TAC-12	A860121-06B	2,980	80.27 ± 1.93	267.9 ± 13.4	3.34 ± 0.19
TAC-13	A860122-01	2,100	42.76 ± 1.07	135.0 ± 6.7	3.16 ± 0.18
TAC-14	A860122-05C	2,440	58.06 ± 1.34	167.1 ± 8.4	2.88 ± 0.16

TABLE 2. CALCULATED EXPOSURE AGES AND EROSION RATES OF SÖR RONDANE MOUNTAIN SAMPLES

ID	^{10}Be Age (10^3 years)	^{26}Al Age (10^3 years)	Average Age (10^3 years)	Erosion rate (10^{-5}cm/year)
TAC- 7	1440 ± 51	1093 ±118	1267 ±245	2.5
TAC- 8	157.5 ± 4.7	135.9 ± 7.3	146.7 ± 15.3	33
TAC- 9	42.9 ± 1.5	28.9 ± 1.9	35.9 ± 9.9	143
TAC-10	1539 ± 65	1207 ±116	1373 ± 234	2.2
TAC-11	695 ± 31	571 ± 38	633 ± 88	6.3
TAC-12	2211 ± 93	1426 ± 157	1818 ± 555	1.5
TAC-13	1998 ± 82	1127 ± 104	1562 ± 615	2.0
TAC-14	2280 ± 93	1099 ± 99	1689 ± 835	1.9

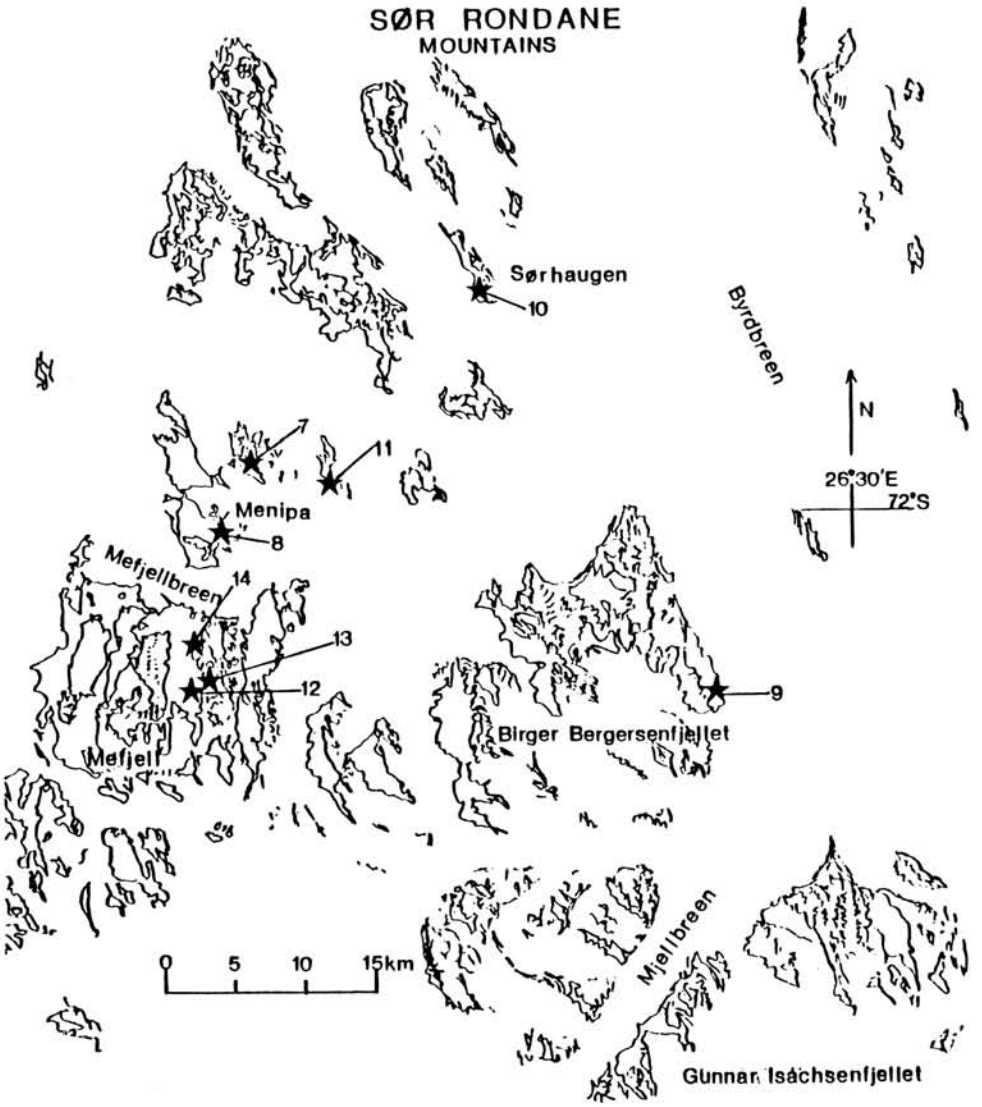

SECOND CONSORTIUM REPORTS OF THE YAMATO 86032 LUNAR METEORITE SAMPLE AND A MINERALOGICAL STUDY.

Hiroshi TAKEDA, H. MORI[1], H. KOJIMA and K. YANAI[2].
[1]Mineralogical Inst., Faculty of Science, Univ. of Tokyo, Hongo, Tokyo 113,
[2]National Inst. of Polar Res., 9-10 Kaga 1 chome, Itabashi-ku, Tokyo 173.

The preliminary reports of the Y-86032 lunar meteorite will be published in three separate papers (1, 2, 3). Many similarities between Y-86032, Y-82192 and Y-82193 have been noted by mineralogical (1) and petrological studies. The chemical compositions of the samples from these three meteorites are uniform for most major elements but not for all minor and trace elements, probably due to inhomogeneity of the source material (2, 3). From the fact that the history of Y-86032 is the same as that of Y-82192/3 as obtained by the noble gas studies, Eugster et al. (3) concluded that these three rocks are pieces of the same meteorite fall. Detailed descriptions of each allocated sample were given in the preliminary report (1).

For the second allocation of the consortium study, a middle right portion of the N view (Photo 495) of Photographic Catalog of Antarctic Meteorites by Yanai and Kojima (4) has been chipped off, producing four large chips and small fragments (,50) 3.875 g in total. Many fragments have slightly weathered (with yellow color) smooth surface, which may be a remnant of fusion crust.

The largest chip (,57) weighing 0.880 g and 1.75 X 1.40 X 0.4 cm in size contains numerous large gray to white clasts as shown in Fig. 3 of Takeda et al. (1). A light grayish clast is similar to the large light clast used for the first allocation (1). An oval shaped white clast 0.3 X 0.2 cm in size, spotted with yellow mafic silicates is similar to granulitic clasts often observed in the PTS. A half of this clast was chipped and used for the INAA study by Fukuoka. The lower half of the chip ,57 was subdivided and allocated to the INAA study by Warren et al. (,69). It contains two large white clasts. One clast 0.3 X 0.1 cm in size contains more mafic silicates than the above granulitic clast.

One chip (,59) weighing 0.521 g and 1.2 X 1.1 X 0.35 cm in size is a typical matrix sample and contains fewer number of large clasts, but numerous small white clasts are densely packed. This chip was subdivided into three samples. A chip with a weathered surface (,67) is kept for the PTS. A chip (,66) weighing 0.206 g was allocated to the noble gas study (Takaoka) and another (,68) weighing 0.125 g was used for the INAA study (Fukuoka), and three very small fragments are kept at NIPR.

The second large chip weighing 0.707 g and 1.1 X 0.9 X 0.55 cm in size has a flat surface, which is a remnant of fusion clast, and includes white clasts in this portion, and another fresh fragmented surface contains a few white clasts, one with brownish mafic silicates. This chap is temporality kept at NIPR. A part of the collections of many small fragments under 0.6 cm in diameter of the first allocation was allocated to isotopic studies (Nyquist) and another part of them will be allocated for a regolith study (McKay).

The results on the investigations of the above samples will be presented at the 14th Symposium on Antarctic Meteorites by the consortium members (5,6). Carbon and nitrogen stable isotope analyses of Y-86032 by Grady and Pillinger (5) have shown that Y-86032 is poorer in presumably spollagenic carbon than ALHA81005, in keeping with the observation that

Y-86032 has not been exposed to cosmic rays and the solar wind. The stepped combustion profile is different from those of Apollo samples. Total nitrogen data are within the range reported for lunar breccia. They suggested that Y-86032 is sufficiently different from lunar counterparts and that some component of meteoritic material has been added from the projectile during the impact. Wang and Lipschutz (6) have analysed volatile/ mobile trace elements in Y-86032 by RNAA. They have found that Y-86032 contains less Au and Sb than do corresponding Y-82192/3 samples. The volatile/mobile trace element patterns of whole-rock (matrix) samples of Y-86032 and Y-82192/3 are similar but Y-86032 contains a somewhat greater proportion of such elements. They concluded that these three lunar meteorites derive from the same impact in the same lunar highlands region, but the parent region was somewhat heterogeneous compositionary. Haramura and Kushiro obtained a bulk chemical composition by the standard wet chemical analysis.

Mori and Taked investigated matrix sample of Y-86032 to see the difference of microtextures by TEM between lunar meteorites of the regolith breccia group (ALHA81005 and Y-791197) and the anorthositic fragmental breccia group (Y-82192/3 and Y-86032). The TEM observation of Y-86032,110 and ,111 showed that the fine grained matrix materials of both ,110 and ,111 are composed of micron-sized angular fragments of plagioclase and very fine-grained (submicron-sized) interstitial material. The very fine-grained material is mainly composed of plagioclase and minor mafic silicate materials with a recrystallized texture. No glassy material was observed in the matrix. It appears that submicron-sized recrystallized materials bind the brecciated fragments. Pronounced differences have not been detected between the two groups, except for that Y-791197 preserves a glassy matrix.

We thank Mr. H. Kojima and Dr. K. Yanai for their help in the sample preparation, and members of the consortium group for their cooperation.

References:

(1) Takeda H., Kojima H., Nishio F., Yanai K. and Lindstrom M. M. (1988) Preliminary report on the Yamato-86032 lunar meteorite I: Recovery, sample descriptions, mineralogy and petrography. Proc. NIPR Symp. Antarct. Meteorites, 2, in press.

(2) Koeberl C., Warren P. H., Lindstrom M. M., Spettel B. and Fukuoka T. (1988) Preliminary examination on the Yamato-86032 lunar meteorite II: Major and trace element chemistry. Proc. NIPR Symp. Antarct. Meteorites, 2, in press.

(3) Eugster O., Niedermann S., Burger M., Krähenbühl U., Weber H., Clayton R. N. and Mayeda T. K. (1988) Preliminary report on the Yamato-86032 lunar meteorite III: Ages, noble gas, isotopes, oxygen isotopes and chemical abundances. Proc. NIPR Symp. Antarct. Meteorites, 2, in press.

(4) Yanai K. and Kojima H. (1987) Photographic Catalog of the Antarctic Meteorites. 289 pp., Natnl. Inst. Polar Res., Tokyo.

(5) Grady M. M. and Pillinger C. T. (1989) Y-86032 and ALHA 81005 - Carbon and nitrogen stable isotope analyses of two lunar meteorites. This volume.

(6) Wang M.-S. and Lipschutz M. E. (1989) Volatile/mobile trace elements in lunar meteorite Yamato 86032. This volume.

CHEMISTRY OF YAMATO-86032 LUNAR METEORITE

Fukuoka, T.[1], Laul, J. C.[2] and Schmitt, R. A.[3]

1. Department of Chemistry, Gakushuin University, Mejiro, Tokyo 171.
2. Chemical Technology Department, Battelle, Pacific Northwest Laboratories, Richland, WA 99352.
3. The Radiation Center, and Departments of Chemistry and Geology and College of Oceanography, Oregon State University, Corvallis, OR 97331.

We analized more than 30 major, minor and trace elements in three white clasts and four matrices from Yamato 86032 meteorite by instrumental neutron activation analysis (INAA). Matrix samples, sub no.68-1 and sub nos.64-2, 64-3 and 109-1 were chipped from opposite side on a meteorite block. Preliminary analytical results are shown in Tabel 1 together with the chemical abundances of the matrices of Yamato-791197, -82192 and -82193 and ALHA 81005 lunar meteorites.

Based on the well-established characteristic lunar and meteoritic ratios of FeO/MnO and Cr_2O_3/V, and C1 chondrites normalized LIL patterns, Y-86032 meteorite is undoubtedly of lunar highland origin like other lunar meteorites and it is an anorthositic gabbro.

The chemial composition of the clast, 64-1 is close to it of the clast, 106-1, and is different from those of the clast, 112-1 and the matrices. This indicates different lithologies for the clasts and that Y-86032 is a complex breccia. The chemical compositions of four matrices are mostly a similar. This imply the matrix of the meteorite was well mixed by previous impact events. There is some small chemical discrepancies between impact melt glass (1) and the other matrices (e.g.FeO and Sc). This is possibly explained by the remove of mafic mineral. Any evidence cannot be seen for loss of the analyzed elements by the impact event. Analyses of volatile elements such as Zn are expected for further discussion of the chemical influence on the impact event.

The similarity of the chemical compositions of matrices (weighted mean) of Y-86032, -82192 and -82193 meteorites suggests that Y-86032 is paird with Y-82192 and Y-82193. The chemical compositions of matrices of Y-86032 meteorite are largely different from those of Y-791197 and ALHA 81005. The lack of an appreciable KREEP component in Y-86032 lunar breccia implies a far side origin of this meteorite as discussed before for the origin of the other lunar meteorites (2, 3).

REFERENCES: (1) Takeda, H. et al.(1988) Abstract 13th Sym. Antarctic Meteorites, 9. (2) Fukuoka, T. et al.(1985) Mem. Natl Inst. Polar Res. Spec. Issue 41, 84. (3) Fukuoka, T. et al.(1986) Abstract 11th Sym. Antarctic Meteorites, 40.

Table 1. Preliminary results of chemical abundances by INAA

		YAMATO 86032								Y82192[1]	Y82193[1]	Y791197[2]	ALHA81005[3]
		clast	clast	clast	matrix	matrix	matrix	glassy matrix	matrix	matrix	matrix	matrix	matrix
		64-1	106-1	112-1	64-2	64-3	68-1	109-1	wtd.mean	wtd.mean	wtd.mean	wtd.mean	wtd.mean
Wt	mg	8.76	5.48	0.629	66.81	14.32	113.8	13.52					
TiO_2	%	0.31	0.23	0.50	0.20	0.19	0.27	0.21	0.24	0.22	0.27	0.30	0.30
Al_2O_3	%	31.6	31.9	25.8	27.8	28.9	27.8	28.9	27.9	27.0	25.8	27.1	25.9
FeO	%	3.57	3.19	4.95	4.37	4.55	4.54	4.20	4.46	4.60	5.70	6.7	5.6
MgO	%	2.8	1.3	5.9	4.7	5.5	5.6	4.5	5.2	4.5	5.1	6.4	8.0
CaO	%	18.1	19.2	14.1	16.1	16.5	15.5	16.3	15.8	15.1	16.7	15.3	15.2
Na_2O	%	0.48	0.45	0.37	0.42	0.42	0.48	0.40	0.45	0.49	0.41	0.34	0.31
K_2O	%	0.006	0.012	0.018	0.011	0.024	0.013	0.014	0.013	0.020	0.037	0.029	0.025
MnO	%	0.054	0.053	0.076	0.065	0.068	0.065	0.064	0.065	0.067	0.081	0.085	0.070
Cr_2O_3	%	0.064	0.057	0.095	0.097	0.098	0.092	0.093	0.094	0.110	0.154	0.120	0.123
Sr	ppm	210	240	130	170	170	190	170	180	190	180	137	140
Ba	ppm	18	18	39	22	29	23	27	23	26	28	39	30
Sc	ppm	7.10	6.33	8.10	8.39	8.78	8.70	7.84	8.55	8.68	12.2	12.9	9.3
V	ppm	12	16	17	26	21	22	22	23	27	31	28	25
La	ppm	0.61	0.57	1.10	1.24	1.34	1.19	1.29	1.22	1.11	1.27	2.17	2.0
Ce	ppm	1.6	1.3	2.5	3.0	3.3	3.1	3.3	3.1	2.7	3.6	5.4	4.9
Nd	ppm	0.9	0.8	1.7	2.1	1.8	2.1	2.1	2.1	1.5	2.0	3.4	3.4
Sm	ppm	0.30	0.29	0.63	0.60	0.63	0.62	0.62	0.62	0.54	0.65	1.04	1.0
Eu	ppm	1.13	1.07	0.74	0.85	0.87	0.94	0.86	0.90	1.10	1.00	0.78	0.74
Gd	ppm	0.60	0.54		0.83	0.92		0.76	0.83	0.80	0.80	1.3	-
Tb	ppm	0.07	0.06	0.10	0.14	0.15	0.14	0.14	0.14	0.12	0.15	0.24	0.20
Dy	ppm	0.6	0.5	0.8	0.9	1.0	0.9	1.0	0.9	0.9	1.0	1.5	1.3
Tm	ppm	0.10	0.10		0.11	0.13		0.13	0.12	0.08	0.11	0.16	0.13
Yb	ppm	0.34	0.33	0.50	0.57	0.65	0.58	0.61	0.58	0.55	0.73	1.03	0.85
Lu	ppm	0.054	0.051	0.073	0.088	0.092	0.087	0.090	0.088	0.082	0.117	0.15	0.13
Zr	ppm				20	20		20	20	20	20	32	30
Hf	ppm	0.19	0.15	0.21	0.39	0.41	0.39	0.43	0.39	0.36	0.45	0.81	0.70
Th	ppm	0.05	0.06	0.06	0.20	0.19	0.16	0.21	0.18	0.14	0.20	0.35	0.31
U	ppm	0.007	0.011		0.032	0.046	0.056	0.046	0.047	0.031	0.040	0.09	-
Ta	ppm	0.04	0.02		0.05	0.05	0.07	0.07	0.06	0.043	0.065	0.11	0.10
Co	ppm	7.7	6.9	11.6	14.4	16.4	15.9	14.9	15.4	14.4	19.2	19.8	20.0
Ni	ppm	46	54		140	181	172	159	162	121	150	180	190
Ir	ppb	2.3	2.1		3.7	5.5	5.7	4.6	5.0	2.9	6.0	6.5	6.2
Au	ppb	0.9			1.3	2.6	1.8	2.1	1.7	0.7	1.3	2.5	2.4

1) Revised from Fukuoka, T. et al. (1986) Abstract 11th Sym. Antarctic Meteorites 40. 2) Fukuoka, T. et al. (1986) Mem.Natl Inst.Polar Res., Spec. Issue, 41, 84. 3) Laul, J. C. et al. (1983) Geophys. Res. Lett., 10, 825.

VOLATILE/MOBILE TRACE ELEMENTS IN LUNAR METEORITE YAMATO 86032

M.-S. Wang and M. E. Lipschutz

Dept. of Chemistry, Purdue University, W. Lafayette, IN 47907.

Four of the 6 lunar meteorites recovered from Antarctica (their only known source on Earth) had already been studied by consortia prior to establishment of the Consortium, led by Prof. H. Takeda, to study Yamato (Y) 86032 and Y-793274. These earlier studies on Allan Hills (ALH A) 81005, Y-791197 and the paired samples Y-82192/3 had shown that all were probably from different regions on the Moon since, for example, each had its own characteristic volatile/mobile trace element pattern (Verkouteren et al., 1983; Kaczaral et al., 1986; Dennison et al., 1987). Other data generally accord with this view and the consensus seems to be that each acquired the shock-induced impulse of $\geq$2.4 km/sec, necessary to travel from the Moon to the Earth, in a separate massive impact (cf. Koeberl et al., 1989).

The leader of the Consortium to study the remaining 2 lunar meteorites provided material from Y-86032 with the cautionary note that it might be paired with Y-82192/3 based on petrologic similarities. [We have not yet received a sample of Y-703274 for study.] Indeed this may well be the case. Refractory lithophile and siderophile trace elements (Lindstrom et al., 1988; Koeberl, 1988; Koeberl et al., 1989) indicate that Y-86032 differs compositionally from ALH A81005 and Y-791197 but resembles Y-82192/3. However, there are subtle differences between Y-86032 and Y-82192/3 in that most lithophile incompatible elements are even lower in the former than in the latter and refractory siderophiles in the two differ. On the other hand, cosmogenic gas contents in Y-86032 and Y-82192/3 are similar (Eugster and Nedermann, 1988) suggesting a single impact in an inhomogeneous target (Koeberl, 1988; Koeberl et al., 1989).

As Consortium members, we received samples of Y-86032 to determine by RNAA our trace element suite, consisting of siderophiles Co, Au and Sb, volatile/mobile Se, Te, Bi, Ag, In, Tl, Zn and Cd, and lithophiles Rb, Cs, Ga and U. [Gallium is normally considered siderophile and/or volatile but seems lithophile in lunar samples.] Our primary goal was to assess the likelihood of a common origin for Y-86032 and Y-82192/3.

We were provided with 2 samples, a 129 mg matrix chip (Y-86032,75 AM) and a 37.4 mg chip of light anorthositic breccia clast (Y-86032,101 AC), both of which had previously been analyzed by Lindstrom et al. (1988) using INAA. In general, we found that, as in Y-82192/3, Y-86032 matrix generally contains equivalent- to higher- amounts of trace elements than do clasts. On the whole, Y-86032 samples contain less Au and Sb than do corresponding Y-82192/3 samples (cf. Lindstrom et al., 1988; Koeberl, 1988; Koeberl et al., 1989). The volatile/mobile trace element patterns of whole-rock (matrix) samples of Y-82182/3 and Y-86032 are similar, but the latter contains a somewhat greater proportion of such elements, corresponding to 2.7$\pm$1.1% Cl equivalent compared with 2.4$\pm$0.8% in Y-82192 (Dennison et al., 1987).

Since both samples contain comparable, high proportions of volatile/mobile trace elements and exhibit similar trends, we believe that Y-82192/3 and Y-86032 derive from the same impact in the same lunar highlands region. The

compositional differences indicate that the parent region was somewhat heterogeneous compositionally. We eagerly await samples of Y-793274.

References

J. E. Dennison, P. W. Kaczaral and M. E. Lipschutz (1987) Proc. Eleventh Symp. Antarctic Meteorites, 89-95.
O. Eugster and S. Nedermann (1988) Meteoritics 23, 268 (abstr.).
P. W. Kaczaral, J. E. Dennison and M. E. Lipschutz (1986) Proc. Tenth Symp. Antarctic Meteorites, 76-83.
C. Koeberl (1988) Meteoritics 23, 280 (abstr.).
C. Koeberl, P. H. Warren, M. M. Lindstrom, B. Spettel and T. Fukuoka (1989) Proc. NIPR Symp. Antarctic Meteorites 2, in press.
M. M. Lindstrom, D. W. Mittlefehldt and R. Score (1989) Proc. NIPR Symp. Antarctic Meteorites 2, in press.
R. M. Verkouteren, J. E. Dennison and M. E. Lipschutz, Geophys. Res. Lett. 10, 821-824.

PETROLOGICAL STUDY OF THE Y-74359 AND Y-74360 UNIQUE METEORITES

Ikeda, Y.

Department of Earth Sciences, Ibaraki University, Bunkyo, Mito 310.

Unique Antarctic meteorites are being studied by a consortium (Leader: Prof. Kushiro). They are small, ranging from 0.6 g to 35 g in weight. Two unique meteorites, Y-74359 (1.5 g) and Y-74360 (3.3 g), are fine-grained and medium-grained respectively, and show holocrystalline igneous textures. They consist of olivine, orthopyroxene, clinopyroxene, and feldspar with minor amounts of chromite, troilite, and Fe-metal. Orthopyroxene and olivine are predominat, and glass is absent. Feldspar occurs in interstitial spaces between olivine and/or orthopyroxene grains. Major element chemical compositions of Y-74359 and Y-74360 (Table 1) were measured using a defocussed beam (about 50 microns in diameter) of an electron-probe micro-analyser with a correction method of Ikeda (1983). The bulk chemical compositions are very similar to average chemical composition of silicate portion of H chondrites except for slightly-low CaO and Al2O3 contents of the unique meteorites.

Olivines show slight chemical zonig from magnesian core to ferroan rim, the MgO/(MgO+FeO) mole ratio ranging from 0.82 to 0.80 for Y-74359 and from 0.83 to 0.78 for Y-74360. Orthopyroxenes also show slight chemical zoning from Ca-poor magnesian core to Ca-rich ferroan rim as shown in Fig. 1. On the other hand, clinopyroxenes show remarkable chemical zoning continuously from pigeonitic core to augitic rim (Fig. 1). Chromites in the unique meteorites are very similar in chemical composition to those in equilibrated H chondrites, and those in Y-74360 show slight chemical zoning from Ti-poor core to Ti-rich rim. Feldspars in Y-74360 are albite, and the An content ranges from 3 to 9. Feldspars in Y-74359 are chemically classified into three groups, Na-rich albite, Na-poor albite, and K-rich feldspar as shown in Fig. 2, and they occur in different portions of Y-74359. Fe-metals occur rarely in the unique meteorites, and the Ni and Co contents are 4-6 wt% and 0.2-0.6 wt%, respectively, which are very similar to those in equilibrated H chondrites.

The remarkable chemical zoning of clinopyroxenes in the unique meteorites mean that they crystallized rapidly in under-cooling conditions similar to those of chondrules. However, the absence of glass suggests that they crystallized more slowly than chondrules. The occurrence of three feldspar groups in Y-74359 suggests that the solid precursor of the unique meteorite included chemically-different feldspars and after the melting crystallization took place rapidly to prevent residual feldspathic melts to homogenize.

Two hypotheses are possible for origin of unique meteorites. First one is as follow: unequilibrated H chondrites were melted without homogenization of feldspathic components, and during the melting Fe-metal and Fe-sulfide components were lost. The silicate melt kept to be chemically heterogeneous and rapidly crystallized olivine, orthopyroxene, and clinopyroxene in this order to produce remarkable chemical zonings of pyroxenes. The rapid crystallization without homogenization of feldspathic components resulted in heterogeneous residual melts which were different in feldspathic composition among the portion. Finally fedspars crystallized interstitially but the chemical compositions were different among the portions of the unique meteorites.

Second hypothesis is as follow: Rapid condensation in the protosolar nebula produced heterogeneous silicate precursors which included chemically-different feldspar grains. They were melted without remarkable homogenization to produce many silicate-melt droplets and silicate-melt blocks, which crystallized rapidly to be chondrules and unique meteorites, respectively. Second hypothesis seems to be preferable to first one, and is shown schematically in Fig. 3.

	75359 K-rich	75359 K-poor	74360	Av.H
SiO2	47.59	46.83	48.20	46.60
TiO2	0.13	0.14	0.15	0.13
Al203	2.25	2.26	2.24	2.61
Cr203	0.97	0.83	0.92	0.60
FeO	14.34	15.44	14.36	15.31
MnO	0.42	0.42	0.43	0.37
MgO	31.31	31.26	30.92	31.03
CaO	1.64	1.67	1.81	2.30
Na20	0.64	1.00	0.86	0.95
K20	0.71	0.15	0.11	0.10
Total	100.00	100.00	100.00	100.00

Table 1. Bulk compositions of Y-74360 and K-rich and K-poor portions of Y-74359. Av.H is average composition of silicate portion of H chondrites (Haramura et al., 1983).

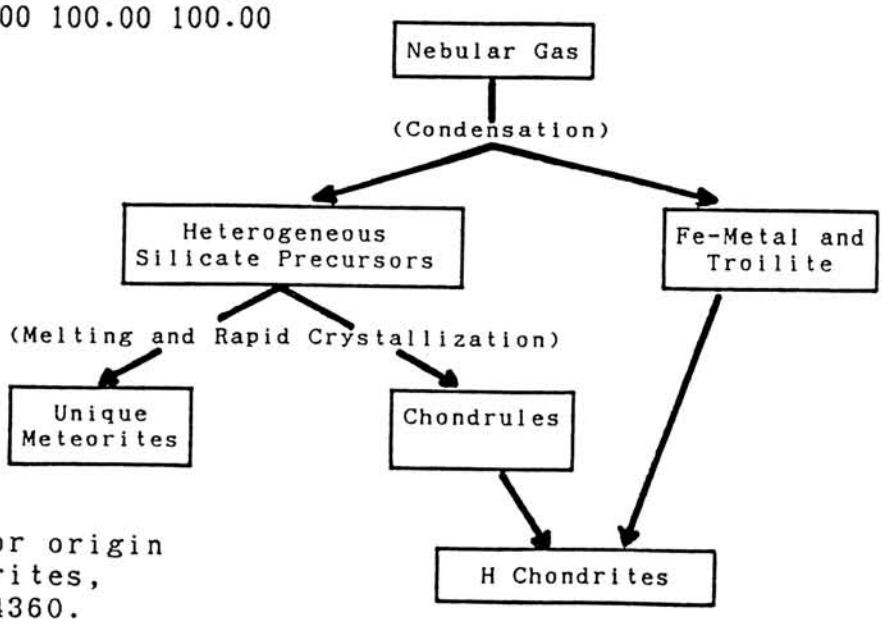

Fig. 3. Model for origin of unique meteorites, Y-74359 and Y-74360.

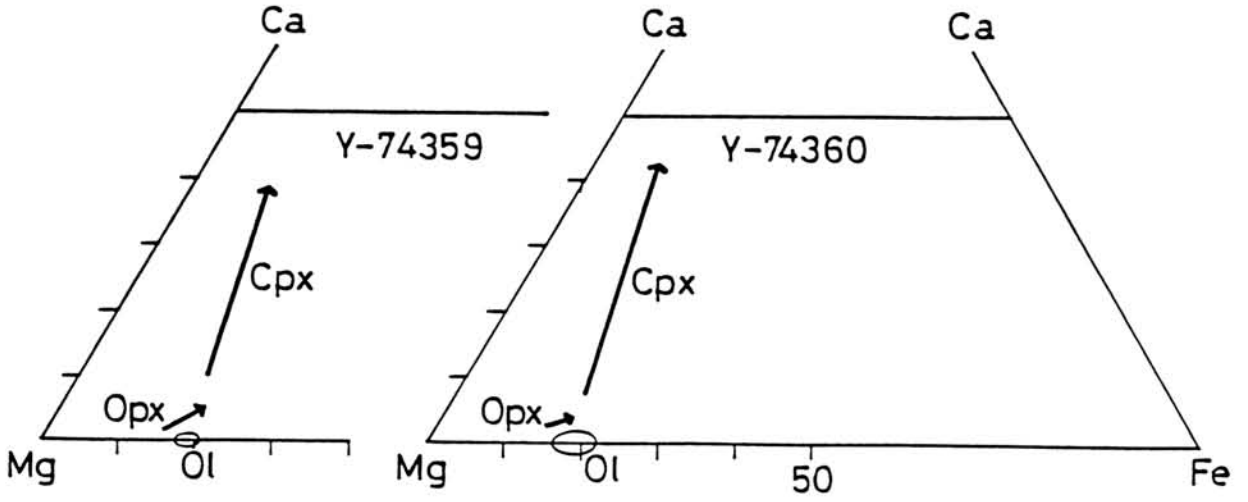

Fig. 1. Olivine(Ol), Orthopyroxene(Opx) and clinopyroxene(Cpx) in Y-74359 and Y-74360 are plotted in Ca-Mg-Fe diagrams. Opx and Cpx show chemical zoning from core to rim as shown by arrows.

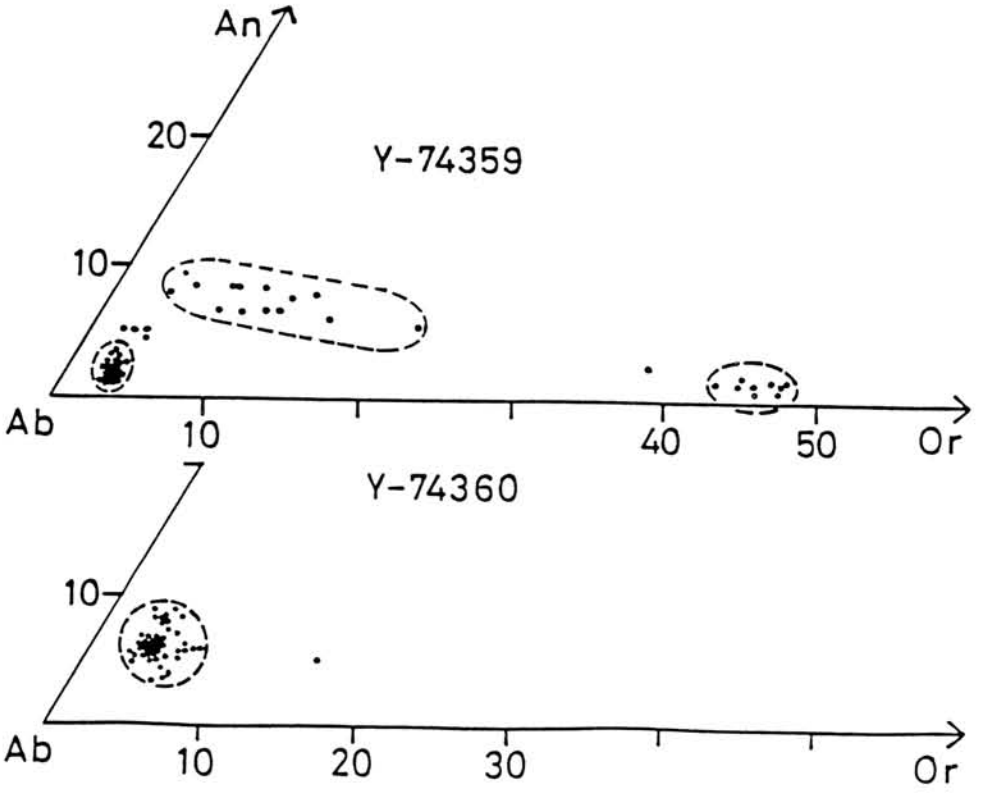

Fig. 2. Feldspars in Y-74359 and Y-74360 are plotted in anorthite(An)-albite(Ab)-orthoclase(Or) diagrams. Three feldspar groups occur in Y-74359.

BELGICA-7904: A NEW KIND OF CARBONACEOUS CHONDRITE FROM ANTARCTICA; MINERALOGY AND PETROGRAPHY

Kazushige Tomeoka, Mineralogical Institute, Faculty of Science, University of Tokyo, Hongo, Bunkyou-ku, Tokyo 113.

INTRODUCTION: Belgica-7904 (B-7904) is one of the unusual carbonaceous chondrites found in Antarctica. Although its general petrographic and chemical characteristics are reportedly similar to CM chondrites [1-5], an oxygen isotopic study indicates that it falls near the CI area in the three oxygen isotopic plot [6]. A previous transmission electron microscope study suggests that B-7904 has experienced thermal metamorphism [3]. Yamato-82162 and -86720 (Y-82162 and -86720) are other two carbonaceous chondrites that resemble B-7904 in many respects [7-11]. These meteorites propose new aspects of carbonaceous chondrite mineralogy and chemistry and potentially provide important information regarding the CI and CM parent bodies. We present here the results of petrographic and scanning electron microscope studies of B-7904. Mineralogical and petrographic characteristics of B-7904 are compared with those of Y-82162, Y-86720, and other CI and CM chondrites.

GENERAL PETROGRAPHY: B-7904 has a variety of olivine-rich chondrules including porphyritic, microgranular, and barred olivine chondrules ranging in size from 100 μm to 1 mm. Isolated grains of olivine (10 to 200 μm in diameter) having a large range of Fe/Mg ratios (Fa_0 to Fa_{45}) also occur. Despite the abundance of olivine, no pyroxene is present. This meteorite has a high abundance of Fe-sulfide, primarily troilite; it occurs in small grains (<10 μm) that are dispersed in the matrix. Relatively large Fe-sulfide grains in a characteristic lath-like shape are common in Y-82162 and Y-86720 [7,8], but they are not present in B-7904. Minor Fe-Ni metal occurs, commonly together with troilite. Magnetite is rare. Minor amounts of Ca-rich material, probably a carbonate, also occur.

CHONDRULES AND AGGREGATES: Their interstitial materials are replaced by a brownish, translucent material, but most olivine grains remain little altered. The replacement products contain major Si, Mg, Fe, and Al and minor Na (1.0 to 2.0 wt% Na_2O) and Cr (1 to 2 wt% Cr_2O_3); they are probably a phyllosilicate. Microprobe analyses are plotted in terms of Fe, Si+Al, and Mg as in a plot described in [12]. Most analyses fall between the serpentine and smectite solid solution lines; thus, they may be a submicron intergrowth of these two phyllosilicates. Chondrules and aggregates in Y-86720 contain two compositionally different replacement products, high-Al and low-Al phases [8]. Most replacement products in the B-7904 chondrules and aggregates are similar to the low-Al phase. Like the replacement products in Y-86720, they show consistently high analytical totals in their microprobe analyses (90.0 to 97.0 wt%).

MATRIX: Broad-beam microprobe analyses indicate that the matrix shows large variations in Fe contents (10 to 35 wt% FeO), and in average, Fe is considerably depleted relative to other CM chondrites. S is also depleted and appears to have weak correlations with Fe. Ni does not show obvious correlations with S, suggesting that Ni occurs as neither sulfides nor tochilinite. The matrix Ni may reside in submicron particles of an Fe-Ni-rich phase (unidentified) that occur in the Y-86720 matrix [8]. The analytical totals of the microprobe analyses are high (85 to 95 wt%) relative to those of ordinary

CM chondrite matrices, being consistent with that this meteorite has a low H_2O content (2.6 wt%) [13].

DISCUSSION AND CONCLUSIONS: Our mineralogical and petrographic studies support the idea that B-7904 is a CM chondrite. In CM chondrites, chondrules and aggregates are altered to various degrees by phyllosilicates [14,15]. Ikeda [14] found that in CM chondrules, mesostasis glass, pyroxene, and olivine were altered in this order with advancing alteration. Based on this criterion, he divided different degrees of alteration into four stages I to IV in order of increasing alteration. In the B-7904 chondrules and aggregates, mesostasis glass and pyroxene were replaced by the phyllosilicate, but olivine remains little altered. On the other hand, the Y-86720 chondrules and aggregates were almost completely replaced by the phyllosilicate [8]. In Ikeda's criterion, aqueous alteration of B-7904 advanced to stage III and that of Y-86720 advanced to stage IV.

Despite the petrographic similarity between B-7904 and ordinary CM chondrites, the alteration products are different. Those in ordinary CM chondrites are predominantly Mg-Fe serpentines [15], whereas those in B-7904 appear to be a mixture of serpentine and smecite and resemble the phyllosilicates in CI chondrites [7,12]. The difference in the phyllosilicate mineralogy suggests that B-7904 and oridinary CM chondrites experienced aqueous alteration in distinct physical-chemical conditions.

Akai [3] found that the matrix in B-7904 contains abundant olivine grains and concluded that they were formed by thermal transformation of the phyllosilicates. Our results confirm his conclusion. Tomeoka et al. [7,8] found similar evidence from the Y-82162 and -86720 matrices. Trace element chemistry also supports the view that they were thermally metamorphosed [5]. The relatively high analytical totals of the chondrule replacement products and the matrix in B-7904 are probably explained by partial alteration of phyllosilicates to olivine. The small grains of troilite dispersed in the matrix presumably resulted from thermal transformation of a thermally labile phase such as tochilinite or S-bearing ferrihydrite, thus resulting in the depletion of Fe and S in the matrix.

B-7904 contains much troilite and minor Fe-Ni metal and little magnetite and pentlandite. The opaque mineral assemblage is similar to that in Y-86720 [8] but differs from those in ordinary CM chondrites. The presence of Fe-Ni metal and the sparsity of magnetite and Ni-rich sulfides suggest that the thermal metamorphism occurred in a relatively reduced condition [8]. If this interpretation is correct, the environments from which B-7904 and Y-86720 were derived differ from those for ordinary CM chondrites in terms of redox condition, because most oridinary CM chondrites were oxidized.

We conclude that B-7904 and Y-86720 are genetically related to each other. They were probably derived from similar precursors and experienced different degrees of aqueous alteration in a common environment. These meteorites and ordinary CM chondrites presumably experienced distinct aqueous alteration conditions and thermal histories, suggesting that they came from different parent bodies.

A NEW CARBONACEOUS CHONDRITE CLASSIFICATION: Since it has been recognized that Y-82162, Y86720, and B-7904 have distinct mineralogical, chemical, and oxygen isotopic characteristics from those of ordinary CI and CM chondrites, there seems to be considerable confusion about a classification of these chondrites. We now know that there are two separate sets of CI and CM (or C1 and C2)

chondrites in the oxygen isotopic plot [11], which may reflect different precursors (or presumably different parent bodies). We propose that the carbonaceous chondrites should be first divided into the separate groups based on oxygen isotopic characteristics. Previous designations CI and CM can be redefined as oxygen isotopic groups. Then, each oxygen isotopic group can be subdivided based on petrographic, mineralogical, and chemical characteristics in a conventional manner, e.g., CI1, CI2, CM1, and CM2. According to such a scheme, B-7904 and Y-86720 are classified as CI2 chondrites, and Y-82162 is classified as a CI1 chondrite. We now recognize that there are two kinds of variations, i.e., aqueous alteration and thermal metamorphism, in the CI and CM chondrites. Thus, we may need further subdivisions to indicate the degrees of such secondary effects.

REFERENCES:

[1] Kojima, H., Ikeda, Y. and Yanai, K. (1984) Mem. Natl Inst. Polar Res., Spec. Issue, 35, 184-199.
[2] Skirius, C., Steele, I.M. and Smith, J.V. (1986) Mem. Natl Inst. Polar Res., Spec. Issue, 41, 243-258.
[3] Akai, J. (1988) Geochim. Cosmochim. Acta 52, 1593-1599.
[4] Kallemeyn, G.W. (1988) 13th Symp. Antarctic Meteorites (Abstr.), 132-134.
[5] Paul, R.L. and Lipschutz, M.E. (1989) Lunar Planet. Sci. XX (Abstr.), 830-831.
[6] Mayeda, T.K., Clayton, R.N. and Yanai, K. (1987) Mem. Natl Inst. Polar Res., Spec. Issue, 46, 144-150.
[7] Tomeoka, K., Kojima, H. and Yanai, K. (1988) 13th Symp. Antarctic Meteorites (Abstr.), 126-127; ---- (1989) Proc. NIPR Symp. Antarctic Meteorites, 2 (in press).
[8] Tomeoka, K., Kojima, H. and Yanai, K. (1988) 13th Symp. Antarctic Meteorites (Abstr.), 130-131; ---- (1989) Proc. NIPR Symp. Antarctic Meteorites 2 (in press).
[9] Watanabe, S., Tsuchiyama, A. and Kitamura, M. (1988) 13th Symp. Antarctic Meteorites (Abstr.), 128-129.
[10] Zolensky, M.E. (1989) Lunar Planet. Sci. XX (Abstr.), 1253-1254.
[11] Clayton, R.N. and Mayeda, T.K. (1989) Lunar Planet. Sci. (Abstr.), 830-831.
[12] Tomeoka, K. and Buseck, P.R. (1988) Geochim. Cosmochim. Acta 52, 1627-1640.
[13] Haramura, H., Kushiro, I. and Yanai, K. (1983) Mem. Natl Inst. Polar Res., Spec. Issue, 30, 109-121.
[14] Ikeda, Y. (1983) Mem. Natl Inst. Polar Res., Spec. Issue, 30, 93-108.
[15] Tomeoka, K., McSween, H.Y. Jr. and Buseck, P.R. (1989) Proc. NIPR Symp. Antarctic Meteorites (in press).

COMPOSITIONAL HETEROGENEITY OF ALTERATION PRODUCTS IN B-7904 CHONDRITE

S. MATSUNAMI, H. NISHIMURA, AND H. TAKESHI: NATURO UNIVERSITY OF EDUCATION, NARUTO, TOKUSHIMA 772, JAPAN.

Phyllosilicates are the most abundant and ubiquitous minerals in the alteration products of chondrules, inclusions and matrix materials in CM chondrites. Especially, formation of PCP and groundmass phyllosilicates in several CM chondrites seems to be records of aqueous alteration processes in the early solar system (McSween, 1979; Ikeda, 1983; Kojima et al., 1984; Tomeoka and Buseck, 1985). They may give clues to understanding of exact formation processes of alteration products.

As already suggested by many investigators, Ca appears to be easily transported from primary Ca-rich materials to Ca-rich alteration product at earlier stage of aqueous alteration (Kojima et al., 1984). The formation of Ca-carbonate observed in several carbonaceous chondrites may be the results of deposition of Ca from aqueous solution. However, detailed behaviour of Ca during aqueous alteration of CM chondrites is poorly known. Detailed study of mode of occurrence of Ca-bearing alteration products may offer clues to clarifying redistribution of Ca during extensive alteration. In this paper, especially, heterogeneous distribution of Ca in alteration products in B-7904 is petrographically described and discussed.

Among characteristics of composition of alteration products, the CaO content appears to be remarkably variable. It is revealed that alteration products from chondrules with opaque rims and inclusions in B-7904 may contain a significant amount of CaO as much as 28 wt%. Using compositional heterogeneities of groundmass phyllosilicates and fine-grained opaque rims, five distinct occurrences of Ca-bearing alteration products are described: type I, type II, type III, type IV, and type V. Type I is characterized by relatively homogeneous distribution of Ca in groundmass phyllosilicates and fine-grained rims. The CaO contents are less than 0.42 wt% (0.05-0.25 wt% CaO in groundmass phyllosilicates; 0.13-0.42 wt% in fine-grained opaque rims). Type II is characterized by homogeneous distribution of Ca in groundmass phyllosilicates and heterogeneity of CaO in fine-grained opauqe rims (0.03-0.49 wt% CaO in groundmass phyllosilicates; 0.16-14.9 wt% CaO in opaque rims). In some chondrules, chlorite is observed as a groundmass phyllosilicate. Ca-rich parts in fine-grained rims are distributed as tiny Ca-rich spots or along micro-cracks. Type III is characterized by relatively homogeneous opaque rims and significant heterogeneity of alteration products in groundmass (0.23-0.46 wt% CaO in rims; up to 20 wt% CaO in altered groundmass). Type IV is Ca,P-rich fine-grained matrix in olivine aggregate. This occurrence is characterized by higher contents of CaO and P_2O_5 (1.87-28.0 wt% CaO; 1.69-28.7 wt% P_2O_5). The CaO content shows a positive correlation with the P_2O_5 content. Ca-phosphate is also observed. Type V is characterized by Ca-rich, Al-rich or Ti-rich spots with the surrounding Ca-rich matrix phyllosilicates (50-56 wt% Al_2O_3: <4.5 wt% TiO_2: <28.2 wt% CaO in several spots; <11.7 wt% CaO in the surrounding matrix). These spots may be alteration products of Ca,Al-rich inclusions.

From these occurrences (especially, types I, II, and III), we can infer redistribution of Ca during alteration of CM chondrites. First, primary Ca-rich phases such as glass or anorthite are converted into SiO_2-poor,FeO-rich,Ca,Al-rich alteration products due to reaction with aqueous solution. Next, the alteration products are gradually converted into chlorite. During this stage, Ca is transported as ions in aqueous solution through micro-cracks from groundmass of chondrules to fine-grained opaque rims finally to be uniformly dispersed in matrix. Some fine-grained rims preserve this stage. The presence of types IV and V suggests that some domains of B-7904 matrix may reflect primary heterogeneities of Ca distribution such as those observed in CAIs and matrix materials with Ca-phosphate.

Mineralogical evidence of heating events in carbonaceous chondrites, Y-82162 and Y-86720

Akai, J.
Dept. Geol. & Min. Fac. Sci. Niigata Univ. Ikarashi, Niigata, 950-21

Carbonaceous Chondrites (CC) have dark fine-grained matrix which consist mainly of phyllosilicates although phyllosilicate types varies with CC types. However, different type of CC was first found in Antarctic CC, Y-793321 and B-7904. Phyllosilicates are not found and evidence of heating has been observed on these CC (Akai, 1986). Y-793321 and B-7904 (CM2) might have experienced heating events at the latest stage in its process before atomospheric entry to the Earth.

In the research consortium of Y-82162, Y-86720, Tomeoka et al. (1988) suggested that they have also been thermally metamorphosed. The author intends to describe these unusual CC especially with mineralogical evidence of heating event in phyllosilicates.

Results of HRAEM examination of matrix

Olivine grains distribute widely and the interstices are often filled with Fe-rich almost amorphous materials. Other mineral species found by EM are as follows; magnetite, Fe sulphides, dolomite, kamacite and taenite. On the other hand, in Y-86720; Fe sulphides (mostly troilite), magnetite, kamacite and taenite. Fig. 1 shows evidence of phyllosilicates transformation to olivine (Y-82162). The shapes are apparently pseudomorph of phyllosilicate. ED pattern of this mineral is suggesting intermediate structure in transformation from serpentine to olivine and is the direct evidence of this trasfomation probably by heating. It resemble to that of Y-793321 (Akai, 1988). However such mineral grains do not distribute so widely but rarely found. Most phyllosilicates are almost utterly changed to olivine.

Y-86720 shows similar textures and also similar ED patterns suggesting the intermediate structure of phyllosilicate transformation to olivine (Fig. 2). The degree of heating may be the same order. Thus, two more examples of CC samples which experienced thermal event are added to Y-793321 and B-7904, although the estimated temperature on Y-82162 and Y-86720 may be different from those on Y-793321 (500～ 600°C) and B-7904 (higher temperature).

Estimation of temperature

To assume transformation temperature sacale of phyllosilicates preliminary heating experiments were carried out on Murchison, a typicall CM chondrite. The Murchison samples were heated at 300, 400, 500, 600, 700, 800, 900, 1000°C, in air for an hour. The 7 A platy serpentine-type phyllosilicates were examined. They were easily identified in shape, AEM data and ED patterns. Based on

rough assumptions as first approximation, phyllosilicates found in Y-82162 and Y-86720 resemble those heated at above 700～800℃. Among all the specimens containing Y-793321 and B-7904, which might have experienced heating events the author tried to arrange them in the order of temperatures, taking account transformation degrees of phylosilicates into consideration. The rough order is as follows ;

B—7904 > Y—82162, Y86720 > Y—793321
～ 800℃ ～ 500°～600°C

However more precise scale must be established and the study is in progress.

Structure of the 'transitional phase' is contained in mineralogical problems. From HREM observations, it is suggested that modified donor and acceptor region model in phase tansformation of serpentine type phyllosilicate may apply. In this model, the reaction may be as follows ;

serpentine
↘ intermediate phase
characterized by 9-13 Å diff. (→→enstatite?)
↘ olivine

REFERENCES

J. Akai (1988) Geoch. Cosmo. Acta 52, 1593.

K. Tomeoka, H. Kojima and K. Yanai (1988) Abs. 13rd Symp. Ant. Meteorite. 126 and 130.

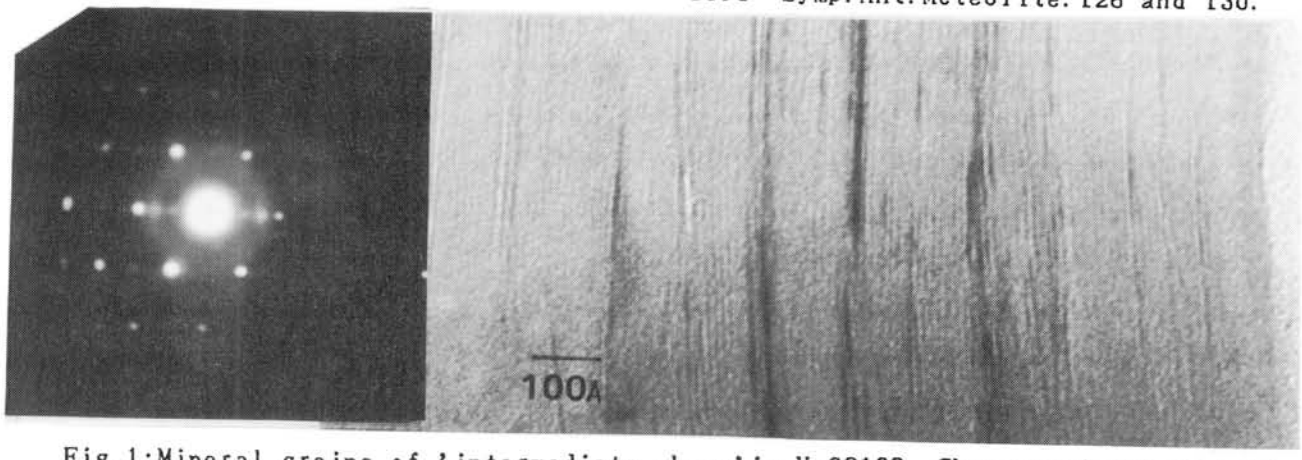

Fig. 1: Mineral grains of 'intermediate phase' in Y-82162. Characteristic ED pattern suggests intermediate structure in transformation from serpentin to olivine.

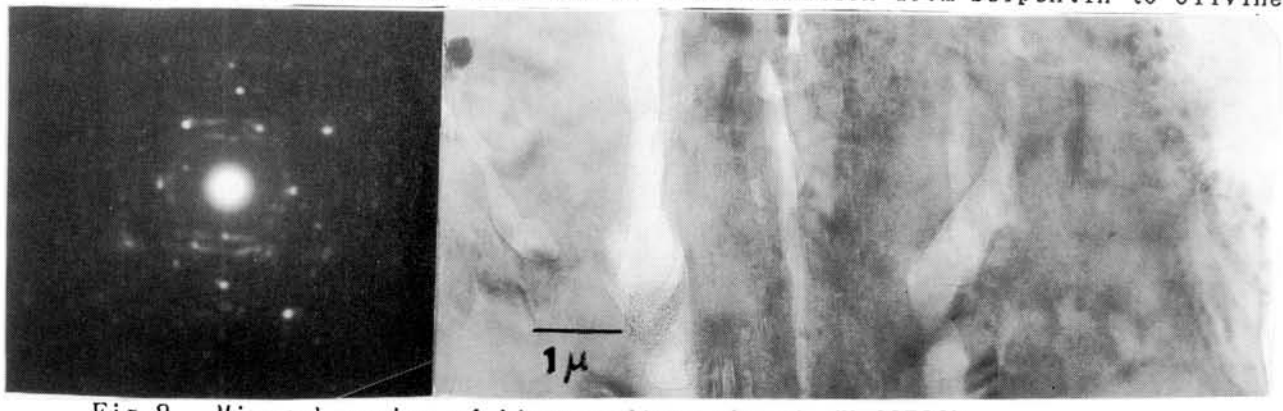

Fig. 2 Mineral grains of 'intermediate phase' (Y-86720)

MINERALOGY AND PETROLOGY OF YAMATO-86720 AND BELGICA-7904

Michael Zolensky[1], Ruth Barrett[2] and Martin Prinz[3], [1]SN2, NASA/Johnson Space Center, Houston, TX 77058; [2]Lockheed Engineering and Science Co., Houston, TX 77058; [3]Dept. Mineral Sciences, American Museum of Natural History, New York, NY 10024.

INTRODUCTION: Yamato-86720 (Y-86720) and Belgica-7904 (B-7904) are CI chondrites [1] which are mineralogically and petrologically unlike any previously described [2], but with similarities to Y-82162 [3-5]. We report here our first results of a study of two thin sections each of Y-86720 and B-7904, by petrographic and electron beam techniques. We can then place these meteorites within their proper petrologic context.

PETROGRAPHY: Y-86720 contains scattered relict chondrules (contain essentially no anhydrous silicates) (<1.5 mm) and lithic clasts (< 1 mm) with dark fine-grained rims, pyrrhotite, clasts of fine grained Ca-carbonate and pyrrhotite, and fine-grained magnetite set within a fine-grained opaque matrix. B-7904 contains type I and II chondrules (<3 mm) and lithic clasts containing anhydrous as well as hydrous silicates (these chondrules will be described in detail in a later report). Most of the chondrules are surrounded by fine-grained opaque rims. The matrix of B-7904 contains abundant fine- to coarse-grained sulfides, olivine, phyllosilicates and magnetite.

MINERALOGY OF Y-86720: Pyrrhotite is found as abundant laths and euhedral pseudohexagonal plates measuring up to ~400 um in greatest dimension. The composition is near stoichiometric FeS (actually $Fe_{.99}S$). Ca carbonate occurs as fine-grained and colloform masses intergrown with fine-grained pyrrhotite. Large individual carbonate crystals were not found. Fairly pure magnetite occurs as fine-grained scattered crystals and aggregates. As noted previously [2], the morphology of magnetite in Y-86720 resembles that found in CM2, not CI1, meteorites. The dominant minerals within the two meteorites are phyllosilicates. They are present as discrete, rounded to irregularly shaped, objects (<1.5 mm) comprising the bulk of the relict chondrules, as smaller (<100 um) rounded grains set within relict chondrules and matrix, and as much finer-grained crystals within matrix. Compositionally, we tentatively conclude that they are mainly antigorite and clinochlore with average compositions:
Antigorite $(Mg_{1.88}Fe_{.74}Al_{.22}Cr_{.08}Ni_{.01})(Si_{2.05}Al_{.02})O_5(OH)_4$
Clinochlore $(Mg_{3.62}Fe_{1.39}Cr_{.03})Al_{.81}(Si_{3.48}Al_{.52})O_{10}(OH)_6$
(water by difference). These (and other) phyllosilicate mineralogical determinations will be verified by HRTEM analyses now in progress. All relict chondrules and most lithic fragments are composed predominantly of phyllosilicates. The compositions of these phases are difficult to determine due to apparent dehydration and intergrowth at a fine scale with matrix phases, apatite, and sulfides.

MINERALOGY OF B-7904: In contrast to Y-86720 (and Y-82162 [2-5]) sulfides (principally pyrrhotite) occur in both matrix and

chondrules as fine-grained masses and larger rounded grains measuring up to 100 um across. Kamacite (<7.5 wt% Ni) is present as scattered grains within olivines. Pyrrhotite has an average composition of $Fe_{.98}S$, and pentlandite is $(Fe_{6.24}Ni_{2.48})S_8$. Most pentlandite is intimately intergrown with pyrrhotite. Olivine varies from Fo100-42 and orthopyroxene from En91-57. Chromite is an important accessory phase in some chondrules and one grain of zircon (2 um) was found in a type I chondrule. Chondrules also contain a very fine-grained mixture of apatite and Ca-carbonate. Phyllosilicates have the same morphological characteristics as in Y-86720, and also fill spaces between olivine and pyroxene crystals in the chondrules. The dominant phyllosilicates are (tentatively) antigorite, ferroan antigorite, and clinochlore, with the average compositions: Ferroan Antigorite $(Fe_{1.63}Mg_{1.08}Al_{.19}Ti_{.04}Cr_{.06}Ni_{.04})(Si_{1.73}Al_{.27})O_5(OH)_4$ Antigorite $(Mg_{1.52}Fe_{.91}Al_{.28}Cr_{.17}Ni_{.02})Si_{2.08}O_5(OH)_4$ Clinochlore $(Mg_{2.84}Fe_{1.54}Cr_{.01}Ti_{.01})Al_{1.24}(Si_{3.51}Al_{.49})O_{10}(OH)_8$ Thus, the phyllosilicates in B-7904 are significantly more iron rich than those in Y-86720. The phyllosilicates within both Y-86720 and B-7904 are similar to those encountered in CM2 chondrites, although those in the former meteorites are far more Al-rich and considerably dehydrated [2]. By comparison, Y-82162 contains a phyllosilicate assemblage dominated by saponite and antigorite, which is more characteristic of CI1 chondrites [5&6].

MATRIX AND FINE-GRAINED RIMS: We performed 48 and 40 analyses of the bulk composition of the matrix and 70 and 42 analyses of fine-grained rims in Y-86720 and B-7904, respectively. The results are shown in Figs. 1 and 2. Fig. 1 compares the average matrix and rim analyses for 12 CI, CM and CV chondrites. Both the matrix and rims for Y-86720 are compositionally similar to CI chondrite matrix, but they are more Fe deficient. This latter observation could be explained by the abundance of relatively coarse-grained pyrrhotite in Y-86720 as compared to the other chondrites. This interpretation is supported by Fig. 2, where the matrix of Y-86720 is also shown to be the most deficient in S (relative to Si) of any of the characterized carbonaceous chondrites. It is of note to observe that when plotted onto a S/Si vs. Fe/Si diagram (Fig. 2), the matrix compositions of the different carbonaceous chondrite groups are clearly discriminated. Data for this figure are adapted from our work [5,7] and that of McSween and coworkers [8,9]. In contrast, Fig. 1 shows that the matrix of B-7904 is compositionally similar to CM2 chondrites. Remarkably, the average composition of the fine-grained rims of B-7904 are far more Fe-rich than the matrix. The compositional difference between matrix and rims for B-7904 is the greatest observed for any carbonaceous chondrite analyzed to date, spanning the entire compositional range exhibited by C2 chondrites. This observation is explained by the abundance of fine-grained sulfides within dark rims in B-7904.

CLASSIFICATION AND CONTEXT: Y-82162, Y-86720, and B-7904 are compositionally CI chondrites. Y-82162 contains no chondrules. In terms of mineralogy and petrology Y-86720 is intermediate between known C1 and C2 chondrites. It contains no true

chondrules, only large aggregates of (dominantly) phyllosilicates which appear to be relict chondrules. Many of the smaller chondrules in B-7904 appear to be like those in Y-86720, containing phyllosilicates, sulfides and magnetite, but the larger olivine and pyroxene-bearing type I and II true chondrules in B-7904 are mainly aggregational. In terms of mineralogy and petrology (hydrous/anhydrous silicates, presence of chondrules and metal, and phyllosilicate species), CI chondrites could be viewed as a petrologic series: Orgueil (or any other CI1), Y-82162, Y-86720, B-7904 (CI2). This CI series may be due to progressive heating (from CI1 to CI2 [10]), progressive aqueous alteration (from CI2 to CI1 [5]), a combination of the two processes [2], or they may have formed sequentially in an evolutionary series without one being derived from the other.

REFERENCES: [1] Clayton and Mayeda (1989) Lunar Planet. Sci. XX, 169-170; [2] Tomeoka et al. (1988) 13th Symp. Antarctic Meteorites, 130-131; [3] Tomeoka et al. (1988) 13th Symp. Antarctic Meteorites, 126-127; [4] Watanabe et al. (1988) 13th Symp. Antarctic Meteorites, 128-129; [5] Zolensky et al. (1989) Lunar Planet. Sci. XX, 1253-1254; [6] Tomeoka and Buseck (1988) Geochim. Cosmochim. Acta 52, 1627-1640, [7] Zolensky et al. (1989) Lunar Planet. Sci. XX, 1249-1250; [8] McSween and Richardson (1977) Geochim. Cosmochim. Acta 41, 1145-1161; [9] McSween (1987) Geochim. Cosmochim. Acta 51, 2469-2477; [10] Paul and Lipschutz (in press) Zeits. Naturforschung.

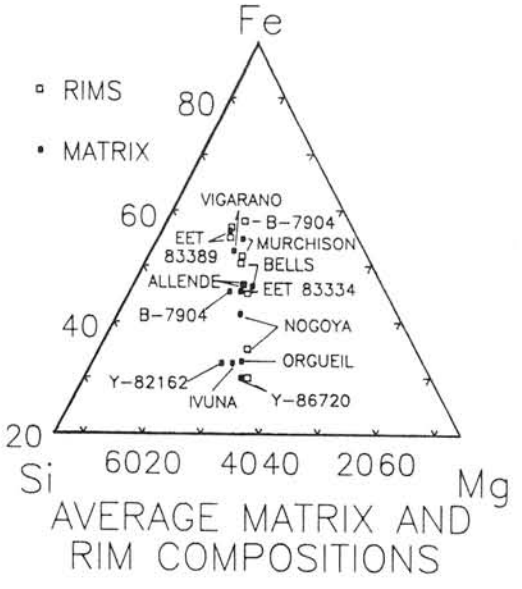

Figure 1

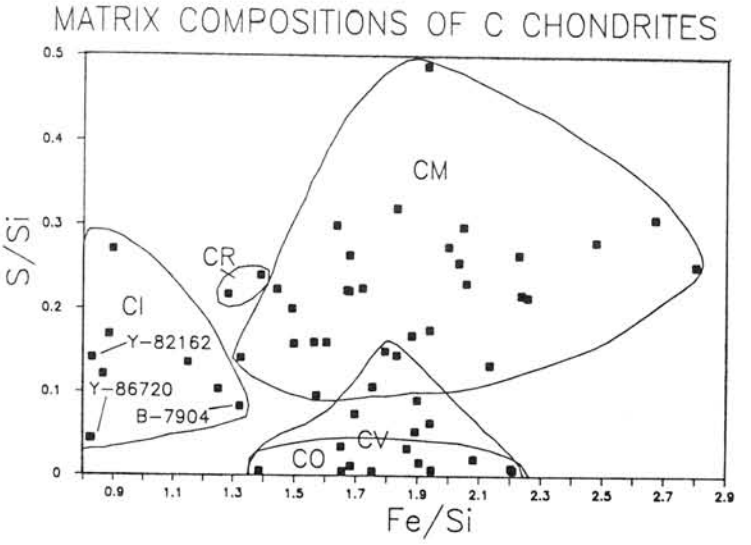

Figure 2

Chemical characteristics and their inference to classification of Yamato-82162 and -86720 meteorites.

Koshi YAMAMOTO and Noboru NAKAMURA

Faculty of Science, Kobe University, Nada, Kobe 657.

Yamato-82162 (Y82162) and -86720 (Y86720) have been widely studied in the research consortium. Oxygen isotope data(1,2), petrologic studies(3,4,5,6) and chemical features obtained by NAA(7) showed that Y82162 belongs to CI chondrites and Y86720 to CI or CM chondrites group. In this study, in order to study more detailed chemical characteristics of lithophile elements including REE and to classify these two meteorites chemically, we made repeated analyses of the meteorites using isotope dilution mass spectrometry(IDMS). Measured elements are REE, Mg, Ca, K, Rb, Sr, Ca and Fe. REE were analyzed by conventional IDMS through column chemistry and the others by the direct loading IDMS(8). Analytical errors for REE, Ca, Mg and Fe are less than 2%, and those for the other elements less than 5%.

Y82162 Analytical results relative to Orgueil CI chondrite(9,10) are shown in Fig.1. This chondrite has elemental abundances of about 0.9-1.5xCI and seems very heterogeneous in several- milligram sizes. The REE abundance patterns, except for that of 5.87 mg fraction, are nearly flat. Whereas, they have parallel and irregular abundance patterns for alkalis, alkaline earths and Fe. The 5.87 mg fraction has a characteristic elemental abundance pattern. That is, the fraction is more depleted in Mg and enriched in Ca and Sr than the other fractions. Also noted is a clear fractionation between LREE and HREE. Since the meteorite is reported to have been subjected to thermal metamorphism and aqueous alteration(5), it is considered that this fractionation was due to re-distribution of elements during the thermal event or aqueous alteration in the parent body. The partition coefficients of minerals and solubilities in aqueous condition for REE, however, can not explain the LREE/HREE fractionation seen in the 5.87mg fraction. Similar fractionations are observed in some kinds of CAI's(11). The enrichment of Ca and fractionation of HREE from LREE are consistent with implication that this chondrite contains high temperature components. The possibility of existence of high temperature component in CI chondrite has already been suggested by NAKAMURA(9). The lack of Yb anomaly in the 5.87 mg fraction, however, is not well explained.

Y86720 As shown in Fig.2, this chondrite has elemental abundances of about 1.4-1.9xCI, except for K and Rb with 0.7-0.9xCI. The depletion of alkalis is well known in the carbonaceous chondrite other than CI. The REE abundance pattern of each fraction shows weak fractionation among REE (slight enrichment of heavier REE) and clear Eu positive anomaly. The degree of Eu anomaly seems to correlate with the abundance level

of REE. That is, the higher becomes the REE abundance, the smaller becomes the Eu anomaly. This fact may suggest that Y86720 contains two components in respect of REE. One component is of low REE abundance with large Eu anomaly, another is of high REE abundance with no or small Eu anomaly.

Classification The average and range of elemental abundances for CI, CM and CO group chondrites relative to Orgueil CI chondrite are shown in Fig.3 together with the data of weighted mean for Y82162 and Y86720. The data points of Y82162 are distributed in the intermediate of CI and CM groups, excepting that the point of Fe is in CV group and those of Mg, Yb and Lu are in CM. On the other hand, those of Y86720 are in the intermediate of CM and CO groups, excepting that those of Fe, Mg, Ca and Eu are in CO and that of K is in CM. To compare abundances in silicate portion, Orgueil normalized abundances are further normalized to Si=1.0(Fig.4). In this Figure, data of Y82162 are plotted along the CI line except for lower abundances of some elements and far below that of CM group. It is probable that this chondrite is classified as a CI chondrite. Whereas the data of Y86720 are again plotted in the intermediate of CM and CO, as in the case of Fig.3. Abundances of LREE and K show good affinity with those of CM chondrites and HREE and Ca do with CO chondrites. Therefore, it is possible that this chondrite is not strictly classified into a previously known group.

(1) Mayeda,T.K., Clayton,R.N. and Yanai,K., Mem. Natl Inst. Polar Res., Spec. Issue, 46, 144-150(1987) (2) Clayton,R.N. and Mayeda,T.K., Lunar Planet. Sci., XX, 169(1989) (3) Kojima,H. and Yanai,K., Abstr. 12th Symp. Antarctic Metrorites, p.15(1988) (4) Watanabe,S., Tsuchiyama,A. and Kitamura,M., Abstr. 12th Symp. Antarctic Meteorites, 128-129(1988) (5) Tomeoka,K., Kojima,H. and Yanai,K. Mem. Natl Inst. Polar Res., Spec. Issue,(in press) (6) Tomeoka,K., Kojima,H. and Yanai,K. Mem. Natl Inst. Polar Res., Spec. Issue,(in press) (7) Kallemeyn,G.W., Abstr. 12th Symp. Antarctic Meteorites, 132-134(1988) (8) Nakamura,N., Yamamoto,K., Noda,S., Nishikawa,Y, Komi,H., Nagamoto,H, Nakayama,T. and Misawa,K. Anal. Chem., 61, 755-762(1989) (9) Anders,E. and Grevesse,N., Geochim. Cosmochim. Acta, 53, 197-214(1989) (10) Nakamura,N. Geochim. Cosmochim. Acta, 38, 755-762 (1974) (11) Palme,H., Wlotzka,F., Nagel,K. and El Goresy,A. Earth Planet. Sci. Lett., 61, 1-12(1982)

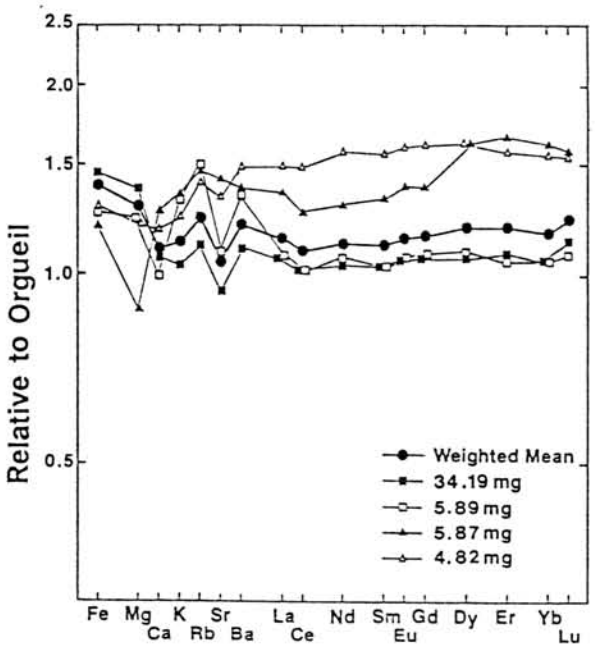

Fig. 1
Analytical data relative to Orgueil CI chondrite for Y82162.

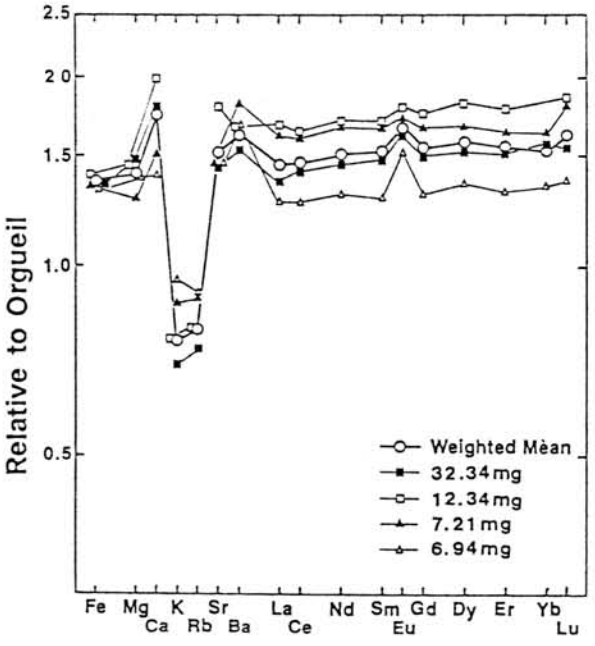

Fig. 2
Analytical data relative to Orgueil CI chondrite for Y86720.

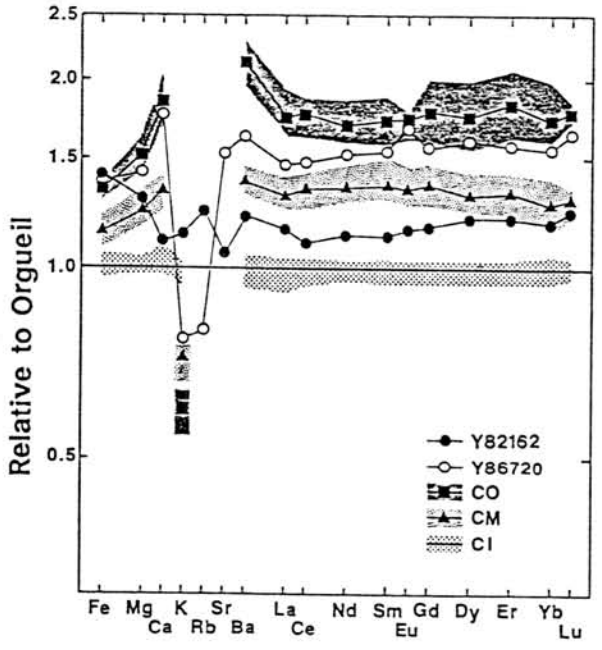

Fig. 3
Average and range of elemental abundances for CO, CM and CI group chondrites relative to Orgueil chondrite. Also plotted are the data of weighted mean of Y82162 and Y86720.

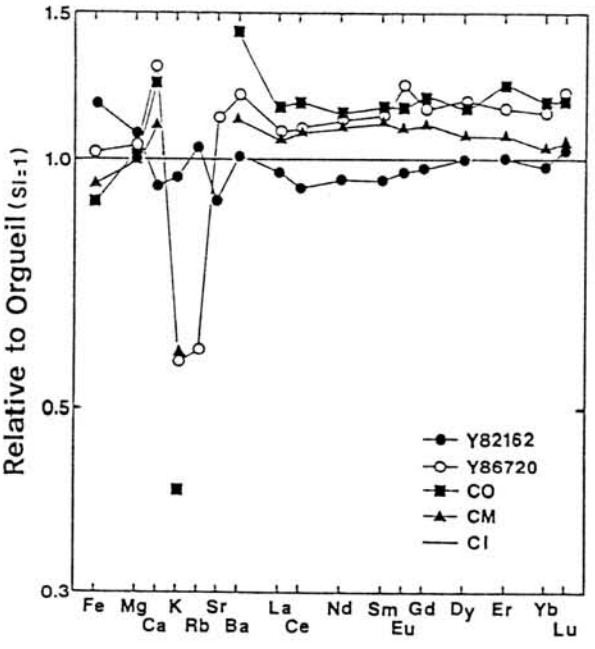

Fig. 4
Plots of mean elemental abundances for Y82162, Y86720, CO, CM and CI chondrites relative to Orgueil (Si=1). Contents of Si of Y82162 and Y86720 are quoted from TOMEOKA et al.(4 and 5), respectively.

ORIGIN OF PCP

Kojima H. and Yanai K.
National Institute of Polar Research
9-10, Kaga 1-chome, Itabashi-ku, Tokyo 173

PCP(poorly or partly characterized phase) is included only in CM carbonaceous chondrite, and is considered as secondary material which was produced by aqueous alteration in a parent body(1, 2). On the other hand, chondrules, inclusions and their fragments of Yamato-74662 and Yamato-791198 have well developed rims. These rims consist mainly of fine phyllosilicates, pyrrhotites and Fe-Ni metals. No PCP is included in rims. PCP is mainly situated out side of rims (Fig 1). This textural feature indicate that PCP situated out side of rims are not altered materials derived from metals and sulphides in chondrules, inclusions and rims, but PCP accretes to rims after rim formation around chondrules, inclusions and their fragments prior to parent body formation.

The chemical compositions of PCP in the CM chondrites which were altered to various degrees are plotted on the two different lines on the Si-Mg-Fe diagram (Fig 2). One is a tie-line between FESON and cronstedtite. The other is a line between Mg-serpentine and 75% cronstedtite on FESON-cronstedtite tie-line. PCP on former line are observed in relatively weakly altered CM chondrites and PCP on latter line are in heavily altered ones. These facts lead following conclusions.

1. FESON reacted with Si-rich material to form cronstedtite prior to parent formation. However this reaction did not proceed completely, FESON was preserved in weakly altered CM chondrites. It is not clean that the FESON is a low-temperature condensation product or alteration product of precursor materials in the nebula.
2. Cronstedtite reacted with SiO_2 and MgO that released from low-Ca pyroxene and olivine to form Fe-serpentine in the stage of aqueous alteration on the parent body.

1) Bunch and Chang (1980) Geochim. Cosmochim. Acta 44, 1543-1577.
2) Tomeoka and Buseck (1985) Geochim. Cosmochim. Acta 49, 2149-2163.

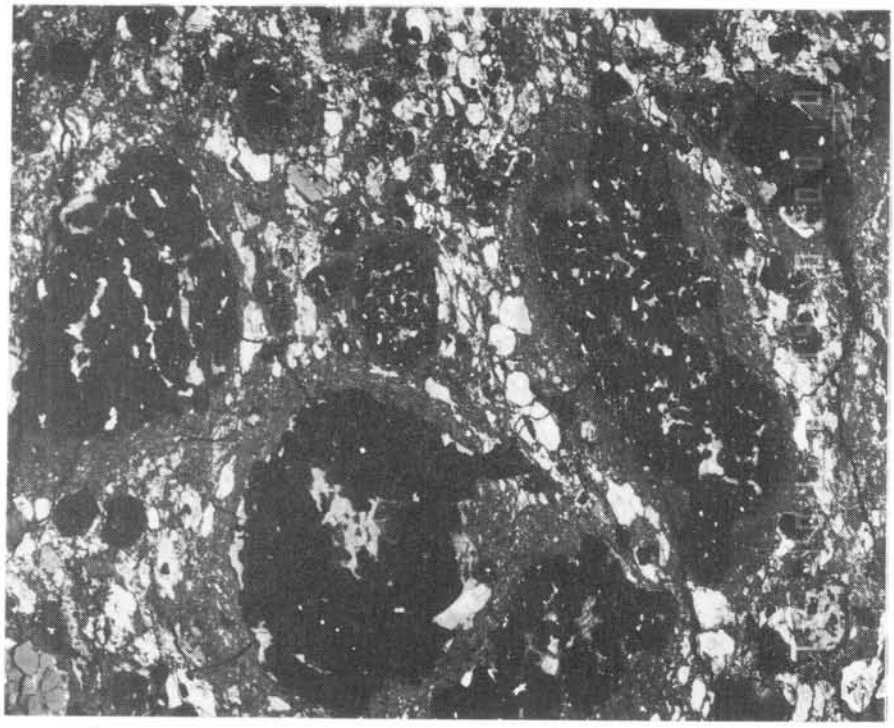

Fig 1. BEI of Y-74662 chondrule and inclusion have well developed rims and PCP is situated out side of rim.

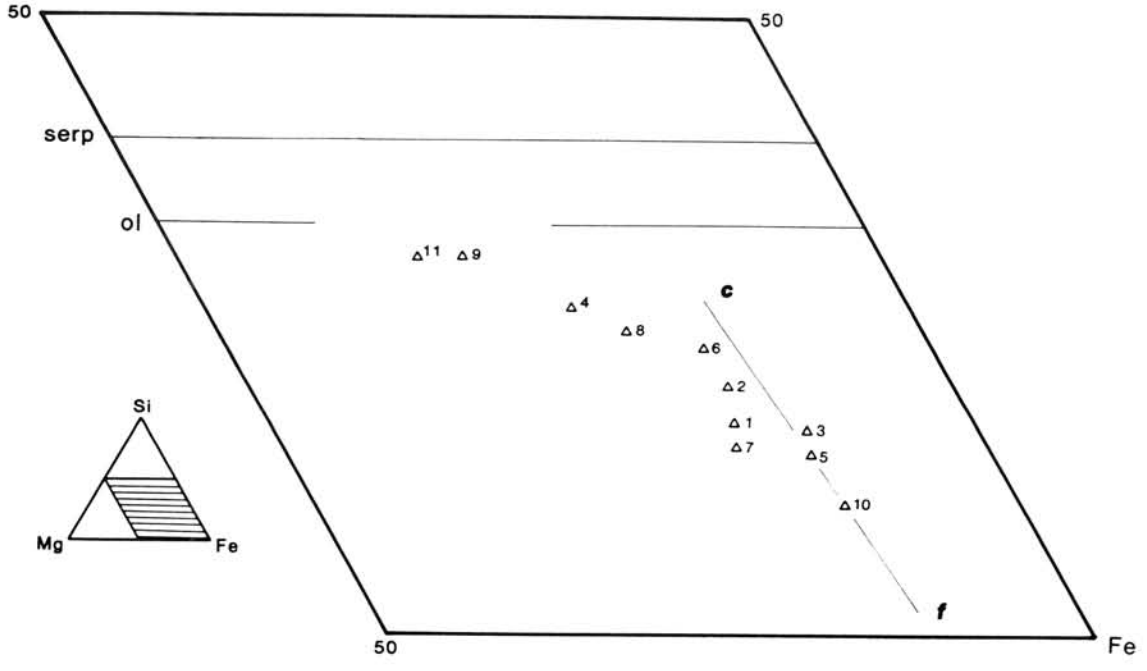

Fig 2. PCP in each carbonaceous chondrite from Antarctica is plotted on Si-Mg-Fe diagram. f: FESON c: cronstedtite

CONSORTIUM REPORT ON CARBONACEOUS CHONDRITES FROM QUEEN MAUD LAND, ANTARCTICA: GLIMPSES OF NEW PARENTS

R. L. Paul and M. E. Lipschutz

Dept. of Chemistry, Purdue University, W. Lafayette, IN 47907.

Among non-Antarctic samples, C1 and C2 chondrites each have well-defined, precise patterns for labile trace elements that clearly distinguish between them (cf. [1,2] and references in these). (We specifically use elemental "volatility" in referring to equilibrium processes during nebular condensation and accretion, and "mobility" to refer to non-equilibrium trace element loss during solid-state metamorphism in a parent body. "Lability" is used when either process could have occurred.) More refractory elements also distinguish between these and other carbonaceous chondrite groups and Kallemeyn and Wasson [3] proposed the terms CI and CM for C1 and C2, respectively, to emphasize that their petrologic and chemical characteristics were of primary nebular origin rather than reflecting secondary, parent-body alteration. We will use the CI-CM terminology to describe mineralogic-petrologic-refractory element - oxygen isotopic trends and the C1-C2 terminology to describe trends established from labile trace elements.

Several recent studies of 4 carbonaceous chondrites from Queen Maud Land, Antarctica suggest peculiar genetic histories [4,5,6], differing from those of analogous non-Antarctic falls. A great deal of evidence suggests that Antarctic and non-Antarctic meteorite populations - even ordinary chondrites - differ in thermal history (cf. [7] and references therein). Consortia were used to investigate these 4 carbonaceous chondrites further and the leaders, Drs. Yanai and Graham (for Yamato [Y] 82042) and Prof. Ikeda (for Belgica [B] 7904, Y-82162 and Y-86720), invited us to join these Consortia and measure Ag, Au, Bi, Cd, Co, Cs, Ga, In, Rb, Sb, Se, Te, Tl, U and Zn by radiochemical neutron activation analysis (RNAA). These trace elements cover a wide lability range and give unique information on thermal histories of meteorites. The results indicate the unique nature of these carbonaceous chondrites.

Our data confirm the earlier view [4] that Y-82042 is a unique meteorite, being CI texturally, CM isotopically in oxygen and C2 chemically. It is clear that all properties of this meteorite are primary nebular condensation/accretion features.

The other three meteorites were thermally metamorphosed in $\geq$2 parent bodies over the 600-700°C range, at relative temperatures B-7904 < Y-82162 < Y-86720. These absolute and relative metamorphic temperatures are established by comparison of labile trace element contents in the 3 Antarctic chondrites with those in Murchison samples artificially heated in the laboratory [8]. Before metamorphic heating, B-7904 and Y-86720 had C2-levels of volatile elements: Y-82162 had uniquely high volatile element contents, at or above C1-levels. To the extent that petrologic data are available for these samples, they are consistent with our conclusions. However, all 3 have CI-like oxygen isotopic compositions. Clearly, Antarctic C1,2 chondrites cannot be described by the classification scheme developed for non-Antarctic specimens.

Hence, the first 4 Antarctic C1,2 chondrites studied are uniquely different from their non-Antarctic brethren, further supporting the idea that

these populations represent different extraterrestrial parent populations [9]. Probably over the extended collecting period of the Antarctic ice sheet, it has sampled a considerable greater proportion of near-Earth asteroids than do current falls.

Similarities in the surface spectral reflectance properties of the numerous C asteroids and non-Antarctic C1 and C2 chondrites have led to the consensus view that these chondrites are "ground truth" for these asteroids [10]. Other asteroid types exist, some of which (B, F, G and T-asteroids) may have surfaces representing altered or metamorphosed C1 or C2 material [10,11]. The 48 carbonaceous chondrite falls or finds outside of Antarctica seem not to include any suitable example of such material. Data for B-7904, Y-82162 and Y-86720 indicate that these 3 samples may derive from thermally altered carbonaceous asteroids and their spectral characteristics should be compared with those of B-, F-, G- or T- asteroids. We predict that a match will be found.

REFERENCES

[1]. H. Palme, J. W. Larimer and M. E. Lipschutz, Chapter 7.5 in Meteorites and the Early Solar System (eds. J. F. Kerridge and M. S. Matthews) 436-461, Univ. of Arizona Press (1988).

[2]. M. E. Lipschutz and D. S. Woolum, Chap. 7.6 in Meteorites and the Early Solar System (eds. J. F. Kerridge and M. S. Matthews), 462-487, Univ. of Arizona Press (1988).

[3]. G. W. Kallemeyn and J. T. Wasson, Geochim. Cosmochim. Acta 45, 1217-1230 (1981).

[4]. M. M. Grady, A. L. Graham, D. J. Barber, D. Aylmer, G. Kurat, T. Ntaflos, U. Ott, H. Palme and B. Spettel, Proc. Eleventh Symp. Antarctic Meteorites, 1986 (K. Yanai, ed.) 162-178 (1987).

[5]. T. K. Mayeda, R. N. Clayton and K. Yanai, Proc. Eleventh Symp. Antarctic Meteorites, 1986 (K. Yanai, ed.) 144-150 (1987).

[6]. R. N. Clayton and T. K. Mayeda, Lunar Planet. Sci. XX, 169-170 (1989).

[7]. P. W. Kaczaral, R. T. Dodd and M. E. Lipschutz, Geochim. Cosmochim. Acta 53, 491-501 (1989).

[8]. S. D. Matza and M. E. Lipschutz, Proc. Lunar Sci. Conf. 8th, 161-176 (1977).

[9]. J. E. Dennison, D. W. Lingner and M. E. Lipschutz, Nature 319, 390-393 (1986).

[10]. M. E. Lipschutz, M. J. Gaffey and P. Pellas, in Asteroids II (eds. R. P. Binzel, T. Gehrels and M. S. Matthews) in press, Univ. of Arizona Press (1989).

[11]. D. J. Tholen, Asteroid Taxonomy from Cluster Analysis of Photometry. Ph.D. Dissertation, University of Arizona, Tucson, 150 pp. (1984).

A NEW CHONDRITE GROUPLET: ALLAN HILLS 85151 AND CARLISLE LAKES 001

Gregory W. Kallemeyn

Institute of Geophysics and Planetary Physics, University of California, Los Angeles, CA 90024, USA

The Carlisle Lakes 001 meteorite was found in 1977 in the Nullarbor Plain region of Western Australia. It was initially classified as a new type of highly oxidized ordinary chondrite (Binns and Pooley, 1979). Allan Hills 85151 was found during the 1985-86 serach for meteorites in Victoria Land, Antarctica. It was initially classified as a C4 chondrite by Mason (1987). Subsequent compositional, isotopic and petrographic studies (Rubin and Kallemeyn, 1989; Weisberg et al., 1989) showed that these meteorites are neither ordinary chondrites nor C4 chondrites. A third possible member of this grouplet is Yamato 75302 which has a very similar petrographic description (Yanai et al., 1985), but its small size (3.6 g.) has precluded compositional studies thus far.

Rubin and Kallemeyn (1989) reported chondrule size and distribution in ALH 85151 and Carlisle Lakes 001 as similar to ordinary chondrites, as well as a similar fine-grained groundmass. But this groundmass makes up a considerably larger volume of the meteorite than normally seen in ordinary chondrites. Both chondrites have similar oxygen three-isotope compositions which are different from any other chondrite group, having a very large $\delta^{17}O$ component (Weisberg et al. 1989).

Replicate chips of ALH 85151 and an homogenized powder sample of Carlisle Lakes 001 were studied by this lab by instrumental neutron activation analysis. Lithophile element (Al, Sc, REE, V, Mg, Cr, Mn, Na and K) abundances for both chondrites generally fall in the range 0.9-1.0× CI chondrites, but Ca is significantly enriched in both. The lithophile element abundance patterns for both chondrites are very similar to one another with only minor differences in rare earth elements and K, and a more significant difference in Ca. A small enrichment in Ca might be explained in the petite (13.9 g) ALH 85151 specimen by the formation of evaporites along crack surfaces during weathering processes, although such enrichment has only been noticed in a very few of the many Antarctic chondrites studied by this lab. The Carlisle Lakes 001 sample was received from Australia as a powder, along with another powdered chondrite sample from the Nullarbor region. The other chondrite sample also shows a very high Ca content, and this would seem to imply that both powdered samples were either contaminated in the environment or during processing. However, the fact that both ALH 85151 and Carlisle Lakes 001, found in widely different environments, have Ca enrichments may be too much of a coincidence, and some small enrichment may be inherent to these chondrites.

Refractory (Os, Ir, Ru) and common (Ni, Co, Fe) siderophile element abundances are also very similar to one another at about CI chondrite levels. Among volatile elements, Au abundances in both meteorites are very low (ALH 85151: 0.37× CI, Carlisle Lakes 001: 0.17× CI); Sb abundances also appear somewhat low relative to the more volatile elements Se and Zn. The unfractionated, CI-level abundances of the common siderophiles implies that they originally condensed together as metal particles. These particles must have rapidly oxidized before Au had the chance to significantly condense into solid solution with them (Rubin and Kallemeyn, 1989). A less attractive alternative would be that the Au became concentrated in a minor phase, possibly during later metamorphic processing, which was subsequently lost during weathering. Petrographic data suggest that ALH 85151 and Carlisle Lakes 001 are of petrologic type 3.6-4.0. This would seem to imply parent body metamorphic temperatures high enough to probably affect the abundance of Zn. Yet Zn abundances in both chondrites are relatively high (0.35× CI); higher than in CO (0.23× CI) and CV (0.25× CI) chondrites and much higher than in ordinary chondrites.

REFERENCES: Binns and Pooley (1979) *Meteoritics* **14**, 349-350; Mason (1987) *Ant. Met. News* **2**, No. 2, 21; Rubin and Kallemeyn (1989) *Geochim. Cosmochim. Acta*, submitted.

Chemical compositions of some primitive carbonaceous chondrites from Antarctica

Ebihara, M. and Shinonaga, T.

Dept. Chemistry, Tokyo Metropolitan Univ., Fukasawa, Setagaya-ku, Tokyo 158, Japan.

As a part of the consortium study on Antarctic meteorites with affinities to C1 chondrites, we analyzed by neutron activation analysis three primitive carbonaceous chondrites from Antarctica, Yamato- (hereafter Y-) 82162, Y-86720 and Belgica- (hereafter B-) 7904.

Oxygen isotope study (1) as well as petrographic (2, 3) and chemical(4) studies suggest that the Y-82162 meteorite is the first C1 (CI) chondrite collected in Antarctica. The remaining carbonaceous chondrites studied in this work have been reported to have some affinities to C1 chondrite more or less, but no definite conclusions for their petrographic classes have been given so far. To assess the primitiveness in chemistry for each carbonaceous meteorite, we determined some major and trace elements in replicate samples of B-7904, Y-82162 and Y-86720 by instrumental and radiochemical NAA.

Table 1 shows the preliminary results by INAA. Considering that the water content in Y-82162 is anomalously low compared with those in other C1 chondrites (2), chemical composition of Y-82162 seems to be among those of C1 chondrites. On the other hand, B-7904 shows the close affinity to C2 in chemistry. The chemical composition data for Y-86720 suggest its position between Y-82162 and B-7904. Experimental study to obtain more conclusive results are now under way.

References

(1) Meyeda T.K., Clayton, R.N. and Yanai, K. (1987) Mem. Natl. Inst. Polar Res., Spec. Issue 46, 144-150.
(2) Kojima. H. and Yanai, K. (1987) Abstr. 12th Symp. Antarct. Meteorites, 15.
(3) Tomeoka, K. (1988) Abstr. 13th Symp. Antarct. Meteorites, 126-127.
(4) Kallemeyn, G.W. (1988) Abstr. 13th Symp. Antarct. Meteorites 132-134.

Table 1. preliminary results by INAA

	error* (1σ/%)	Y-82162,87		Y-86720,88		B-7904,101	
Mg/%	1.2-1.3	10.7	10.7	13.5	12.5	15.1	
Al	0.6-1.2	0.94	0.96	1.26	1.20	1.22	
Ca	6.4-7.1	1.03	1.28	1.12	1.07	0.98	
Na	2.4-3.1	0.42	0.48	0.27	0.26	0.47	
Mn	0.8-1.0	0.22	0.189	0.172	0.172	0.160	
Ti/ppm	21-31	430	390	480	430	490	
V	1.8-2.6	51	49	63	65	70	
La	15-29	0.26	0.24	0.45	0.50	0.40	0.37
Sm	2.3-5.1	0.21	0.20	0.25	0.26	0.28	0.26
Yb	27-85	0.14	0.086	0.14	0.26	0.18	0.16
Au/ppb	1.3-3.3	82	73	186	175	154	158
Ir	1.2-1.8	580	480	560	560	540	570

*range of error (1σ) due to counting statistics.

ON THE RELATION OF CARBON AND NITROGEN CONTENTS IN CARBONACEOUS CHONDRITES

Tetsuo Yamamoto[1] and Takashi Kozasa[2]
1) Institute of Space and Astronautical Science
2) Department of Physics, Kyoto University

It is considered that most of the carbon and nitrogen atoms in carbonaceous chondrites occur as organic polymers. Recently Shimoyama et al.[1] have measured contents of carbon and nitrogen in Antarctic carbonaceous chondrites, and have found that C and N contents in the Antarctic carbonaceous chondrites show the linear relation in terms of the logarithmic contents:

$$d\ln N/d\ln C = \alpha > 1. \qquad (*)$$

This relation holds as well[1] when including non-Antarctic carbonaceous chondrites[2,3] (see Fig. 1). The constant α equals 1.84 for the Antarctic carbonaceous chondrites (with the correlation coefficient $r = 0.97$), and $\alpha = 1.34$ (with $r = 0.90$) when including the non-Antarctic ones. Note that $\alpha > 1$. The relation (*) places a constraint upon mechanisms of the formation and processing of carbon and

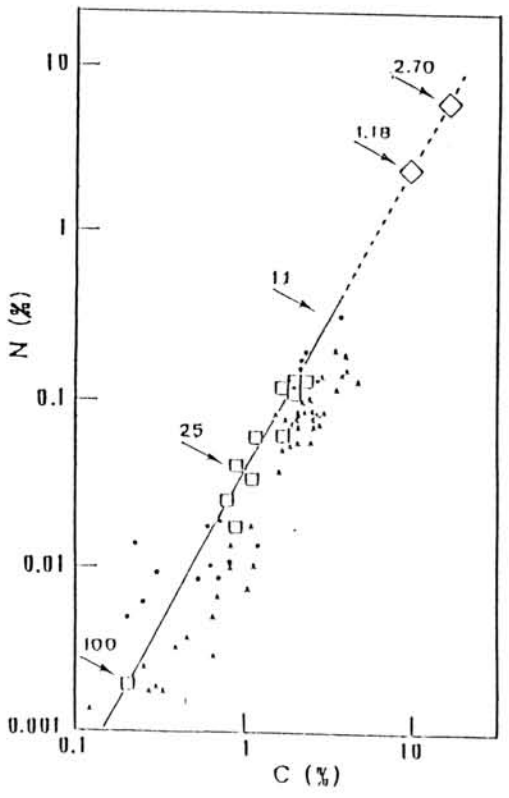

Figure 1: C and N contents of carbonaceous chondrites. The open squares stand for Antarctic ones, and the filled symbols for non-Antarctic ones. The two open diamonds at upper right show the cross points of the line of the C/N ratio = solar (see text) with the line for log N = 1.84 log C - 1.46 (Shimoyama et al. 1987). The numbers attached to arrows show the C/N ratio along the line.

nitrogen polymers found in carbonaceous chondrites.

We have examined processes that lead to the relation (*) on the basis of chemical kinetic consideration. Two kinds of processes have been examined as the candidates: a) thermal process, and b) irradiation of energetic particles or photons. For irradiation, we considered the following two types: (i) a hard type: the radiation that penetrates through the grains, which are raw materials of carbonaceous chondrites. Cosmic ray is one of the types of this radiation; and (ii) a soft type: the radiation that is absorbed at the surface of the grains. Ultraviolet photons are one of the types of this radiation.

The result are summarized as follows:

(1) Destruction of refractory organic polymers by radiation of the hard type can reproduce the linear relation (*) (see Fig. 2). This process is not effective for bodies as large as meteorites, but for small grains that formed carbonaceous chondrites. In this process, it is required that the destruction efficiency of the polymers is much larger than the production efficiency in order to realize the linearity in the measured interval of C and N contents.

(2) The relation (*) does not arise from polymerization of volatiles (i.e. ices) by irradiation. This process, however, may be responsible for the formation of the original organic polymers or their precursor radicals from volatiles. It is

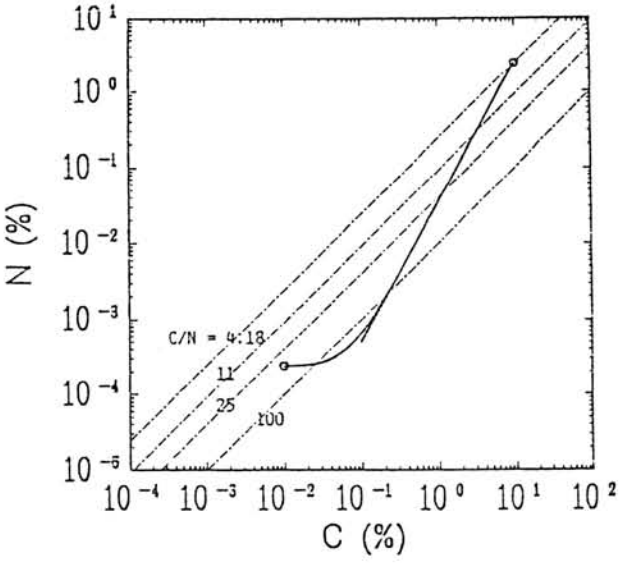

Figure 2: A locus of (X_C^P, X_N^P) for irradiation of the penetration type, and the dotted line showing the relation (*) for $0.1 < C(\%) < 10$. The dash-dotted lines are those for C/N = 4.18 (solar), 11, 25, 100. The parameter values adopted here are ; $(\beta_C/\alpha_C, \beta_N/\alpha_N) = (10^{-3}, 10^{-4})$, $\alpha_N/\alpha_C = 1.84$, $(X_C^P(0), X_N^P(0)) = (9.96, 2.38)$.

characteristic that the contents of C and N in this case vary along a line of C/N = constant for both hard and soft types of irradiation.

(3) From an analysis of an idealized thermodynamic system, it is expected that thermal processes will not yield (*) under chemical equilibrium. To confirm this conjecture, however, we need a study for realistic systems including thermal chemical reactions.

(4) It is to be pointed out that our theory can be tested by an experiment of irradiation of protons to powdered carbonaceous chondrites.

The authors thank Dr. A. Shimoyama of University of Tsukuba for attracting our interest to the problem discussed in this article and enlightening discussion.

References

1) Shimoyama, A., Harada, K., and Yanai, K., 1987, Carbon and Nitrogen Contents of Carbonaceous Chondrites and Their Implications for a Primitive Condensate in the Early Solar System, *Chem. Lett.* pp. 2013-2016.
2) Gibson, E.K., Moore, C.B., and Lewis, C.F., 1971, Total Nitrogen and Carbon Abundances in Carbonaceous Chondrites, *Geochim. Cosmochim. Acta.* **35**, 599-604.
3) Kerridge, J.F. 1985, Carbon, Hydrogen and Nitrogen in Carbonaceous Chondrites: Abundances and Isotopic Compositions in Bulk Samples, *Geochim. Cosmochim. Acta* **49**, 1707.

Stable Isotope and Abundance Measurements of Solvent Extractable Compounds in Murchison.

I.A. Franchi[1], R.A. Exley[2], I. Gilmour[3], C.T. Pillinger[1]

[1] Dept. of Earth Sciences, Open Univ., U.K.; [2] V.G. Isotech Ltd., Cheshire, U.K.; [3] Enrico Fermi Inst., Univ. of Chicago, U.S.A..

The organic material in the carbonaceous chondrites has been investigated for many years and by many different techniques, yet many important problems remain unresolved, particularly as to the origin and the formation of these intriguing materials. Stable isotopic measurement of the organic material is one of the more under-used techniques although, when this has been applied, it has been done so with good effect. Lancet and Anders (1) noted that the isotopic fractionation between CO_2 and the organic material synthesised during Fischer-Tropsch Type (FTT) reactions (≈50‰) is of the same sign and magnitude as the difference in $\delta^{13}C$ between the carbonates and organic material in meteorites. This observation has consequently been used to support the argument that the organic material in meteorites formed by FTT processes acting on simple precursors such as CO, NH_3 and H_2 in the presence of suitable catalytic grains in the early solar system (2).

However, more recent stable isotopic measurements of individual volatile hydrocarbons and carboxylic acids ($\leq C_6$) from the Murchison meteorite has cast doubt on some of these earlier conclusions (3). Both the hydrocarbons and the carboxylic acids displayed well defined trends of decreasing $\delta^{13}C$ with increasing carbon number indicating a kinetic effect. However, the CO liberated from the meteorite ($\delta^{13}C$ = -32‰) is considerably lighter than the organic material ($\delta^{13}C$ = 0 to +23‰) and CO_2 (+29‰) analysed, a fractionation that is in the wrong direction if the CO liberated from the meteorite is the residual of the precursor gas for FTT synthesis. Analysis of four non-volatile hydrocarbons ($\geq C_{15}$) from Murchison revealed a trend increasing $\delta^{13}C$ with molecular weight (4), the opposite to that of the volatile hydrocarbons and incompatible with a kinetically controlled formation process.

The saturated non-volatile hydrocarbons in meteorites tend to be dominated by the straight chain isomers (maximum abundance around n-C_{19}, although from the complexity of gas chromatograms obtained from the appropriate fractions a multitude of other isomers appear to be present, producing a similar abundance pattern to that yielded by FTT processes (5). However, the relationship between the volatile and non-volatile hydrocarbons remains unclear. Stable isotope measurements of suitable fractions should help resolve this problem. The $\delta^{13}C$ of total solvent extracts of meteorites are similar (up to +10‰) to those of the volatile hydrocarbons (6,7), although the four fractions analysed by Gilmour and Pillinger (4) were considerably lighter (-19 to -25‰).

Therefore, to extend the work of Gilmour and Pillinger (4) a number of samples of the Murchison meteorite have been solvent extracted with mixtures of methanol and toluene: JB2 - 100 to 1000 μm size fraction (73g), JB3 - 30 to 100 μm size fraction (17g), JB4 -1 to 30 μm size fraction (24g) and DM1 - a de-mineralised HF/HCl residue. In each case the total extracts were subdivided by adsorption chromatography on silica gel by elution with n-hexane, toluene and methanol to afford the saturated hydrocarbons, unsaturated hydrocarbons and polar organics respectively. The hydrocarbon fractions have been characterised on a capillary G.C. (column = BP-5; 25m x 0.32mm).

As expected the n-hexane fractions were dominated by the straight chain alkanes, ranging from n-C_{15} to n-C_{25}. The most abundant alkane in JB2 was n-C_{19} (0.095 ppm) whereas in JB3 n-C_{20} was the most abundant (0.90 ppm), indicating that there is no discernible variation in the distribution of these compounds within the meteorite. Chromatograms of the toluene fractions were very similar to that obtained by Basile *et al.* (8), the major components being the unsubstituted three and four ring polycyclic aromatic hydrocarbon (PAHs) compounds anthracene, fluoranthene and pyrene. Unlike the saturated hydrocarbons the unsaturated hydrocarbons appear to be concentrated in the finer size fraction, with almost 2 ppm of fluoranthene in JB3 compared to only 0.75 ppm in JB2. Possibly the PAHs are concentrated at the surface of some specific, but currently unidentified, component within the meteorite, possibly even some catalytic material involved in their formation. As yet a solvent extract on the 1 to 30 μm size fraction (sample JB4) has not been analysed. The $\delta^{13}C$ of the individual straight chain alkanes and the resolved PAHs is being measured on a recently designed gas-chromatograph - isotope-ratio-mass-spectrometer (GC-IRMS) system developed by V.G. Isogas Ltd. (the Isochrom II), the results of which will be presented at the meeting and their significance discussed.

Polar fractions cannot be gas chromatographed without derivitisation. Since this will change their isotopic composition the methanol fractions have been analysed using stepped combustion using a technique modified from Boyd *et al.* (9) to study in the first instance nitrogen. The methanol fraction of JB2 showed two major releases of isotopically heavy nitrogen around 200°C ($\delta^{15}N \approx +110‰$) and 600°C ($\delta^{15}N \approx +100‰$) (Figure 1a). A third, minor component around 400°C is also discernible. The 20‰ dip in the isotopic composition at 225°C indicates the presence of a light nitrogen component, which although unidentified, is most probably a terrestrial component. In contrast, analysis of the de-mineralised sample (Figure 1b) shows that the only release of isotopically heavy nitrogen is around 450°C, which corresponds closely with that of the minor component present in JB2. Possibly there are two different types of soluble organic material present at different locations within the meteorite, one of which is shielded by mineral grains, indicating that this is a relatively early formed component around

which other material has formed. Characterisation of the material in the methanol extracts may reveal important clues as to the formation of these components.

References:

(1) Lancet, M.S. and Anders, E. (1970). *Science*, **170,** 980-982. (2) Anders, E. *et al.* (1973). *Science*, **182**, 781-790. (3) Yuen, G. *et al.* (1984). *Nature,* **307**, 252-254. (4) Gilmour, I and Pillinger C.T. (1985). *Meteoritics*, **18**, 302. (5) Studier, M.H. *et al.* (1972). *Geochim. Cosmochim. Acta*, **36**, 189-215. (6) Kvenvolden, K. *et al.* (1970). *Nature*, **228**, 923-926. (7) Becker, R.H. and Epstein, S. (1982). *Geochim. Cosmochim. Acta*, **46,** 97-103. (8) Basile, B.P. *et al.* (1984). *Organic Geochemistry,* **5**, 211-216. (9) Boyd, S.R. *et al.* (1988). *J. Phys. E: Sci. Instrum.*, **21**, 876-885.

Figure 1a

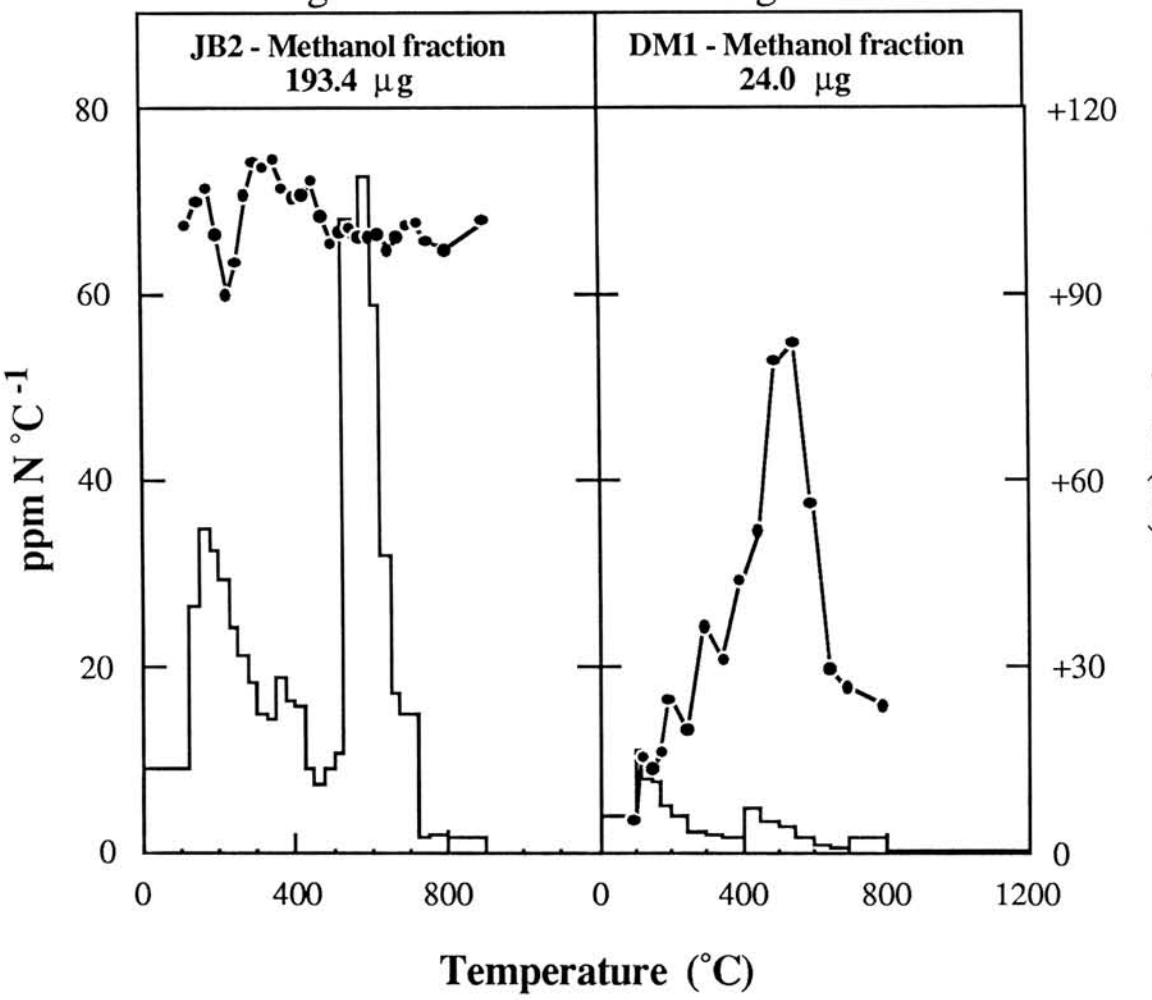

Figure 1b

PURINES IN ANTARCTIC CARBONACEOUS CHONDRITES

Shimoyama, A., Hagishita, S., and Harada, K.

Department of Chemistry, University of Tsukuba, Tsukuba 305

We have examined organic compounds in Antarctic carbonaceous chondrites and found indigenous amino acids, carboxylic acids, and hydrocarbons. We extended our analysis to purines and pyrimidines, basic constituents of nucleic acids in living organisms. We report here the result of our analysis for thesenitrogen bases.

The samples we examined were four Antarctic C2 chondrites, namely, Yamato-74662, Yamato-791198, Yamato-793321, and Belgica-7904. These chondrite samples were analyzed briefly as follws: Each chondrite sample was powdered and extracted in succession with water(60 ^{o}C, 3h), formic acid(60 ^{o}C, 2h), and HCl-HF(80 ^{o}C, 8h). Each extract was desalted by an ion exchange column and examined for purines and pyrimidines by a HPLC with a multi-channeled uv detector in the range of 210 to 350 nm.

We found guanine, hypoxanthine, and xanthine in the formic acid extract of Yamato-74662(Fig. 1) and Yamato-791198, but not of Yamato-793321 and Belgica-7904. The amounts of the three nitrogen bases are listed in Table 1. Purines and pyrimidines were not found in the water and HCl-HF extracts of the four chondrite samples examined.

Our previous examinations showed indigenous amino acids were found from Yamato-74662[1] and Yamato-791198[2], but little from Yamato-793321 and Belgica-7904[3]. The present result of the nitrgen bases gives a similar finding as to which chondrites yield those extractable organic compounds, although the amounts of the nitrogen bases are much smaller than those of amino acids.

In comparison to studies on the nitrogen bases in non-Antarctic carbonaceous chondrites, our results is somewhat similar to those reported by Schwartz's group.[4]

The origin of these nitrogen bases in carbonaceous chondrites is yet to be solved. In sumilation for prebiotic organic synthesis, the three nitrogen bases were formed from HCN solution through one intermidiate compound.[5] It seems that HCN is an important compound for the formation of the nitrogen bases, as well as amino acids, in carbonaceous chondrites.

Table 1. Purines recovered from Antarctic carbonaceous chondrites(ng/g)

Chondrite	Guanine	Hypoxanthine	Xanthine
Yamato-74662	417	120	320
Yamato-791198	229	30	36
Yamato-793321	n.d.	n.d.	n.d.
Belgica-7904	n.d.	n.d.	n.d.

n.d.: not detected above 5 ng/g

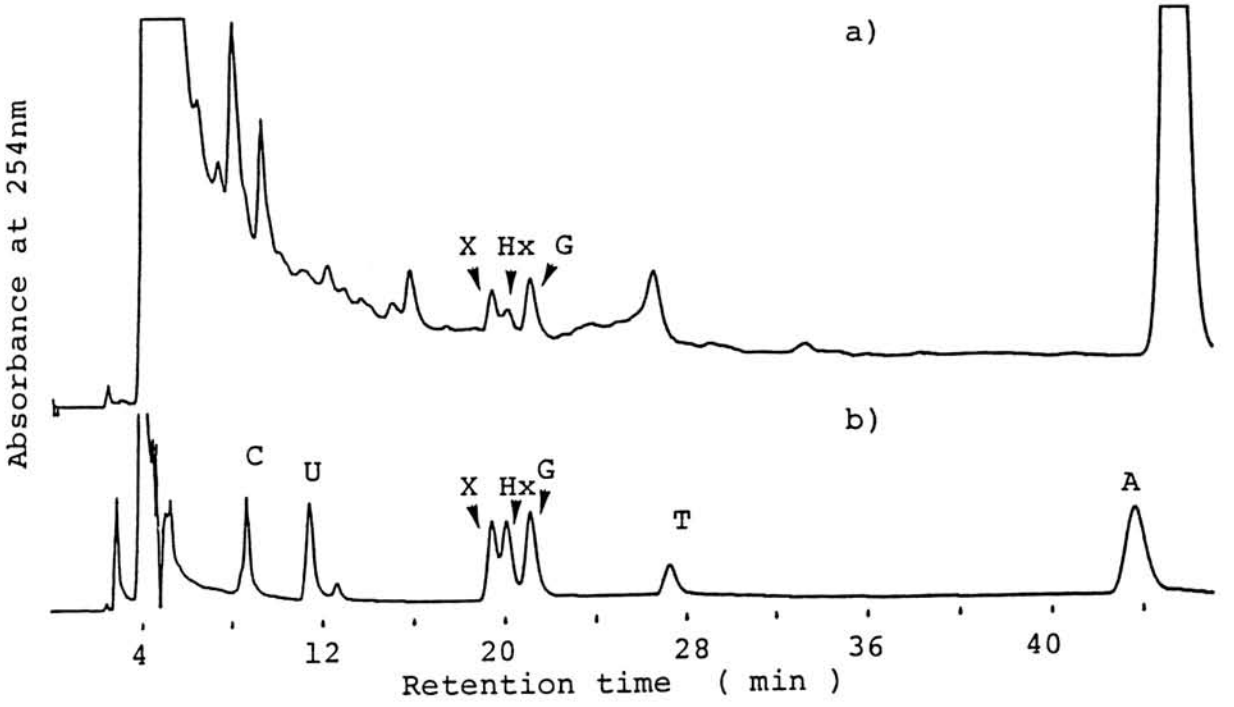

Fig. 1. HPLC chromatograms of the formic acid extract from Yamato-74662 and a mixture of authentic compounds.
a) Yamato-74662, b) authentic compounds.
Abbreviations: A=adenine, C=cytosine, G=guanine, T=thymine, U=uracil Hx=hypoxanthine, and X=xanthine.

References

1. Shimoyama, A., Ponnamperuma, C., and Yanai, K. (1979) Nature, 282. 394.
2. Shimoyama, A., Harada, K., and Yanai, K. (1985) Chem. Lett., 1985, 1183.
3. Shimoyama, A. and Harada, K. (1984) Geochem. J., 18, 281.
4. Stoks, P.G. and Schwartz, A.W. (1981) Geochem. Cosmochem. Acta, 45, 563.
5. Oro, J. and Kimball, A.P. (1962) Arch. Biochem. Biophys., 96, 293.

TG-MS ANALYSIS OF INSOLUBLE ORGANIC MATTER IN ANTARCTIC CARBONACEOUS CHONDRITES

Komiya, M., Shimoyama, A., Naraoka, H., and Harada, K.

Department of Chemistry, University of Tsukuba, Tsukuba 305

Organic compounds in carbonaceous chondrites are present largely as insoluble polymer(s). Because of this non-extractable chemical property, it is difficult to characterize the polymer chemically. We attempted to examine the polymer by a thermal treatment in which components released from a carbonaceous chondrite sample were analyzed by a mass spectrometer(MS) at every 50 ^{o}C during heating from room temperature to 1000 ^{o}C.[1] In the present study we improved the analysis in a way that major components released were continuously detected during the heating. We report here the result of the continuous detection as well as the discontinuous one at every 50 ^{o}C.

The procedures in our examination are briefly as follows: About 40 mg of a powdered carbonaceous chondrite were heated under He flow in a DTA-TG instrument from room temperature to about 1000 ^{o}C at the inceaseing rate of 10 ^{o}C/min. As soon as components were released from the sample during the heating, they were introduced directly into a MS(continuous detection), or they were collected in a cold trap tube for 3 min and introduced into a MS by heating the trap tube for 2 min(discontinuous detection). The total of 5 min corresponds to the temperature increase by 50 ^{o}C. MS scanning was done about every 2 sec.

In the continuous detection, released components were assigned by only corresponding molecular ions. Therefore, the identification was not confirmed. However, in comparison to the result of the discontinuous detection, the assignment of several important components was probably correct. In the discontinuous detection, the cold trap tube performed to a certain extent a role of a gas chromatographic column upon heating. In this case, not only molecular ions but also fragmented ions were obtained for several important compounds.

In order to characterize the insoluble polymer, we examined Yamato-791198 sample which had been already extracted with a mixture of benzene and methanol and had yielded various aliphatic and aromatic hydrocarbons.[2] In comparison, we also examined the fresh sample of the same chondrite. The two samples released H_2O, CO_2, SO_2, and SO far more abundantly than organic components. Figures 1 and 2 show the weight loss(TG) curve and major organic components released by the thermal examination. Large parts of the thermal release took place over the temperature range from 200 to 500^{o}C. The release patterns of a given component between the continuous and discontinuous detections were very similar to each other, so that the two analyses suppoted the result each other.

Among organic components released, benzene was the most abundant follwed by toluene and naphthalene. Our finding from the fresh sample clearly indicated that these aromatic compounds were major organic components released from the polymer. In turn, the main constituents of the polymer were very likely those aromatic components. Saturated and unsaturated light aliphatic hydrocarbons were also founds. These compounds were not identified precisely because of the limitation of our experiment.

Thiophene was also found rather abundantly in the released components. However, it is not clear that this compound was a constituent of the polymer. During heating the chondrite sample sulfur compounds were released,

therefore, it is possible to form S-containing aromatic compounds. Possible presence of other heterocyclic compounds, such as pyrrole and furan, was also noted in the released components. To decide if these heterocycles were constituents of the polymer has to wait for further examination.

We also examined Yamato-793321, because the chondrite is known to lack extractable organic compounds.[3] Organic components released from this sample were much smaller in amount than those from Yamato-791198. Only benzene was noted significantly. This difference may reflect that the polymer in Yamato-793321 consists of a rather simple number of constituents than those in Yamato-791197 and/or poses more simple structure.

Insoluble organic polymer(s) in carbonaceous chondrites is probably complex in composition and complicated in structure. So far, thermal analysis(or pyrolysis) seems the best method to characterize the polymer. Our present finding revealed only a part of the polymer. Step by step examination is neccessary to clarify the polymer.

References

1. Shimoyama, A., Komiya, M., and Harada, K. (1988) Proc. Sym. Ant. Met. 13th, 16.
2. Naraoka, H., Shimoyama, A., Komiya, M., Yamamoto, H., and Harada, K., (1988) Chem. Lett., 1988, 831.
3. Shimoyama, A. and Harada, K. (1984) Geochem. J., 18, 281.

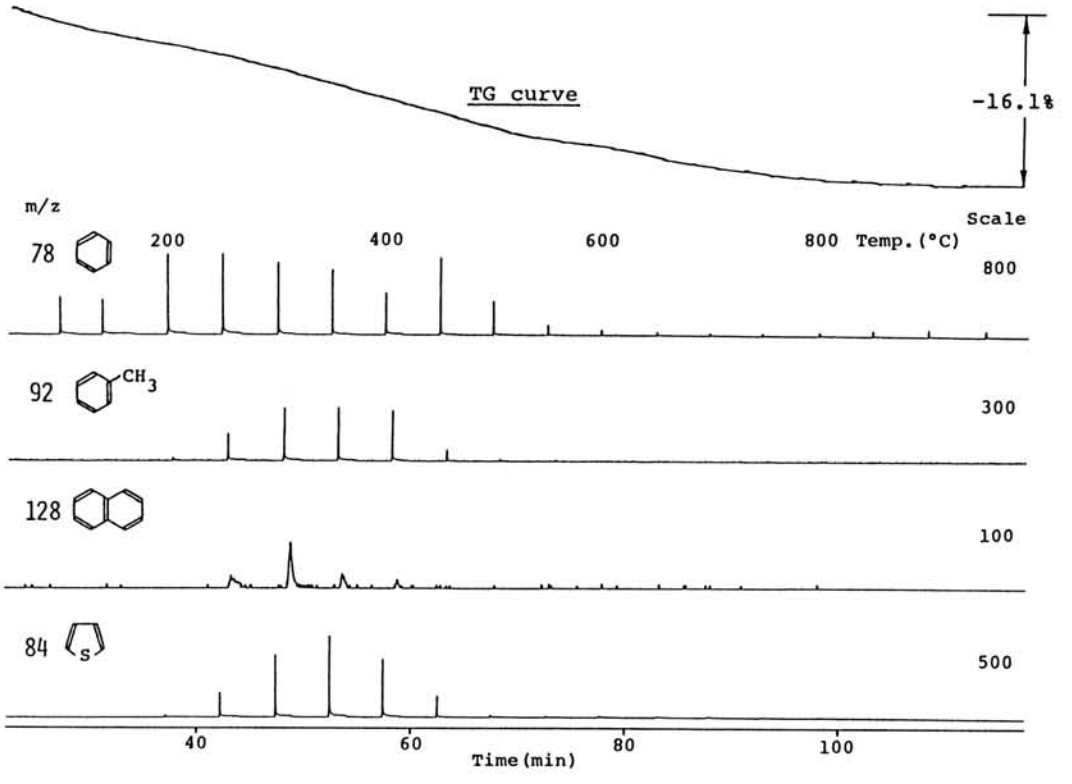

Fig. 1. Thermal release patterns of ions for components released from Yamato-791198 pre-extracted with a mixture of benzene and methanol.

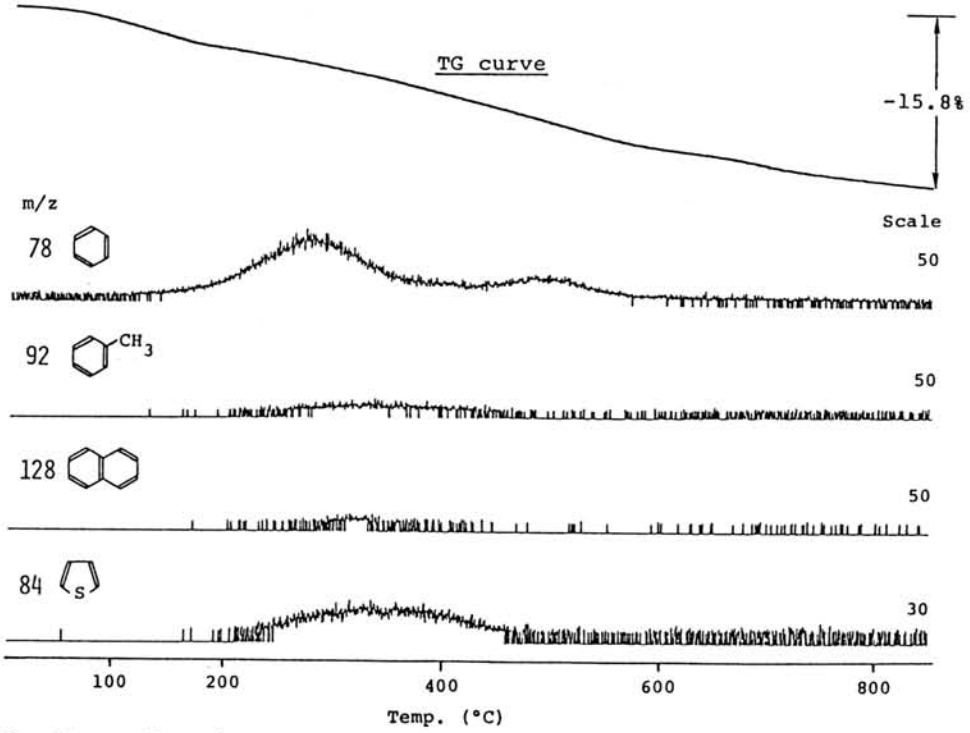

Fig. 2. Thermal release patterns of ions for components released from Yamato-791198 pre-extracted with a mixture of benzene and methanol.

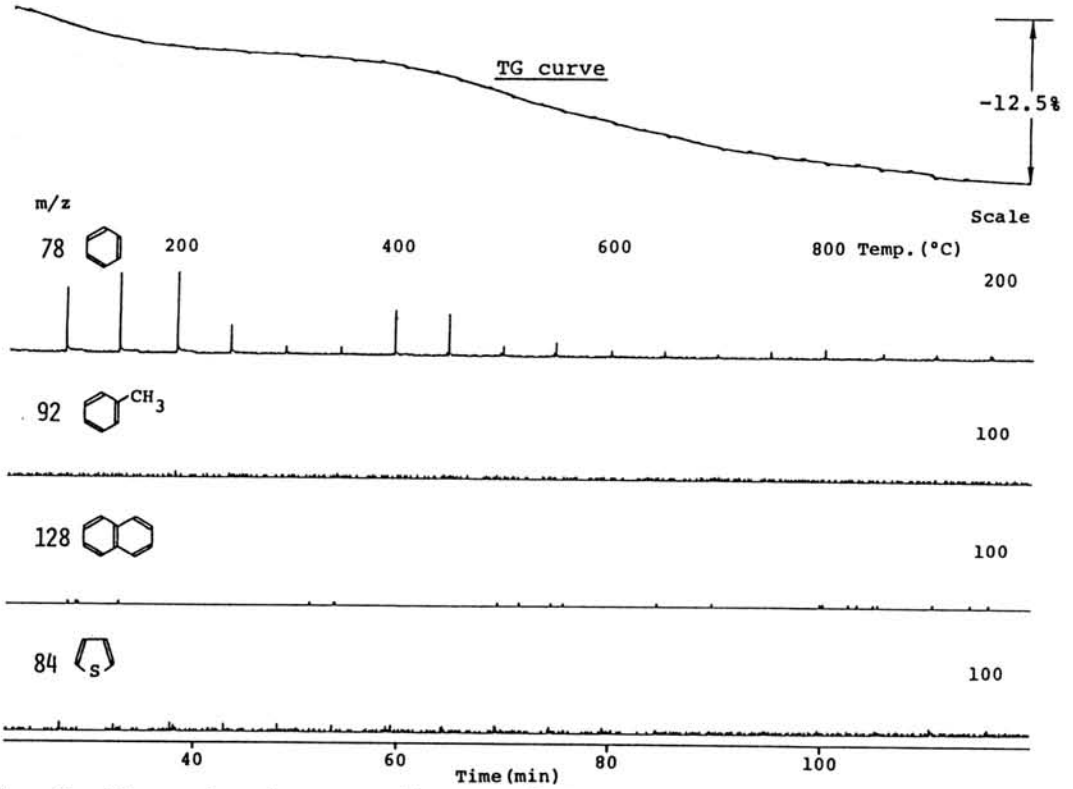

Fig. 3. Thermal release patterns of ions for components released from Yamato-793321.

STUDIES OF CARBONACEOUS RESIDUES OBTAINED FROM CARBONACEOUS CHONDRITES BY ACID TREATMENTS

Murae, T., Masuda, A., and Takahashi, T

Department of Chemistry, Faculty of Science, University of Tokyo, Bunkyo-ku, Tokyo 113

Major organic components of carbonaceous chondrites are organic polymers. We proposed a highly condensed aromatic hydrocarbon structure bearing edge defects (Fig. 1) (1). This structure can interpret many results observed by various methods. The polymers concentrate in residues obtained by treatments with HCl and HF. We have suggested possible occurrence of an alteration of the structure of the organic polymer in the chondrites on acid treatments (2). Most of characterization of the organic polymer has been done on the HCl and HF residues. We consider that the residues exhibit more clear nature of basic skeleton of the polymer (structure bearing less edge defects). We measured IR and mass spectra of the acid residues in order to obtain more informations about its structure.

The sample used in this work was a residue obtained from ALH-77307 by repetition of HCl and HF treatments. The carbon contents of the residue was 45%. We measured the IR spectra using a Horiba FT-300 Fourier transform infrared spectrophotometer equipped with diffuse reflectance attachment. The mass spectrum was determined using a Shimazu LAMS-50K laser ionization time of flight mass spectrometer.

The IR spectrum (Fig. 2) showed weak peaks at 3070, 1580, 1490, 810, and 720 cm^{-1}. These peaks are characteristic for aromatic compounds. This means that the organic polymer contains aromatic groups like phenyl group as a major part of its edge defects but the ratio of the edge defects to the polyaromatic center is low. If substituents like ester, ether, acetal, and corresponding thioderivatives (acid labile edge defects) were connected to the aromatic center, most of these acid labile bonds would have been hydrolyzed on the acid treatments. Therefore, the aromatic edge defects is probably connected to the aromatic center with acid stable carbon-carbon bond which can be cleaved on pyrolysis.

The carbons contained in the most outside carbon circle and the second outside carbon circle of the molecule (Fig. 1) are assumable as average of various aromatic edge defects which will be lost on pyrolysis. On the assumption we can estimate the molecular size (molecular weight) roughly using the ratio of the amount of lost carbon on pyrolysis to the amount of carbon present before pyrolysis. The results are shown in table 1. Although the molecular weights of these compounds are too high to be determined by conventional mass spectrometers, we could observe a peak which is considered to indicate possible molecular weight of the organic polymer in the acid residue using the laser ionization time of flight mass spectrometer (Fig. 3). If the observed peak indicates the molecular ion, the average size of the molecule including edge defects is 10.4 nm.

Additional supports for our proposed structure

for the organic polymer in carbonaceous chondrites were obtained in this work.

References: (1) Murae, T., Masuda, A., & Takahashi, T. (1987) Mem. Natl Inst. Polar Res., Spec. Issue, 46, 196. (2) Murae, T., Masuda, A., & Takahashi, T., (1988) Abstracts of 13th Symposium on Antarctic Meteorites, 21.

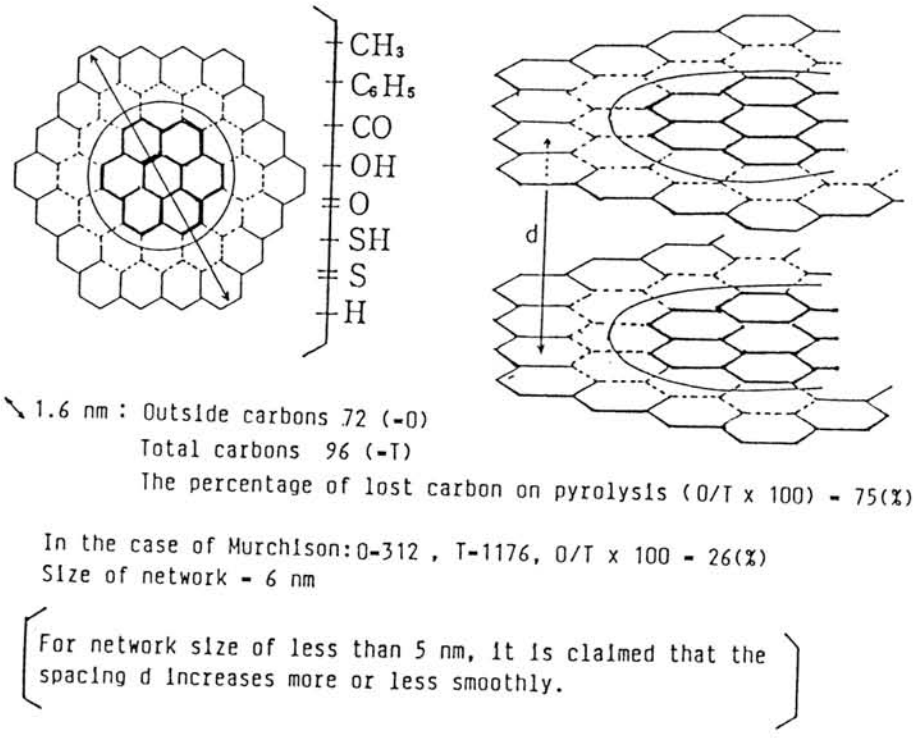

Fig. 1. Simplified model of molecular structure of organic polymer in carbonaceous chondrites.

Table 1. Estimated size and molecular weight for organic polymers in carbonaceous chondrites.

Meteorite	Class	Lost carbon on pyrolysis (%)	Estimated size (nm)	Molecular weight
Murchison	C2	26	6	14,112
Y-74662	C2	19	8	28,800
Y-793321	C2	19	8	28,800
B-7904	C2	14	12	52,488

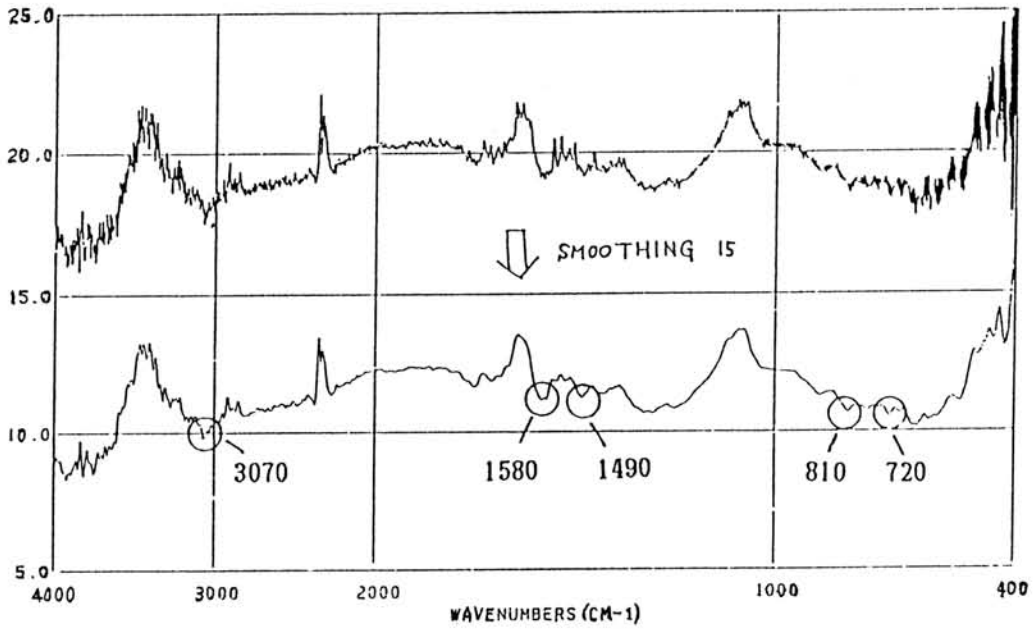

Fig. 2 Diffuse reflectance infrared spectrum of the acid residue from ALH-77307.

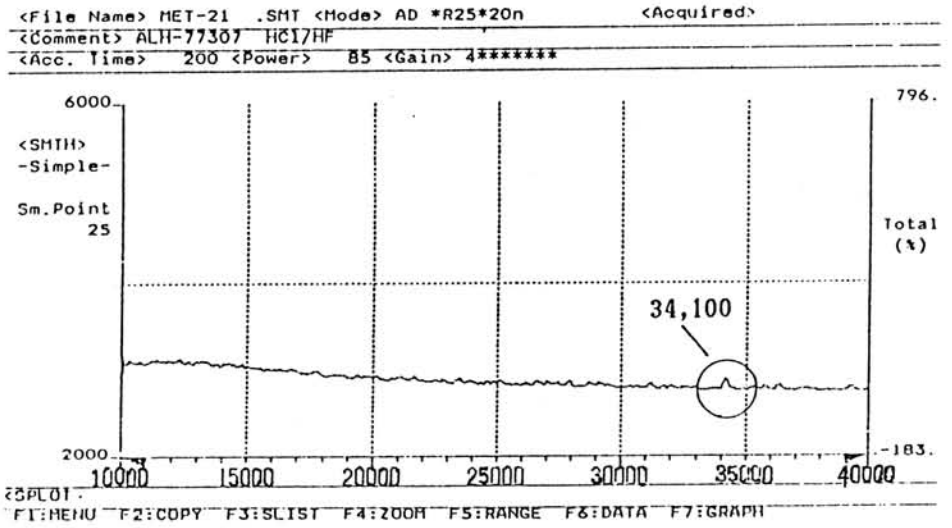

Fig. 3 Laser ionization time of flight mass spectrum of the acid residue from ALH-77307.

HOMOGENIZATION PROCESS IN PYROXENE OF ORDINARY CHONDRITES

Fujita,T., Tsuchiyama,A. and Kitamura,M

Department of Geology and Mineralogy, Kyoto University, Sakyo Kyoto 606.

In chondrites, increasing number of petrologic types is accompanied with the homogenization of olivine and pyroxene. In the present study Fe-Mg heterogeneity in clinoenstatite of ordinary chondrites was investigated with an optical microscope (OM), scanning electron microscope (SEM) and an analytical transmission electron microscope (ATEM) to discuss the homogenization process in pyroxene of ordinary chondrites.

Heterogeneous texture in clinoenstatite.

Clinoenstatite in type 3 and some type 4 chondrites have Fe-Mg heterogeneous texture which is characterized by the striated heterogeneity parallel to (100) plane. In the texture, Fe/Mg ratio changes gradually in the direction parallel to (100) plane, while it changes sharply in the direction normal to (100) plane (Tsuchiyama et al.,1988; Noguchi, 1988) (Fig.1). Fe-rich parts of the pyroxene should have been formed by the exchange of Fe-Mg with Fe-rich matrices. Observation of ultra-thinsections under an OM and SEM and analytical electron microscopy strongly suggests that the exchange process in pyroxene is constrained by cracks normal to the c-axis and (100) plane defects such as twin boundaries and ortho-clino phase boundaries; Fe-rich parts in the striated heterogeneity are considered to be formed by Fe-Mg diffusion from the cracks in the pyroxene. The variation of the chemical composition across the (100) plane defects (Fig.2) suggests that the defects acted as barriers for diffusion and formed the sharp compositional boundaries. The heterogeneous texture of pyroxene is regarded as the transitional texture frozen in the course of homogenization process in pyroxene of chondrites.

Olivines are almost homogenized in upper subtype of type 3 chondrites. Those homogeneous olivines and the heterogeneous pyroxenes are considered to be formed in the same metamorphic process of chondrites.

Thermal condition.

Thermal conditions for the metamorphic process were estimated from the time -temperature - mean diffusion distance (T-T-D) diagram (Fig.3) in which the mean diffusion distance, d, is calculated from the equation of $d = (2Dt)^{1/2}$, where D is the diffusion coefficient and t is the time. Data for Fe-Mg diffusion in orthopyroxene (Wilson,1982) and olivine (Misener, 1974) were adopted in the calculation.

Mean diffusion distance of the Fe-Mg exchange in the clinoenstatite along the c-axis can be assumed to be the length of the Fe-rich part (about 10um for typical samples in upper subtypes 3 chondrites). Therefore, time and temperature conditions of the homogenization process in pyroxene should be on the 10um iso-distance line for pyroxene in Fig. 3. On the other

hand, the diffusion distance of homogeneous olivine should be larger than half length of the largest grain (100um). Then, the homogenization process in olivine should have occurred in the region upper than the 100um iso-distance line (Fig. 3). Since these two lines for pyroxene and olivine cross around 1200-1300°C, coexisting of heterogeneous pyroxene and homogeneous olivine can be allowed only in the region below about 1200-1300°C.

The conditions estimated from the diagram are further constrained by other data on the transition temperature of enstatite and the cooling rate of chondrules.

Firstly, homogenization of pyroxene should have occurred below the transition temperature between proto-clinoenstatite (1300°C for clinoenstatite ($En_{80}Fs_{20}$); Heubner and Turnock, 1980), since the (100) plane defects formed by the transition constrained the striated heterogeneity. This constraint is not conflict with the conditions of homogenization pyroxene estimated from T-T-D diagram.

Secondly, cooling rate of type 3-5 L chondrite around 1000°C (800-1100°C) is estimated to be a few to 10°C/hr (Watanabe et al., 1985). This rather fast cooling rate suggests that the homogenization of pyroxene have not occurred around 800-1000°C.

Thirdly, clinoenstatite partly inverted to orthoenstatite. This inversion takes place in a few hours to a few days when the temperature is about 700-900°C (Smith, 1974). Since the time around the temperature required for the homogenization is considered to be too long to preserve the monoclinic structure of clinoenstatite, the homogenization have not occurred around 700-900°C.

Fourthly, cooling rate of H4 and L4 chondrites around 600°C are estimated to be faster than 44°C/Ma and 6.2°C/Ma, respectively (Pellas and Stolzer,1981). The time around 600°C estimated from the diagram is too long to be consistent with the rates.

As a result, high temperature condition at about 1000-1200°C or low temperature condition at 600 - 700°C is expected as the homogenization process in pyroxene of ordinary chondrites.

Reference

Freer,R (1981) Contrib.Mineral.Petrol.,76,440-454.
Heubner and Turnock (1980) Am.Mineral.,65, 225-271.
Noguchi (1988) paper presented to 13the Symps. Antarc. Metor.,38-40
Pellas and Stolzer (1981) Proc. R. Soc. Lond. A 374, 253-270.
Smith (1974) Am. Mineral., 59, 345-352.
Tsuchiyama et al. (1988) Proc. NIPR Symps. Antarc. Metor., 1, 173-184.
Watanabe et al. (1985) Earth Planet. Sci. Lett., 72, 87-98.
Wilson, A.H. (1982) J.Petrol., 23, 240-293.

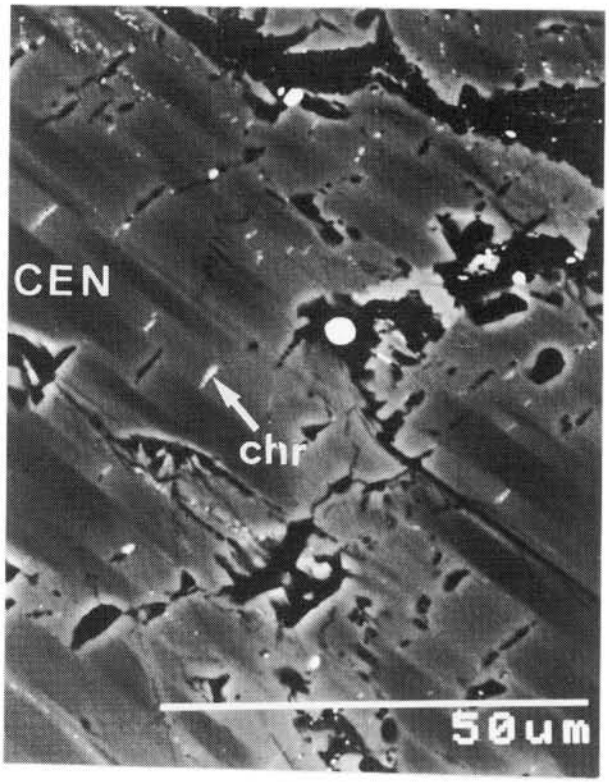

Fig.1 BEI image of a clinoenbstatite in ALH-77304 showing striated heterogeneity.

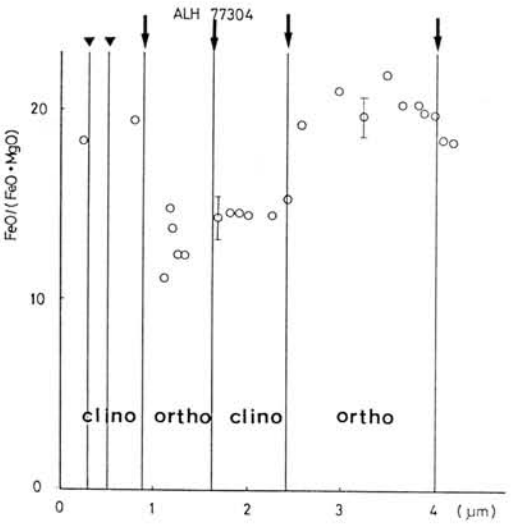

Fig.2 Relation between (100) plane defects and the variety of composition in a clinoenstatite. Triangles and allows represent twin boundaries and phase boundaries respectively.

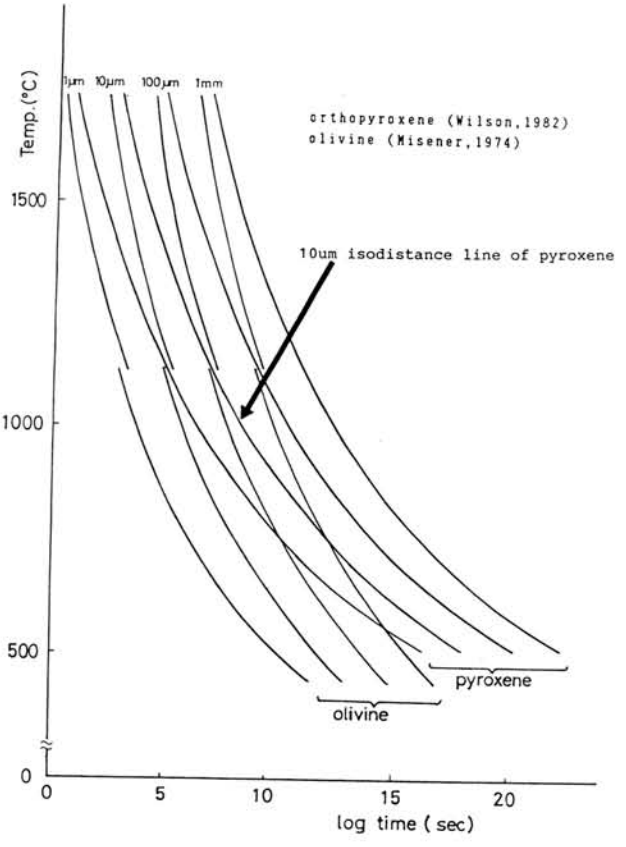

Fig.3 Time-Temperature-Mean diffusion distance diagram.

Variations of compositional changes of pyroxenes and olivine in L chondrites. Evaluation of "petrologic type"

Noguchi, T., Geol. Inst., Univ. Tokyo, Hongo, Tokyo 113

Investigation of compositional variations of minerals such as olivine, pyroxenes and metals is important for understanding "metamorphism" of ordinary chondrites. Olivine composition has already been studied since early 1970s: Lux et al. (1980) showed that the Mg/(Mg+Fe) ratio of olivine in H chondrites decreases as petrologic type increase. Rubin et al. (1988) showed, however, that they did not show such relationship.

One of the reasons for this confusion may be that classification of petrologic type is qualitative. In this paper, the extent of homogenization of pyroxenes is evaluated by the average and standard deviation of chemical compositions of pyroxenes. Meteorites studied are Saratov, Tennasilm, Bald Mountain, Homestead, Arapahoe, Malakal, Taiban, Knyahinya, Elenovka, Knashak, Tourinnes-la-Grosse, and their "petrologic type" ranges from 4 to 6.

Fig. 1 shows average values and standard deviations of Mg/(Mg+Fe) ratio of low-Ca pyroxenes and those of Mg/(Mg+Fe) ratio, Al_2O_3 content and Wo content of Ca-rich pyroxene. Average Mg/(Mg+Fe) ratio of low-Ca pyroxenes increases as Wo content of Ca-rich pyroxene increases and Al_2O_3 content of Ca-rich pyroxene decreases. Along with this change, the standard deviations of these values decrease.

In Fig. 1, petrologic types of each chondrite are also presented. The averages and their standard deviations vary in harmony with "petrologic type" with some exceptions. The exceptions are especially noted in Wo and Al_2O_3 contents of Ca-rich pyroxene. Except for some chondrites being discordant with the change of average and standard deviation, each petrologic type corresponds to the following ranges of the averages and standard deviations:

type 4: average Wo content of Ca-rich pyroxene: >40,
type 5: average Wo content of Ca-rich pyroxene: 40 to 45,
type 6: average Wo content of Ca-rich pyroxene: >45 and standard deviation of it <1.5 .

In chondrites with low extent of homogenization, inverted protopyroxene, orthopyroxene and pigeonite can be divided by their compositions. These three low-Ca pyroxenes display specific Fe-Mg heterogeneity texture (Tsuchiyama, 1988). Except for the texture, there is another specific heterogeneity texture, that is patchy occurrence of ferrous pyroxene (>Fs25) in the rim of pyroxene crystals. Because such texture is seldom observed in pyroxenes in type 3s, it may be related to the metamorphism of ordinary chondrites. Among these low-Ca pyroxenes, inverted protopyroxene is homogenized much faster than orthopyroxene. In chondrites, in which Ca-rich pyroxene has homogeneous Mg/(Mg+Fe) ratio and heterogeneous Wo content, the texture described by Tsuchiyama et al. 1988) cannot be observed in inverted protopyroxene (striated orthopyroxene) but can be seen in orthopyroxene in some meteorites with lesser extent of homogenization.

Contrary to pyroxenes, standard deviation of Mg/(Mg+Fe) ratio is almost the same in types 4 to 6. The average Mg/(Mg+Fe) ratios of pyroxenes and olivines, however, systematically varies from type 4 to 6 as shown in Fig. 2. With increase in the petrologic type, the Mg/(Mg+Fe) ratios decrease. This result is similar to that reported for H chondrites (Lux et al., 1980). The systematic variation of Mg/(Mg+Fe) of olivine and pyroxenes may be due to either difference in bulk composition or difference in redox state. Brett and Sato (1984) suggested that chondrites with higher petrologic types had been under more reducing conditions from intrinsic oxygen fugacity measurement. The increase in the average Mg/(Mg+Fe) ratio as increase in the "petrologic type" is inconsistent with what is expected from their interpretation. If their measurement is reliable, the differences of the Mg/(Mg+Fe) ratio among petrologic types may be due to the difference in the bulk composition, which have already pointed out for H chondrites, by Lux et al. (1980) and Morgan et al. (1985).

References:
Lux et al. (1980): Geochim. Cosmochim. Acta, 44, 841-855.
Morgan (1985): Geochim. Cosmochim. Acta, 49, 247-259.
Rubin et al. (1988): in Meteorites and their origins, 488-511.
Tsuchiyama et al. (1988): Proc. NIPR Symp. Ant. Meteorites, 1, 173-184.

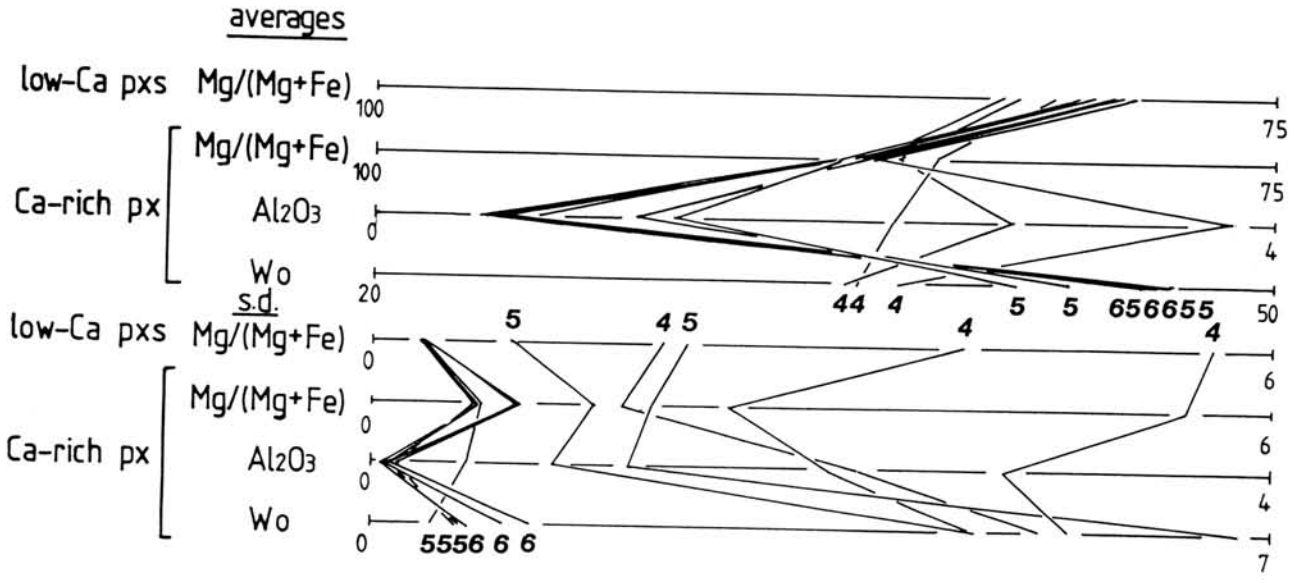

Fig. 1 Averages and standard deviations of Mg/(Mg+Fe) ratio of low-Ca pyroxenes, and those of Mg/(Mg+Fe) ratio, AL_2O_3 content and Wo content of Ca-rich pyroxene. Numbers (4, 5 and 6) are petrologic types.

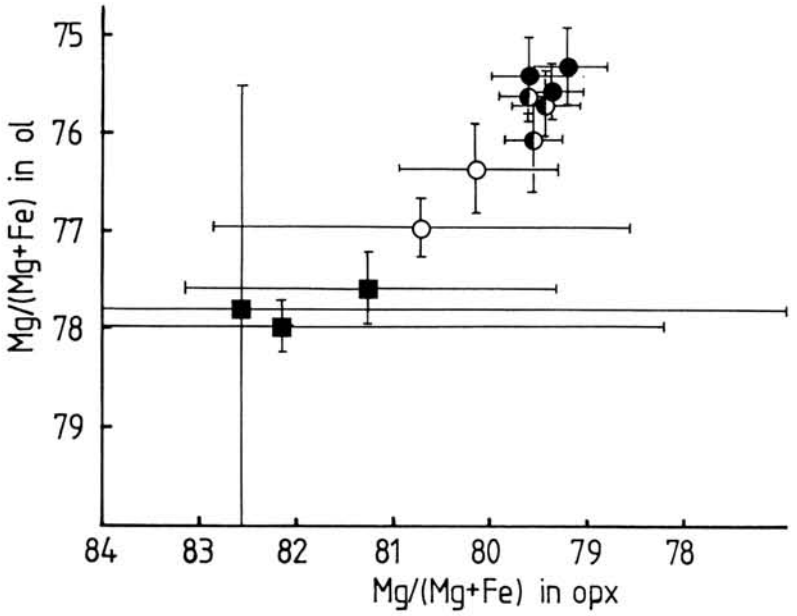

Fig. 2 Mg/(Mg+Fe) in low-Ca pyroxenes versus Mg/(Mg+Fe) in olivine. Mg/(Mg+Fe) ratios in both minerals decrease as petrologic type increases.
solid square: type 4s, open circle: type 5s, half filled circle: type 5s with indistinguishable composition with type 6, solid circle: type 6s. Error bars are one sigma of analyses.

Allende III: A SEM study of its glassy phases

G. Sanchez-Rubio, A. M. Reyes-Salas and A. Nieto
Instituto de Geologia (UNAM), Ciudad Universitaria,
Delegación Coyoacán, 04510 México, D. F., Mexico

Wednesday, June 7, 1989

0900 - 1715 ***Symposium, Auditorium***

MINERALOGICAL AND SPECTROSCOPIC STUDIES OF PRIMITIVE ACHONDRITES WITH REFERENCE TO THE S-TYPE ASTEROIDS.

Takahiro HIROI, Jun SAITO, and Hiroshi TAKEDA.
Mineralogical Institute, Faculty of Science, University of Tokyo,
Hongo, Tokyo 113, Japan.

Two primitive achondrites ALH-78230 and ALH-77081 and an H6 chondrite Y-82111 are examined by mineralogical and spectroscopic methods, and are compared with other primitive achondrites and asteroid 29 Amphitrite.

1. Mineralogy of ALH-78230 and ALH-77081.

ALH-78230,51-2 shows medium grained texture of orthopyroxene, olivine, Ni-Fe metal, and minor plagioclase, augite, and sulfides. Their modal abundances and chemical compositions are summarized in Table 1. ALH-77081,80 (0.355g) was examined by Takeda et al. [1]. The modal abundance and pyroxene composition of ALH-78230 are plotted in diagrams with other primitive achondrites [2] and shown in Fig.1. This meteorite is very similar to winonaites and probably different from lodranites. According to the mineral assemblage of Amphitrite assumed by the method of Hiroi and Takeda [3], ALH-78230 is a good candidate for the surface material of Amphitrite as shown in Fig.1.

2. Spectroscopy of ALH-77081 and Y-82111.

Spectral reflectances of ALH-77081 and Y-82111,62 (1.102g) chips were measured and compared with those of Amphitrite [4] and iron meteorite Mundrabilla. Fig.2(a) shows those spectra and absorption band assignments. Spectral reflectance of Amphitrite shows an inclination similar to Mundrabilla and absorption bands similar to ALH-77081 and Y-82111. Therefore, we expect that Amphitrite spectrum can be synthesized with these spectra. The results are shown in Fig.2(b). Absorption band wavelengths and profile are well fit, however, absorption band depths are deeper than Amphitrite. This difference shows that silicate grains of Amphitrite are smaller than those of ALH-77081 and Y-82111. More detailed calculations are required to clearly explain this difference.

3. Conclusion

Amphitrite surface material may have primitive achondrite or H6 chondrite like assemblage whose metal abundance is larger and grain size is smaller than those meteorites.

REFERENCES: [1]Takeda H., Mori H., Yanai K., and Shiraishi K. (1980) Mem. Natl Inst. Polar Res., Spec. Issue, 17, 119-144. [2]Prinz M., Nehru C. E., Delaney J. S., and Welsberg M. (1983) Lunar Planet. Sci. XIV, 616-617. [3]Hiroi T. and Takeda H. (1989) Lunar Planet. Sci. XX, 418-419. [4]Bell J. F., Gaffey M. J., Gradie J. C., Hawke B. R., and McCord T. B. (1985) Lunar Planet. Sci. XVI, 47-48.

mineral	modal abundance(%)	chemical composition (range)
metal & sulfides	21	kamasite (6.7-7.0 wt% Ni) taenite (16-18 wt% Ni) troilite
olivine	25	Fa 10.4 (9.6-11.1)
orthopyroxene	43	Fs 9.6 (8.9-10.2), Wo 1.4 (1.1-1.8)
augite	3	see Fig.1(b)(c)
plagioclase	7	An 14.6 (13.8-16.0)

Table 1. Mineral assemblage of ALH-78230.

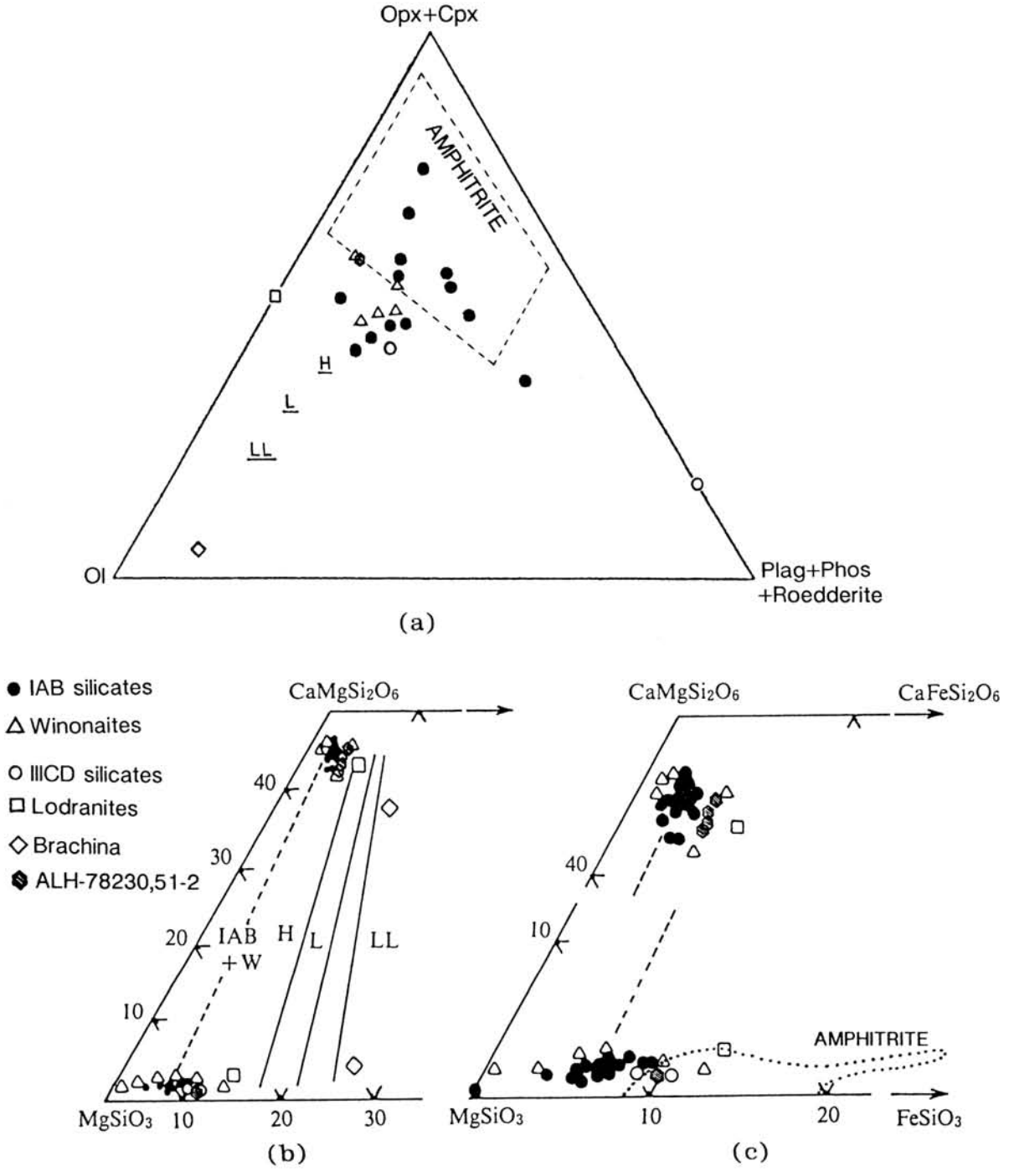

Fig.1. Mineralogy of ALH-78230 with reference to Amphitrite plotted in diagrams by Prinz et al. (1983).
(a) Modal abundance.
(b) Pyroxene chemical compositions.
(c) Magnified figure of (b).

(a)

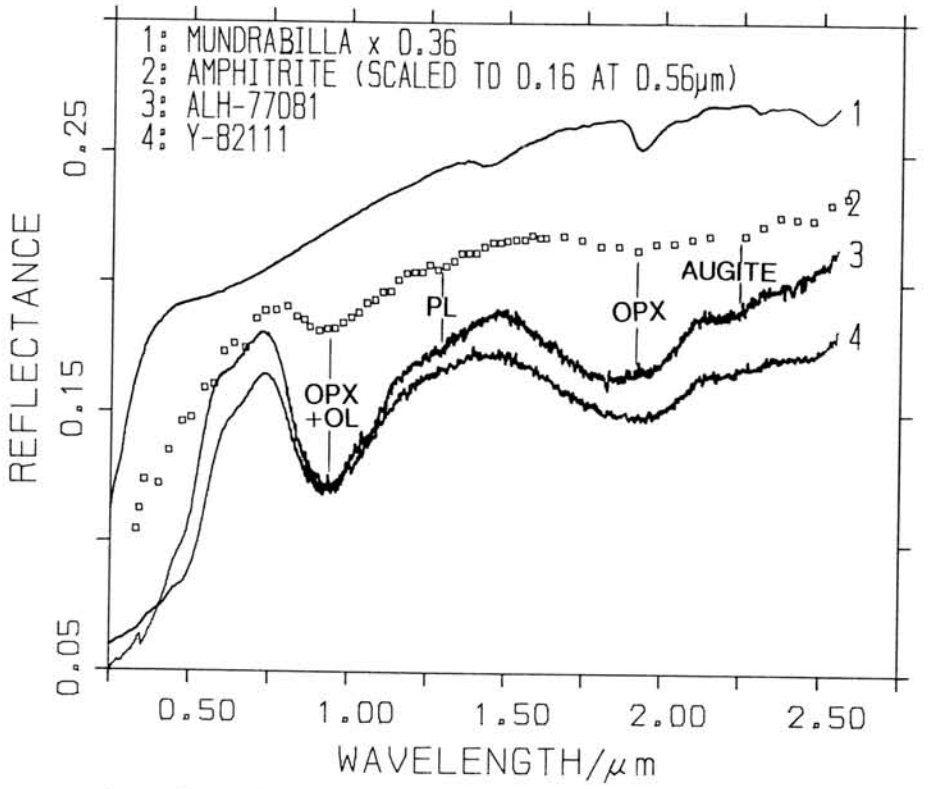

(b)

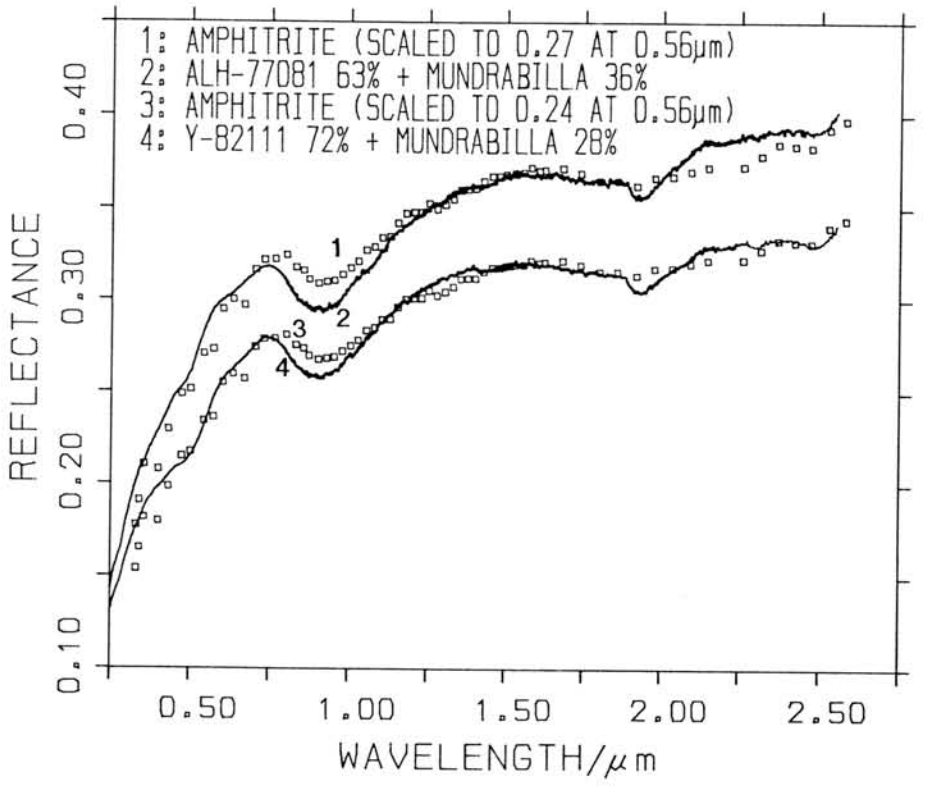

Fig.2. Spectral reflectances of ALH-77081 and Y-82111 with reference to Amphitrite and Mundrabilla.
(a) Assignments of absorption bands to mafic minerals.
(b) Approximation of reflectance spectra of Amphitrite with (1) ALH-77081 and Mundrabilla, (2) Y-82111 and Mundrabilla by least-squares method.

Mineralogical Study of the Yamato-8448 ureilite and some thoughts on the origin of ureilite

Saito, J., Nakamura, T. and Takeda, H.

Mineralogical Institute, Faculty of Science, University of Tokyo, Hongo, Tokyo 113 Japan

Among Yamato meteorites, some unique ureilites such as a Fe,Ca-rich Y74130 and Mg-rich Y791538 have been found. Because the preliminary study of Yamato-8448 shows variations of chemical compositions of olivine and pyroxene (1), we studied this meteorite in order to identify the origin of chemical variations by electron probe microanalysis and optical microscopy. A revised model of ureilite genesis is also given.

The polished thin section of Y-8448,61-2 revealed that olivine and pyroxene crystals are elongated. Although we studied a small number of olivine crystals, Y-8448 olivines to display a tendency for preferred orientation of their crystal axis, as was found in some non-Antarctic ureilites (2). The electron probe microanalysis shows that the chemical compositions of mafic silicate cores of Yamato-8448 are uniform; Fa_{22}, for olivine and $En_{72.5}FS_{18.5}Wo_{9}$, for pyroxene. The pyroxene rims have lower Fe content. Along the margin of this section, there are dark colored areas with many rounded holes, around which dendritic materials are grown. These areas are about 1mm in width, and appeared to be fusion crusts. These dendritic materials consist of olivines and pyroxenes, which shows chemical zoning. Thus, the variations of chemical compositions of Y-8448 olivines and pyroxenes may be attributed to zoning of these dendritic crystals in fusion crusts and pyroxene rims.

Y-8448 has been found to be one of normal ureilites (2), with relatively thick fusion crusts including dendritic olivines and pyroxenes. This ordinary ureilite belongs to the type I subgroup of Clayton and Mayeda according to the mafic silicate chemistry (3). They demonstrated that Fa contents are correlated to the degree of oxygen isotope anomalies, and we expect that the oxygen isotope of Y-8448 may not be too anomalous. The preferred orientation of olivine crystals of ureilites has been attributed to the evidence for cumulate model of ureilite origin(2). Olivine crystals of Y-8448 also may show such elongation, though we have only a small number of olivine grains. However, Tsukahara and Yamazaki (4) have shown that the ureilite texture can be produced without necessitating conventional "setting-type" cumulates. Their study suggests that very elongated crystals may be grown by a temperature gradient zone refining process.

We studied the chemical zonings and variations of pyroxene and olivine in Y-8448 in order to gain better understandings of the way how the Ca-Al-Fe-S melt was removed from the partially melted source material. However, these chemical variations and zonings turned out to be attributed to rims of mafic silicate and dendritic crystals in fusion crusts. We just mention some thoughts on the origin of ureilites in terms of the above

growth model.

According to the planetesimal scale collision model (5,6), ureilites is thought to be formed by preferential melting and crystal growth of carbonaceous chondrite-like source materials by planetesimal scale collisions. This model requires a removal of Ca-Al-Fe-S melts from the source material. It has not been fully understood, however, how the Ca-Al-Fe-S melt was removed from the partially melted source material.

During the planetesimal-scale collision, shock waves traverses the interior of the planetesimal, and phenomenon similar to an earthquake will take place. One way of removing liquid from the mixtures of melts and solids during such process condition is the liquefaction phenomenon. The liquefaction is a phenomenon that a wet sandy soil behave like liquid, and liquids seep out of a ground when earthquake occurs. The reason why we refer to this phenomenon is that this is the process which can easily remove a liquid from a solid-liquid mixture when vibration occurred in the mixtures of solids and liquids. Applying this process to the preferential melting of ureilite source material, the Ca-Al-Fe-S melts may be removed from the partially melted source material when the shock waves traverse during the planetesimal-scale collision. If a small amount of vapors is present, removal will be much efficient. Distribution of partially melted zone within the planetesimal will induce a process similar to temperature gradient zone refining. This growth mechanism is in time with elongation of mafic silicates. The liquids concentrated at the end of crystal growth will accumulate incompatible elements, which should be removed from the source materials.

The process of removing melt (or melts) from the ureilite source material is very important to explain the ureilite formation from source material because the oxygen isotope anomaly has to be retained during this process. Further study including an experimental approach must be required in order to reveal the mechanism of the removal of melt from the source material (or materials) of ureilite.

We thank National Institute of Polar Research for meteorite sample, and Ohbayashi Corporation for discussions about a liquefaction phenomenon.

REFERENCES:

(1)Yanai, K. and Kojima, H. (1987) Photographic Catalogue of The Antarctic Meteorites, p219; (2) Berklay, et al. (1980) GCA 44, 1579; (3)Clayton, R. N. and Mayeda, T. K. (1988) GCA 52, 1313; (4)Tsukahara, H. and Yamazaki, T. (1976) Journ. Geol. Soc. Japan 82, 751; (5) Takeda, H. (1987) EPSL 81,358-370; (6)Takeda, H. et al. (1988) Proc. NIPR Symp. Antarct. Meteorites, 1, 145

MINERALOGY OF YAMATO 791466 AND 791438 ACHONDRITES AND THE EVOLUTION OF MATERIALS IN THE HED PARENT BODY.

Hiroshi Takeda, Kazuo Saeki and Tokuhei Tagai.
Mineralogical Inst., Faculty of Science, Univ. of Tokyo, Hongo, Tokyo 113.

A preliminary description of Yamato 791466 by Yanai and Kojima (1) showed that it is one of the Y-75032-type achondrites. The texture with heavily shocked pyroxene fragments set in a dark glassy matrix is similar to Y-75032. Yamato 791438 is a monomict eucrite (1) with pyroxene compositon similar to those of Mg-rich cumulate eucrites. Because pyroxene compositions of the Y-75032 group cover the entire range from Fe-rich diogenites to cumulate eucrites, we compared Y-791466 with Y-791438 to decipher pyroxene crystallization trend and the evolution of materials in the HED (Howardites, Eucrites, Diogenites) parent body. The pyroxene crystallization and the relation between the anorthite content (An) of plagioclase and the mg number=100XMg/(Mg+Fe) of the coexisting pyroxene in these specimens will give us information on the fractional crystallization in the HED body. The diagram of the Y-75032 group revealed two crystallization trends: One trend is intermediate to that of the Mg-rich suites of the lunar highland crust and that of ferroan anorthosite, and the other is a trend with a steep decrease in the An content, while the mg numbers of the pyroxene remain effectively constant. A model involving crystal fractionation in a shallow magma ocean or intrusion in the parent body has been proposed by Takeda and Mori (2).

(1) Mineral Chemistry.

The pyroxene textures of Y-791466 indicate that many of them crystallized as low-Ca pigeonite, and some as orthopyroxene. Later shock events which produced glassy matrix modified the original inversion and exsolution textures of pyroxene. The pyroxene chemical compositions distribute within small range (mg=68 to 63), which is similar to Y-75032 (Fig. 1). Augites are present as blebs and exsolution lamellae. Small amounts of plagioclase are present both as a small grain in a lithic clast and fragments in the glassy matrix. The plagioclase compositions (Fig. 2) show large variation in the An content (95 to 72). These trends are similar to Y-75032, Y-79 1000 and Y-91199, which are typical diogenite-rich materials. Y-791439, Y-791200, Y-791201 are rich in cumulate eucrite components and show small range in the An content and the larger range in mg number.

Y-791438 is a rare crystalline eucrite found in Antarctica, but its texture is slightly disturbed by shock events. The texture is intermediate between subophitic and equant, and lath shapes of plagioclase can be recognized. The modal abundance of plagioclase (20 vol. %) is smaller than that of pyroxene. Pigeonite crystals show fine exsolution textures parallel to (001) comparable to those of Juvinas and the augite lamellae are barely resolvable by the microprobe. A large grain of pigeonite may be partly inverted in different orientations. The bulk composition of the pigeonite is $Ca_8Mg_{50}Fe_{42}$, which is more Mg-rich than those of Moore County and Y791195 and is comparable to those of cumulate eucrites, Serra de Magé and Nagaria. The An contents of plagioclase range from 95 to 90, which represent the original chemical zoning during rapid crystal growth. The range is smaller than Juvinas but is larger than Nagaria (Fig. 2).

(2) Chemical Trends and Crystal Fractionation.

Each data point of the An versus mg number diagram (Fig. 3) represents an average of 3 to 10 measurements obtained by an electron microprobe for a coexisting pyroxene-plagioclase pair of a lithic clast in the Y-75032 group specimens and Y-791466. The region from cumulate eucrite to ordinary eucrite trend (dotted line in Fig. 3) is taken from Takeda and Mori (2). Open squares show the range of crystalline clasts for four diogenite-rich meteorites of the Y-75032 group (Y-75032, Y-791199, and Y-791422). The Y-75032 group, except for cumulate-eucrite-rich members (Y-791200, Y-791201 and Y-791439) defines the vertical trend with nearly constant mg number. Because the mg numbers of pryoxenes in these diogenite-rich rocks are within a small range (64 to 69), the trend is defined by the An values of plagioclase fragments from 91 to 60. The values of the interstitial plagioclases differ very much from one clast to another within one meteorite. Because plagioclase is rare in diogenitic clasts, previously measured data poorly defined the diogenitic vertical trend. Now, the Y-791466 clasts define more clearly the vertical trend and extend to more An poor side (Fig. 3). The variation of the chemical compositions and the interstitial occurrence of plagioclase between pyroxene crystals indicate crystallization from intercumulus trapped liquid.

The nearly horizontal trend is defined by cumulate eucrite clasts in Y-791201 (solid circle) and partly by those in Y-791200. Some Clasts in Y-791200 are within the diogenitic trend. The data of Y-791201 appear to distribute in the cumulate eucrite to ordinary eucrite trend. This main eucritic trend may represent crystal fractionation in the HED magma ocean. It is to be noted that the two trends start at a point where the first phase to appear from the eucritic partial melt.

Bulk chemical compositions of the Y-75032 group analysed by H. Haramura (personal communication, 1983) were utilized to compare Al_2O_3 versus CaO (wt %) plots with those of the known HED achondrites (5,6,7). All the data of the Y-75032 group in these figures are located intermediate to diogenite and the most Mg-rich cumulate eucrites and howardites. The bulk composition of Y-791466 has not been analysed but the existence of plagioclase suggests that it will plot in this region. The bulk chemical composition of Y791438 estimated by the modal combination method plots near Binda. The texture of Y-791438 is not cumulate and one explanation for it is that Y-791438 reflect a liquid composition of the HED magma ocean in an early stage. From the bulk Y-791438 composition and a partition coefficient of Mg/Fe between pyroxene and liquid, we computed the mg number of a pyroxene, which will be crystallized from a magma of the bulk Y-791438 composition. The value we obtaind (mg=80) is well in the magnesian range of diogenites commonly found in normal howardites. Discovery of a magnesian eucrite with ordinary eucrite (non-cumulate) textures and the An-variation trend of diogenite suggests the presence of a Mg-rich magma that may have crystallized diogenites as a cumulate and supports the plausibility of the fractional crystallization model.

Phase equilibrium constraints on the HED association by Longhi and Pan (3) showed that simple fractionation crystallization at 2 kbar can account for many of the mineral and chemical features of the diogenite-eucrite association. However, its plausibility was strained by the absence of volcanic equivalents of the Mg-rich magma that crystallized the diogenites. Now, since we found such a Mg-rich volcanic eucrite and the cumulate

orthopyroxene trend, the differentiation from the HED magma ocean seems plausible. The magma ocean at 2kbar appears to be too deep, but if we accept a two stage model by Takeda et al. (4), the crystal fractionation can take place in a shallow magma ocean. The two stage model assumes that accreating source materials to the surface of the magma ocean bring the magma composition back on the olivine-pyroxene cotectic line, where crystal fractionation of pyroxene still proceed.

We thank National Inst. of Polar Res. (NIPR) for the sample and the Mitsubishi Foundation for support.

References: (1) Yanai K. and Kojima H. (1987) Photo. Catalog of the Antarctic Meteorites. 298 pp. NIPR, Tokyo. (2) Takeda H. and Mori H. (1985) Proc. Lunar Planet. Sci. Conf. 15th, JGR 89, C636-C648. (3) Longhi J. and Pan V. (1988) Proc. Lunar Planet. Sci. Conf. 18th, 459-470. (4) Takeda H., Mori H., Ikeda Y., Ishii T. and Yanai K. (1984) Mem. Natl Inst. Polar Res., Spec. Issue No.35, 81-101. (5) Mason B. (1962) Meteorites, 274 pp., Wiley, New York. (6) Mason B., Jarosewich E., and Nelen J. A. (1979) Smithson. Contrib. Earth Sci., 22, 27-45. (7) Fredriksson K., Noonan A., and Brenner P. (1976) Meteoritics, 11, 278-280. (8) Stolper E. (1977) Geochim. Cosmochim. Acta 41, 587-611.

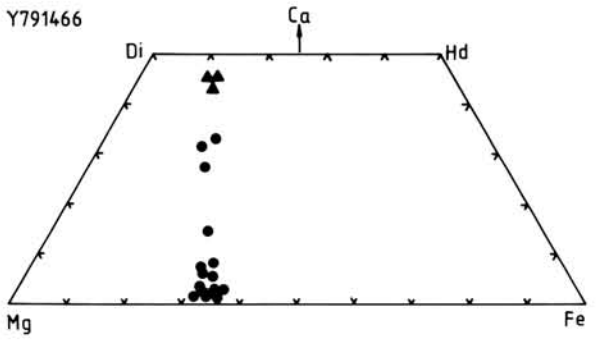

Fig. 1. Pyroxene quadrilateral of Y-791466 achondrites. A dot represents the composition of one pyroxene grain by point analysis.

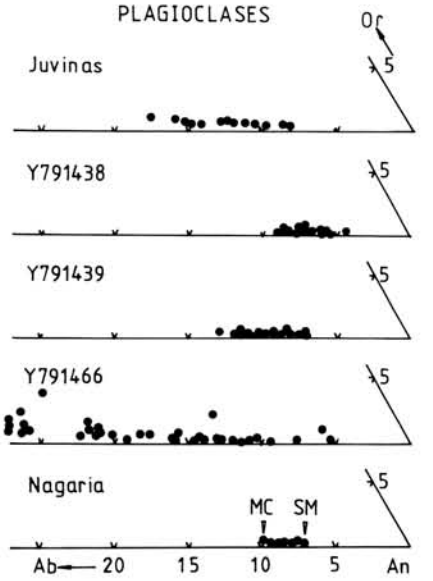

Fig. 2. Plagioclase compositions of Y-791466 and related HED's. MC and SM: cumulate eucrites.

Fig. 3. The relation between An of plagioclase and the mg numbers= MgX100/(Mg+Fe) in coexisting pyroxene in the HED crust. Solid squares: Diogenitic clasts in Y-791466: open squares: Y-75032, Y-791000, Y-791199; open circles: clast in Y-791200; solid circles: cumulate eucrite clasts in Y-791201; dotted lines: ordinary and cumulate eucrites (6). Hexagon: first phase to appear from the eucritic melt (8).

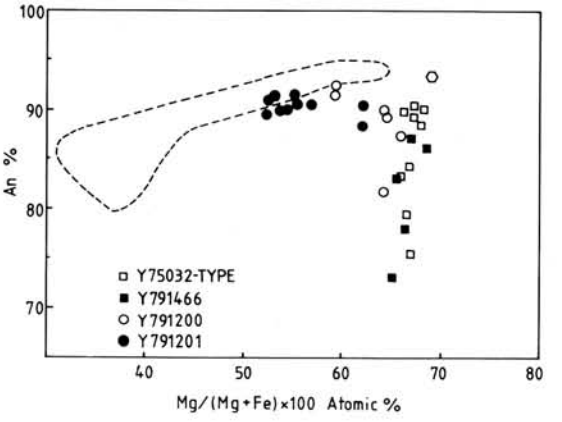

EUCRITIC ENCLAVES IN THE MT.PADBURY AND VACA MUERTA MESOSIDERITES

Ikeda, Y.(*), Ebihara, M.(**), and Prinz, M(***).
(*) Ibaraki Univ., (**) Tokyo Metropolitan Univ., and (***) Amer. Mus. Nat. His.

Three eucritic enclaves from Mt. Padbury, six eucritic enclaves from Vaca Muerta, and one eucrite ("Chile") which might be an enclave from Vaca Muerta, were petrologically studied. Their texture, grain size, and degree of exsolution of pigeonites are shown in Table 1. They consist mainly of plagioclase and pigeonitic pyroxene with minor and variable amounts of silica-mineral, orthopyroxene, chromite, ilmenite, phosphate, rutile, troilite, and Fe-metal. Plagioclases range from An_{82} to An_{97}; those are the most sodic in enclave Z (An_{82-91}), and the most calcic in enclave H (An_{95-97}). Chemical compositions of pyroxenes in each enclave are shown in Fig. 1. The MgO/(MgO+FeO) mole ratio (mg) of low-Ca pigeonites ranges widely from 0.30-0.35 in enclave Z to 0.60-0.63 in enclave H. Clinopyroxenes in enclave Z show remarkable continuous zoning from ferroan pigenite core to magnesian augite rim. This suggests that crystallization of augite in enclave Z took place under a reducing condition. Orthopyroxenes in enclave Z are magnesian (mg= 0.63-0.66) and occur in mesostasis together with magnesian augite. Orthopyroxenes in enclaves 4630, 4633, 891, and H, occur surrounding pigeonite grains, showing a replacing texture. They are always more magnesian than replaced pigeonites (Fig. 1), indicating that reduction took place under a reducing condition at subsolidus temperatures. Chromites show chemical variation similar to that of chromites in HED meteorites. Ni contents of Fe-metals range from 2 wt% up to 20 wt% except for those in eucrite 4627 where the Ni content is zero. Rutiles occur in enclave 4632 as exsolution lamellae or single grains in ilmenite. Phosphates are mostly whitlockite although fluorapatite occurs in enclave 4627 and Fe-phosphate in 4631.

Bulk chemical compositions of enclaves were obtained using a broad beam (about 50 microns in diameter) of an electron-probe micro-analyser with a correction method of Ikeda (1983), and neutron activation analyses were carried out for enclaves 4631, 4632, 4630, and 4633 and eucrite 4627. They show remarkable positive Eu anomaly, and C1-normalized REE contents are larger than 1 for 4627, 4631, and 4632, but those are smaller than 1 for 4630 and 4633. Petrography, mineral composition, and bulk chemical compositions suggest that enclaves Z, U, 914, 4631, and 4632 and eucrite 4627 are non-cumulate, and enclaves H, 891, 4630, and 4633 are cumulate or crystal mush.

Five enclaves among nine enclaves studied have suffered

reduction during late-stage crystallization or at subsolidus temperatures, and these facts suggest that eucritic enclaves in mesosiderites came from a parent body different from that of HED meteorites.

Table 1. General remarks on the enclaves studied.

Enclave	Mesosiderite	Grain size	Texture	Exsolution	Subsolidus reduction
Z	Mt. Padbury	fine	ophitic	no	no
U	Mt. Padbury	medium to fine	subophitic to porphyritic	moderate	no
H	Mt. Padbury	coarse	gabbroic to granular	remarkable	remarkable
891	Vaca Muerta	coarse	gabbroic to granular	remarkable	moderate
914	Vaca Muerta	coarse	gabbroic to granular (prefered Ori.)	moderate	no
4630	Vaca Muerta	coarsae	gabbroic	moderate	remarkable
4631	Vaca Muerta	medium	gabbroic	moderate	no
4632	Vaca Muerta	medium	subophitic to porphyritic	moderate to weak	no
4633	Vaca Muerta	coarse	gabbroic to granular	remarkable	weak
4627	Vaca Muerta(?)	coarse	gabbroic	weak	no

Fig. 1 (next page). Chemical compositions of pyroxenes in nine enclaves and one eucrite (4627). Small solid circles are pigeonite, augite, and mixtures of pigeonite, augite, or hypersthene, and large solid circles are hypersthene. Note that clinopyroxenes in enclave Z show remarkable zoning from ferroan pigenite core to magnesian augite rim and that hypersthenes are always more magnesian than coexisting pigeonites.

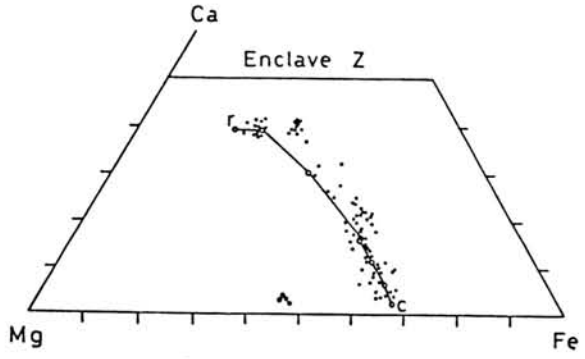
Ca
Enclave Z
Mg
Fe

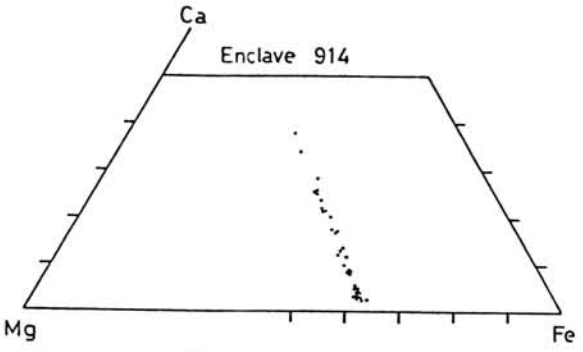
Ca
Enclave 914
Mg
Fe

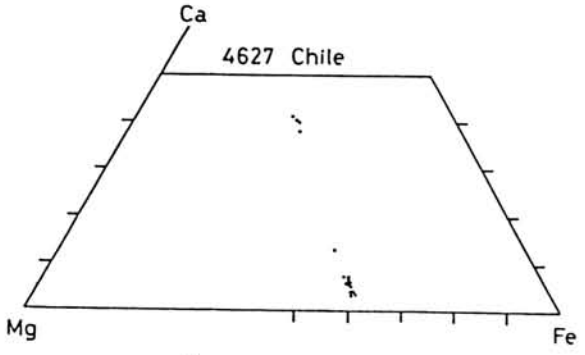
Ca
4627 Chile
Mg
Fe

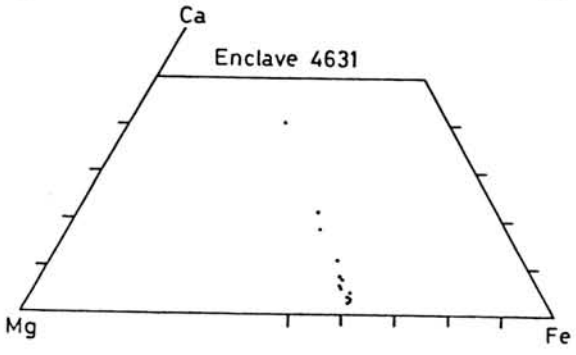
Ca
Enclave 4631
Mg
Fe

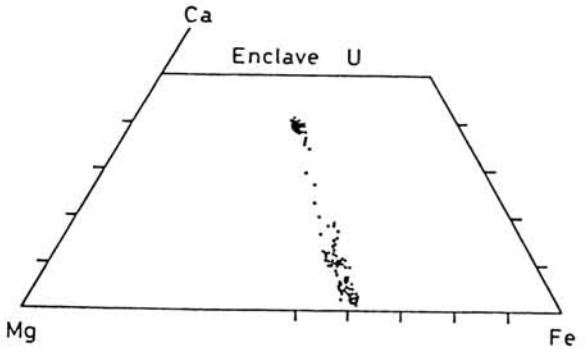
Ca
Enclave U
Mg
Fe

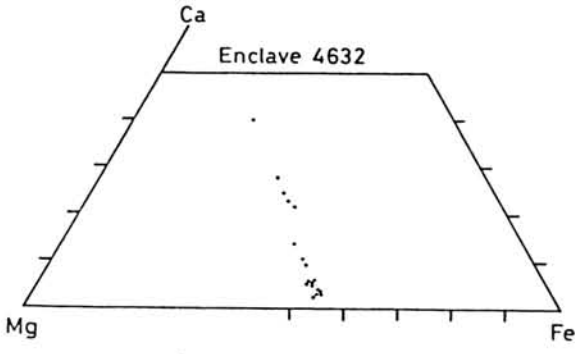
Ca
Enclave 4632
Mg
Fe

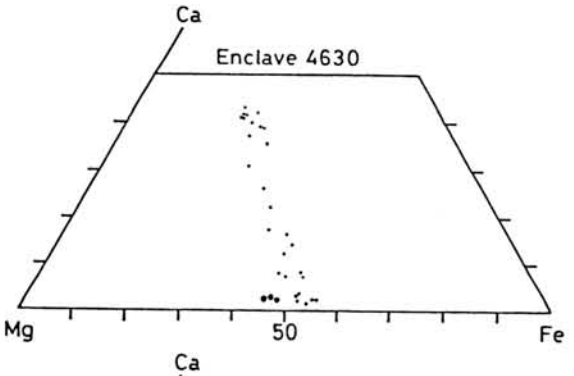
Ca
Enclave 4630
Mg
50
Fe

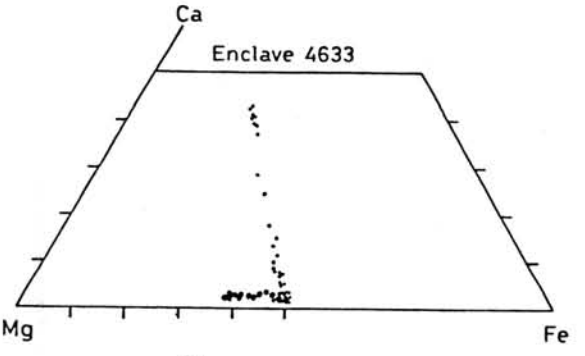
Ca
Enclave 4633
Mg
Fe

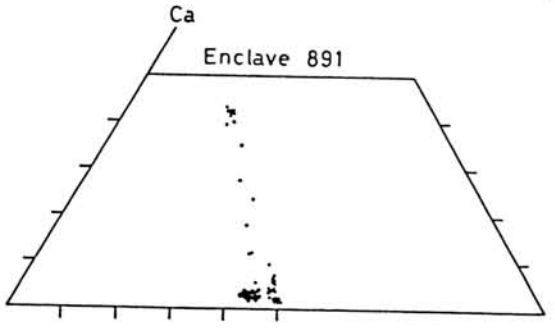
Ca
Enclave 891

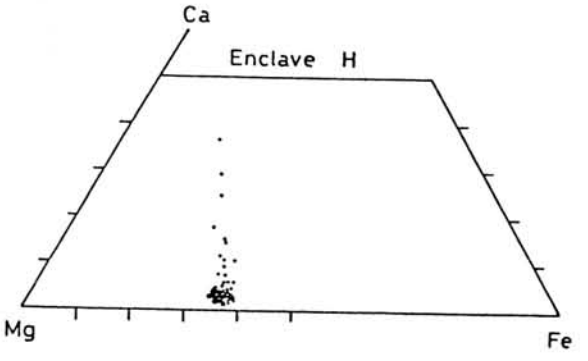
Ca
Enclave H
Mg
Fe

DENSITIES OF EXPERIMENTAL REPRODUCED DIOGENITIC PYROXENES AND EUCRITIC MELTS

ISOBE, Hiroshi

Dept. of Environ. Safety Res., Japan Atomic Energy Res. Inst.,
Tokai, Ibaraki, 319-11

The howerdite, eucrite and diogenite (HED meteorites) are generally considered to have been fractionated during a magmatic process in their parent body. The essential mechanism of this differentiation processes should be the separation of crystals from the liquid. In order to determine separation behaviors of crystals in the liquid, the difference in density among crystals and the liquid and the viscosity of the liquid. Supposing that coexisting crystals and the liquid keep an equilibrium, the bulk composition of the system determine the compositions of the crystals and the liquid at the given temperature. These chemical compositions has been then used to calculate densities and viscosities of the system.

Previously, we have carried out phase equilibrium experiments of a chondritic material to simulate the evolutional processes of the HED and pallasite parent body, [1] and examined the possibility of separation of olivines from the coexisting melt in the system [2]. Based on our results, an initially chondritic material has partially melted to yield the pallasitic olivine and the melt. The composition of the liquid can be considered to be a mixture of diogenites and eucrites at around 1400°C (Fig. 1) [1]. In this system, the sinking velocity of olivines was maximum also at around 1400°C based on the calculation of density difference and viscosity. Therefore, it has been concluded that the first stage of the fractionation process should have occured at around 1400°C [2].

In the present study, the second stage of the fractionation process is examined based on the results of the phase equilibrium experiments of the starting material whose composition is the mixture of 55% diogenite and 45% eucrite. In the run products, pyroxenes, minor olivines and chromites coexist with melts in the temperature range of 1140°C to 1330°C. Plagioclases are also found below 1160°C. Compositions of pyroxenes in this temperature range are plotted in a pyroxene quadrilateral (Fig. 2). Crystallized pyroxenes are orthopyroxenes from 1330°C to 1180°C, and pigeonites below 1160°C. On the other hand, compositions of melts are plotted in the 'pseudo-liquidus' diagram [3] (Fig. 1). Their compositions are very close to noncumulate eucrite at around 1200°C.

Because diogenites consist mainly of orthopyroxene (En 73~77, Wo ~1), the compositions of melts and pyroxenes in the temperature range of 1180°C to 1330°C are determined as functions of temperature. Densities of melts are then calculated by using

the equation of Bottinga and Weill [4] and their viscosities are also calculated by using the tables of Bottinga and Weill [5]. Densities of orthopyroxenes at room temperature can be calculated by their molar volume and unit cell parameters. Their thermal expansion coefficient increases linearly under 1000°C [6,7]. Consequently, the densities of orthopyroxenes at temperatures of 1140°C to 1330°C are calculated by extraporating this linear function.

The calculated densities of melts and orthopyroxenes are shown in Fig. 3. The density of melt slightly increases at temperatures below 1240°C. On the other hand, the density of pyroxene decreases monotonously. A curve labeled 'A' represents its density for the case that the expansion coefficient of Sueno et al [6] is simply extraporated to higher temperatures and a curve labeled 'B' represents the density on the extreme exagaration that expansion coefficient above 1000°C is ten times larger than that at lower temperatures. In any case, density differences between melts and pyroxenes increase with decreasing temperature.

Sinking velocities of a same size of pyroxenes calculated from viscosities and density differences increase with increasing temperature. Calculated typical sinking velocity of 1mm pyroxene is 10^{-6}m/sec and this is one tenth of that of pallasitic olivine [2]. However, the sinking velocity of crystals is proportinal to the square of the crystal diameter. Consequently, the separation process of diogenitic pyroxene depends chiefly upon its grain size and so its cooling and crystal growth histories should be considered. These data provide bases for the reconstruction of evolutional processes of HED and pallasite parent body.

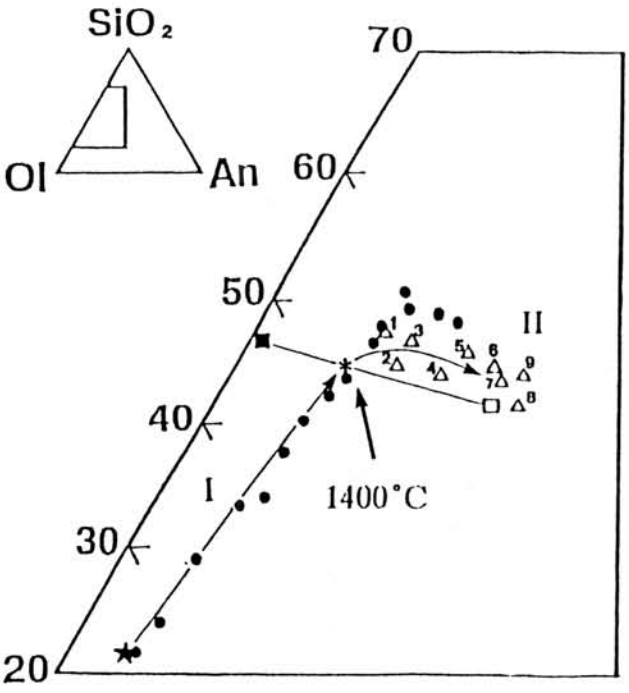

Fig. 1 Compositional change of melts shown in the 'pseudo- liquidus' diagram [3] for the two series of phase equilibrium experiments at different temperatures.
■ : Average diogenite
□ : Average noncumulate eucrite
I: First experiments [1]
★ : Starting material
● : Melt compositions from 1600°C to 1280°C
II: Second experiments
✻ : Staring material
△ : Melt compositions
Numbers coreespond to the following temperatures (°C):
1:1330, 2:1300, 3:1280, 4:1250, 5:1220, 6:1200, 7:1180, 8:1160, 9:1140

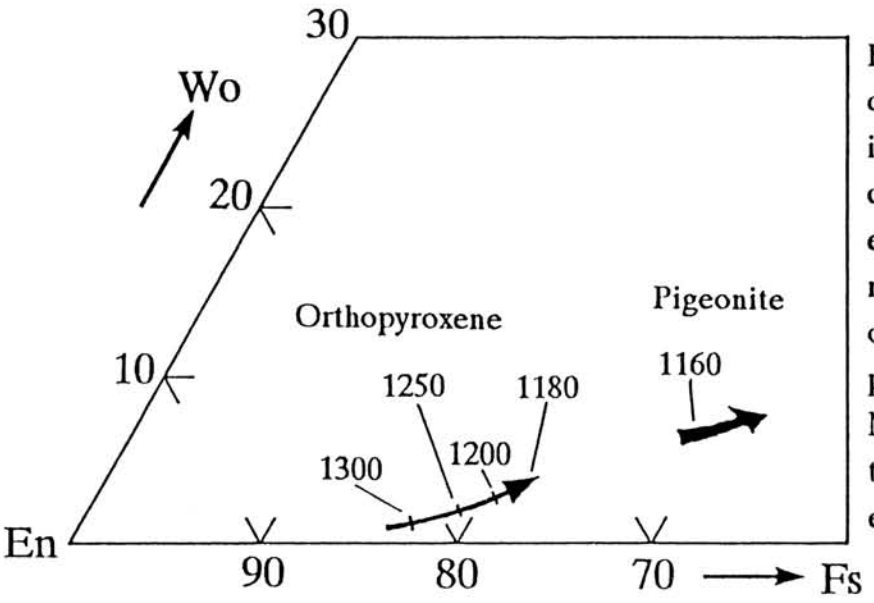

Fig. 2 Compositional change of pyroxenes shown in a pyroxene quadrilateral during the second experiments. Two arrows represent trends of orthopyroxenes and pigeonites, respectively. Numbers correspond to the temperatures of the experiments.

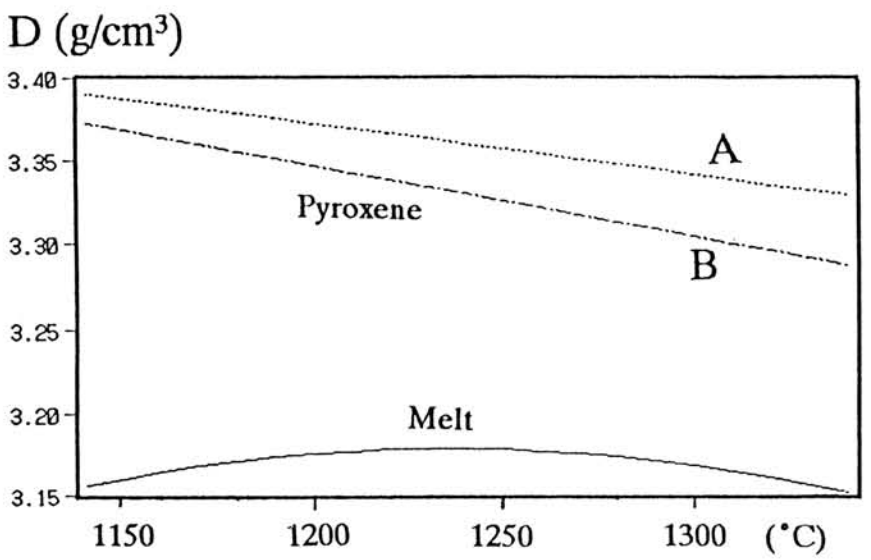

Fig. 3 Calculated densities of pyroxenes and melt. Curve B is calculated based on the thermal expansion coefficient which is ten times larger than that of A above 1000 °C.

References: [1] Isobe, H. et al, (1988) Abstr. 19th Symp. Antarctic Meteorites, 65-67, NIPR. [2] Isobe, H. (1989) Abstr. Symp. "Meteorites and the Origin of the Solar System", 45-47. [3] Stolper, E. (1977) Geochim. Cosmochim. Acta, **41**, 587-611. [4] Bottinga, Y. & Weill, D. F. (1970) Amer. Jour. Sci., **269**, 169-82. [5] Bottinga, Y. & Weill, D. F. (1972) Amer. Jour. Sci., **272**, 438-75. [6] Sueno, S. et al, (1976) Amer. Mineral., **61**, 38-53. [7] Smyth, J. R. (1973) Amer. Mineral., **56**, 636-48.

HIGH DISLOCATION DENSITIES OF RELICT MINERALS IN CHONDRULES

Seiko Watanabe and Masao Kitamura
Department of Geology & Mineralogy, Faculty of Science, Kyoto University, Sakyo, Kyoto 606, Japan

Fine textures of relict minerals in chondrules can give informations on the formation of chondrules. Watanabe et al. (1984) studied dislocation structure of a relict olivine grain, and suggested that chondrules may have formed by shock melting. On the other hand, Kitamura et al. (1988b) carried out shock experiments and supported shock origin of chondrules. In this study, dislocation structure of relict olivine grains in a chondrule and that of anomalous pyroxene grains in ALH-77015 (L3) were studied by a transmission electron microscopy (TEM) to confirm that the high dislocation density is common to the relict grains.

olivine

A porphyritic chondrule consists mostly of olivine, pyroxene (Fs_{-2}), troilite and glass. Olivine grains have dusty core and clear rim, but central parts of the cores are inclusion-free. Here the central inclusion-free and the outer inclusion-rich parts of the core are mentioned as inner- and outer-core, respectively. Composition of olivine by EPMA is about Fa_7 around the inner-core and about Fa_{15} around the outer-core and rim. The dusty inclusions are Fe-metal by qualitative analyses.

Analytical electron microscopy (AEM) shows that Fe/Mg of the olivine changes not monotonically around the boundary between the rim and core; it decreases gradually in the rim toward the core, once increases abruptly, and then decreases inwards again in the core. Kamacite inclusions were identified by electron diffraction and AEM in the outer-core. In addition, tiny and coarser Cr-spinel grains were observed in the inner- and outer-core, respectively. Both types of Cr-spinel have crystallographic relation with host olivine. Most dislocations of the olivine have Burgers vector of [001]. Dislocation densities are 10^7-10^8 cm^{-2} in the rim, and $5x10^8$-10^9 cm^{-2} in the outer-core. In the inner-core, dislocations are relatively low in density, and are localized around the Cr-spinel. The dislocations are of screw and mixed types in the rim and outer-core, and screw, edge and mixed types in the inner-core.

pyroxene

Two types of pyroxene grains were studied by TEM.

(i) pyroxene with SiO_2 inclusions

In a pyroxene chondrule, clinoenstatites have many SiO_2 inclusions. Rim of the clinoenstatites is inclusion-free, and poorer in Fe (Fs_{2-4}) than core (Fs_{2-4}) with the inclusions. Similar pyroxene grains were reported in Y-691 (EH3) as relict (Nagahara, 1985; Kitamura et al., 1988a), and were also found in Y-82038 (H3).

Under TEM, the clinoenstatite shows polysynthetic (100) twinning and dislocations. The dislocation density of the clinoenstatite is 3×10^{8} - 10^{9} cm^{-2}. Burgers vector could not be determined. Diffractions pattern from the SiO_2 inclusions was similar to that of low-temperature cristobalite.

(ii) pyroxene with olivine inclusions

An orthopyroxene grain as a mineral fragment has many olivine inclusions in a constant extinction position. Similar pyroxene grains were reported in Y-691 (EH3) as relicts (Kitamura et al., 1988a), and were observed in other ordinary chondrites.

In the orthopyroxene, (100) twinning and dislocations were abundantly observed by TEM. The dislocation density was 10^{8} - 10^{9} cm^{-2}. Burgers vector of the dislocations could not be determined, but at least was not [001], which are commonly reported for pyroxenes. Between the olivine inclusions and host orthopyroxene, no simple relation in the crystallographic orientation was found by electron diffraction.

The high densities of the [001] dislocations in the relict olivine grains in this and previous studies indicate that they are common characteristics of relict olivine. The high dislocation densities of the anomalous pyroxene grains suggest that they also are relicts. In olivine, the Burgers vector of [001] predominates to [100] not in usual terrestrial rocks but in a shock experiment product (Mori et al., 1982). This fact and the high dislocation density in the cores suggest a shock event during or before the chondrule formation. Therefore, shock melting is preferred as a model for the formation of chondrules.

[REFERENCES]

Kitamura et al., (1988a) Proc. NIPR Symp.Antarct.Meteorites, 1, 38-50.

———— (1988b) Papers presented to the 13th Symp. Antarct. Meteorites, 121-122.

Mori et al. (1982) Mineral.Soc.Japan, 1982 Annual Meeting Abstracts with Programs, 66.

Nagahara (1985) Papers presented to the 10th Symp. Antarct. Meteorites, 12-14.

Watanabe et al. (1984) Mem.Natl.Inst.Polar Res., Spec.Issue, 35, 201-209.

SHOCK-MELTING ORIGIN OF CHONDRULES

Masao KITAMURA, Akira TSUCHIYAMA, Seiko WATANABE,
Department of Geology and Mineralogy, Faculty of Science,
Kyoto University, Sakyo, Kyoto 606, Japan

Yasuhiko SYONO and Kiyoto FUKUOKA
Institute for Materials Research, Tohoku University,
Katahira, Sendai 980, Japan

Origin of chondrules has been presented as the most attractive theme of meteoritics. Findings of relict minerals survived from melting during the chondrule formation gave an incontestable evidence of the existence of precursor materials of chondrules. Textures of relict minerals gave informations on both the precursor materials and the process of chondrule formation. High dislocation density of the relict olivine and pyroxene in chondrules (Watanabe et al., 1984; Watanabe and Kitamura, 1989) suggests the shock melting of the chondrule formation.

A few shock experiments have been carried out on chondrites (e. g. Sears et al., 1984). A shock experiment on the complete melting of a porous mineral-mixture with solar abundance has also been carried out (Arakawa et al., 1987). However, the melting process of chondritic material by shock-loading has not been clarified. Recently, Kitamura et al. (1988) carried out shock experiments of both a chondrite and its powders with different porosities. Some of the run products have clusters of brecciated minerals and melt pockets. In the present paper, the textures and compositions of the clusters and the melt were studied, and dislocation structures of olivine and pyroxene were observed under a transmission electron microscope (TEM). The characteristics of the run products were compared with those of chondrites. From their resemblance, we support shock-melting as an origin of chondrules.

Three types of specimens (Cedar, H6) with different porosities were shock-loaded (Kitamura et al., 1988) ; (I) a rock chip (the porosity is a few %), (II) powders of the chondrite with porosity of about 28 %, (III) powders with porosity of about 43 %. Two different speeds of a flyer were chosen for each type of the specimen; 1.20 and 1.94 km/sec, which correspond to the pressure on the capsule of 25 and 45 GPa, respectively. The actual pressure on the specimen, however, was not be estimated because shock impedances of the specimens have not been obtained.

The type I specimens show no melting textures but shock veins running at about 45^{o} with the direction of the shock propagation. In the type II and III specimens, the shock veins were not found clearly. Back-scattered electron images revealed that interstices among large grains of olivine, pyroxene and plagioclase (maskelynite) are the cluster of brecciated minerals or the melt pockets. Eutectic melting of Fe and FeS was also observed. The number of the clusters and the melt pockets

increases with the porosity and the shock pressure.

The clusters of brecciated minerals consist of fine grains of olivine, pyroxene, plagioclase (maskelynite), Fe-metal, FeS, and the interstices of glass. Fe content in the bulk composition of the clusters varies widely, because of the heterogeneous distribution of Fe and FeS. Except for the Fe content, the bulk compositions of the clusters scatter only in a small range around that of the starting materials . This suggests that all kinds of the silicate minerals in the starting materials were brecciated and gathered in the clusters.

The melt pockets are surrounded by large grains of olivine, pyroxene and plagioclase (maskelynite), and sometimes include these minerals, Fe metal and FeS. The compositional range of the glass avoiding Fe-blebbs is similar to that of the bulk composition of the clusters, and then that of the starting materials. Therefore, the bulk compositions of the melt pockets indicate that the melting occurred through the formation of the clusters.

One of the run products (type III specimen) was ion-thinned for TEM. Clear glass and fine grained aggregates were found among large grains of pyroxene, olivine and others. Olivine grains have high dislocation density of more than 10^9 cm^{-2}. Pyroxene grains have lots of twins and also high dislocation density. These textures of olivine and pyroxene grains resemble to those of the relict minerals in chondrules (Watanabe and Kitamura, 1989).

Ordinary chondrites generally include chondrules, coarse grained lithic fragments and fine-grained aggregates (FGA's) which are chondrules with small degree of partial melting (Watanabe et al., 1987). The bulk compositions of chondrules and FGA's scatter around the solar abundance.

The clusters and the melt pockets have the similar compositional range as chondrules and FGA's. The clusters resembles FGA's in their textures such as grain size. The texture that the melt pockets include olivine and other minerals also resembles to that of chondrules including the relict minerals. The high dislocation densities of the relict minerals are well explained by the shock-loading. These facts suggest that shock melting can produce similar materials as chondrules and FGA's. Coarse grained lithic fragments in chondrites can also be explained to be formed from brecciation of minerals by shock-loading.

Among the constituents of ordinary chondrites, only matrix is not simply explained by the shock-loading of the precursor materials. However, the shock-loading might lead vaporization of the starting materials. Vapor generated by the shock-loading can spread out to some extent as an adiabatic expansion. This adiabatic expansion leads the lowering of pressure and temperature of the gas, resulting in rapid crystallization of dust from the gas. The origin of the matrix materials can be explained in this kind of the process after the shock-loading of the materials.

References

Arakawa,M., Sawamoto,H., Urakawa,S., Kato,M., Mizutani,H. & Kumazawa,M. (1987) Experiment of shock-compression for the chondritic materials. Abstract in "Koatsu-toronnkai". 3C13.

Kitamura,M., Tsuchiyama,A., Watanabe,S., Syono,Y. & Fukuoka,K. (1988) Melting and deformation of a chondrite by shock-loading. 13th Symposium on Antarctic meteorites (abstract) pp.121-122.

Sears,D.W., Ashworth,J.R., Broadbent,C.P. & Bevan,A.W.R. (1984) Studies of an artificially shock-loaded H group chondrite. Geochimica et Cosmochimica Acta vol. 48, 343-360.

Watanabe,S., Kitamura,M. & Morimoto,N. (1984) Analytical electron microscopy of a chondrule with relict olivine in the ALH-77015 chondrite (L3). Mem. Natl. Inst. Polar Res., Spec. Issue 35, 200-209.

Watanabe,S., Kitamura,M. & Morimoto,N. (1987) Fine-grained aggregates in L3 chondrites. Earth Planet. Sci. Lett., 86, 205-213.

Watanabe,S. and Kitamura,M. (1989) High dislocation densities of relict minerals in chondrules. 14th Symposium on Antarctic Meteorites (abstract).

Mechanical and Morphological Characterization of Shock Effects in Antarctic Meteorites (II) - Hardness & Grain Shape Analysis of Metallic Particles-

Horii,Y., Fujii,N.
Dept. Earth Sci., Faculty of Sci., Kobe Univ., Nada, Kobe 657

Takeda,H.
Mineral. Inst., Faculty of Sci., Univ. Tokyo, Bunkyo, Tokyo 113

Introduction

Shock effects recorded in meteorites have been described by mineralogical-petrochemical approaches, such as undulation of plagioclase and Olivine grains (Dodd 1981), and hardness of metallic grains (Sears et al., 1984). Although these approaches are compared with results of shock experiments. It is likely that most of shock effects in porous and mechanically heterogeneous samples must be inhomogeneous in micro-scale observations. We intended to obtain quantitative parameters of shock effects. In this paper, we focused on the mesurements of [1] Ni content by SEM-EDS, [2] Micro Vickers Hardness, [3] Fractal dimension of metallic grains (Fe-Ni & FeS), in four shocked chondrites (Y-82163[H],Y-790964[LL], Y-790519[LL],Y-790964[LL]), and seven unshocked chondrites (ALH-77233[H4],ALH-77115[H6],Y-74191[L3],ALH-77230[L4],ALH-77254 [L5],ALH-77231[L6],Y-75258[LL6]).

Micro Vickers Hardness Testing

Micro Vickers Hardness Testing is one of hardness indicators by indentation of a diamond and it reflects the hardness of a flat surface area of about 10 microns.

Hardness in metallic grains

Fig.1 shows a histgram of hardness in metallic grains. Among these shocked LL chondrites, the largest amount of vesicules are obtained in Y-790964 and the least in Y-790345 (Sato et al., 1982). Results shows that the larger amount of vesicules, the lower the average of hardness.

Ni-content & Hv

Fig.2 shows the relation between hardness and Ni-content in Fe-Ni grains. Most of grains (Ni-content of 4 - 7 wt%) are kamacite, and others are taenite (more than 15 wt%). In taenite grains, the hardness increases with increasing amount of Ni-content, although the presence of transform ε-iron is not confirmed yet.

FD & Hv

Using micro computer aided image processing system, we also analyzed shape of metal grains for polished sample surfaces, and estimated the Fractal Dimension (FD), which is one of the indicators of shape irregulality (Fujii et al., 1983). Fig.3 (a) and (b) show the relations between hardness and FD about H and LL type chondrites. It is concluded that higher values of FD (that is higher irregularity) would correspond to the lower hardness for stacking shock effects more strongly. Fig.4 is an illustlation of Fig.3 (a) and (b).

Fig.1

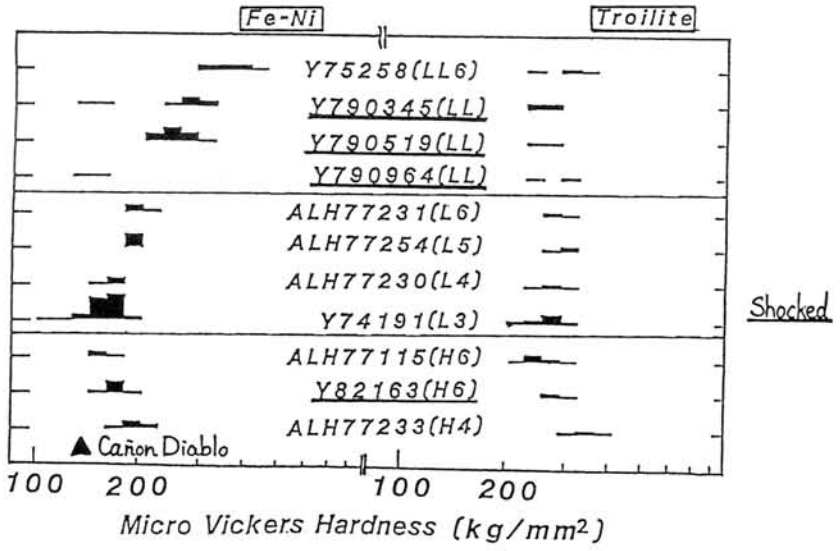

Fig.2

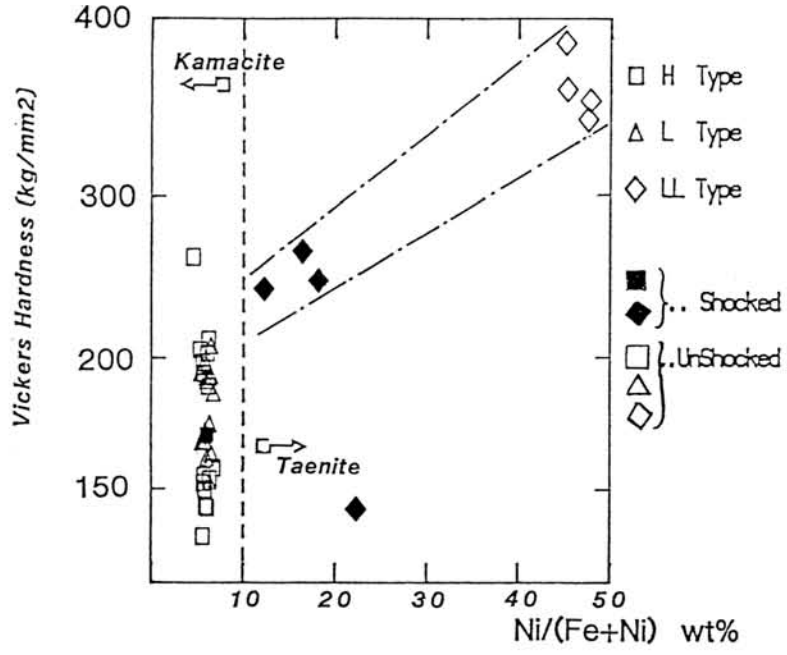

Conclusions

[1] In Taenite grains, the more Ni-content, the higher the value of hardness.

[2] In shocked LL type chondrites, the larger amount of vesicules, the lower the average hardness.

[3] Shock effects are heterogeneous even in microscopic scale, and irregular grains show shock effects more strongly.

Discussion

Shock effects may cause increase of dislocation density so that one might expect the plastic hardening in metallic grains. However our result indicate opposite, which may be explained by thermal annealing properties of Fe-Ni grains, such as cooling rates and the highest temperatures of the samples.

Reference

Sears,D.W., et al.,(1984) Studies of an artificially shock-loaded H group chondrites. Geochim. Cosmochim. Acta,48 343-360.

Dodd (1981) Meteorites ; A Petrological-Chemical Synthesis, 432 pp. Cambridge University Press, Cambridge

Sato et al.,(1982) Impact Melted LL-chondrites of YAMATO 79-collection8th NIPR abstract.

Fujii,N., et al.,(1983) Shape of Fe-Ni grains and magnetic susceptibility anisotropy.NIPR, 30, 389-402

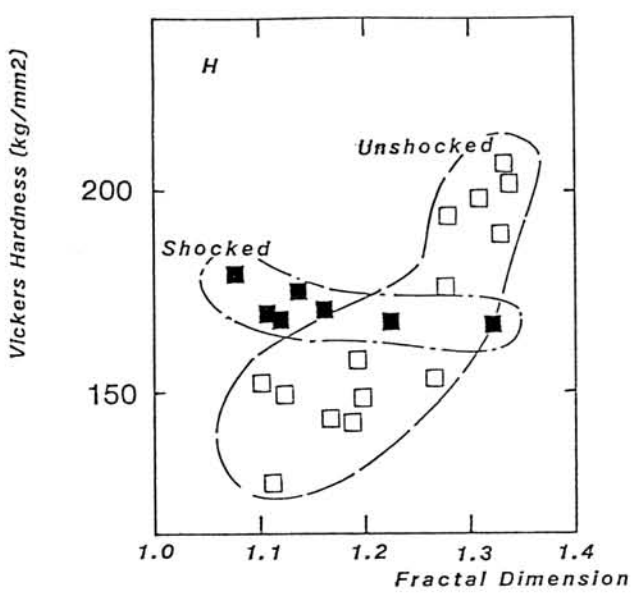

Fig.3(a)

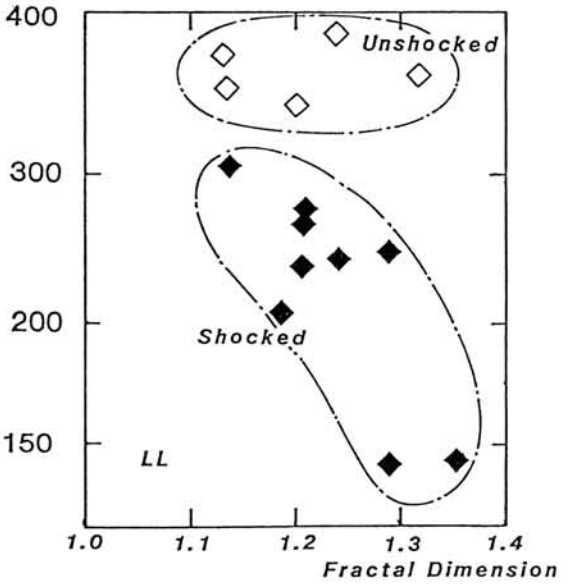

Fig.3(b)

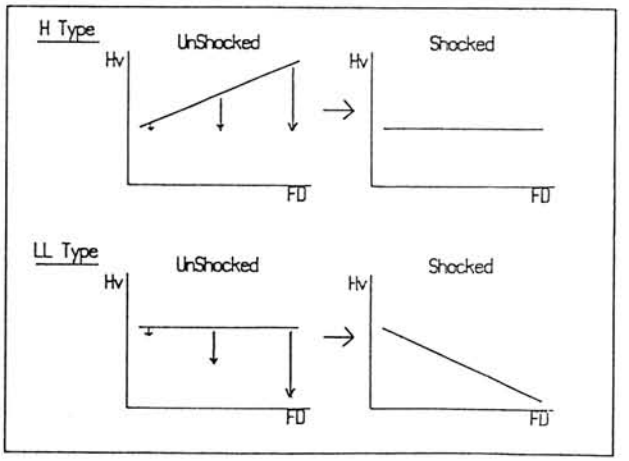

PLAGIOCLASE COMPOSITIONS OF YAMATO-691 CHONDRITE

Yasunori MIURA and Yoshihisa HANAURA
Faculty of Science, Yamaguchi University, Yamaguchi, 753.

1. Introduction

Plagioclase compositions in Yamato-691 chondrite have been reported by Miura (1986) and Ikeda (1988). The purposes of this study are (1) investigation of feldspar crystals with plagioclase composition, and (2) atomic substitution types of Mg-rich plagioclase composition by using optical microscope, EPMA (X-ray color mapping method), SEM, X-ray singlediffraction and computer simulation.

2. Optical, X-ray and SEM images

Na-rich plagioclases in the matrix of the enstatite chondrule are all maskelynite (i.e. glass), though the Ca-rich plagioclases of $An_{70}Or_{1.6}$(core) to $An_{61}Or_{1.1}$(rim) coexisted with Enstatite ($En_{54}Wo_{45}$) and olivine (Fo_{99}) show partly crystalline (Fig. 1).

3. EPMA data and computer simulation

Twenty-nine plagioclase compositions within 3% deviation from stoichiometric chemical formulae show wide range from albite to bytownite (Fig. 2), which are anomalous feldspar data from the previous E chondrite. The plagioclase compositions have been checked by the following "mixing" models and "Mg atomic substitution types" (cf. Fig. 3).

1) Mixing models: Three typical data in the Y-691 are classified as An_{59} (with higher Mg, Si & Ca and lower Al), An_{69} (with standard Si & Al without Mg), and An_{80} (with lower Si, & higher Al higher without Mg). The following three mixing models are used in the analyzed compositions of fassite, enstatite and forsterite. It is found that plagioclase compositions with pyroxene and olivine show lower Al value, and An_{59} plagioclase contains Mg from pyroxene component. Five plagioclase compositions are considered to be the mixing compositions (i.e. maskelynite glass).

2) Mg atomic substitution type from An_{60} to An_{90}: From four types of Mg atomic substitution, the present EPMA data suggest that Mg atoms substitute M-site (i.e. Na site) or T-site (i.e. Al site) from albite composition. But the Mg substitution from the anorthite compositions

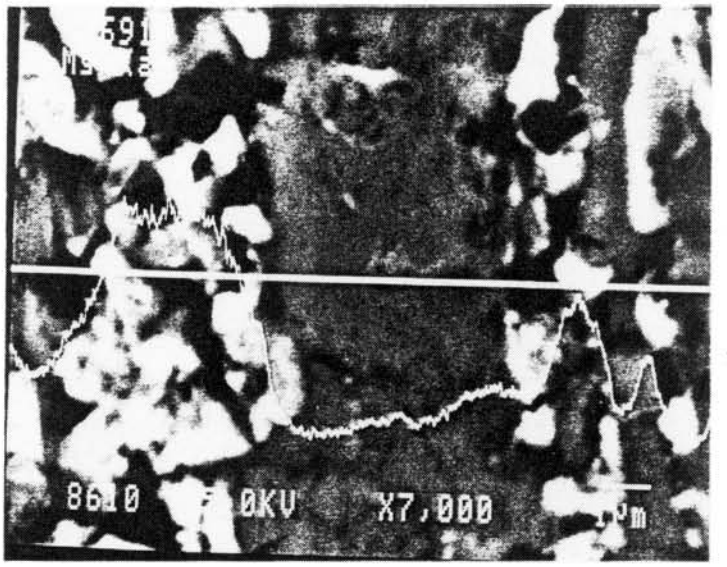

Fig. 1. Plagioclase (An_{70-62}) in pyroxene ($En_{54}Wo_{45}$) chondrule. Line profile of MgKα is crossed between the above two phases.

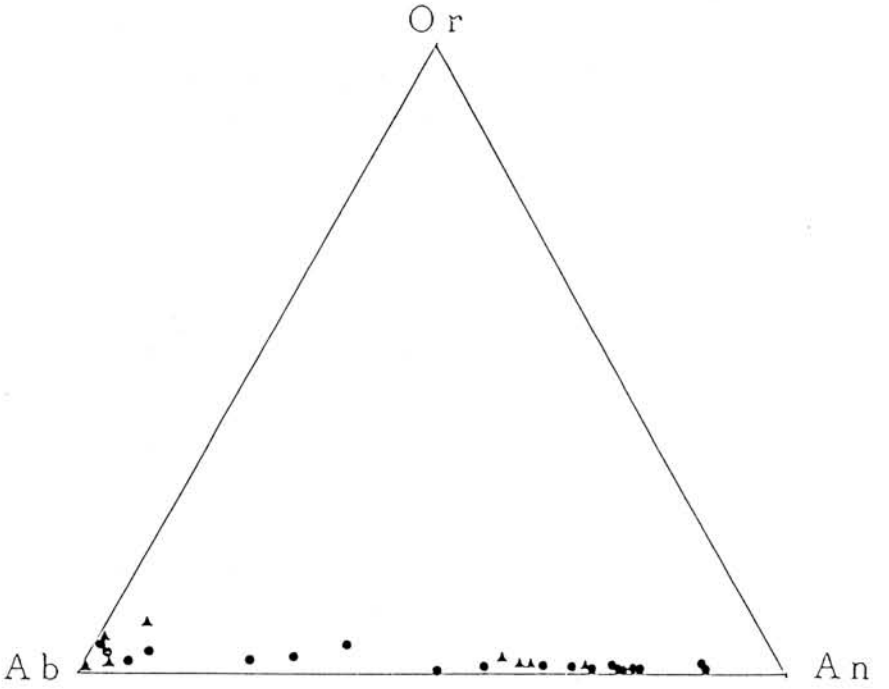

Fig. 2. Plagioclase compositions of Y-691 chondrite in Or-Ab-An diagram.

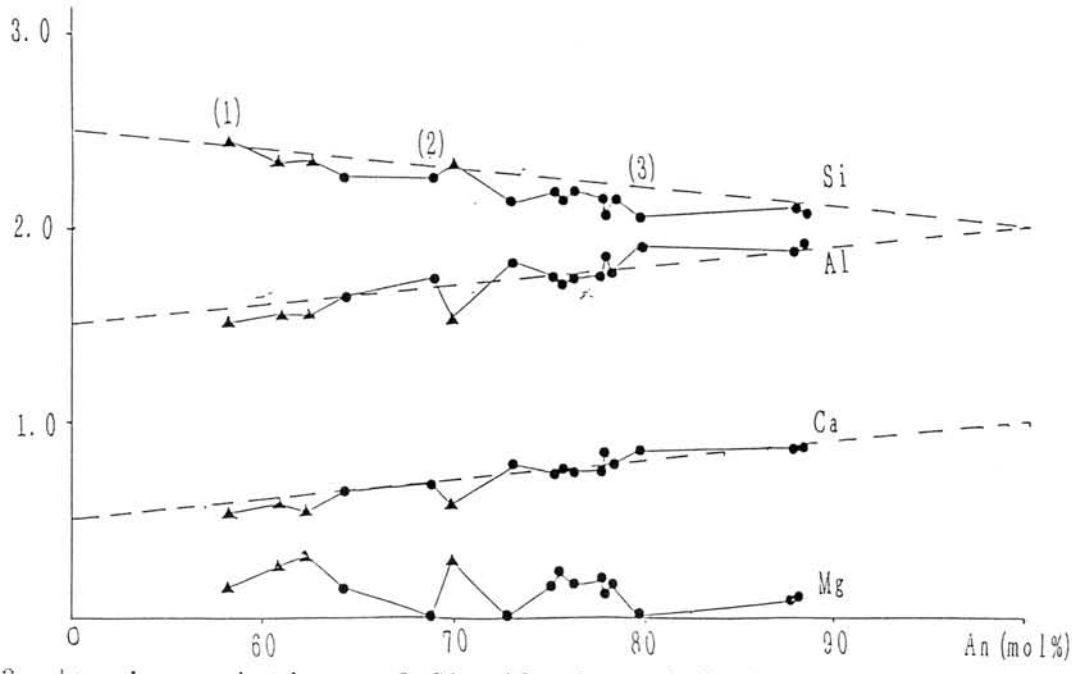

Fig. 3. Atomic variations of Si, Al, Ca and Mg in plagioclase compositions of Y-691 chondrite in An content and atomic ratio in the structural formula (O=8).

is only found in the M-site. Mg atoms increase in Na-rich labradorite composition, which is consistent with the previous result that maskelynite glasses are found in albite or labradorite composition.

4. Formation process

Plagioclase compositions of the Y-691 chondrite are considered to be formed at the various conditions as follows:

(1) reaction of maskelynite with albite composition,
(2) relatively lower temperature reaction to form Mg-bearing plagioclase (at M-site) from albite (-like) composition,
(3) relatively higher temperature and pressure reactions to form Mg-bearing plagioclase (at T-site) from albite (-like) composition,
(4) relatively lower temperature reaction to form Mg-rich anorthite (at M-site) from anorthite (-like) composition.

References:

Ikeda, Y. (1988): Proc. NIPR Symp. Antarctic Meteorites, 1, 1-37.
Miura, Y.(1984): Mem. Natl Inst. Polar Res., Spec. Issue,35,226-242.
Miura, Y.(1986): 11th Symp. Antarctic Meteorites, 101-103.
Miura, Y. and Kato, T. (1989): LPSC XX , 703-704.

VAPORIZATION EXPERIMENTS IN THE SYSTEM PLAGIOCLASE-HYDROGEN: 2. COMPOSITION OF THE GAS AND RESIDUE

Hiroko Nagahara[1], Ikuo Kushiro[1], and Kazushige Tomeoka[2]
1) Geol. Inst., Univ. Tokyo, Hongo, Tokyo 113, Japan, 2) Mineral. Inst., Univ. Tokyo

At the last Antarctic meteorite symposium, we presented results of vaporization experiments in the plagioclase-hydrogen system and demonstrated that plagioclase vaporized incongruently to non-stoichiometric residue and gas with cation ratios with Na:Al:Si=1:1:1 which corresponds to those of nepheline [1] . Additional experiments on plagioclases with different compositions have revealed that the "nepheline" composition was occasionally formed but the gas composition is strongly dependent on starting material composition.

Plagioclases with four different compositions were prepared for starting materials: An_{79} (PL1), An_{62} (PL2), An_{54} (PL3), and An_{30} (PL4). They were heated at 1150° to 1300°C and 10-6 to 1 torr with or without hydrogen gas for 6 to 120 hrs in a furnace placed in a vacuum chamber. After partial vaporization, compositional and textural changes of the residues were studied with SEM, EPMA and TEM.

The chemical compositions of residues and gases are independent of temperature or pressure but are simply dependent on the starting material composition. Chemical compositions of the gases can not directly be analyzed, and those of the residues were plotted on various diagrams to estimate gas compositions. Compositions of the gases must lie on the extension of residue compositions to the opposite side of plagioclase solid solution line. Because the compositions of the residues are on plagioclase join when projected from Si apex of the Si-Na-Ca-Al tetrahedron, the residue and gas compositions must be on a plane including Si and plagioclase solid solution. A question arised is whether the gas contains Ca or not; if the gas does not contain Ca, it should be on the Si-Na-Al-plane and if it does, it should be between the plane and plagioclase. Composition of the gas from PL1 is close to Na:Al:Si=1:1:1 as discussed before [1] , which suggests that the gas consists of Na, Al, and Si and does not have Ca. Accordingly, the gas compositions may be on the Si-Na-Al plane, which indicates that the Na/Al ratio of the gas is always 1 and the (Na+Al)/Si ratio varies with starting material composition. This further indicates that the reaction is shown by a decomposition equation of albite component:

$$NaAlSi_3O_8 \rightarrow NaAlO_2(SiO_2)_x \text{ <gas>} + (3-x)SiO_2 \text{ <residue>}$$

Although the reaction is shown by the equation, gas species are not known. $NaAl_2(SiO_2)_x$ represents bulk composition of the gas, and will be decomposed into several gas species.

Most residues are zoned from less non-stoichiometric core to highly non-stoichiometric surface due to partial vaporization. Highly non-stoichiometric residue which contains scarce Na gives X-ray defraction pattern characteristic to anorthite in spite of non-stoichiometric composition. TEM observation showed that it comprises anorthite and silica. Silica is rectangular or platy and the size is up to 0.1 um, which may be exsolution. It is still not known whether it is crystalline or amorphous.

The present study shows that plagioclase vaporizes non-stoichiometrically which is a function of starting material composition. This is different from olivine which vaporizes stoichiometrically to magnesian residual olivine and gas with iron-rich olivine composition. The difference would be due to the difference in mineral structure.

[1] Paper presented to the 13th symposium on Antarctic meteorites, 34 (1988)

EXPERIMENTAL AND THEORETICAL STUDIES OF SOLID-GAS EQUILIBRIA AND THEIR IMPLICATION TO REDOX REACTIONS IN THE NEBULA.

Tsuchiyama, A.

Department of Geology and Mineralogy, Kyoto University, Sakyo, Kyoto 606.

In the last few years experimental studies of condensation and vaporization have been developed to understand thermal processes in the solar nebula (e.g., [1-4]). Tsuchiyama [5] carried out condensation experiments in the system Mg-Si-O-H, and concluded that correspondence between the condensation experiments and thermochemical calculation for equilibrium was established in this simple but most important system. This strongly suggests that applicability of solid-gas equilibria to condensation in the nebula at high temperatures is verified by experiments.

In the present paper, chondrite formation including redox reactions are discussed based on solid-gas phase diagrams [6] constructed by thermochemical calculations.

Solid-gas phase diagrams. The previous thermochemical calculations (e.g., [7]) have been made in complex natural systems. Accordingly, it was hard to view overall features of solid-gas equilibria, such as redox conditions and fractionation paths for different chemical compositions. It was proposed that phase diagrams in simple systems are useful for the overall view [9]. Furthermore, it was found that the diagrams are simple under nebula conditions ($p(total)=p(H_2)<10^{-3}$bar) (some vaporous boundaries are fixed irrespective of the pressure and the refractory elements/H ratio).

In this point of view, several phase diagrams were constructed for some simple systems including chemically active major elements (H, O, C, Mg, Si, Fe, S and Al). Solid-gas equilibria of non-cosmic compositions [8] as well as those of the cosmic composition can be treated easily in these diagrams.

Redox conditions of chondrites. Redox equilibria can be discussed in phase diagrams by changing H, O and C-contents. Thus, redox conditions of chondrites were estimated from the phase diagrams.

The assemblage of metallic iron and Fe^{2+}-bearing silicates is found in ordinary chondrites. This assemblage is possible at high temperatures only for extremely low H/O ratios compared with the cosmic composition. Thus, ordinary chondrites were considered to be formed under more H-depleted conditions than those in the nebula with the cosmic composition. On the other hand, silicon is dissolved in the metallic iron in enstatite chondrites. This is possible under more reduced conditions (e.g., higher C/O ratio) than those in the nebula with the cosmic composition. It is also seen from the phase diagrams that these reduced conditions were hardly attained by usual solid-gas fractionation because a thermal barrier is present between the

reduced conditions and those in the nebula.

Chondrite formation. Chondrites have the following three features; (1) they are composed of a variety of objects with various chemical compositions (chondrules, lithic and mineral fragments, mineral aggregates, and matrix), (2) the bulk chemical composition is rather uniform in a specimen size for each chemical group of chondrites, and (3) the bulk compositions are different from the cosmic composition except for CI chondrites even for major elements.

The chemical compositions of chondrites were also examined by using the phase diagrams. The Mg/Si and Fe/Si ratios of chondrites can be explained by fractionation of forsterite and iron in the phase diagrams. The following model is favorable for explaining the above features and the estimated redox conditions: (1) formation of pre-chondritic materials in the nebula by solid-gas fractionations from the cosmic composition (the pre-chondritic materials correspond to lower temperature components including ices, and the refractory element compositions were fixed in this process), (2) aggregation of the pre-chondritic materials to form pre-chondritic bodies, (3) formation of chondrites (formation of chondrules, fragments and matrix by impacts of the pre-chondritic bodies [9]) under H-depleted conditions with redox reactions (the redox conditions depends on mineral/ice/organic material ratios of the pre-chondritic bodies; e.g., enstatite chondrites were formed from materials containing a large amount of C-rich organic materials).

References: [1] Mysen,B.O. & Kushiro,I. (1988) Amer. Mineral. 73, 1. [2] Nagahara,H., Kushiro,I., Mysen,B.O. & Mori,H. (1988) Nature, 331, 513. [3] Tsuchiyama,A., Kushiro,I., Mysen,B.O. & Morimoto,N. Proc. NIPR Antarc. Meteorites, 1, 185. [4] Hashimoto,A. (1989) Lunar Planet. Sci., XX, 385. [5] Tsuchiyama,A. (1989) Lunar Planet. Sci. XX. [6] Tsuchiyama,A. & Kozasa,T. (1989) Proc. Meeting on Origin of Comets. [7] Grossman,L. & Larimer,J.W. (1974) Rev. Geophys. Space Phys., 12, 71. [8] Wood,J.A., Hashimoto,A. & Holmberg,B.B. (1989) Lunar Planet. Sci., XX, 1215. [9] Kitamura,M., Tsuchiyama,A., Watanabe,S., Syono,Y. & Fukuoka,K. (1989) Abstract of this symposium.

THE MAGNESIUM ISOTOPE ABUNDANCE OF SILICATES PRODUCED FROM GAS-CONDENSATION FURNACE

Chiaki Uyeda, Jun Okano and Akira Tsuchiyama†

College of General Education, Osaka University, Toyonaka, Osaka
†Dept. Geology and Mineralogy, Kyoto University, Sakyo, Kyoto

In recent years, large mass fractionations in magesium as well as silicon isotopes have been reported on particular types of inclusions in Allende meteorites. Esat et al.(1986) have measured the Mg isotopic abundance of laboratory distillated samples and the mass fractionation of condensate and residue samples with respect to starting material amounted to -14‰ and +27‰, respectively. The results indicated that the large mass fractionations seen between coarse and fine grained CAI in Allende meteorite can be caused from natural distillation process. However, the total pressure of the experimental system was about 5×10^{-5}torr which is considerably low compared to that estimated for the primitive solar nebula. The condensation temperature was kept constant around room temperature.

Meanwhile, Tsuchiyama(1988,1989) has carried out gas-condensation experiment in the Mg-Si-O-H system using a newly constructed furnace. The H_2 gas pressure was kept constant at 1.4×10^{-5} barr which is fairly close to that of the estimated primitive solar nebula. The starting material(powders of synthetic forsterite crystals) was evaporated at about 1630 °C. Under these conditions, forsterite, mixtures of forsterite and enstatite and Mg-rich amorphous material condensed between 1400 °C-900 °C, 900 °C-600 °C and below 600 °C, respectively. In the present study, the relation of Mg isotope abundance and condensation temperature T_c was investigated for condensates produced in the above experiment, since the temperature dependence of the mass fractionation may give an imporant key to investigate the mechanism of mass fractionation due to evaporation-condensation process. A modified Hitachi IMA-2A ion microprobe analyser was used for the measurement of the magnesium isotope abundance. The primary ions were 9keV O_2^+ ions with a beam current of about 1μA. The spot size was 200μm in diameter. The Mg isotope measurements were carried out for 8 to 20 spots on each sample. The scattering of $^{26}Mg/^{24}Mg$ values due to instrumental effect was estimated to be less then +4‰ in the present measurement. Details in the ion probe analysis have been shown elsewhere (OKANO et al.,1985)

Fig.1 shows the relation between the amount of mass fractionation and condensation temperature T_c for seven condensate samples produced in a single experiment. The vertical axis show the mass fractionation for $^{26}Mg/^{24}Mg$ ratio with respect to the starting material,

$$\Delta 26 = \{(^{26}Mg/^{24}Mg)_{sample}/(^{26}Mg/^{24}Mg)_{starting}-1)\times 1000 \quad ‰ .$$

○ and ▣ represent the condensates and residue, respectively. The sample which condensed at room tempereture were highly fractionated in the light Mg isotope($\Delta 26 = -52\pm4$‰). However $\Delta 26$ tend to increase with T_c, and at T_c=1400 C, 26 amounted to +12+5‰. The residue was enriched in the heavy isotope and $\Delta 26$ was $\Delta 26=+8\pm4$‰ . The results indicate that the Mg mass fractionation in silicates produced through evaporation -condensation process strongly depends on its condensation temperature, and that the condensates are not necessarily enriched in light isotopes. The mechanism of this large mass fractionation of condensates will be discussed based on the correlation of $\Delta 26$ and T_c.

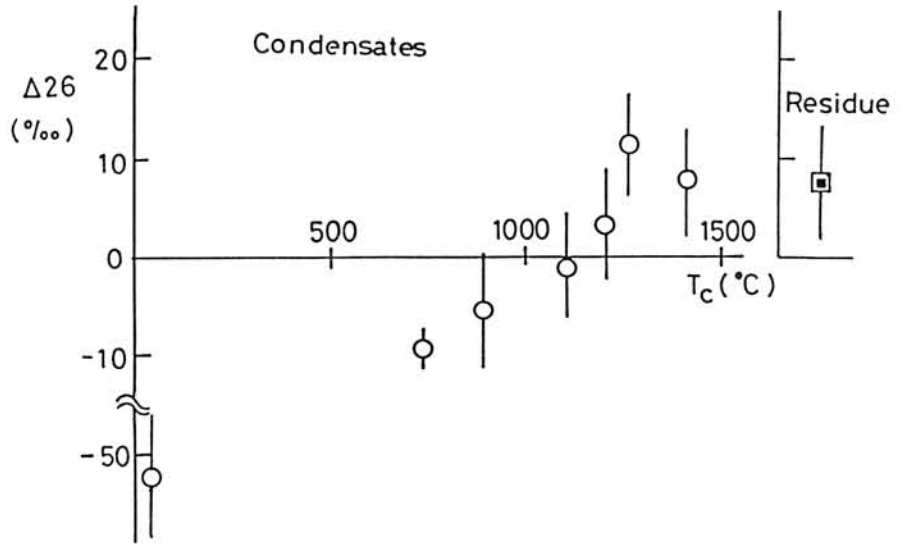

Fig.1 The relation between the amount of mass fractionation and condensation temperature T_c for products of gas-condensation experiment.

References

1) ESAT,M.T.et al.(1986):Nature 319,576-578.
2)Tsuchiyama,A.(1988):Abstract of the 13th symp.antarctic meteorites, national institute of polar res.123-125.; Tsuchiyama,A.(1989): Lunar and Planetary Science XX.
3) OKANO,J. et al.(1985):Mass Spectroscopy 33, 245-253.

Rb-Sr age of diogenite younger than that of eucrite.

*Kazuya Takahashi, Hiroshi Shimizu and Akimasa Masuda
*Department of Chemistry, University of Tokyo, Hongo, Tokyo 113
*Institute of Physical and Chemical Research, Wako, Saitama 351

Diogenites are a group of achondritic meteorites, which have been regarded to have a genetically close relationship with eucrites. Ages around 4.5-4.6 b.y. have been obtained for several eucrites by many workers. In this study, precise Rb-Sr measurements were carried out on several diogenite and diogenitic samples to compare with the data for Juvinas eucrite. Furthermore, REE (rare earth elements) abundances were determined. The samples we analyzed are listed in Table 1 with the results of Rb-Sr dating.

As shown in Table 1, eight diogenite samples (four samples from Tatahouine and four from Johnstown) define the age with quite small errors. The isochron for these samples is displayed in Fig. 1. On the Fig. 1, the data of Tatahouine-1 and -2 are close to each other, while the data of Tatahouine-3 and -4 are also close to each other, and fall on the separate position from the above one for Tatahouine-1 and -2. From this isochron, the age of 4.394 $\pm$0.011 b.y. has been obtained; a small uncertainty is noteworthy. In this figure, the dotted line is the isochron for Juvinas eucrite which shows the age of 4.52 b.y. The age of diogenite is apparently younger than the age of eucrite and these diogenites are considered to have little genetic relationship with eucrite as discussed later. On the other hand, the Rb-Sr data for Roda and Yamato-791422 fall near the isochron formed by eucrite with the age of 4.52 b.y., as shown in Fig. 2. Y-791422 is classified as Y-75032 type diogenite. This group of diogenite has been recognized as a unique type of diogenite and considered to have close relationship with eucrite, based on the mineralogical and chemical study (Takeda and Mori, 1981). These observation on Rb-Sr systematics suggests that diogenites would be roughly divided into two groups. The first group, to which Tatahouine and Johnstown belong, have the younger age than eucrite and the other group, to which Roda and Y-75032 type diogenites belong, have a close relationship with eucrite. This speculation can be confirmed by the REE patterns shown in Fig. 3. The REE patterns of Roda and Y-791422, giving the 4.5 b.y. age, are highly similar to the pattern of pyroxene fraction of Juvinas eucrite, while the REE pattern of Tatahouine and Johnstown, giving the 4.394 b.y. age, have some unique characteristics, such as the concave curvature between La and Sm. Though the REE patterns for matrix samples of Johnstown appear rather similar to those of Roda, the Johnstown samples are distinguished from Roda on the Rb-Sr isochron-plot (Fig. 2).

As discussed above, regarding the age and the characteristics of REE pattern, Tatahouine and Johnstown, typical diogenites, are from the eucrite group and some unique diogenite (Roda and Y-75032 type). For the genesis of diogenite, one possibility is that the typical diogenites, such as Johnstown or Tatahouine, would have been formed through secondary igneous process from Roda or Y-75032 type diogenite. However, if it were correct, the

isochron line of 4.394 b.y. and that of 4.52 b.y. should cross each other around the data point of Roda or Y-791422 in Fig. 2. As shown in Fig. 2, these two isochrons cross near the $^{87}Sr/^{86}Sr$-axis. Namely, initial values of these isochrons are close to each other within the range of the error. This fact indicates that Tatahouine and Johnstown were formed from the material with lower Rb/Sr abundance ratio than 0.014. Therefore, it is considered that these typical diogenites were formed by the distinct process from the Roda or Y-75032 type achondrite and the diogenite parent body had kept some igneous activity for about hundred million years after parent body formation. The data obtained here is open to the possibility that the eucrites as represented by Juvinas and the diogenites such as Johnstown and Tatahouine came from different parental bodies.

References:
Takeda, H. and Mori, H. (1981) Meteoritics,16, 390-391.

Table 1 Sample list and the results of Rb-Sr dating.

diogenite	sample name
Tatahouine (No.1644)	Tatahouine-1, -2
Tatahouine (Me 2651)	Tatahouine-3, -4
Johnstown (AMNH#2497)	Jt-Opx clast, Matrix-1, -2, -3
Roda(#640)	
Yamato-791422	

Age:	Tatahouine (4 samples)	4.398 ±0.028 b.y.
	Johnstown (4 samples)	4.390 ±0.035 b.y.
	Tatahouine + Johnstown (8 samples)	4.394 ±0.011 b.y.
	Roda, Y-791422	4.5~4.6 b.y.

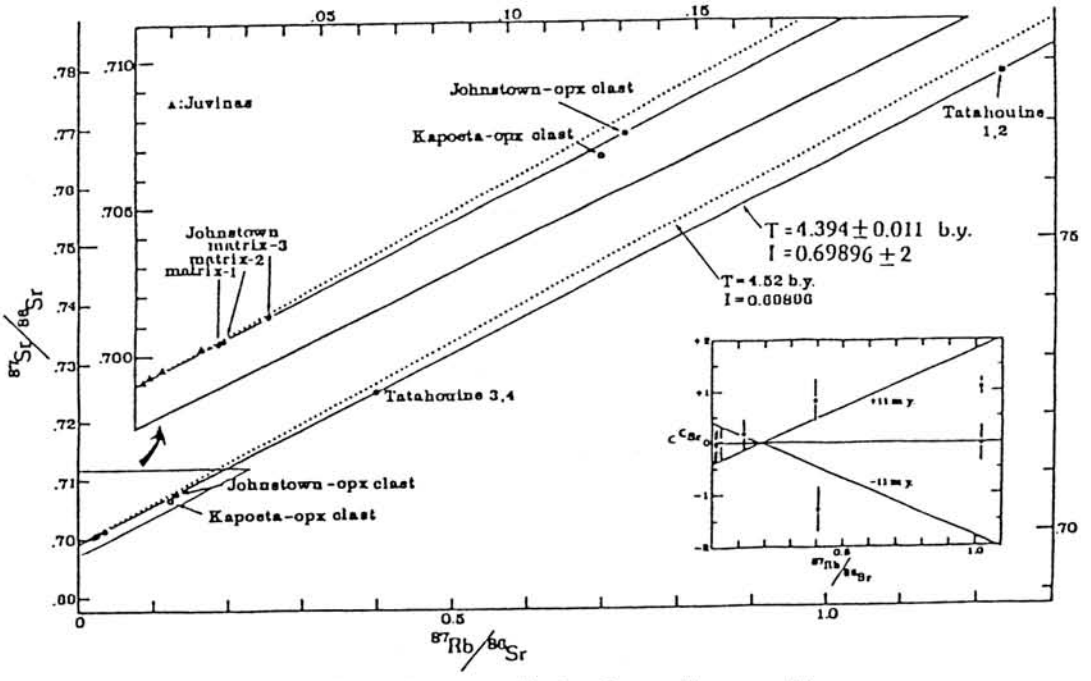

Fig. 1 The Isochron plot for diogenites.

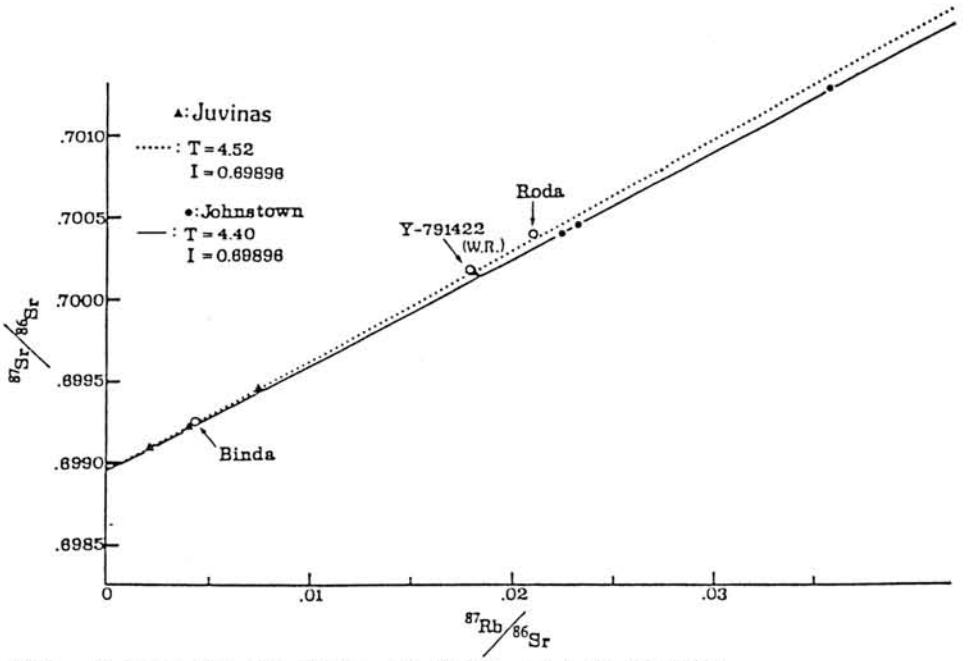

Fig. 2 The Rb-Sr data of Roda and Y-791422. This plot corresponds to the area for $^{87}Rb/^{86}Sr$ smaller than 0.035 in Fig. 1.

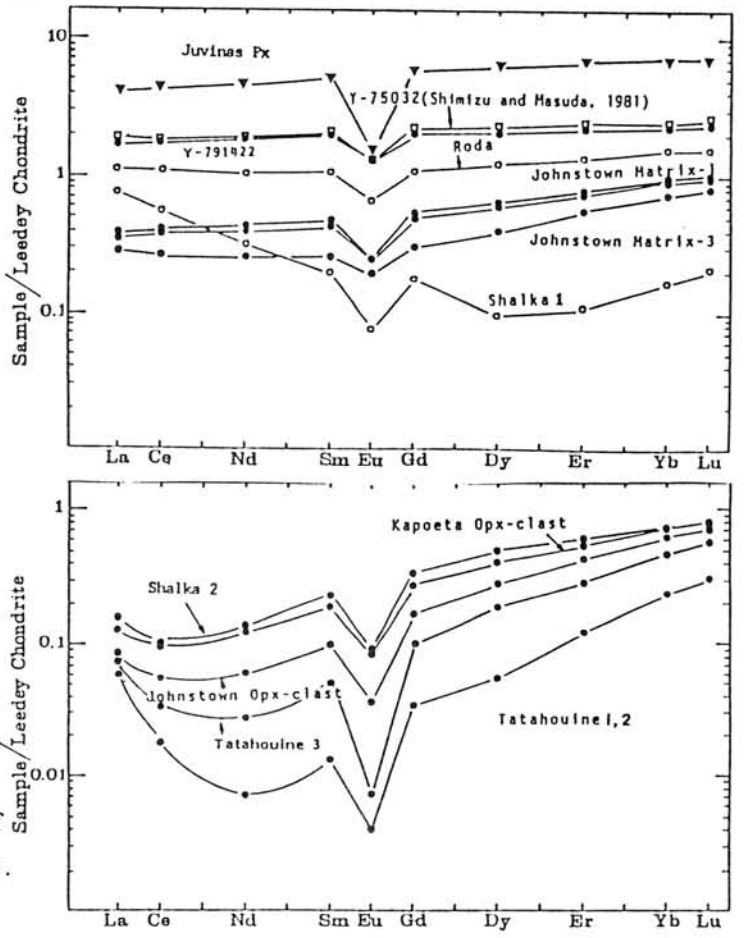

Fig. 3 The REE pattern of diogenite samples.

Alteration of Antarctic meteorites and their anomalous abundances of Halogens.

Shinonaga, T. (1), Ebihara, M. (1), Nakahara, H. (1), Kondoh, A. (2), Honda, M. (2), Miyamoto, M. (3), & Kojima, H. (4)
(1)Dept. Chemistry, Tokyo Metropolitan University, Setagaya, Tokyo 158, Japan,
(2)Dept., Chemistry, Nihon University, Setagaya, Tokyo 156, Japan,
(3)College of Arts and Sciences, University of Tokyo, Meguro, Tokyo 153, Tokyo, Japan,
(4)Natl. Inst. Polar Res., Itabashi, Tokyo 173, Japan.

Of trace elements, halogens have such chemical features as high volatility and easiness in chemical leaching, hence determining and investigating halogens in Antarctic meteorites have a great significance in considering the effect of weathering in Antarctica. From this viewpoint, halogens in different types of Antarctic meteorites were first analyzed by Dreibus et al. (1). They found significantly high abundances of iodine in Antarctic meteorites. Such a mysterious iodine-overabundance in Antarctic meteorites was later confirmed by Heumann et al.(2). Neither of them found correlation between the iodine concentration and weathering index or terrestrial age. Even though Heumann et al. found that the iodine concentration shows a significant decrease from the surfaces to the centers of Antarctic rocks, they presented no definite conclusions for the cause of iodine-overabundance.

In this study, we have determined the depth profiles of iodine, chlorine, and bromine in ALH-77231 Antarctic L6 chondrite. Halogens were determined by radiochemical neutron activation analysis. We have also measured the spectral reflectance for an aliquot of each sample by using a Fourier transform infrared spectrometer and calculated the integrated intensity of absorption band (hydration band) near 3μm due to the presence of hydrous minerals.(3).

Fig.1 shows the sampling positions in the ALH-77231 meteorite. Table 1 shows the analytical results of iodine and integrated intensity of absorption band in different positions of the chondrite. Errors due to counting statistic (1σ) also are given. A significant decrease of iodine concentration is found from the surface to the interior of ALH-77231 meteorite. A-1 in the outermost part contains 11.2ppm I, whereas B-9 in the innermost part contains only 0.08ppm I. As noticed obviously in Table 1, there is an apparent correlation between iodine contents and integrated intensities of hydration band. These results strongly suggest that iodine-overabundance is due to weathering.

DEPTH+PROFILES OF HALOGEN AND HYDRATION BAND NEAR 3u: Ebihara M. et al.

Table 1 iodine content and integrated intensity of absorption band near 3μ

sample name	I/ ppm	error/ %(1σ)	integrated intensity
A-1	11.2	2.1	197
A-2	4.7	1.8	201
A-4	0.11	15.0	116
B-1	0.70	6.0	197
B-3			110
B-5			102
B-7			102
B-9	0.08	20	149

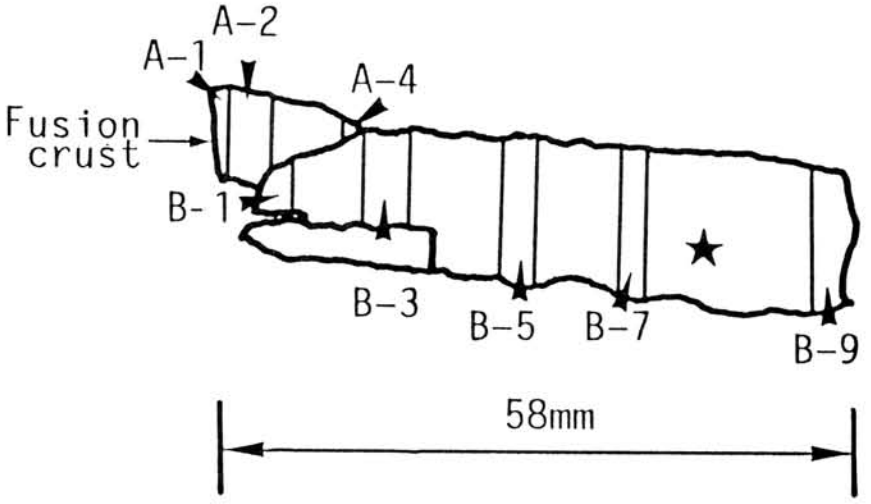

Fig. 1 Sampling positions in ALH-77231 (L6). The center of meteorite is marked by a star.

References
(1) Dreibus G., Wanke H. and Schultz L. (1985) Workshop on Antarctic Meteorites, 11-13.
(2) Heumann K.G., Gall M. and Weiss H. (1987) Geochim. Cosmochim. Acta 51, 2541-1547.
(3) Miyamoto M. (1988) Earth Planet. Sci. Lett. 89, 398-402.

Neutron Activation Analyses for Rare Earth Elements in Meteorites and others

Shigekazu Yoneda, Hisanori Mihara, Hisao Nagai and Masatake Honda
College of Humanities and Sciences, Nihon University

In previous works [1], the REE abundances in Allende inclusions and in evaporation-experiment products were determined by the isotope dilution method in surface ionization mass spectrometry (ID-MS). Although ID-MS measurement of REE has the merit of sensitivity and accuracy, mono-isotopic element (Pr, Tb, Ho, Tm; Y, Sc) concentrations cannot be determined except for introducing long-lived radio nuclides as the spikes. However, some meteorite inclusions, for example Group II [2], have extremely anomalous REE patterns and mono-isotopic REE abundances are important to study the origin of these anomalies.

In this study, the REE, especially mono-isotopic elements, abundances in some meteorites, in evaporation residues of chondrites and in some GSJ standard rocks [3] were determined by radiochemical neutron activation analyses. The analytical data were compared with those by ID-MS. Samples were irradiated in the S pipe of JRR4 reactor for 6 hours; because of small sample sizes (<10mg)), high neutron flux was necessary. For measurements of ^{142}Pr (Half Life : 19.2h) and ^{166}Ho (26.7h), gamma ray countings must be started in the next day after the irradiation. In the quantitative group separation of REE+Y by cation exchange , Sc was removed beforehand using a citric acid - ammonium chloride mixed solution, because ^{46}Sc (83.8d) interfered with the measurements of long lived ^{160}Tb (72.1d) and ^{170}Tm (128.6d). After this process Sc remained in the REE fraction was less than 5%.

The REE recovery was estimated by (1) re-irradiation measurements of 6 species of REE carriers, (2) comparing with the simultaneous nondestructive determination of some sensitive REEs, (3) gamma ray counting for the recovery of a tracer ^{228}Ac, ^{90m}Y or ^{88}Y.

REE patterns found in the JB-3 standard rock (basalt) and the fusion crust of the Ness County chondrite (L6) are shown in Fig. 1. REE abundances of JB-3 are normalized to the La content because of poor standard recovery, but relatively they are in good agreement with the reference values (1986) [3]. REE found in the fusion crust sample show a slightly enriched pattern among the light REE members and a small Ce negative anomaly. These facts seem to suggest the preferential evaporations occurred in the atmosphere. A positive anomaly of Eu seen in the pattern measured by ID-MS is probably due to laboratory contaminations. The Tm abundance has not been determined yet, because ^{160}Tb (86.7keV) and Pb-X ray (84keV) interfered with ^{170}Tm (84.3keV).

Determinations of Y contents in these samples by the gamma ray counting of ^{90m}Y (3.19h) or ^{88}Y (106.6d) has a very poor sensitivity because of low cross sections of ^{89}Y (1mb to ^{90m}Y and low yield of (n,2n) reaction). A beta ray counting of ^{90}Y (64h, σ=1.3b, Eβmax 2.3MeV) was performed selecting hard components of ^{90}Y β, differentially employing two thick Al absorbers. The counting data of the JB-3 are shown in Fig. 2. Subtracting the small contributions of REE standard mixture from the gross data, the net ^{90}Y activity can be observed. Calculating from the decay curve, the Y content of JB-3 was estimated to be 30.2 ± 2.2 ppm (reference value : 28 ppm [3]). Similarly the contents in two chondrite samples were also estimated to be 2.3 ± 0.3 ppm (ref. : 2 ppm [4]).

References

[1] Yoneda et al. (1988) Papers presented to the 13th Symposium on Antarctic Meteorites, 62-64

[2] Martin and Mason (1974) Nature 249, 333-334

[3] Ando et al. (1987) Geostandards Newsletter 11, 159-166

[4] Schmitt et al. (1963) Geochim. Cosmochim. Acta 27, 577-622

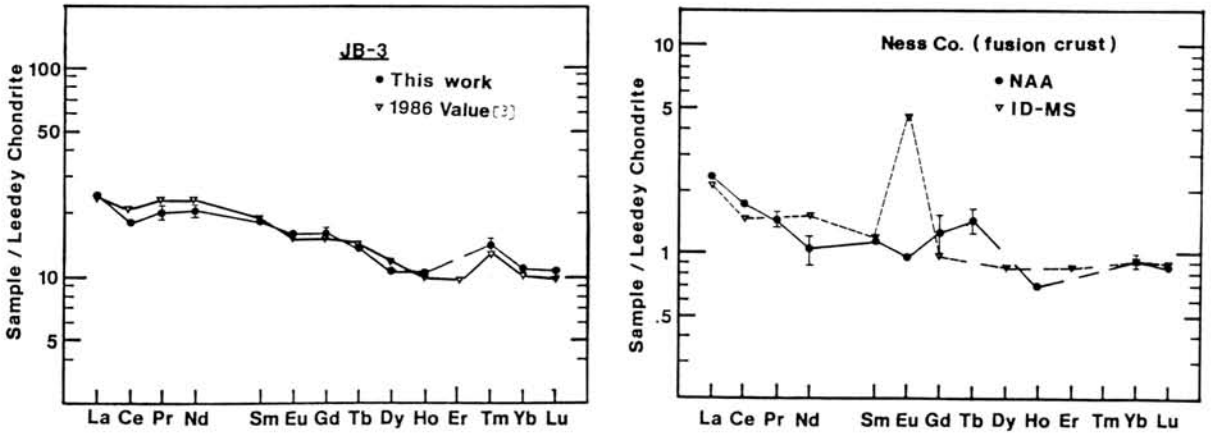

Fig. 1 REE patterns of JB-3 and the fusion crust of the Ness County chondrite (L6)

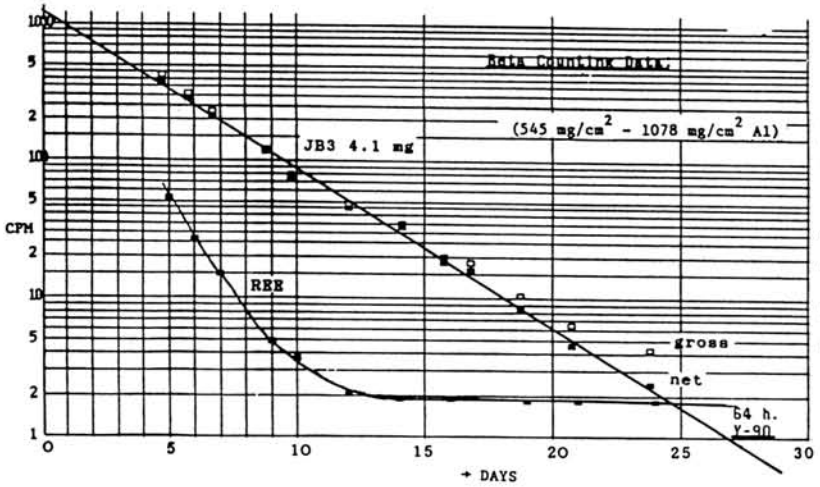

Fig. 2 Beta ray counting data of JB-3 REE
(GM counter back ground : 6 cpm)
After a cooling for several days, waiting for decays of hard beta emitters, such as ^{152m}Eu, ^{142}Pr, ^{166}Ho and other impurities, the ^{90}Y β activity became predominant for the following days.

Further characterization of fractionated and unfractionated REE and alkali metal abundances in the Allende (CV3) chondrules - part 1 -

Hitoshi MATSUDA and Noboru NAKAMURA

Department of Earth Sciences, Faculty of Science, Kobe University, Nada, Kobe 657

Previously, it has been reported that individual chondrules from the Allende (CV3) meteorite show more or less fractionated REE patterns and have various alkali metal abundances with CI-chondritic Rb/K ratio (1). In this work, in order to obtain further chemical characteristics of the chondrule formation events and precursors, additional twenty-three chondrules and a Ca, Al-rich inclusion from Allende were analyzed for trace and major elements (K, Rb, Sr, Ba, REE, Ca and Mg) by direct-loading IDMS analysis (2) and major mineral compositions by electron probe microanalysis.

alkali metal fractionation Fig. 1 illustrates relationship between K content and CI-normalized Rb/K ratio. Most chondrules with higher K content (> CI level) have CI-chondritic Rb/K ratio as reported by Misawa and Nakamura (1), but chondrules with lower K (< CI) clearly show higher Rb/K ratio than CI-chondritic. The CI-normalized Rb/K ratio increases with decreasing K content. Such Rb/K fractionation is observed for vaporization residues of the Etter (L5) chondrite heated at 1300 °C for more than several minutes (3). In addition, chondrules with higher Rb/K ratio exhibit more depletion of K relative to CI-chondritic K/Ca ratio (Fig. 2). Fig. 2 shows that porphyritic type chondrules have a weak positive correlation between K and Ca contents, while barred olivine chondrules show no clear trend. Moreover, the average of Fa contents in olivine grains in individual chondrules positively correlate with bulk K content for barred olivine chondrules (Fig. 3). Similar correlation is not observed for porphyritic type chondrules. Since olivine grains in barred olivine chondrules are considered to have been formed from total melts, Fa content of barred olivine chondrules may reflect a redox state in the chondrule formation melting which might have controlled the volatilization rate of sodium from silicate melts (4). Therefore, it is possible that barred olivine chondrules accompanied with lower K contents and high Rb/K ratios were subjected to vaporization loss of alkali metals in more reduced conditions.

From these observations, it is suggested that barred olivine chondrules were formed from two types of precursors with alkali-rich refractory and CI-chondritic components which had CI-chondritic Rb/K and K/Ca ratios and were more or less subjected to volatilization and fractionation of alkali metals during the chondrule formation melting, and that porphyritic type chondrules were formed by mixing of two different types of precursors; one component is enriched in alkali metals and has CI-chondritic Rb/K and K/Ca ratio, and another is poor in alkalis and have

fractionated alkali metal abundances.

REE abundances As reported previously (1), four of six chondrules analyzed in this work also show variable REE abundances in absolute sense and mostly flat REE patterns with small anomalies of Ce, Eu and Yb (Fig. 4). Two plagioclase-rich microporphyritic chondrules (PP-26, PP-27) are quite similar to each other in major chemical compositions and petrographycal features. They, however, display a marked difference in REE pattern. PP-27 shows Group II REE pattern and PP-26 shows Group III REE pattern. Although a few chondrule with Group II REE pattern has been reported (5,6,7), Group III REE pattern for PP-26 is the first clear identification as chondrules. Details of chemical and petrological features of these two chondrules are discussed by Nakamura and Matsuda (8).

REFERENCES: (1) Misawa K. and Nakamura N. (1988a) Geochim. Cosmochim. Acta 52, 1699-1710 (2) Nakamura N. et al. (1989) Anal. Chem. 61, 755-762 (3) Nakamura N. and Shimaoka T. (1989) Lunar Planet. Sci. XX, 756-757 (4) Tsuchiyama A. et al. (1981) Geochim. Cosmochim. Acta 45, 1357-1367 (5) Misawa K. and Nakamura N. (1988b) Nature 334, 47-50 (6) Rubin A. E. and Wasson J. T. (1987) Geochim. Cosmochim. Acta 51, 1923-1937 (7) Kring D. A. and Holmen B. A. (1988) Meteoritics 23, 282-283 (8) Nakamura N. and Matsuda H. (1989) this volume (9) Noda S. and Nakamura N. (1989) Lunar Planet. Sci. XX, 794-795

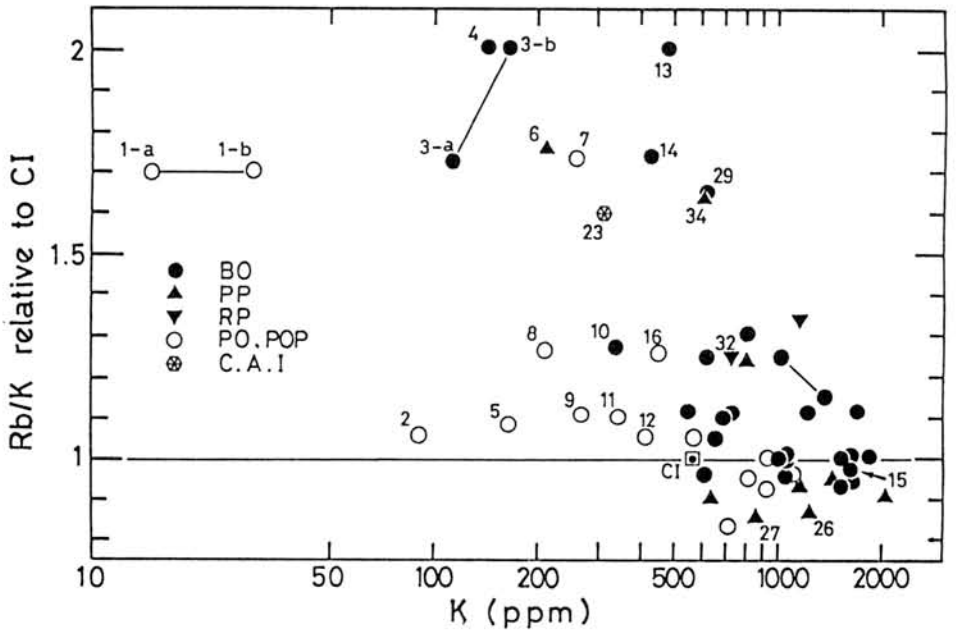

Fig. 1
Relationship between K content (ppm) and CI-normalized Rb/K ratio for the Allende chondrules. < data partly from ref.(1) and ref.(9) >

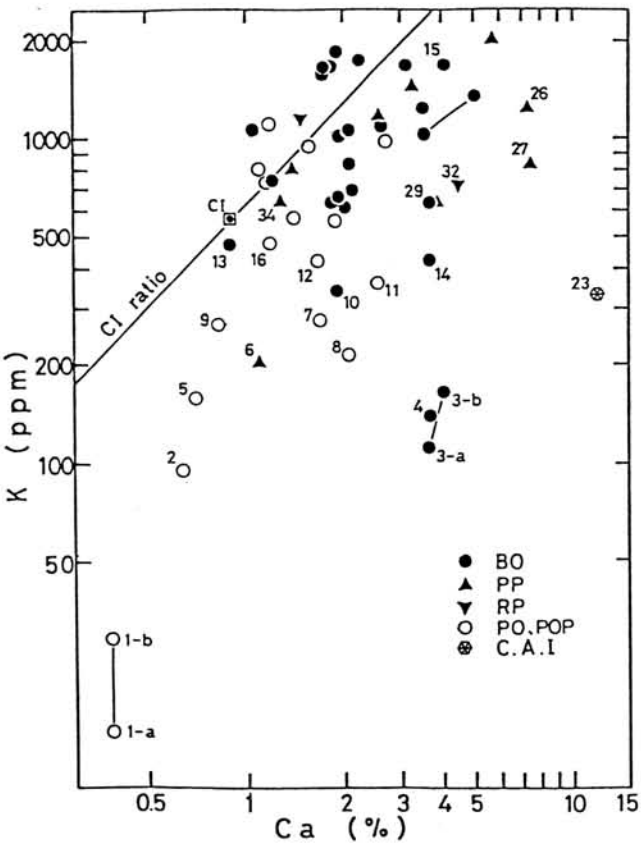

Fig. 2
Plots of K (ppm) versus Ca (%) for the Allende chondrules ‹ data partly from ref.(1) and ref.(9)›

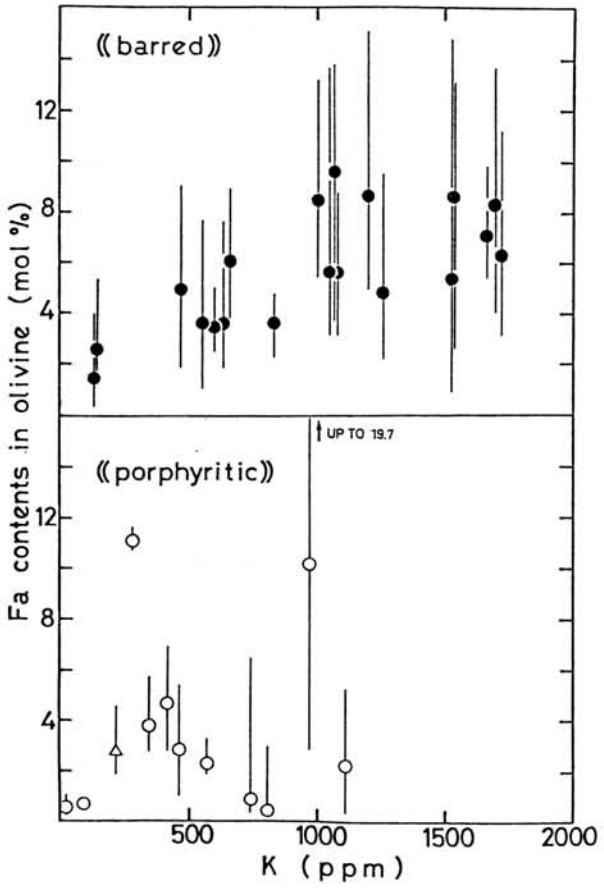

Fig. 3
Relationship between bulk K content and Fa content in olivine for the Allende chondrules. ‹ data data partly from ref.(1) ›

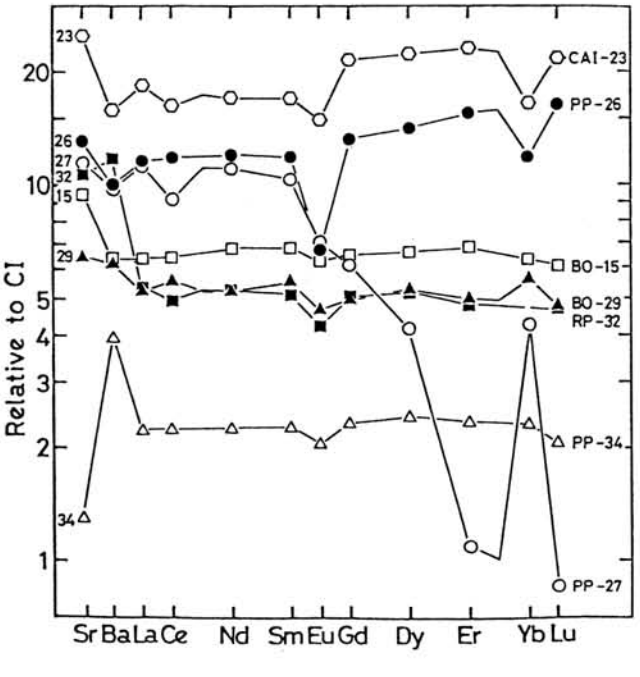

Fig. 4
CI-normarized REE patterns for chondrules and a Ca, Al-rich inclusion from the Allende meteorite.

FURTHER CHARACTERIZATION OF FRACTIONATED AND UNFRACTIONATED REE AND ALKALI METAL ABUNDANCES IN THE ALLENDE (CV3) CHONDRULES (II)

Noboru Nakamura and Hitoshi Matsuda

Dept. of Earth Sci., Faculty of Sci., Kobe Univ., Nada, Kobe 657

During our search for detailed trace element chemical characteritics of the Allende (CV3) chondrules, we have encountered with two microporphyritic chondrules (PP-26 and PP-27) with unique REE fractionations [1]. In order to obtain further chemical aspects of chondrule formation, detailed chemical and petrological examinations for these chondrules were carried out with EPMA and SEM together with analyses by direct-loading IDMS [2].

Both chondrules have quite similar textural features with core-mantle structures, consisting of mainly glassy materials, plagioclase (core An_{95-98}, mantle An_{85}) and pyroxene (core Wo_{1} $Fs_{2.2}$, mantle $Wo_{2-3}Fs_{0.6-7}$), and minor olivine (core Fa_{3-8}, mantle Fa_{10-33}). The chondrule-cores belong to CA-chondrules [3, 4] but chondrule-mantles to typical ferromagnesian type (Figs. 1, 2). In spite of such similarities, two chondrules have markedly different REE fractionations. PP-26 (core) shows a ~15xCI-chondritic, flat REE pattern with negative anomalies at Eu and Yb (Group III REE) but PP-27 (core) indicates a unique REE pattern with large light/heavy REE fractionation (~10xCI for light REE and ~1xCI at Er and Lu) and positive Yb anomaly (Group II REE) (see Fig.3). Group II REE pattern has been well-documented for many CAI's and also for some chondrules [5]. Although similar REE patterns to that of PP-26 (core) have been occasionally found in Allende chondrules [5], such a typical Group III REE pattern for PP-26 may be the first observation in chondrules. Two unique but different REE patterns observed for chondrule-cores suggest that their precursors were formed under different physical conditions at high temperatures in the nebula. The existence of similar CA-type material carring different refractory precursors together with surrounding ferromagnesian type material seems to shed new light on interrelationships of fractionated refractoies and common ferromagnesian precursors. We have suggested that the majority of Allende chondrules was formed from alkali-rich refractories with more or less fractionated REE and non-refractory (common ferromagnesian) components [5]. The identification of such components with divergent chemical natures within two associated, complex chondrules suggests that they were in close genetic relations. Then it is considered that the gas/dust fractionation yielding to formation of refractory precursors, their transportation, mixing and aggregation with common ferromagnesian precursors, and melting to form chondrules were all closely processed. Therefore, large temperature gradients and transient physical conditions in space and/or time seem to have existed in chondrule-formation regions of the nebula.

References: [1]H. Matsuda & N. Nakamura, this volume [2]N. Nakamura et al., Anal. Chem. 61, 755-762(1989) [3]H.Y. McSween Jr GCA 41, 1843-1860(1977) [4]D.A. Wark, GCA 51, 221-242(1987) [5]K. Misawa & N. Nakamura, Nature 334, 47-50(1988); GCA 52, 1699-1710 (1988) [6]A.S. Kornaki & B. Fegley, Jr. EPSL 79, 217-234(1986)

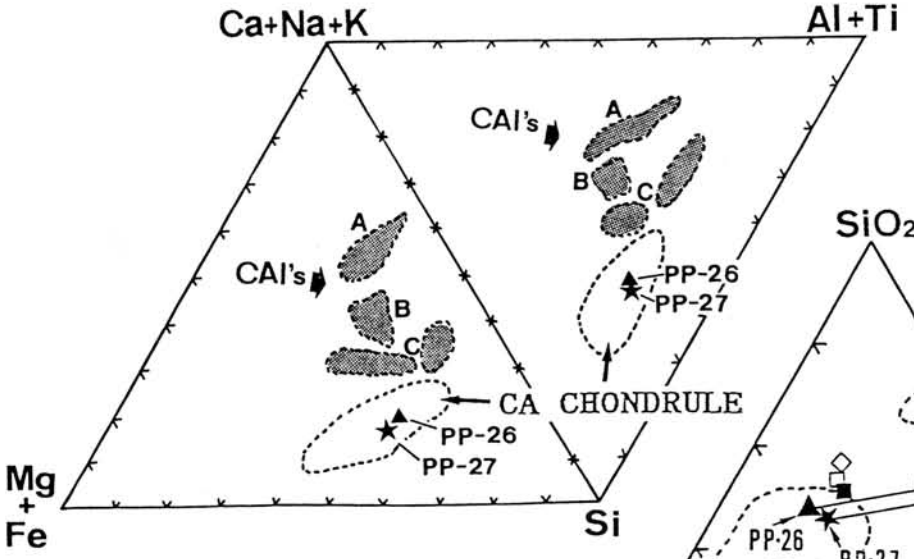

Fig. 1
Projections of compositions of cores and mantles of PP-26 and -27 chondrules.
[3]

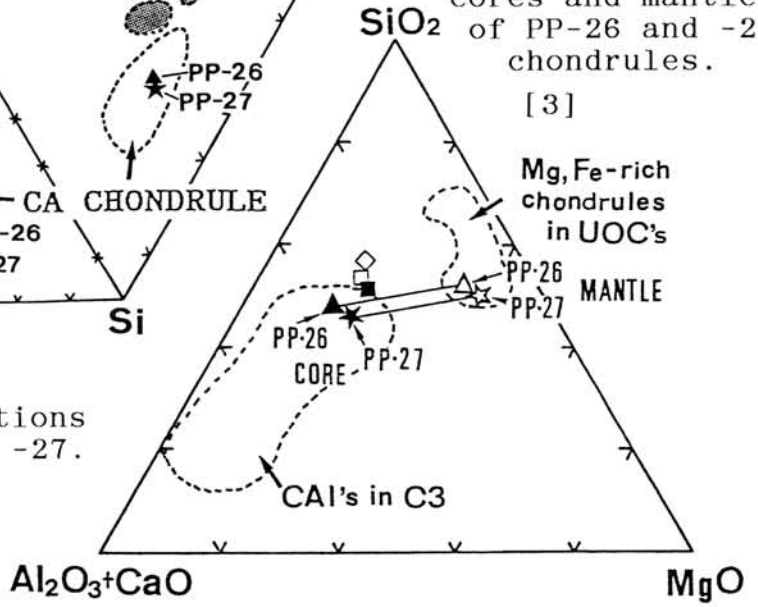

Fig. 2
Projections of compositions of cores of pp-26 and -27.
[4]

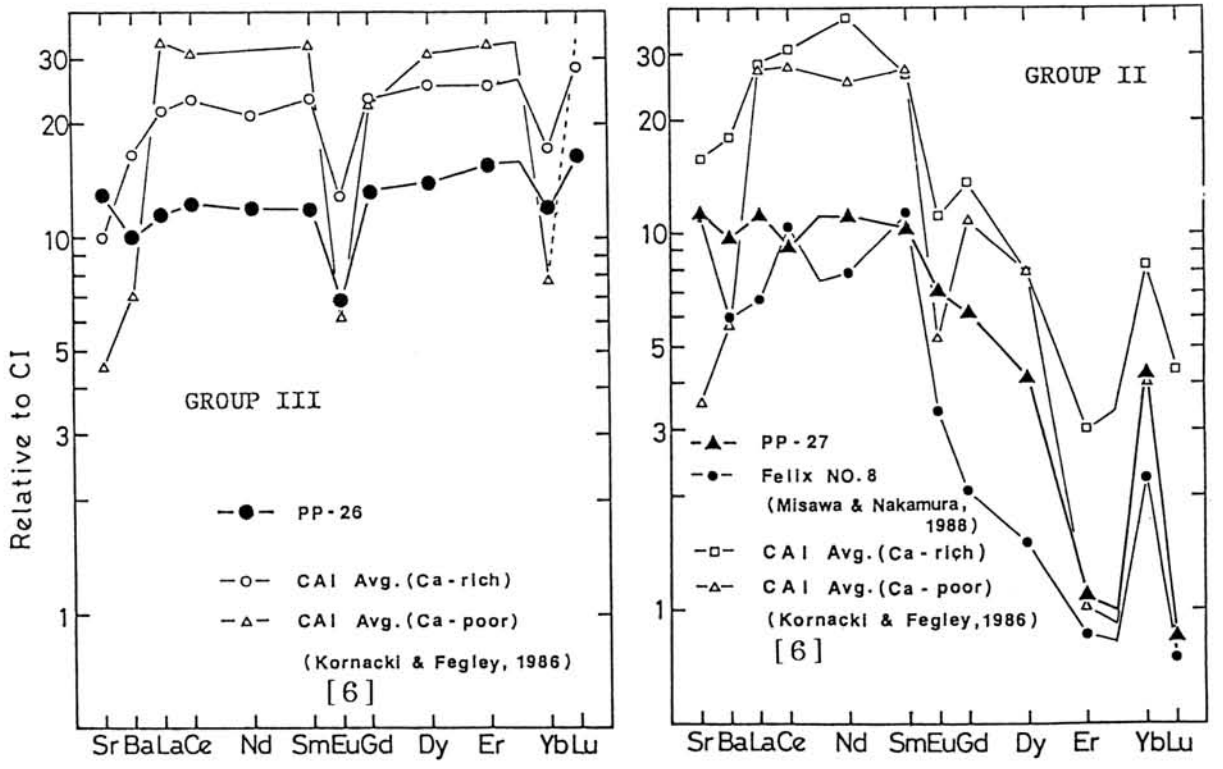

Fig. 3 Comparison of REE patterns of PP-26 (a) and PP-27 (b) with those of CAI's in carbonaceous chondrites.

BE-10 AND AL-26 IN METAL AND STONE PHASES OF METEORITES.

Nagai,H. and Honda,M. Nihon Univ.Setagaya-ku,Tokyo,156
Imamura,M. Inst.Nuclear Study, Univ.Tokyo,Tanashi,Tokyo
Kobayashi,K.Res.Cent.,Nuclear Sci.Techn.,Univ.Tokyo,Bunkyo-ku,Tokyo
Ohashi,H. Inst.Cosm.Ray Res.Univ.Tokyo,Tanashi,Tokyo

Cosmogenic ^{10}Be and ^{26}Al were determined in separated metal and stone fractions of meteorites by AMS, accelerator mass-spectrometry. The tandem van de Graaf accelerator at the Univ. of Tokyo was employed for these measurements by applying the internal beam monitor method (2).

Chondrites, including antarctic chondrites and fragments of the Jilin chondrite, and stony irons were processed to separate their metal and stone phases. Because of higher ^{26}Al contents in their stone phases, extensive purifications for the metal grains had to be performed. The contamination levels must be lower than 1% stone in metals, and small stone corrections can be made. The sample sizes were 50-400 mg of metals and ca.100 mg of stones. The metal sample size was limited mainly by the shortage of available samples. Smaller amounts of carriers were added for metal samples, down to 200 and 500 micro g.Be and Al respectively, and the observed atomic ratios of $^{10}Be/Be$ and $^{26}Al/Al$ of the samples were approximately 10^{-11}.

Some examples of recent determinations are shown in Table 1 (4). The fragments of the Jilin are characterized by the contents of ^{21}Ne and other products. They reflect the depth profile of the 1st stage irradiation, by 2 pi geometry for 10 million years and the smaller contributions near the surface of the 2nd stage, 4 pi for about 0.4 million years. The latter can be estimated from the deepest samples for stable and long-lived activities and are used for corrections to the net contributions in the first stage. Tese are expected to be exponentially distributed with depths except near the surface.

In general, the following equation, or the equivalent expression, can be applied for the statistical estimations of production rates, P ,of various high energy reaction products in iron and stone meteorites (1).

$$P(A,Z) = f(A,Z) * k_1' * (\Delta A + a)^{-k_2'},$$

where a=4 can be used as an empirical term; f is a partial yield of product, A,Z ,among isobar,A,; k_1' indicates a production level in Fe target; ΔA is a mass difference between 56 and A, between A=54 and 20. This formula has been developed originally for iron meteorites. In extensive applications of the formula for ^{3}He and ^{4}He in Fe and for the products in the targets other than iron,the f value is generally used as a proportional coefficient and the equivalent ΔA can be assigned as an effective parameter.

The two sets of linear relations are obtained by plotting $\log[P(^{10}Be)/P(^{53}Mn)]$ vs. shielding index, k_2', for stones and metals. An effective ΔA for ^{10}Be in metal is estimated at 18 (and f=0.11), in a wide range of k_2'= 1.8 to higher than 3. This is the same as ^{38}Ar and ^{3}He. Therefore $P(^{10}Be)$ is relatively constant within the chondrite group. For ^{10}Be in stones, ΔA=8 (and f=0.12) can be assigned, in the range k_2'=1.8-2.4, as reported previously(3). A smilar relation is seen In achondritic targets as has been shown in mesosiderites. This pattern is extended to the Jilin and to the lunar samples. The distributions of net ^{53}Mn and ^{10}Be in the 1st stage of the Jilin can be refered to the galactic productions near the lunar surface. Under the 2 pi irradiation, the depth profiles of both nuclides show exponential variations. Therefore, k_2's, expressed by the logarithmic functions of the ratio of the contents of the two products, increase linearly with depth except at the very top of the surface.

Similar relations were observed for ^{26}Al. Production ratios of $(^{26}Al/^{53}Mn)$ can also be compared with k_2's. In the stone phases of chondrites of ordinary sizes, the ratios were essentially constant at about 0.13. In other words, the ΔA for ^{26}Al in the stone phases is assigned to be 3 which is equal to that of ^{53}Mn. When the reproducible ^{26}Al data available, the ratio of $^{53}Mn/^{26}Al$ in metals is considered to be the most sensitive indicator for the shielding throughout stony and iron meteorites. This ratio has been applied to determine the above ΔA for ^{10}Be(2).

Ref. (1) M.Honda(1985) EPSL 75,77-80; (1988) Meteoritics 23, 3-12. (2) H.Nagai et al(1987)Nucl.Instr.Method, B29,266-270; (1987) Meteoritics 22,467-469. (3) H.Nagai et al(1988) 13th Symp. Antarctic Meteorites,Jun.Tokyo. (4) H.Nagai et al(1989) Workshop Cosmogen. Nuclide Produc. Rates,Jun.Vienna,LPI,Houston, in press.

TABLE 1 BE-10 AND AL-26 FOUND IN METAL AND STONE FRACTIONS

SAMPLE	CLASS	ID	METAL FRACTION sample mg.	METAL FRACTION dpm/kg Be-10	METAL FRACTION dpm/kg Al-26	stone %	STONE FRACTION sample mg.	STONE FRACTION dpm/kg Be-10	STONE FRACTION dpm/kg Al-26	Mn-53*	k'2
CHONDRITES:											
A77299	H3		116	4.58±.25	3.41±.26	.13	31.9	17.7±1.1	43±2	317	1.95
Y7301	H5		115	3.93±.22		.04				102	
Y74117	L6		144.7	4.64±.19			107.5	16.4±.9		240	
Y74455	L6		235	5.94±.27	3.4 ±.2	.15	106	18.3±1.1	49±2	278	1.90
Y74663	L6		129	5.55±.27	3.0 ±.2	.03	114	18.1±1.1	39±1	255	1.79
ETTER	L6	H47,260	430	2.36±.13		.46	119.4	16.6±.7		(158)	
LA CRIOLLA	L6	1985	227	3.63±.18		.01	107.4	20.0±.7	63±2		
NEW CONCORD	L6	1860	178	3.95±.15		.12	100	17.0±.6	69±3	(174)	
NUEVO MERCUR.	H5	1978	402	4.37±.13		.20	120.1	22.4±1.4		(506)	
TSAREV	L5		87.2	1.41±.11		.12	107.1	5.21±.46			
JILIN	H5	1976									
	fragm.	$^{21}Ne*10^{-8}$cc/g									
TOKYO A, No.1		1.64	150	1.93±.09		.34	104	11.4±.3	39±1	187	2.6
K2,Carneg.Inst		(1.4)	181.5	1.76±.11	1.49±.13	.34	225.9	12.0±.6	24±3	149	2.7
MAINZ B, No.1		0.99	197	1.23±.05						179	2.8
TOKYO B, No.1		0.82	256.3	0.86±.06		.24	256.8	8.6±.4		112	3.0
TOKYO E, No.1		0.62	443	0.93±.06	0.69±.04	.27	107.7	10.3±.4	31±1	68	3.1
TOKYO 4AB,No.4		0.51	225.2	0.78±.09	0.82±.06	.26	108.0	6.3±.2	26±3	85	3.2
MAINZ A, No.4		0.43	371	0.91±.04						81	3.3
HEIDELB.I,No.1		0.42	132.7	0.87±.07		.48	154		26±1	77	3.3
HEIDELB.II,No.4		0.38	119.1	0.87±.11	0.80±.17	.36	95.3	6.5±.5	25±1	75	3.5
STONY IRONS and IRONS:			#: Begemann et al(1976)								
BENCUBBIN	MES	#	61.1	5.04±.24		.50	104.3	26±1	80±2	525	2.43
BUDULAN	MES	#	85.6	3.28±.18	2.55±.28	.40	104.0	20±.6	119±6	398	2.7
CRAB ORCH.	MES	#	133	4.21±.16	2.99±.18	.04	108.3	24±.8	82±3	520	2.62
EMERY	MES	#	299	5.97±.48			104.1	22±.9	92±3	422	2.11
			58.7		4.15±.33	.52					
UDEI STATION	IA	#	230	3.8 ±.3			107	22±.8		575	2.6
			70		4.0±.4	.32					
TAWALLAH V.	IVB		130	5.26±.20	3.55±.19						
TOCOPILLA	IIA		618	2.28±.17	1.17±.09					(214)	
TRENTON	IIIA	AII-22+2	324	3.35±.11	2.54±.12					(590)	

* literature: K.Nishiizumi,Nucl.Tracks Rad.Meas.,13,209-273(1987).

NOBLE GAS ISOTOPIC COMPOSITIONS OF NINE CHONDRITES FROM ANTARCTICA

Nagao, K.[1], Miura, Y.[2] and Koh, T.[2]
1) Institute for Study of the Earth's Interior, Okayama University, Misasa, Tottori 682-02.
2 Department of Mineralogical Sciences and Geology, Faculty of Science, Yamaguchi University, Yoshida, Yamaguchi 753.

Noble gas concentrations and isotopic compositions of meteorites are important and useful data which inform us i) the chronological events such as collisional metamorphism on a parent body, cosmic-ray exposure age, terrestrial age, ii) paired meteorites of a single fall, iii) presolar materials in some primitive meteorites, etc. In this work we measured nine antarctic chondrites (see Table 1) collected on various ice fields. They are ALH(Allan Hills), Y(Yamato), RKP(Reckling Peak), BTN(Bates Nunataks), and MET(Meteorite Hills). Since Y-82095 is low petrologic type (L3), noble gases were analyzed employing stepwise heating (700, 900, 1100, 1300, 1500, 1800 °C).

Concentrations of all noble gases and isotopic ratios of He, Ne and Ar are given in Table 1. As cosmogenic Ne is predominant in all the samples, He in these samples should be composed of only two components, i.e. radiogenic and cosmogenic He. However, a small amount of trapped Ar can be seen in all the samples.

Cosmic-ray exposure ages in the table were calculated with the concentration of cosmogenic ^{21}Ne and the production rate equation proposed by Eugster(1988). The equation includes the correction factors for chemical compositions and for shielding effect. The cosmic-ray exposure ages T21 obtained for the samples are from 4.6 to 25 Ma, which are in the nomal rane for the ordinary chondrites. The exposure ages obtained with cosmogenic ^{3}He and its production rates are in good agreement with T21, which indicates no He loss in recent stage.

K-Ar ages were also estimated on the assumption that K content of these meteorites is 850 ppm. Although errors seem to be large, three L6 chondrites indicate an intensive Ar loss at about 0.5 Ga ago. Since it is well known that many L chondrites lost radiogenic Ar about 0.5 Ga ago by collisional shock event, these L6 chondrites seem to belong to the group of shocked L chondrites. However, since their exposure ages are distinctly different from each other, they can not be paired. K-Ar ages of other samples are in the range of 2.1-4.0 Ga.

Stepwise heating experiment on Y-82095(L3) showed that the maximum release temperatures for radiogenic ^{4}He and ^{40}Ar, cosmogenic Ne, and trapped Ar, Kr and Xe were 900, 1300, and 1300 °C, respectively. The lowest ^{40}Ar/^{36}Ar ratio of 66 in 1500 °C fraction indicates the relatively high concentration of trapped Ar in this meteorite.

REFERENCE:

Eugster, O. (1988) Geochim. Cosmochim. Acta, 52, 1649-1662.

Table 1. Noble gas concentrations, isotopic ratios, cosmic-ray exposure ages, and K-Ar ages.

unit: 3/4($\times 10^{-4}$) He,Ne,Ar($\times 10^{-8}$cc/g) Kr,Xe($\times 10^{-10}$cc/g)

Sample	4He	3/4	20Ne	20/22	21/22	36Ar	38/36	40/36	84Kr	132Xe	P21[1]	T21(Ma)[2]	T40(Ga)[3]
ALH-77232	809	73.1	1.64	0.855	0.943	0.904	0.345	3530.	0.93	1.9	0.396	4.6	3.3
(H4)		± 0.7		±0.004	±0.004		±0.004	±40					
RKP-78002	1350	75.8	2.19	0.867	0.931	0.900	0.420	860	0.59	1.1	0.369	6.4	3.8
(H4)		± 1.2		±0.006	±0.003		±0.004	±60					
Y-81132	1720	170	4.92	0.842	0.893	0.908	0.631	320	0.80	0.88	0.297	18	4.0
(H6)		± 3		±0.003	±0.004		±0.007	±90					
Y-82095	503	760	8.10	0.885	0.881	9.22	0.279	169	8.3	8.9	0.299	27	2.3
(L3)													
Y-8011	1180	319	8.94	0.854	0.931	2.15	0.474	410	0.52	0.47	0.396	25	4.1
(L6)		± 4		±0.004	±0.002		±0.008	±20					
ALH-78112	396	935	5.80	0.829	0.863	0.680	1.138	900	0.25	0.44	0.272	22	2.1
(L6)		± 9		±0.002	±0.002		±0.007	±20					
ALH-78130	248	1370	6.64	0.839	0.896	1.54	0.796	105	0.29	0.49	0.324	22	0.43
(L6)		±20		±0.002	±0.002		±0.002	± 1					
BTN-78002	220	1150	4.46	0.856	0.899	0.619	1.023	430	0.37	0.57	0.328	14	0.67
(L6)		±10		±0.002	±0.002		±0.004	± 3					
MET-78028	172	571	2.21	0.871	0.880	0.681	0.461	506	1.6	1.6	0.296	7.5	0.82
(L6)		± 7		±0.003	±0.003		±0.002	± 2					

1) Production rates of cosmogenic 21Ne (10^{-8}ccSTP/g per Ma) calculated with the equation by Eugster(1988).

2) Cosmic-ray exposure age.

3) K-Ar ages were calculated on the assumption that K content of these meteorites is 850 ppm.

^{40}Ar-^{39}Ar AGE AND NOBLE GAS ISOTOPES OF A CLAST(H) IN A SHOCKED L6 CHONDRITE Y-75097

Kaneoka, I.*, Takaoka, N.** and Yanai, K.***
* Earthquake Research Institute, University of Tokyo, Bunkyo-ku, Tokyo 113
** Department of Earth Sciences, Faculty of Science, Yamagata University, Koshirakawa-cho, Yamagata 990
*** National Institute of Polar Research, Kaga 1-chome, Itabashi-ku, Tokyo 173

In the L6 chondrite Yamato-75097(Y-75097), many inclusions are observed and they are composed mostly of olivine and with lesser amount of plagioclase(1). On the basis of oxygen isotope studies, these inclusions have been identified to be classified into the H-chondritic group(2). This is the first example found that a chondrite contains clasts of the different chondritic group(1). Recently, it has been found that the L6 chondrite Barwell also contains clasts of the H-type clast(3). Barwell is reported to be an unshocked meteorite(3),whereas the Y-75097 meteorite shows evidences of shock effects(1).

For the host meteorite of Y-75097, noble gas compositions and ^{40}Ar-^{39}Ar ages were studied before (4,5). The results indicate that the later degassing event for the meteorite occurred at about 490Ma or slightly younger age. To reveal the degassing characteristics from a meteorite, these clasts would give us a unique example by comparing the result with that of the host meteorite. Hence, ^{40}Ar-^{39}Ar ages and noble gas isotopes were examined for the clast of Y-75097.

^{40}Ar-^{39}Ar age analyses of the clast indicate that it shows a U-shaped pattern in the ^{40}Ar-^{39}Ar age diagram. In the 800 and 900°C fractions, it indicates the youngest ^{40}Ar-^{39}Ar age of about 480Ma. More than 90% of ^{39}Ar were degassed below 1100°C. In the higher temperature fractions of more than 1200°C, the clast shows much older ^{40}Ar-^{39}Ar ages than those observed in the host meteorite. This indicates that the clast seems to retain more inherited radiogenic ^{40}Ar than the host meteorite. Apparently very old ^{40}Ar-^{39}Ar ages observed in the higher temperature fractions of the clast would imply the incorporation

of radiogenic ^{40}Ar due to a shock.

Noble gas isotopes were examined in the two temperature fractions(600°C and 1650°C). Most noble gases were degassed in the 1650°C fraction, including He and Ne. He and Ne are mostly of cosmogenic origin. A high $^{129}Xe/^{132}Xe$ ratio of about 30 was observed for the clast, indicating a rather high $^{129}I/Xe$ ratio in the source materials of the clast.

References:

(1) Yanai, K., Matsumoto, Y. and Kojima, H. (1983) Mem. Natl Inst. Polar Res., Spec. Issue No.30, 29.

(2) Prinz, M., Nehru, C. E., Weisberg, M. K., Delaney, J. S., Yanai, K. and Kojima, H. (1984) Meteoritics, 19, 292.

(3) Hutchison, R., Williams, C. T., Din, V. K., Clayton, R. N., Kirshbaum, C., Paul, R. L. and Lipschutz, M. E. (1988) Earth Planet. Sci. Lett., 90, 105.

(4) Takaoka, N., Saito, K., Ohba, Y. and Nagao, K. (1981) Mem. Natl Inst. Polar Res., Spec. Issue No.20, 264.

(5) Kaneoka, I., Takaoka, N. and Yanai, K. (1988) Proc. NIPR Symp. Antarct. Meteorites, 1, 206.

EXPERIMENTAL PROCEDURES OF MEASURING NITROGEN ABUNDANCES AND ISOTOPES, AND A PRELIMINARY RESULTS FOR LL CHONDRITES

K.Hashizume and N.Sugiura
Geophysical Institute, University of Tokyo, Tokyo Japan.

The nitrogen measurement system is shown diagramatically in Fig.1. The gas extraction system is similar to that of Frick and Pepin [1].

After heating the sample chamber well enough to remove the contamination, the sample placed in a branch of the chamber is dropped to the bottom. About 5 torr of oxygen is introduced from the zeolite chamber and the temperature is raised using a temperature controller. The maximum temperature is kept for 25 min. before cooling. At the end of this heating period, liquid nitrogen is put on the Trap-1, and remaining gas is exposed to Cu at 500 C. The residual gas (mainly nitrogen, argon and other rare gases) is transferred to the purification line where Trap-2 is set at liquid nitrogen temperature. If the amount of the gas is too much, then appropriate splitting is made. The residual gas is adsorbed on the nupro-p1 at liquid nitrogen temperature. Condensable gases are pumped out while the nitrogen is in the nupro chamber. The same process is repeated using the Trap-3 and nupro-q1 for further purification. The purified gas is then introduced to the QMS. Masses 26-30 are measured 20 times, which takes about 250 seconds.

Nitrogen is measured as nitrogen molecules and it has two isotopes, i.e. mass 14 and 15. Therefore we need to measure masses 28 and 29 to determine the isotopic ratio of nitrogen if there is no interference. Actually, there are many interfering molecules and we need to measure masses 26-30 to make the correction. The major interferences are carbon monoxide interference at masses 28-30 and hydrocarbon interference at masses 26-30. Two assumptions are needed to make the correction. 1) The isotopic ratios of carbon and oxygen are known. 2) The relative abundance of hydrocarbon at masses 26-30 is known. With these assumptions, we are able to get a unique solution for the unknowns (abundance of nitrogen, carbon monoxide, hydrocarbon and the isotopic ratio of nitrogen). The correction is quite small (less than a few per mill in most cases), so even if the assumptions we made is not strictly valid it does not affect the isotopic ratio significantly.

To minimize the effect of mass discrimination, we always measure rather constant amounts of nitrogen (3-15 ng). The isotope anomaly is calculated from the difference of the 15/14 ratio between the sample and the STD at the same amount of nitrogen.

The performance of our system is compared with other systems in the world (Table 1). The Clayton's system uses a dynamic mass-spectrometer, while the others use static mass spectrometers.

Canyon Diablo (IA) was measured to confirm that we can reproduce the isotope anomaly reported by Prombo and Clayton[2]. Ar is also measured to provide evidence for the

origin of nitrogen.

LL chondrites, Chainpur(LL3), Yamato74442(LL4) and St.Severin (LL6) have been measured so far. The nitrogen abundances range from 4.1 to 70.5 ppm, while the bulk isotopic ratios range from -13.8 to 8.2 permil. The respective values are shown in table 2. Duplicate measurements on Chainpur and St.Severin show that isotopic ratio vs. temperature diagram is fairly reproducible, while nitrogen release pattern could be variable at sample sizes of 50 mg. It was observed that at the highest temperatures (1100 - 1200 C) nitrogen isotope tends to be heavy, which may be due to cosmogenic nitrogen. At low temperatures, it is not easy to distinguish contamination (adsorbed air and organic nitrogen) from indigenous nitrogen. Similar release patterns of nitrogen and 36-argon in many samples suggest that contamination is not serious. On the other hand, a slight bump on isotope profile at 500 C suggests some contamination. If the data at 700 - 900 C are selected to avoid the effect of possible contamination and that of cosmogenic nitrogen, then a trend of increasing isotopic ratio with the increase in petrologic type is observed.

Table 1 Comparison of nitrogen measurement systems

	THIS STUDY	F.& P.[1]	PILLINGER[3]	CLAYTON[4]
Dynamic range (ng)	3-15	0.1-250	0.6-14	>50
Error (per mill)	3	20-2	3-0.1	<1
Blank (pg/min.)	1.5	10	1	-
Time (min.)	4	5-20	20-30	-
Cold blank (ng)	0.5	0.1	0.5	2000
Hot blank (ng)	3	1	1	<100

Errors are one standard deviation.

Table 2 Bulk results for nitrogen and 36-argon.

Sample	Nitrogen(ppm)	Delta-15N(permil)	36-Argon(ccSTP/g)
Chainpur	23.2	-13.8	4.2e-7
Chainpur	70.5	-9.1	6.3e-7
Y74442	7.0	-10.1	4.8e-8
St.Severin	4.1	+7.8	4.5e-8
St.Severin(S)	6.8	+8.2	2.4e-8
Canyon Diablo	21.7	-45.6	8.4e-8

(S) for St.Severin denotes silicate portion.

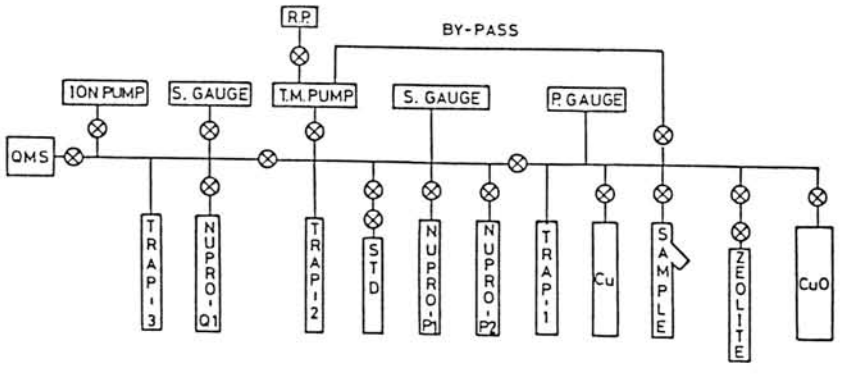

References: [1] U.Frick and R.O.Pepin (1981) Earth Planet.Sci.Lett. 56,64. [2] C.A.Prombo and R.N.Clayton (1983) Lunar Planet. Sci. XIV, 620. [3] S.R.Boyd, I.P.Wright, I.A.Franchi and C.T.Pillinger, Submitted to J. Phys. E. [4] C-C. Kung and R.N.Clayton (1978) Earth Planet. Sci. Lett. 38, 421.

NE ENRICHMENT IN SILICA GLASSES PRODUCED BY SHOCK AND IN OBSIDIANS

Matsubara, K., Yajima, H., Yamamoto, K. and Matsuda, J.

Faculty of Science, Kobe University, Nada, Kobe 657.

We measured major elements and noble gases in seven obsidians and three pieces of a Darwin glass. The obsidian samples were obtained from Turkey (NE1, NE2, NE3 and ME1), U.S.A. (US115, US330a and US8123) and Japan (7473104). We used 60-100 mesh fraction except for the sample NE3 in order to obtain diffusion constants of noble gases by the step-wise heating technique. Darwin glass (DG#1 and DG#2 were chipped sample, DG#3 was 60-100 mesh fraction) was obtained from Mt. Darwin crater in Australia, and was considered as being produced by impact melting during meteorite collision.

Major element compositions were analyzed by the X-ray fluorescence spectrometry, except for Na_2O. H_2O was measured by using the method given by Sugisaki (1). $H_2O(+)$ was detected only for ME1. For all samples, $H_2O(-)$ was too low to be determined. SiO_2 contents of obsidians were ranging from 71 to 76%. Whereas that of Darwin glass was 84.9%, much higher than those of obsidians. TiO_2 and MgO contents in Darwin glass were higher than those in obsidians. CaO, Na_2O and K_2O contents were lower than those in obsidians. There seem no clear differences in major element compositions among obsidian samples used in this study, except for that CaO contents in obsidians obtained from Turkey were lower than those in other obsidians from U.S.A. and Japan.

About 0.3-1g sample was used for determing noble gas abundances by mass spectrometry. ^{4}He and ^{132}Xe concentrations were only as upper limits in many samples. ^{20}Ne, ^{36}Ar and ^{84}Kr concentrations varied by one to three orders of magnitude, though SiO_2 content was nearly the same in obsidians.

From the results of the step-wise heating experiments for the sample ME1, ^{36}Ar was released at 800 to 1400°C and ^{84}Kr mainly at 1200 to 1400°C. Although the 800°C fraction of ^{132}Xe was highest, considerable amounts of ^{132}Xe was released even at 1600 °C. As almost all ^{20}Ne was released below 800°C, we did the step-wise heating experiment of Ne below 800 °C for the samples NE2, ME1, 7473104 and DG#3. For all samples, ^{20}Ne was released mainly at 400 to 500°C.

The fractionations of noble gases in obsidians seemed to show the monotonic changes from ^{36}Ar to ^{132}Xe, relative to the atmospheric abundance. There are both directions of increasing and decreasing of the fractionation with increasing the mass number. Whereas, the fractionations of ^{20}Ne to ^{36}Ar in obsidians were variable. The elemental abundance patterns of noble gases in obsidians and Darwin glass showed ^{20}Ne

enrichment relative to the atmospheric abundance, except for the samples US1823 and NE3. The whole patterns of fractionations were very similar to the type 2 which was observed in submarine glasses (**2**, **3**). The fractionations of heavy noble gases in obsidians were smaller than those in submarine glasses. The noble gas abundance patterns of tektites had a high F(20) about 10 to 1800 (**4**, **5**). F(20) is the fractionation factor defined by a following equation,

$$F(20)=(^{20}Ne/^{36}Ar)_{sample}/(^{20}Ne/^{36}Ar)_{atmosphere}.$$

The Ne enrichment in impact glass and tektite indicates that the Ne excess should have occured on the Earth's surface, rather than at the magma generation inside the Earth. Bogard et al. (**5**) and Wiens and Pepin (**6**) reported that shock-implanted noble gases in silicates showed no elemental fractionations, and that the Ne/Ar ratios were lower than that of the ambient atmosphere in their experiments. The step-wise heating experiment showed that Ne is released at low temperatures of 200-400°C, suggesting that diffusion of Ne from these samples readily occurs (**5**). Ne in shock-produced diamonds was tightly trapped, being released at temperature as high as 2000°C, but the elemental fractionation pattern of noble gases showed small depletion of light noble gases relative to the atmospheric abundance (**7**). These experiments suggest that the Ne excess which is now observed was not shown in the noble gas pattern of impact glass immediately after the shock event on the Earth's surface. The Ne/Ar ratio of the Darwin glass should be lower or almost the same as that of atmosphere when it was formed. This suggest that Ne excess occured by gas-solid interaction during the time since the impact glass had solidified. Therefore, the possible mechanism to produce Ne excess would be a diffusion process in a gas-solid interaction, where the light noble gases enter the material more easily than heavy noble gases.

The diffusion coefficients of noble gases in obsidian (ME1, NE2 and 7473104) and Darwin glass were determined from the step-wise heating data. The activation energy and the diffusion constant of noble gases in obsidians and Darwin glass were listed in Table. The diffusion coefficients of Ne in three obsidians were very similar, and seem to lie on the straight line, corresponding to the activation energy of 18-20 Kcal/mole. Although the linearity was not good, the diffusion coefficients of Ne in Darwin glass were similar to those in obsidians. The difference of diffusion coeffients of Ar and Kr in obsidians is smaller than those of Ne and Ar in them. This could be the main cause of the Ne excess.

REFERENCES

(1) Sugisaki, R. (1981), J. Geol. Soc. Jpn., **87**, 77-85.
(2) Dymond, J and Hogan, L. (1973), Earth Planet. Sci. Lett., **20**, 131-139.

(3) Ozima, M. and Zashu, S (1983), Noble gas Geochemistry, Cambridge Univ. Press.
(4) Hennecke, E. W., Manuel, O. K. and Sabu, D. D. (1975), J. Geophys. Res., **80**, 2931-2934.
(5) Bogard, D. D., Horz, F. and Johnson, P. H. (1986), Proc. Lunar Planet. Sci. Conf. 17th; J. Geophys. Res., **91**, E99-E114.
(6) Wiens, R. C. and Pepin, R. O. (1988), Geochim. Cosmochim. Acta, **52**, 295-307.
(7) Matsuda, J. and Nagao, K. (1989), Geochim. Cosmochim. Acta (in press).

Table The activation energy (E) and the diffusion constant (D_0) of noble gases in obsidians and Darwin glass.

Sample	Noble gas	Temp. (°C)	E (Kcal/mole)	D_0 (cm^3/sec)
NE2(obsidian)	Ne	300- 600	17.5	$5.5X10^{-4}$
ME1(obsidian)	Ne	300- 600	18.6	$7.2X10^{-4}$
	Ar	800-1400	18.1	$3.3X10^{-6}$
	Kr	800-1400	30.2	$6.9X10^{-5}$
7473104(obsidian)	Ne	200- 500	20.1	$6.9X10^{-3}$
DG#3(Darwin glass)	Ne	300- 700	21.7	$3.4X10^{-3}$

Noble gases in ureilite — Constraint on origin —

Nobuo Takaoka(Department of Earth Sciences, Yamagata University)

ALH-77257(Ur) contains large amounts of trapped noble gases (Takaoka,1983, 1984; Takaoka and Sekii,1985). The isotopic compositions of Ne and Ar trapped in carbon veins are summarized in Table 1. The isotopic composition of trapped Ne is in good agreement with that for Ne-U (Ott et al.,1984). The lowest value of trapped $^{40}Ar/^{36}Ar$ ratio is 1.2×10^{-3}, which is comparable with the ratio for Kenna carbon (Göbel et al.,1978).

Table 1. Isotopic compositions of trapped Ne and Ar in ALH-77257(Ur) carbon.

Sample	$^{20}Ne/^{22}Ne$	$^{21}Ne/^{22}Ne$	$^{38}Ar/^{36}Ar$	$^{40}Ar/^{36}Ar$
ALH-77257(this work)	10.46 ±.20	0.0285 ±.0021	0.1915 ±.0025	0.0012±.0004
U-Ne(Ott et al.1984)	10.4 ±.3	0.027 ±.003	---	---
Kenna(Göbel et al.,1978)	---	---	0.190 ±.003	0.0017±.0003

It is not clear what mechanism enriched noble gases in the carbon veins and how it was related to the origin of ureilites. Most of noble gases in the carbon veins are trapped in diamonds (Göbel et al.,1978). Diamonds in ureilites were produced by shock at collision on the parent body(Lipschutz,1964), or by crystal growth in the proto-solar nebula (Fukunaga et al.,1987; Miyamoto et al.,1988). If the diamonds were produced by shock in a noble gas-containing atmosphere and trapped the noble gases at this time, the shock could implant the noble gases into silicates (Begemann and Ott, 1983).

We separated the silicate and carbon phases by hand-picking and chemical etching, respectively. We compare the noble gas data for the silicates with those for the carbon residues (Table 2). Spallogenic He and Ne dominate in the silicate phase. Minor part of ^{20}Ne can be assigned to trapped Ne because the $^{20}Ne/^{22}Ne$ ratio is slightly larger than one. The $^{38}Ar/^{36}Ar$ ratio of 0.196 means that 99.7 % of ^{36}Ar is trapped and 0.3 % is spallogenic. For ^{40}Ar, we can give only an upper limit because of large blank correction. The isotopic compositions of Kr and Xe are indistinguishable from those in the carbon phase (Fig. 1). This indicates that Kr and Xe in the silicates are trapped. The estimated amounts of trapped gases are given in parentheses. The estimation of trapped ^{4}He is difficult because of no data available on the U content in the silicate fraction. The trapped ^{132}Xe in the silicate fraction is 1/3500 times

attributed to oxidation of diamond by solid silicates and/or gaseous oxygen. The large amounts of trapped gases in the ureilite diamond mean that the ureilite diamonds were in a reducing condition during the shock heating.

References

Begemann and Ott(1983): Geochim.Cosmochim.Acta 47,975; Fukunaga et at.(1987): Nature 328,141; Göbel et al.(1978), J.Geophys.Res. 83,855; Lewis et al.(1975): Science 190,1251; Lipschutz (1964): Science 143,1431; Matsuda et al.(1989): Proc.Symp.Solar Sci.(10th) 1; Miyamoto et al.(1988): Geophys.Res.Lett .15,1445; Ott et al.(1984): Meteoritics 19,287; Pepin et al.(1963): J.Geophys.Res. 69, 1406; Takaoka(1983): Abstr.8th Symp.Ant.Met. 50; Takaoka(1984): Abstr.9th Symp. Ant.Met. 46; Takaoka and Sekii(1985): Abstr.10th Symp.Ant.Met. 65; Wacker(1986): Geochim.Cosmochim.Acta 50,633.

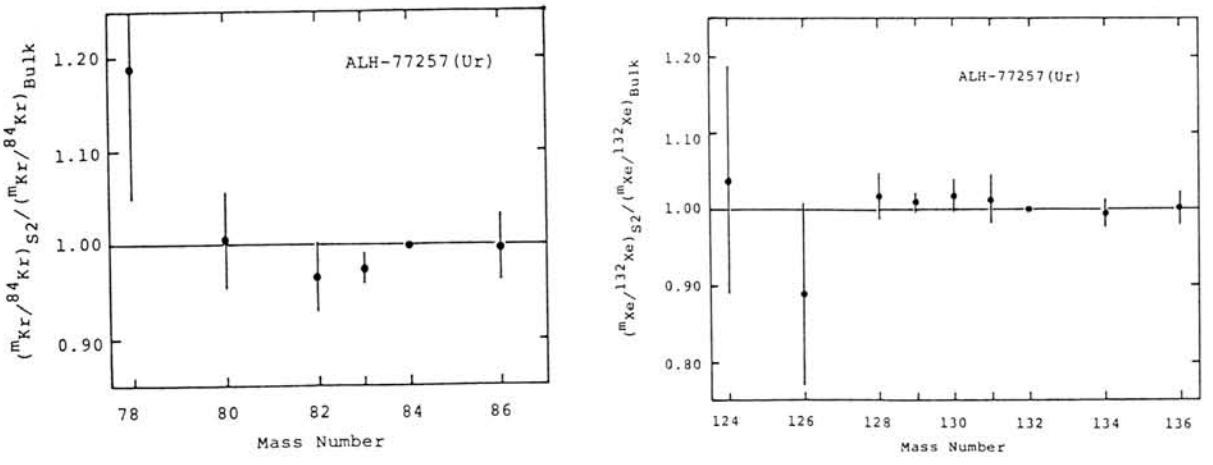

Fig. 1, Comparison of isotopic ratios of Kr and Xe between silicates and bulk of ALH-77257 (Ur.) Kr and Xe in bulk are contained in diamond. The isotopic ratio at ^{78}Kr is disturbed by a large hydrocarbon peak.

that in the carbon fraction.

There are two possible interpretations of the trapped gases found in the silicate fraction: One is owing to noble gases trapped in the silicates and the other is contamination of noble gases trapped in the carbons. The mixing of 0.03 % carbons intruded into the silicates by the shock can explain the trapped gases found in the silicate fraction. Such a low content of carbon must have been exhausted for reducing part of the silicates and the evolved gases possibly except He could be contained in the silicates. A part of He may have been lost by diffusion during a high-temperature period. The equal isotopic compositions of Kr and Xe between the silicates and the carbons suggest that the silicates underwent no large losses of these gases because the large losses could change the isotopic compositions (Begemann and Ott,1983).

A large amount of Ar was implanted into meteorite silicates by a 600 kb shock pressure (Pepin et al.,1963). This and the low noble gas content in the ureilite silicates imply that the ureilite carbons did not aquire the noble gases by the shock event on the parent body but had trapped the gases probably at the formation of carbonaceous matter, for which the vapor growth of diamond in the protosolar nebula has been proposed (Fukumoto et al.,1987). A recent result on the noble gases in vapor growth carbon polimorphs (Matsuda et al.,1989) seems to be compatible with the result on the primordial gases in the unshocked, diamond-free ureilite ALHA-78019(Wacker, 1986).

Table 2. Noble gases in silicates

Isotope	Silicates	Carbon/Silicate
^{3}He	205	0.77
^{4}He	901	99.9
^{20}Ne	40.6(2.0)	50.0(1000)
^{21}Ne	40.5	0.148
^{22}Ne	47.5	4.08
^{36}Ar	139(138.6)	2800(2800)
^{38}Ar	27.2	2700
^{40}Ar	<40	>360
^{84}Kr	0.76(0.76)	4600(4600)
^{132}Xe	0.65(0.65)	3500(3500)

Concentrations in 10^{-9} ml/g

From these discussions, we suppose that the trapped gases found in the silicate fraction are assigned to the contamination of the trapped gases in the carbon fraction. This is compatible with that the trapped gases in primitive meteorites such as carbonaceous chondrites are contained in the carbon phase, but not in the silicate phase (Lewis et al.,1975).

There is a considerable difference in noble gas release patterns beween the pure carbons and the carbons mixed with the silicate minerals of ureilite. The pure carbons release the gases at about 1900 C, while the carbon-silicate mixture does at 1200 - 1400 C for 30 - 60 minutes. The gas release at 1900 C is due to conversion of diamond to graphite. The release at 1200 - 1400 C can be

COMPARISON OF THE PREVIOUS CARBON-14 TEREESTRIAL AGES

Yasunori MIURA[1] and Roelf BEUKENS[2]

1) Faculty of Science, Yamaguchi University, Yamaguchi, 753.
2) IsoTrace Laboratory, University of Toronto, Toronto, Ontario M5S 1A7

1. Introduction

The previous ^{14}C terrestrial ages are largely different between the counting method and the accelerator mass spectrometry (AMS). It is also found that five Tandtron AMS facilities (Toronto, Arizona, Gif-Sur-Yvette, Nagoya and Oxford) have been reported the different C-14 data and concentrations of the Bruderheim (L6) chondrite.

It will be discussed that the major differences of the previous C-14 data.

2. C-14 data interpretation

The real ^{14}C concentration should be discussed in the contamination, efficiency and measurement methods, which are summarized as follows:

1) Determination of the ^{14}C terrestrial ages requires careful removal of the **terrestrial contamination.**
We use step-wise extraction up to 1,600 °C (melt fraction) (cf. Simoneit et al.).
Other methods are step-wise combustion, extraction and/or combustion at temperature below 1,000 °C.

2) For every method the important parameters are **efficiency** and **contamination.**
The efficiency will be compared for the different methods by comparing the ^{14}C concentration (dpm/kg) extracted from the Bruderheim chondrite, which has been analyzed by every method.
The contamination will be compared for those methods for which has been analyzed.

3) Our step-wise extraction method will be discussed in detail, mainly:

a) In the Bruderheim spallation ^{14}C is extracted in the 500 °C to 1,000 °C fraction (≈24%) as well as in the high temperature melt fraction(≈76%). This will be shown by the extraction of ^{14}C from irradiated Bruderheim samples.
No "weathering" carbon is extracted from Bruderheim as expected.

b) Our extraction efficiency is ≈40% greater than for the low temperature extraction methods.

c) The contamination in our method has been checked very carefully. We will show the contamination from Fireman's extraction CuO oxidation system, as well as the contribution of the crucible to the ^{14}C for the temperature fractions of <500 °C, 500 °C to 1,000 °C and 1,600 °C (melt).

4) The consequences for the interpretation of our results ans those of others will be discussed.

First, for **absolute measurements**, e.g. in situ produced ^{14}C, the value (quoted by Jull et al.) is too low by ≈40%.

Secondaly, for the **relative measurements**, e.g. terrestrial ages of the Antarctic meteorites, some results are in correct, some are reasonably accurate because two errors nearly cancel.

Thirdly, **"weathering" ages** determined by others are incorrect as the spallation ^{14}C extracted at low temperatures have not taken into account. If possible, we will discuss the effect of contamination on the older meteorites.

<u>References:</u>

Beukens R. P. et al. (1988): <u>Proc. NIPR Symp. Antarctic Meteorites,</u> 224-230.

Fireman E. L. (1983): <u>Mem. Natl Inst. Polar Res., Spec. Issue,</u> 30, 246-250.

Jull A. J. T. et al. (1984): <u>Proc. Lunar Planet. Sci. Conf.,</u> 15th, C329-C335.

Simoneit B.R. et al. (1973): <u>Proc. Lunar Sci. Conf.,</u> 4th, 1635-1650.

TERRESTRIAL ^{81}Kr-Kr AGES OF ANTARCTIC EUCRITES

Nagao, K. and Ogata, A.

Institute for Study of the Earth's Interior, Okayama University, Misasa, Tottori-ken 682-02.

Because of a long residence of Antarctic meteorites, their terrestrial ages have special importance for the investigations of concentration mechanism of meteorites on blue ice fields, of time dependent variation of infall meteorite species, and of movement of ice sheet on Antarctica. However, only a few data on the terrestrial age are available for Antarctic meteorite collection of Japan. Recently, we started to measure the terrestrial age of these meteorites by ^{81}Kr as a comparative study of terrestrial age with other methods such as ^{14}C, ^{26}Al, TL, etc.

Kr isotopic compositions as well as other noble gases were measured for five Yamato eucrites Y-791186, -791960, -791962, -792510 and -792769. Cosmogenic radionuclide ^{81}Kr as well as the cosmogenic stable isotopes of Kr were detected clearly for these eucrites, and ^{81}Kr-Kr method was applied to them to estimate the terrestrial ages. Other noble gas isotopic compositions are also useful for an identification of paired meteorites of a single fall, for the estimation of the duration of cosmic-ray exposure, etc.

^{81}Kr-Kr method was developed by Marti (1967) and Eugster et al. (1967) to determine the cosmic-ray exposure age, and was modified by Schultz (1986) and Freundel et al. (1986) to calculate the terrestrial age. According to them, the ^{81}Kr-Kr exposure age is evaluated by,

$$T = (1/\lambda)(0.95/2)(^{80}Kr/^{83}Kr + ^{82}Kr/^{83}Kr)(^{83}Kr/^{81}Kr)$$

where $\lambda = 3.25 \times 10^{-6}$/y, which is the decay constant of ^{81}Kr. If this equation is applied to the meteorite of long terrestrial age, the calculated age is "an apparent exposure age **Ta**" which is larger than a true exposure age due to the radioactive decay of ^{81}Kr during the residence on the earth. If the true exposure age **Te** is determined by other method, the terrestrial age **Tt** can be calculated by,

$$Tt = (1/\lambda)\ln(Ta/Te).$$

For the calculation of true exposue age, Freundel et al. (1986) presented an equation to estimate cosmogenic ^{38}Ar production rate as a function of chemical composition of individual meteorite.

The terrestrial ages determined with these equations are listed in Table 1, in which the data for other Yamato eucrites are also included for comparison. K-Ar ages were also estimated for these eucrites. Our tentative conclusions are followings;

1) Five eucrites belong to three groups as shown in Table 1, based on the noble gas data.
2) The terrestrial ages are in the range of 0.23-0.35 Ma which are relatively older than the ages reported for other Yamato eucrites (Nishiizumi, 1986; Schultz, 1986).
3) Though the data on the terrestrial ages of Yamato eucrites obtained until now are very limitted, two groups of eucrites from two different ice fields designated as Eucrite-A and -B (Takeda and Yanai, 1982) may have different terrestrial ages; the eucrites from B have longer terrestrial ages than the eucrites from A.
4) $^{78}Kr/^{83}Kr$ ratio of cosmogenic Kr is sensitive to the shielding effect. Accordong to the calculation on the relationship between ^{38}Ar production rate and $^{78}Kr/^{83}Kr$ ratio for eucrite meteoroids with different radii (Freundel et al., 1986), the preatmospheric body of Y-791186 and -792510 was smal (about 10 cm in diameter), whereas that of Y-791960 and -791962 might be about 1 m in diameter, in which -791960 was near the surface and -791962 was in the center.
5) K-Ar age for both Y-791186 and -792510, which are paired monomict eucrites, is 2.7+/-0.2 b.y. The ages for Y-791960 and -792769 are 3.2+/-0.2 and 3.0+/-0.2 b.y., respectively.

Though the nobel gas compositions obtained by us and Schultz (1986) suggest the pairing of Yamato eucrites as shown in Table 1, it may be in contradiction to the field observation. Do the different groups of polimict eucrites concentrate at the same area on the blue ice field ? More systematic investigation on the Yamato eucrites is needed to solve such a contradictory problem.

REFERENCES:

Marti, K.(1967) Phys. Rev. 18, 264-266.
Eugster, O., Eberhardt, P. and Geiss, J. (1967) Earth Planet. Sci. Lett., 2, 77-82.
Schultz (1986) Mem. Natl Inst. Polar Res., Spec. Issue, 41, 319-327.
Freundel, M., Schultz, L. and Reedy, R.C. (1986) Geochim. Cosmochim. Acta, 50, 2663-2673.
Takeda and Yanai (1982) Mem. Natl Ins. Polar Res., Spec. Issue, 25, 97-123.
Nishiizumi (1986) LPI Tech. Rept, 86-01, 71-73.
Nagao, K., Ogata, K., Takaoka, N. and Saito, K. (1983) Mem. Natl Inst. Polar Res., Spec. Issue,30, 349-361.
Kamaguchi, A. and Okano, J. (1979) Mem. Natl Inst. Polar Res. Spec. Issue, 12, 178-185.

Table 1. Cosmogenic noble gases, production rate of 38Ar P(38), true exposure age T38, apparent exposure age Ta, and terrestrial age Tt, of Antarctic eucrites.

Sample	type	21Ne	38Ar	P(38)	T38 (Ma)	Ta (Ma)	Tt (Ma)	(78Kr/83Kr)	K-Ar age(b.y.)	Ref.
Y-791186	mon	2.80	1.80	0.135±0.014[1]	13.33±1.38	29.5±2.1	0.24±0.04	0.2038±0.0088	2.7 ± 0.2	a)
Y-792510	mon	2.89	1.55	0.133±0.012[1]	11.65±1.05	24.8±1.8	0.23±0.04	0.2313±0.0095	2.7 ± 0.2	a)
Y-791960	pol	2.35	0.797	0.117±0.010[1]	6.81±0.58	16.5±1.4	0.27±0.04	0.2023±0.0096	3.2 ± 0.2	a)
Y-791962		2.28	0.438			14.6±1.1		0.1642±0.0218		a)
Y-792769	pol	1.51	0.541	0.145±0.013[2]	3.73±0.33	11.7±0.5	0.35±0.03	0.2386±0.0087	3.0 ± 0.2	a)
Y-74159	pol	12.6	9.80						3.8 ± 0.2[5]	b)
		9.02	9.98	(0.139)[3]	72	63.	-41	0.1860±0.0097	3.9 ± 0.2[5]	b)
Y-74450	pol		9.56	0.131±0.007	73.0 ±6.4	65.8±7.7	-32 ±44		4.1 ± 0.2[6]	c)
Y-75015	pol	15.3	9.99					0.2129±0.0231		d)
Y-790007	pol		9.61	0.131±0.008	73.3 ±7.2	66.6±3.6	-29 ±34		4.2 ± 0.2[6]	c)
Y-790122	pol			0.126±0.008	24.4 ±1.7	35.1±2.5	0.11±0.03			c)
Y-790260	pol			0.120±0.008	21.6 ±1.7	34.1±2.4	0.14±0.03			c)
		3.38[4]	2.74[4]	(0.120)	22.8	32	0.10		3.3 ± 0.2[7]	b)
Y-790266	pol			0.133±0.008	21.9 ±1.6	35.8±2.8	0.15±0.03			c)

[1] Chemical compositions by Haramura were used(Takeda: private communication), [2] Bulk chemical compositions presented by Takeda and Yanai(1982) were used. [3] Mean production rate of eucrite(Freundel et al., 1986) [4] Mean value of duplicate analyses, [5] K content of 550ppm (Kamaguchi and Okano, 1979) was used, [6] Calculated with the data by Schulz (1986), [7] K content by Schultz(1986) was used.

a) This work b) Nagao(unpublished) c) Schultz(1986) d) Nagao et al.(1983)

51

TERRESTRIAL AGE OF ANTARCTIC METEORITE MEASURED BY THERMOLUMINESCENCE OF FUSION CRUST

A.Nakanishi, H.Ono and S.Miono

Department of Physics, Osaka City University, Osaka 558

Terrestrial age of Antarctic meteorites are estimated by means of thermoluminescence(TL) intensity of fusion crusts. The TL intensity is reset to zero, because of the heat during its passing through atmosphere. Subsequently the TL intensity increases with time due to environmental radiation(1). Samples are filed out from fusion crusts by diamond grinder sheet in the water and magnetic component is removed. After sample is dried, 5 mg of each is measured. 12 Yamato meteorites are measured. 6 of these have known terrestrial ages measured by ^{14}C(2) and 2 is considered to be paired, so our results are compared with these data.

Reference
(1) NINAGAWA, K., MIONO, S., YOSHIDA, M. and TAKAOKA, N., Lett. al Nuovo Cimento 38(1983), 33
(2) MIURA, Y. , private communication(1988)

Thermoluminescence study of ordinary chondorites by TL spatial distribution readout system

Ninagawa, K.

Okayama University of Science, Ridai-cho 1-1, Okayama 700

In principle, there are two methods to determine the terrestrial ages of the meteorites by the thermoluminescence[TL] technique. One is the method to measure the TL grown on the earth using surface materials, which was annealled by heating during the atmospheric passage(1,2). The other is the method to measure the magnitude of the fading using interior samples (3,4). This time, TL emission spectra of ordinary chondrites, ALH-77294(H5) and ALH-77216(L3), are measured by a time-resolving spectroscopy system. Then TL images of sliced samples of these meteorites are measured by the TL spatial distribution readout system and local TL glow curves are analized.

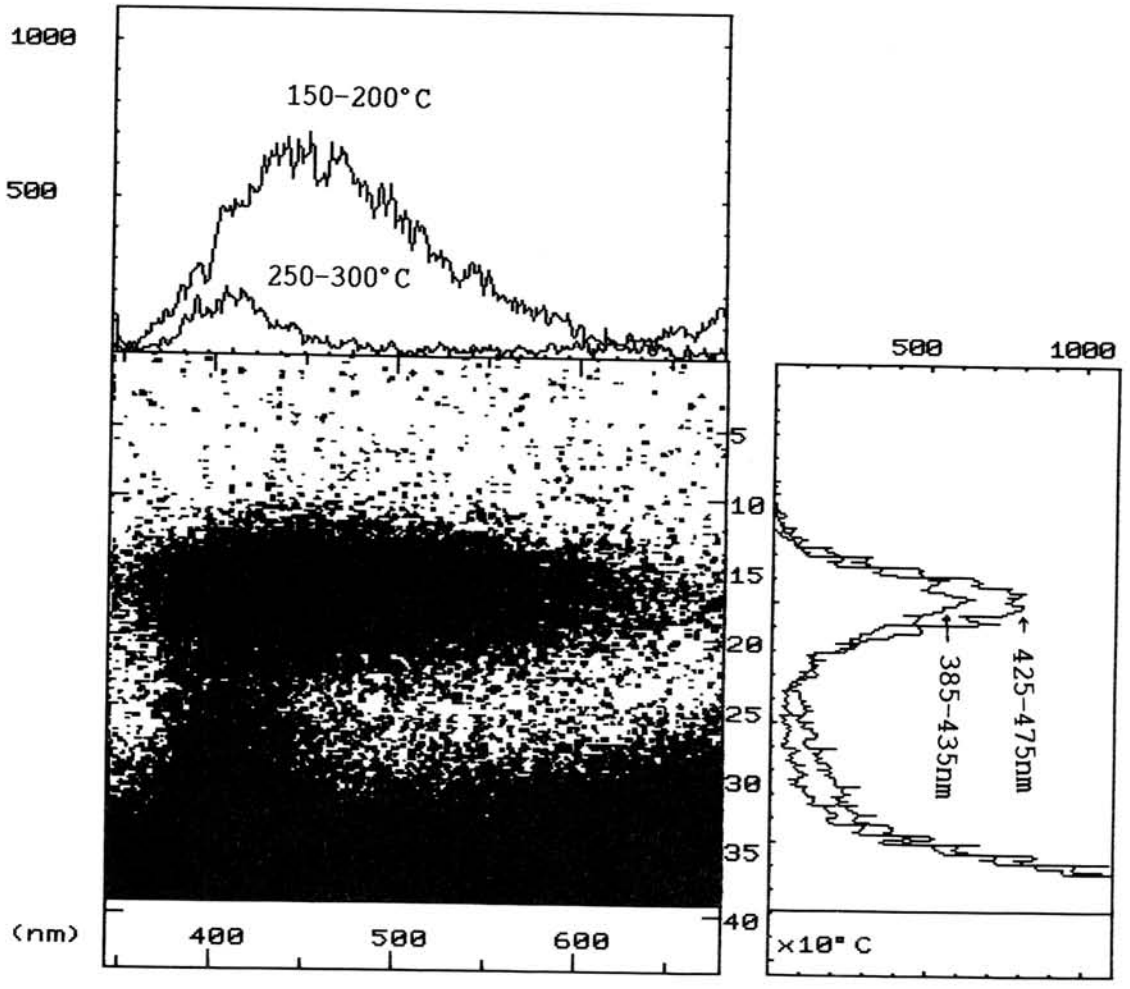

Fig.1 Emission spectrum of natural TL [ALH-77294]. The position of high TL intensity is put by black points.

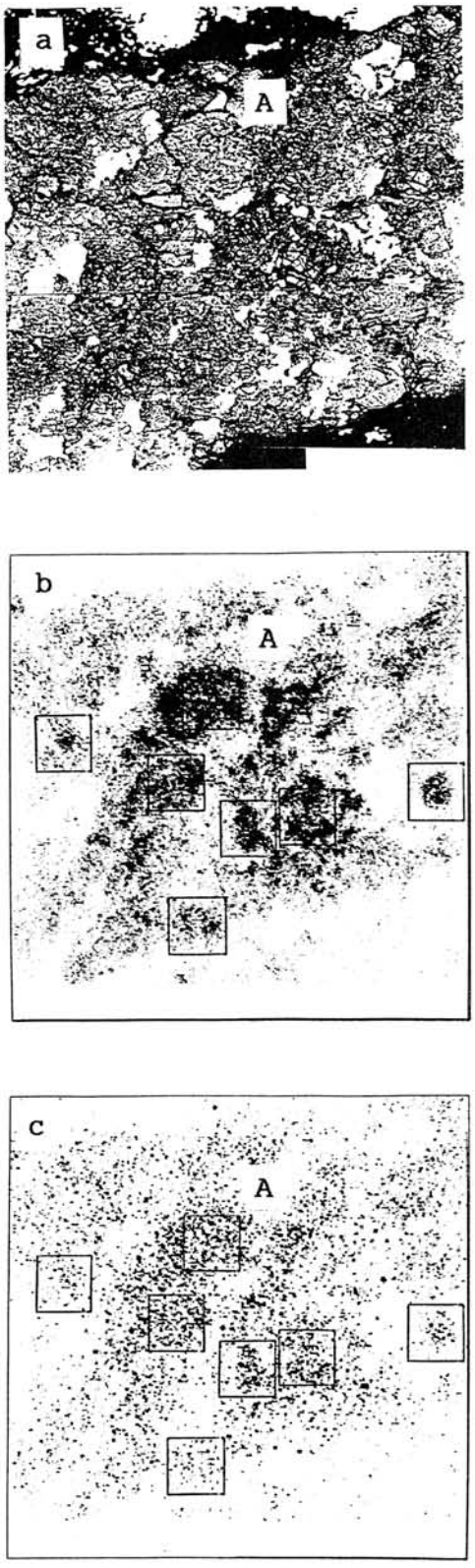

A time-resolving spectroscopy system is constituted of the TL spatial distribution readout system and a spectroscope(5). This system is improved to collect much light using a parabolic millar. Emission spectra of the first glow (natural TL) and the second glow of these chondrites are measured. That of the first glow [ALH-77294] is shown in Fig.1. Their emission spectra are consistent with those of Allegan, Barwell, Olivenza and Farmington measured by Strain et al.(6). TL emission spectra of these ordinary chondrites at low temperature is different from that at high temperature. The TL emission peak at low temperature (150-200°C) is 450nm with 130nm FWHM. That at high temperature (250-300°C) is 400nm with 60nm FWHM. This means that L/H (the ratio low temperature peak to high temperature peak), which is a indicator of the terrestrial age, depends on the TL measuring system as mentioned by Strain et al.(6) and that there is a possibility that the material responsible for the TL at low temperature is different from that at high temperature.

Figure 2a is a BEI of a sliced sample [ALH-77294]. This sample is heated and TL images are measured by the TL spatial distribution readout system. Figures 2b and 2c show TL images at low temperature(160-184°C) and at high temperature(340-362°C), respectively. The position of high TL intensity is put by deep black points. The TL image at low temperature resembles that at high temperature.

Fig.2 BEI of a sliced sample [ALH-77294] and TL images.
a)BEI of a sliced sample. b)TL image at low temperature(160-184°C). c)TL image at high temperature(340-362°C)

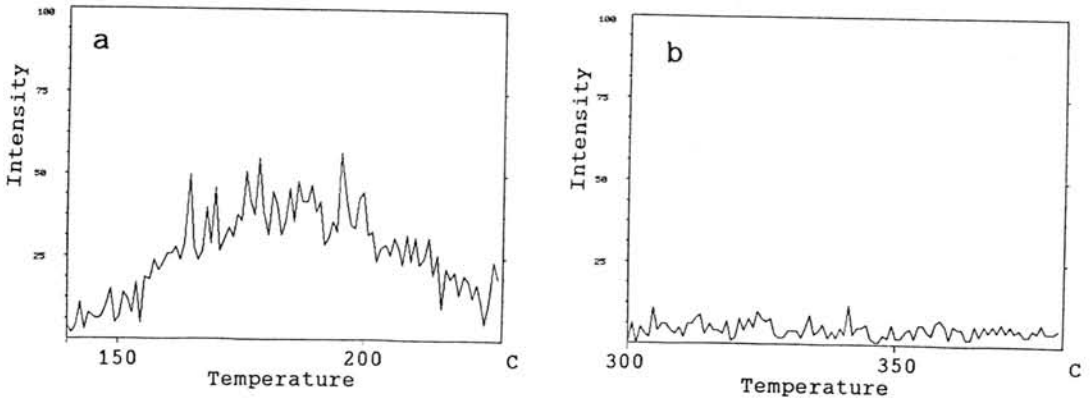

Fig.3 Glow curves of the square part A indicated in Fig.2
a)low temperature region. b)high temperature region.

This implies that the materials responsible for the TL at low temperature are the same as those at high temperature.

Local TL glow curves are also analized by 2-dimensional photon counting method(7) to investigate whether the L/H ratio is the same at any parts of the chondrites. The glow curves of the square part A is shown in Figures 3a and 3b. Many a chondrules of the high TL intensity are judged by Dr.Matsunami to be porphyritic.(8)

References

(1)Ninagawa,K., Miono,S., Yoshida,M. and Takaoka,N. (1983) Mem. Natl. Inst. Polar Res., Spec. Issue, **30**, 251-258
(2)Bhandari,N. and Senqupta,D. (1988) Papers presented to the 13th symposium on Antarctic meteorite, 103-105
(3)Melcher,C.L. (1981) Geochim. Cosmochim. Acta, **45**, 615-626
(4)Hasan,F.A., Haq,M. and Sears,D.W.G. (1987) J. Geophys. Res., **92**, E703-E709
(5)Ninagawa,K., Nakamura,M., Imaeda,K., Takahashi,N., Tomiyama,T., Yamamoto,I., Takano,Y., Yamashita,N., Yamashita,Y. and Wada,T. (1986) Bull. Okayama Uni. Sci. **21A**, 49-54
(6)Strain,J.A., Townsend,P.D., Jassemnejad,B. and McKeever,S.W.S (1985) Earth Planet. Sci. Lett. **77**, 14-19
(7)Yamamoto,I., Imaeda,K., Takahashi,N., Ninagawa,K., Tomiyama,T., Wada,T. and Yamashita,Y. (1987) Nucl. Instrum. & Methods, **A256**, 567-575
(8)Nagahara,H. (1983) Mem. Natl Inst. Polar Res., Spec. Issue, 30, 61-83.

Thursday, June 8, 1989

0900 - 1435 ***Symposium, Auditorium***

1435 - 1555 ***Special Lecture***

Professor Michael E. Lipschutz

(Purdue University)

DIFFUSION OF NOBLE GASES IN DIAMONDS

Yajima, H. and Matsuda, J.

Department of Earth Sciences, Faculty of Science, Kobe University, Nada, Kobe 657

Diamond is resistant to chemicals and mechanical stresses, and is known to be very old. It is recently proposed that natural diamonds may have preserved in situ "ancient" noble gases of the mantle (1,2). However, it is likely that noble gases move through diamond crystalline structure by diffusion process without a destruction of the diamond structure. Therefore, it is very important to determine the diffusion coefficients of noble gases in diamonds to discuss the retentivity of the ancient noble gases. In general, natural diamonds or industrial diamonds synthesized under hydrostatic pressure contain very small amounts of noble gases. This makes us difficult to estimate the diffusion coefficients of noble gases in them, especially at low temperature below 1200°C. Some workers estimated the diffusion coefficients of helium in terrestrial diamonds or extra-terrestrial diamonds in meteorites at temperatures higher than 1200 °C (2,3,4,5,6). For other noble gases of neon, argon, krypton and xenon, there has been few or no estimation of the diffusion coefficients.

Matsuda and Nagao (7) showed that shock-produced diamonds contained noble gases much larger than those of natural or industrial diamonds, and that these gases were closely trapped in the diamond structure, being released at temperature of about 2000 °C. A large amount of noble gases in shock-produced diamonds makes us possible to determine the diffusion coefficients of noble gases at low temperatures. Making use of this feature, we tried to estimate the diffusion coefficients of noble gases in diamonds.

We selected DP diamonds, synthesized by du Pont Corporation, as shock-produced diamonds. According to the explanatory note, DP diamonds are produced as follows; graphite with metal catalyst is exposed to an explosive, then a part of graphite is transformed into micro-crystals of diamond of 100 angstroms size, a cluster of such micro-crystals forms poly-crystalline diamond particle of up to 100μm size. We used three size fractions; DPF3(2-4μm), DPF9(6-12μm) and DPF30(22-36μm). Noble gases in some 200mg of these samples were analyzed by mass spectrometry using the stepwise heating technique. The analytical procedure is precisely described in another work (8).

The diffusion coefficient D (cm^2/sec) was obtained by the stepwise degassing method. The diamond particles were assumed as spherical bodies of "a" (cm) in half diameter. The values of diffusion coefficients D/a^2 (sec^{-1}) were computed from the data of release fraction of noble gases per total abundance and the duration time of heating the sample. We considered "a" as an unknown factor by following reasons. The values of D/a^2 for ^{20}Ne, ^{36}Ar and ^{84}Kr were plotted in Arrhenius diagram (Fig. 1),

of which slope gives the activation energy. The data of ^{4}He and ^{132}Xe are not displayed because of their uncertainties.

We point out two important features in this diagram. The first is that two slopes are admitted in this figure. The sharp one above 1600 °C seems to be caused by the graphitization of diamonds, and another below 1600 °C may suggest the diffusion process of noble gases in diamonds. The size dependence of noble gas atoms on the low temperature slopes is consistent with this hypothesis. The smaller noble gas atom gives the higher diffusivity. Meanwhile, the differences of the activation energies are small for graphitization process. The second feature is that the values of D/a^2 determined for any samples are identical at each extraction temperature, though the size of diamond grains are different from each other. If effective radius "a" was expressed by the size of diamond grain, the D/a^2 value would have differed between DPF3 and DPF30 by two order of magnitude. This result seems to suggest that the effective radius "a" has a common value for these diamonds. According to an explanatory note of du Pont, the du Pont diamonds consist of micro-crystals of 100 angstroms size, which agree with our observation from Arrhenius diagram. We estimated the value of "a" as about 50 angstroms. Based on this assumption, the D values of Ne, Ar and Kr were estimated to be from $1x10^{-18}$ to $1x10^{-20}$ (cm^2/sec) at about 1300 °C.

References (1) Ozima,M., Zashu,S. and Nitoh,O. (1983), Geochim. Cosmochim. Acta 47, 2217-2224. (2) Honda,M., Reynolds,J.H., Roedder,E. and Epstein,S. (1987), J. Geophys. Res. 92, 12507-12521. (3) Ozima,M., 1989, submitted to Anu. Rev. Planet. Sci. (4) Kurz,M.D., Gurney,J.J., Jenkins,W.J., and Lott III,D.E. (1987), Earth Planet. Sci. Lett. 86, 57-68. (5) Lal,D., Wacker,J.F., Poreda,R. and Craig,H. (1987), Meteoritics 22, 437-438. (6) Göbel,R., Ott,U. and Begemann,F. (1978), J. Geophys. Res. 83, 855-867. (7) Matsuda,J. and Nagao,K. (1989), Geochim. Cosmochim. Acta (in press). (8) Matsuda,J., Matsubara,K., Yajima,H. and Yamamoto,K. (1989), (in preparation)

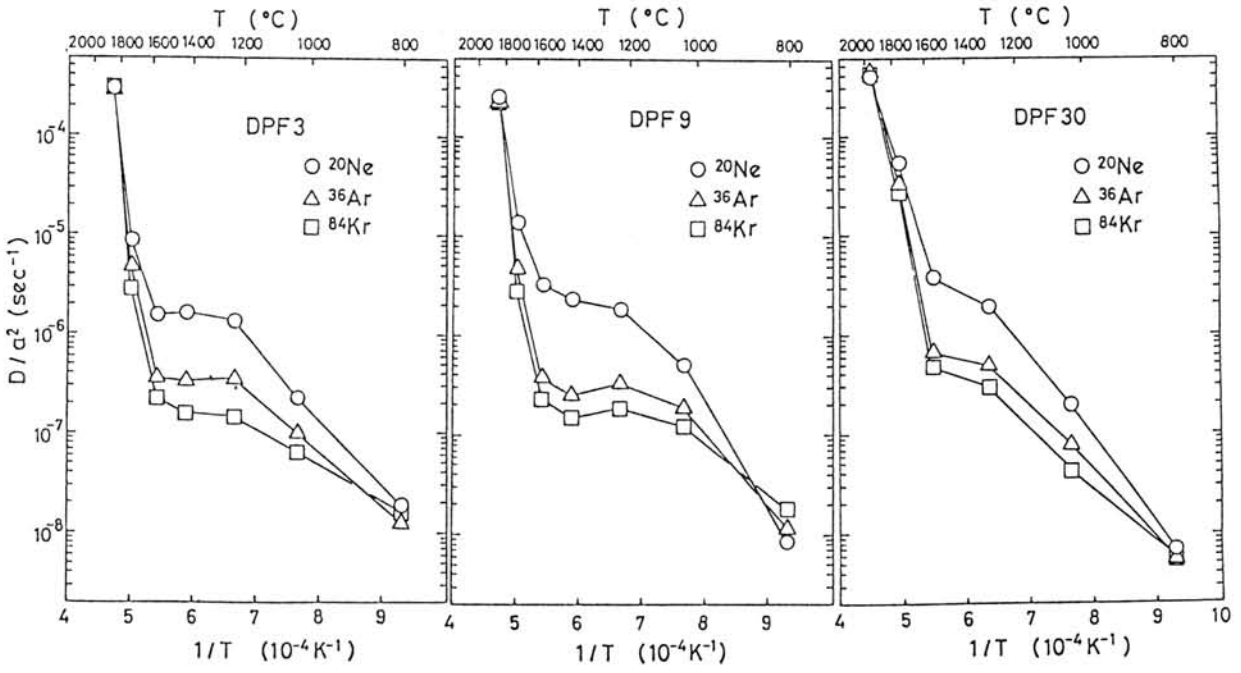

Fig. 1 Arrhenius diagram of diffusion coefficients D/a^2 (sec^{-1}) of ^{20}Ne, ^{36}Ar and ^{84}Kr trapped in three fractions of shock-produced diamonds. The values at the same temperature are identical for any samples, suggesting that the value of "a" is common among these samples. There seem two components in this diagram; the gentle slope below 1600 °C represents diffusion process of noble gases in diamonds, and another above 1600 °C suggests graphitization process of diamonds.

ISOTOPIC COMPOSITION OF RARE GASES IN VAPOUR GROWTH DIAMOND

Fukunaga, K., Matsuda, J. and Ito, K.

Department of Earth Sciences, Faculty of Science,
Kobe University, Nada, Kobe 657

Ureilites are known to have diamonds. It has been generally accepted that these diamonds were produced under high pressure by shock. Diamond is one of the rare gas carries, whereas graphite is gas-free in ureilites. We synthesized diamond by chemical vapour deposition (CVD) using microwave from gaseous mixture of H_2 and CH_4 including Ar, and examined Ar trapped in diamond by mass spectrometry. The vapour growth diamonds contained a large amount of Ar, while graphite was almost gas free. So we concluded that the diamonds in ureilites have been formed by CVD from the primitive solar nebula (1). However, the subsequent work (2) showed that the shock-produced diamonds also trapped rare gases as large as those in the vapour-growth diamonds and that their elemental ratios were similar to those of the ambient atmosphere.

Diamonds in ureilite contain 'planetary' type rare gases which is highly fractionated to be enriched in heavy gases. In this study we made diamonds by CVD from gaseous mixture including all rare gases to examine the fractionation of these gases.

Schematic drawing is shown in Fig.1. The experimental apparatus was essentially the same as that given by Fukunaga et al.(1) except that we used the mixture of all rare gases. The concentrations of CH_4 were 1% and rare gas mixtures (1% He, 1% Ne, 96% Ar, 1% Kr and 1% Xe) were 0.1%, 0.3% and 1%, respectively. Total pressures were 23 torr. A typical deposition period was about 50 hrs. According to X-ray diffraction analysis, only diamond was detected.

Rare gases were examined by mass spectrometry employing stepwise heating technique. A typical temperature steps are 800°, 1100°, 1400°, 1700° and 2000°C, respectively. We examined the concentrations of all rare gases and isotopic composition of Ne, Ar, Kr and Xe at each step. Most of rare gases were released at 2000°C step. For Ar, Kr and Xe , the elemental abundance patterns for the diamonds show strong fractionations favoring the heavy gases. These patterns provide good matches to the fractionation patterns observed in the ureilites. This result suggests that diamonds in ureilites were directly formed from solar nebula. These patterns also show good matches to the calculated ion abundance ratio under plasma conditions. For heavy rare gases, it is apparent that plasma condition plays an important role in trapping rare gases. However, for light rare gases, the elemental abundance patterns show fractionations favoring the light gases. This pattern can not be explained by the plasma process. From these facts, we concluded that there are two mechanisms for trapping rare gases. One is the plasma process and the other gives effect on light rare gases trapping like solution.

Xenon isotopic compositions of diamonds agree within error

limits with the composition of terrestrial Xe. Krypton isotopic composition is also approximately the atmospheric composition. The results of negligible isotopic fractionation at the trapping also agree with ureilite data (3).

We synthesized diamond by CVD not only using microwave but also using a hot tungsten filament. Schematic drawing of a apparatus using hot filament is shown in Fig.2. Gas mixture was decomposed by thermal electron. The temperature was maintained at 800°C by the furnace. Diamonds synthesized by hot filament method contain much less rare gases than diamonds synthesized by microwave method. This result may be caused by the difference of plasma condition.

References:
(1) Fukunaga, K., Matsuda, J., Nagao, K., Miyamoto, M. and Ito, K. (1987) Nature, 328 141-143
(2) Matsuda, J. and Nagao, K. (1989) Geochim. Cosmochim. Acta (in press)
(3) Gobel, R., Ott, U. and Begemann, F. J. Geophys. Res., 83 855-867

Fig.1

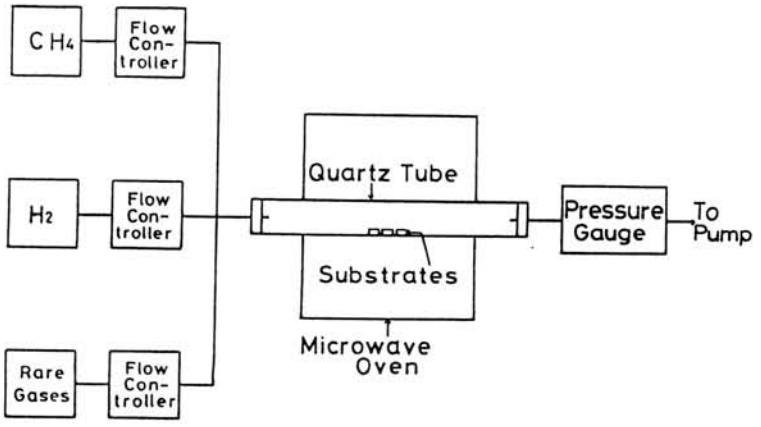

Fig.2

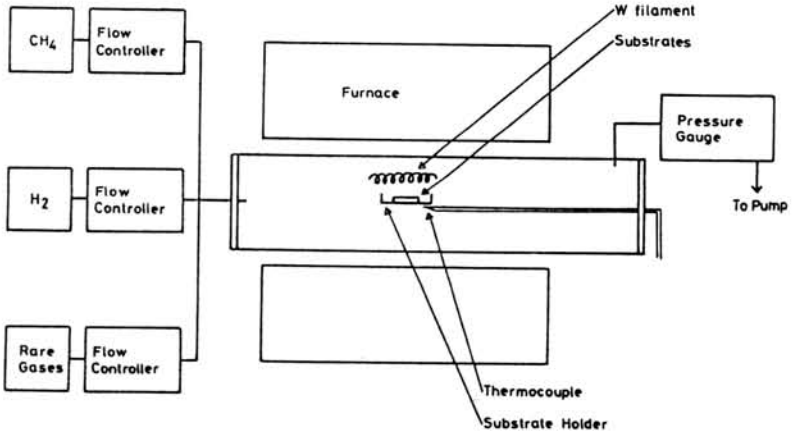

FRACTIONATION OF NOBLE GASES IN THE CARBON MATERIAL SYNTHESIZED BY GLOW-DISCHARGE CVD

Suzuki, K. and Matsuda, J.

Department of Earth Sciences, Faculty of Science,
Kobe University, Nada, Kobe 657, Japan

Noble gases in synthesizing carbon material have been studied to account for the trapping mechanism of them in meteorites. The synthesized carbonaceous materials, such as propane soot and electron-discharge kerogen etc. have been reported to be efficient trappers of noble gases (1). Dziczkaniec et al. (2) reported that the carbyne synthesized in a radio frequency plasma trapped large amounts of noble gases. Similarity, Fukunaga et al. (3) and Matsuda et al. (4) reported that vapor-growth diamond synthesized by microwave plasma was a good noble gas carrier.

We have synthesized carbon material used by glow-discharge CVD from the gas mixture of H_2, CH_4 and noble gases, and analyzed the elemental and the isotopic composition of noble gases in the synthesized carbon material. A schematic drawing of our synthesizing apparatus is shown in Figure 1. The reactant gas mixture consisted of H_2, CH_4, and noble gases (1% He, 1% Ne, 96% Ar, 1% Kr, 1% Xe ; atmospheric isotopic composition for each gas) are led to the discharge quartz tube through gas flow meter by being pumped out with a rotary pump. Total gas pressures measured with oil-manometer were about 2 torr. The discharge tube was heated at 800°C with an electric furnace. A black matter was deposited on the substrate patched on the electrode. As it had no lines by X-ray diffraction, it was identified to be amorphous carbon.

The noble gas contents of the materials were measured by mass spectrometer using stepwise heating technique. Our synthesizing materials were extremely enriched in noble gases, especially heavy noble gases. For example, the sample KS-97 was synthesized under the condition of 1% partial pressure of noble gases mixture, of which ^{132}Xe concentration was 1.2×10^{-3} ccSTP/g . The stepwise heating analysis showed that the trapped noble gases were mainly released at 1200°C. This release temperature was apparently different from that of adsorbed component and from that for diamonds (3, 4).

The elemental abundance patterns for the synthesizing material was characterized by large enrichment of ^{4}He, ^{20}Ne, ^{84}Kr, and ^{132}Xe relative to ^{36}Ar when compared to the original gas compositions. A fractionation factor F(132), being defined by $(^{132}Xe/^{36}Ar)_{sample}/(^{132}Xe/^{36}Ar)_{ambient\ atmosphere}$, was as large as about 10^3 in our material. The heavy noble gas pattern was similar to the trend of calculated ion abundance in plasma condition by Göbel et al. (5). The trend of the glow-discharge synthesizing material was very close to the ion abundance pattern at the electron temperature of 6000-7000K. But for the light noble gases, their trend could not be explained by the same process. This result suggested that there were two mechanisms for trapping noble

gases. One is the plasma process, and the other gives strong effect on trapping light noble gases .

Although strong elementary fractionation was found on our synthesizing material, no significant mass fractionations were detected for isotopic patterns of noble gases in glow-discharge synthesizing carbon material.

References

(1) Frick, U., Mack, R., and Chang, S. (1979) Proc. Lunar Planet. Sci. Conf. 10th, 1961-1973. (2) Dziczkaniec, M., Lumpkin, G. R., Donohoe, K. and Chang, S. (1981) Lunar Planet Sci. 12, 246-248. (3) Fukunaga, K., Matsuda, J., Nagao, K., Miyamoto, M. and Ito, K. (1987) Nature 328, 141-143. (4) Matsuda, J., Fukunaga, K. and Ito, K.(1989) Lunar Planet. Sci. 20. (in press) (5) Göbel, R., Ott, U. and Begemann, F. (1978) J. Geophys. Res. 83, 855-867

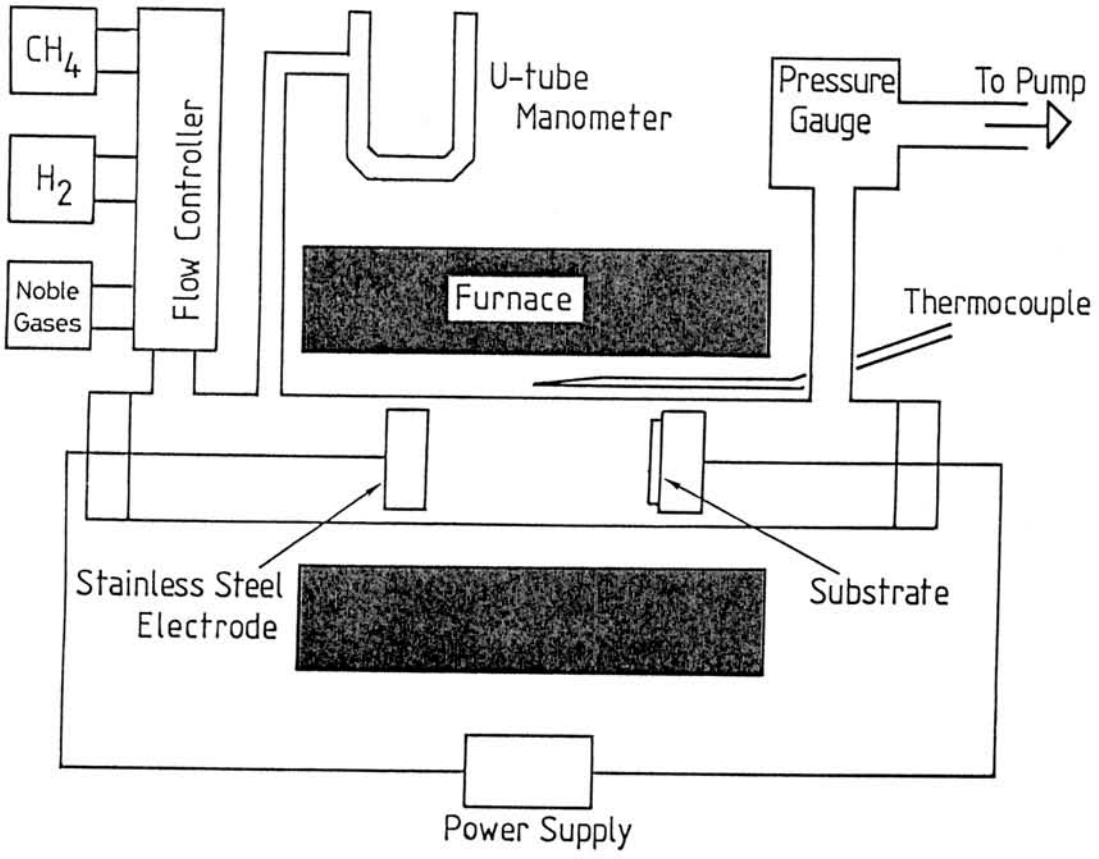

Figure 1. Schematic diagram of the experimental arrangement.

DETAILED MEASUREMENT OF POTASSIUM 40 ELECTRON CAPTURE DECAY, AND THE COMPRESSIONAL AND CHEMICAL EFFECT TO ITS DECAY CONSTANT

Kusaba, M.[1], Imamura, M.[2], Yagi, K.[3], Ozima, M.[1], Watanabe, S.[4], & Hiyagon, H.[1]

[1]Department of Geophysics, Faculty of Science, University of Tokyo, 3-1, Hongo, 7-chome, Bunkyo-ku, Tokyo 113

[2]Institute for Nuclear Study, University of Tokyo, Midori-cho, Tanashi-shi, Tokyo 188

[3]Institute for Solid State Physics, 7-22-1, Roppongi, Minato-ku, Tokyo 106

[4]Department of Physics, Faculty of Science, University of Tokyo, Tokyo 113

Introduction

We studied the effects of (1)pressure [P < 30Kbar] and (2)chemical form on the decay constant of ^{40}K. Such imformation is vital for K-Ar dating.

The electron capture of ^{40}K is known to be unique first-forbidden with ^{40}K a 4^- state and the 1.46 Mev state of ^{40}Ar a 2^+ state. For such a unique first-forbidden decay, the (L+M+N)/K electron capture ratio is estimated to be 0.34± 0.08 for ^{40}K, mostly depending on the L3/K ratio [1]. If the 2P and/or 3P orbital electrons were to be changed due to the changes in external conditions, this would result in a significant change of the decay constant. To evaluate the effect, we made a detailed measurement of ^{40}K EC decay constant (λ_e) (1)under high pressures and (2)in different chemical forms i.e., crystal and aqueous solution.

Experimental Method

Since the background due to natural K from surroundings was very large, we used a detector within a heavily shielded housing (Average 10 cm thick lead and 5cm thick of HC Copper). A very small amount of ^{22}Na(NaCl) was added to KCL samples for nomalization. The γ ray intensity of ^{40}K(1.4062Mev) relative to that of ^{22}Na(1.2746Mev) was measured. Such relative measurements would reduce errors resulting from changes in the efficiency and other sources in the γ ray detection system.

To investigate the compressional effect, we pressed KCL(^{40}K 3.15% enriched) crystal with a diamond anvil and measured the γ ray peak intensities of ^{40}K and ^{22}Na with a HP Ge detector (ORTEC Pop Top type: Efficiency 16.4%).

In the search for the chemical effect, we prepared pulverized KCL crystal (about 20g; ^{40}K not enriched) and its aqueous solution and measured the relative intensities. In this measurement, we also used another HP Ge detector(CANBERRA Coaxial type:Efficiency 20.6%) in a less shielded housing (Average 12.5 cm thick lead). [^{40}K is much more abundant than in the samples of compressional experiment.] It was necessary to correct for the difference of γ ray attenuation factor between KCL crystal and solution. In both cases, the decay constatnt of ^{22}Na is considerably large and it was necessary to correct for its decay during the measurments.

Results

As to the compressional effect, the experimental results are equivocal[fig. 1] mainly because of too small sample amounts(about 0.2mg) in the anvil. However, in the case of chemical effect, there may be a slight difference between crystal and aqueous solution [fig.2]. This should be confirmed by further experiments.

【Fig. 1】 Pressure Dependence of λ_e

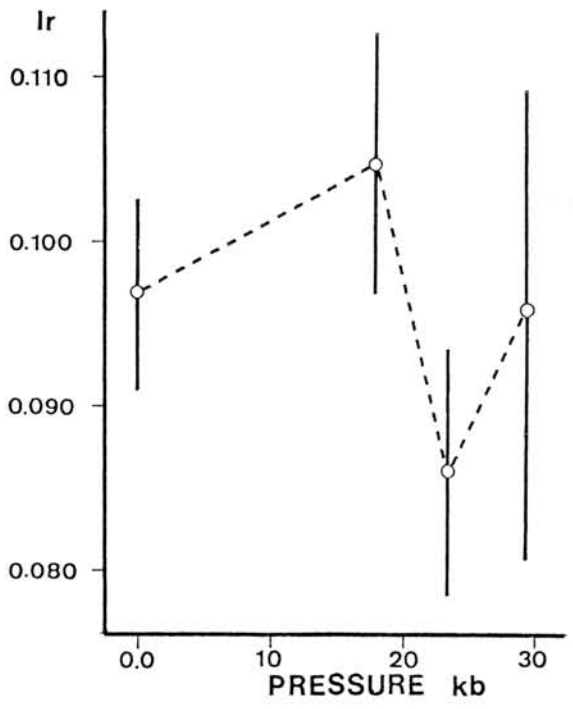

【Fig. 2】 The change of λ_e between KCL Crystal and Solution

EXPERIMENT No. 2 /DETECTOR = CANBERRA

Sample[2]	ρ [g/cm^3] (KCL[g])	number of trial	I_r[1]	Error
Crystal	1.061 (22.676)	5	0.4088	0.19%
Solution	1.275 (5.906)	2	0.4042	0.54%

$\Delta \lambda_e$ = 1.13%

EXPERIMENT No. 3 /DETECTOR = ORTEC

Sample[2]	ρ [g/cm^3] (KCL[g])	number of trial	I_r	Error
Crystal	1.094 (23.380)	5	0.4826	0.39%
Solution	1.245 (5.290)	3	0.4776	0.85%

$\Delta \lambda_e$ = 1.04%

[1] I_r : Relative γ Intensity
[2] In each experiment, a solution sample was prepared by dissolving a crystal sample.

Discussion

A very samll pressure effect has been observed experimentally in the EC of ^{7}Be [2]. As for the compressional effect of ^{40}K, there is some theoretical estimate by M. Bukowinski [3], but he considered only the change of total charge in the nucleus. In his estimates, the change of the λ_e may be underestimated, since in the case of potassium λ_e depends on the outer orbital electrons, like 2P or 3P, as much as on the inner ones.

Presently we are calculating the charge density of each orbital electron in the potassium nuculeus of KCL crystal and solution by the cluster method [4] to compare the results with the experiments. We will also report on the precise λ_e obtained in these experiments.

References

[1]McCann, M. F., Lewis, G. M., and Smith, K. M. Nuclear Physics A98, 577-584(1967)
[2]Hensley, W. K., Basset, W. A. , and Huizenga, J. R. Science 181, 1164-1165(1973)
[3]Bukowinski, M. S. T. , Geophy. Res. Lett. Vol. 6 No. 9, 697-699(1979)
[4]Watanabe, S , Kamimura, H , J. Phys. Society. Japan Vol. 56 No. 3, 1078-1088(1987)

^{244}Pu FISSIOGENIC Xe IN THE MANTLE

Ozima, M., Azuma, S.and Hiyagon, H.

Geophysical Institute, University of Tokyo, Tokyo 113.

Mantle-derived materials such as MORBs and mantle xenoliths often show excesses in ^{129}Xe and in $^{131\text{-}136}$Xe relative to the air Xe. The excess in ^{129}Xe has been reasonably attributed to extinct nuclide ^{129}I. Although the excess in $^{131\text{-}136}$Xe must be due either to ^{238}U spontaneous fission or to ^{244}Pu spontaneous fission, it has not been possible to resolve their origin because of experimental difficulties. Cosmic elemental abundance,if applied to the Earth,strongly favours ^{244} Pu, since ^{244}Pu-fissiogenic Xe would be more than an order of magnitude abundant than ^{238}U-fissiogenic Xe in the Earth (1). However, xenon isotopic analyses on a CO_2 well gas from New Mexico, which contained a sufficient amount of Xe for a precise isotopic determination clearly showed ^{238}U fissiongenic Xe isotopic pattern as well as excess in ^{129}Xe, setting a maximum limit of 20% for ^{244}Pu fissiogenic Xe(2). Lately, CO_2 well gases from Colorado and Australia were also reported to have ^{238}U fissiogenic Xe excess and excess in ^{129}Xe(3). Hence, some authors suggested that excesses in $^{131\text{-}136}$Xe in the mantle derived materials are also due to ^{238}U fission(4). In this report we reexamined the problem in the light of all the published data on mantle-derived materials and our newly obtained data on diamonds. We will show that excesses in $^{131\text{-}136}$Xe are best explained by ^{244}Pu fission.

Samples used in this study are MORBs, and diamonds,both representing mantle noble gas states. However, it is important to note that while MORBs represent the present mantle, diamonds represent the ancient mantle. Diamond samples include both uncoated and coated diamonds. Although uncoated diamonds are generally believed to occur in the upper mantle, the origin of the coated diamonds are complex.

In Fig.1 we plotted ^{136}Xe/^{130}Xe v.s. ^{129}Xe/^{130}Xe for mantle derived samples, which shows a linear array. Such a linear array was first reported for MORBs by Staudacher and Allegre (5). Allegre et al.(4) interpreted that the linear trend is a mixing line between the air-type Xe of the lower mantle origin and a upper mantle Xe which has excesses in ^{129}Xe and $^{131\text{-}136}$Xe. They further suggested that the excess in ^{129}Xe is due to ^{129}I and excess in ^{136}Xe to ^{238}U fission.

A remarkable feature in Fig.1 is that both diamonds and modern basalts form the same linear array. Though the age of the diamonds are not known, they must be much older than MORBs, some of them being of Precambrian age. Since ^{238}U fissiogenic Xe has been still evolving($T_{1/2}$ = 4.47 Ga), it is difficult to see why these samples formed at entirely different age should form the same linear trend. We expect that modern basalts (MORBs) would be more enriched in ^{136}Xe excess than the diamonds if excess ^{136}Xe were due to ^{238}U fission, giving rise to a different mantle Xe or a different mixing

line with a less slope. The similar linear trend both for modern basalts and ancient diamonds strongly suggest that the mantle Xe with excesses in ^{129}Xe and ^{136}Xe has been established long before, at least before the crystallization of the diamonds. This would leave ^{244}Pu as a more likely parent of the excess ^{136}Xe in the mantle.

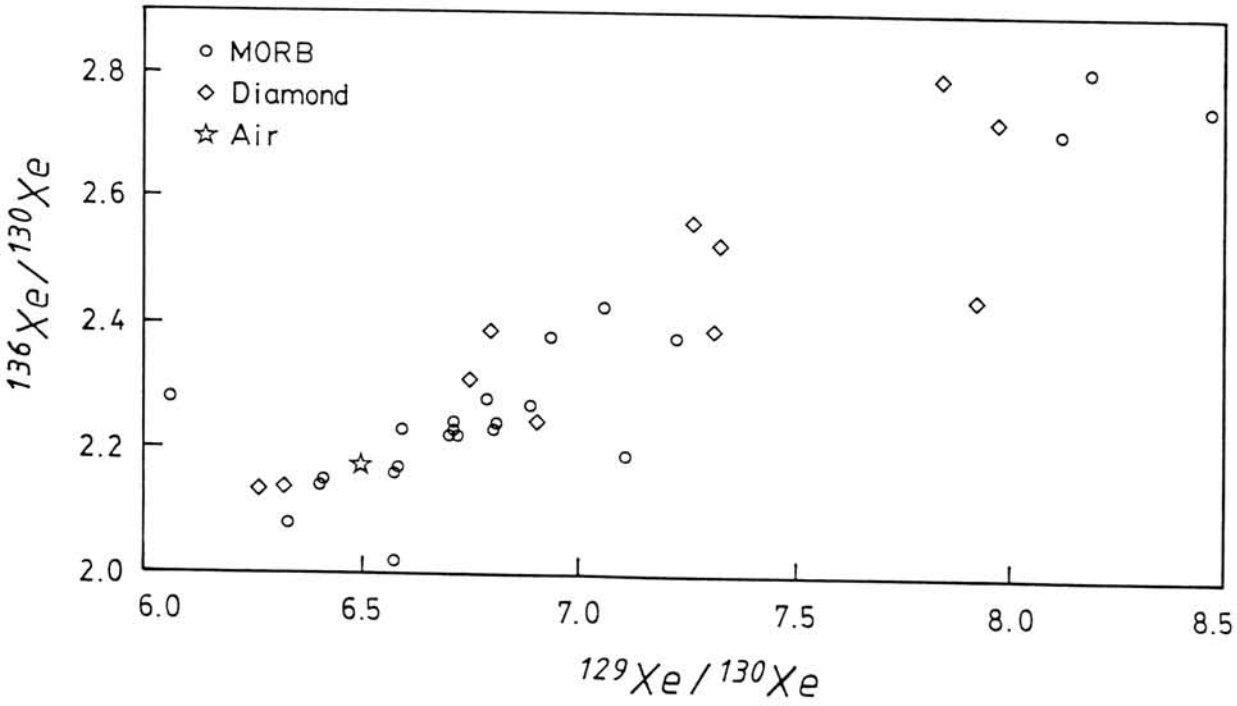

Fig. 1. $^{136}Xe/^{130}Xe$-$^{129}Xe/^{130}Xe$ diagram. Note that both MORBs and diamonds form nearly a same linear trend.

Moreover, if the linear array in Fig.1 were to be interpreted to be a mixing line, we must have a well defined mantle Xe with uniform isotopic compositions as one of the end member. It is then very difficult to see how the still evolving ^{238}U-fissiogenic Xe mixed with ^{129}I-radiogenic excess ^{129}Xe could give rise to such an uniform $^{136}Xe/^{129}Xe$ ratio, unless we assume either extremely efficient mantle homogenization or uniform distribution of uranium and xenon in the mantle. If the excess Xe were derived from ^{129}I and ^{244}Pu,however, various geodynamical processes in the mantle throughout the Earth's whole history would have homogenized the isotopes to give rise to the uniform mantle Xe. The argument again favour the ^{244}Pu-origin of the excess ^{136}Xe.

We also examined correlation between the excess in ^{136}Xe and ^{238}U-derived nucleogenic isotopes ^{4}He and ^{21}Ne. If the excess ^{136}Xe was derived from ^{238}U, we should see a positive correlation between them. We observed no such correlation,again suggesting a ^{244}Pu-fissiogenic origin.

Cosmochemical considerations also support ^{244}Pu-fissiogenic origin of the excess ^{136}Xe in the mantle. Assuming the latest estimate on a

chondritic value of $(^{244}Pu/^{238}U)_o$ = 0.0067 + 0.001 (6) for the whole Earth(suffix o indicate 4.5 Ga ago), we can show that the ^{238}U-fissiogenic ^{136}Xe produced for 4.5 Ga is less than 4 % of ^{244}Pu-fissiogenic ^{136}Xe. Assuming no large fractionation between Pu and U during the accretion of the Earth or meteorite parent bodies , it can be argued that if ^{238}U-fissiogenic Xe were significant in the Earth, there should be more ^{244}Pu-fissiogenic Xe.

Pepin and Phinney(7) have shown that the air Xe contains about 6.7% of ^{129}I-radiogenic ^{129}Xe and about 4.7% of ^{244}Pu-fissiogenic ^{136}Xe. With additional meteorite Xe isotopic data and by means of multivariate data analyses, Igarashi (8) concluded that 3.1 + 1.0 % of air ^{136}Xe is ^{244}Pu-fissiogenic. Adopting the latter value, it is easy to show that the air Xe has a $(^{136}Xe)_{Pu}/(^{129}Xe)_U$ ratio of 0.155. Since ^{244}Pu has a much longer half life ($T_{1/2}$ = 82 Ma) than ^{129}I ($T_{1/2}$ = 17 Ma), the ratio$(^{136}Xe)_{Pu}/(^{129}Xe)_U$ in the degassed mantle must be larger than that value in the air. The argument also strongly suggests that ^{244}Pu-fissiogenic ^{136}Xe must be more abundant than ^{238}U-fissiogenic ^{136}Xe in the degassed mantle.

In conclusion, excess ^{136}Xe in mantle-derived materials is best explained by ^{244}Pu spontaneous fission.

References:

1. Bernatowicz, T. and Podosek, F.A.: In Terrestrial noble gases. ed. by Alexander, E.C. Jr and Ozima, M., pp99-135, Japan Sci Soc. Press (1978).
2. Phinney, D., Tennyson, J. and Frick, U.: J. Geophys. Res., 83, 2313-19 (1978).
3. Caffee, M.W., Hudson, G.B., Uclsko, C., Alexander, E.C. Jr, Huss, G. R., and Chivas, A.R.: In Lunar Planetary Sci. Conf. XIV, 154-5 (1988).
4. Allegre, C.J., Staudacher, T. and Sarda, P.: Earth Planet. Sci. Letters, 81, 127-50 (1986/7).
5. Staudacher, T. and Allegre, C.J.: Earth Planet. Sci. Letters, 60, 389-406 (1982).
6. Hudson, G.B., Kennedy, B.M., Podosek, F.A. and Hohenberg, C.M.: Proc. 19th Lunar Planet. Sci. Conf. (1988).
7. Pepin, R.O. and Phinney, D., Moon and Planets (in press).
8. Igarashi, G., Ph. D. Thesis, University of Tokyo (1988).

INVESTIGATION OF HIGH $^3He/^4He$ RATIO IN DEEP-SEA SEDIMENTS

Matsuda, J.*, Murota, M*. and Nagao, K.**

* Department of Earth Sciences, Faculty of Science, Kobe University, Nada, Kobe 657.
**Institute for study of the Earth's Interior, Okayama University, Misasa, 682-02.

Merrihue (1) first reported noble gas data on a magnetic and a nonmagnetic separate of a pacific red clay, suggesting the occurrence of extraterrestrial material in the deep-sea sediments. Ozima et al. (2) and Takayanagi and Ozima (3) reported the noble gas data of bulk sediments from world wide, and concluded that there are significant amounts of global fallout of extraterrestrial material into deep-sea sediments. Fukumoto et al. (4) reported that Ne isotopes were also of extraterrestrial origin whereas heavy gases were of terrestrial atmospheric origin, which was confirmed by Amari and Ozima (5) although they insisted that Ne isotopes were of solar flare origin rather than of solar wind origin proposed by the former authors. At any rate, it is now established that there exist the extraterrestrial noble gases in deep-sea sediments. The problem is what kind of cosmic material carries the extraterrestrial noble gases.

Amari and Ozima (6) got the magnetic fraction of 0.22% of the bulk sediments, which contained nearly 30% of the total ^3He. Krylov et al. (7) and Matsuda and Nagao (8) reported that the high $^3He/^4He$ ratios was observed in the sediments dissolved in HCl or HNO_3. In order to search the host phase of extraterrestrial noble gases, Fukumoto et al. (4) prepared the magnetic fraction and the chemically leached fractions of deep-sea sediments, respectively. The magnetic separate of only 0.75% of the bulk sediment contains about 50% of the total ^3He. The magnetic fraction did not lost its ^3He during the 98% HNO_3 treatment. The HCl resistant fraction, comprising 70% of the bulk sediments, contains about 70% of the total ^3He, but lost its ^3He during HCl-HF treatment. In this study, we dissolved the magnetic fraction of deep-sea sediments with HCl, and measured the He and Ne concentrations and their isotopes by the stepwise heating technique.

We used the deep-sea sediments of pelagic clay sampled at 14° 29.61'S, 158°52.98'W on a cruise of R/V Hakureimaru, Geological Survey of Japan. The sediments are the same as that used by Fukumoto et al. (4). We took another aliquot of wet sediments, and dried completely at 110°C in air. The weight loss was 69%, the water content of the wet sediments. We gently pulverized the dried sediments to fine grains and homogenized the sample which was designated M0. A 42.11g aliquot of the dried sediment M0 was again suspended in a distilled water, and yielded 0.2249g of the magnetic fraction M2M. The separation procedure was done by using a small magnet bar of a magnetic stirrer, which was the same as that described by Fukumoto et al. (4). About 0.06g aliquot of M2M were dissolved in 5ml 3M HCl at room temperature, yielding M2M-1 for two days and M2M-2 for three days. The sample M2M was dissolved in 3M HCl for three days at room temperature and once

rinsed with distilled water, then dissolved again under the same condition for additional three days, which yielded the sample M2M-3. The whole scheme of the procedure is given in Fig. 1 where the weight fractions are given relative to the dried sediment M0.

Elemental abundances and isotopic compositions of noble gases were determined for M0, M2M, M2M-1 and M2M-3. The analytical procedure of noble gases were essentially the same as those of our previous studies (4, 8, 9). The results are given in Table 1. High $^{3}He/^{4}He$ ratios and solar $^{20}Ne/^{22}Ne$ ratios (12-14) were observed in all temperature fractions in the magnetic separate and its leached samples. The bulk sample M0 and its magnetic fraction M2M are considered to be the same samples as B0 and B2M in Fukumoto et al. (4), respectively. The ^{4}He content ($5.9X10^{-7}$ccSTP/g)of M0 seem to agree with that ($5.1X10^{-7}$ccSTP/g) of B0 when we judged from 10% error of each measurement, but $^{3}He/^{4}He$ ratio ($1.30X10^{-8}$) of M0 is much higher than that ($0.90X10^{-4}$) of B0. ^{20}Ne concentration of M0 is also higher than that of B0. These results suggest that distribution of the extraterrestrial material is quite inhomogeneous in deep-sea sediments. Similar inhomogeneity of $^{3}He/^{4}He$ ratios within a few centimeters were also reported by Takayanagi and Ozima (3). In the meanwhile, the magnetic separate M2M agrees very well with B2M in both elemental abundances and isotopic compositions of He and Ne. Therefore, the inhomogeneity of the bulk sediments may be simply due to the inhomogeneous distribution of the magnetic fraction. The HCl-leached sample M2M-1 agree very well with the severely leached sample M2M-3 in noble gas data. ^{4}He and ^{20}Ne contents of M2M decreased to about a half the original concentration by HCl leaching, and $^{3}He/^{4}He$ ratios decreased and $^{20}Ne/^{22}Ne$ ratio seemed to be increased very slightly. The weight loss from M2M to M2M-1 was 37%, whereas the loss of ^{3}He was about 60%, which may suggest that the extraterrestrial He is in the fine particles or on the surface area of grains. However, the leached samples M2M-1 and M2M-3 still have high $^{3}He/^{4}He$ ratios and the solar $^{20}Ne/^{22}Ne$ ratios, indicating that extraterrestrial noble gases are also tightly trapped inside the grain. The release temperature of ^{4}He is at 800 and 1000° C, whereas that of ^{20}Ne is rather uniform and seems to be slightly high. The small release peak of ^{20}Ne is admitted

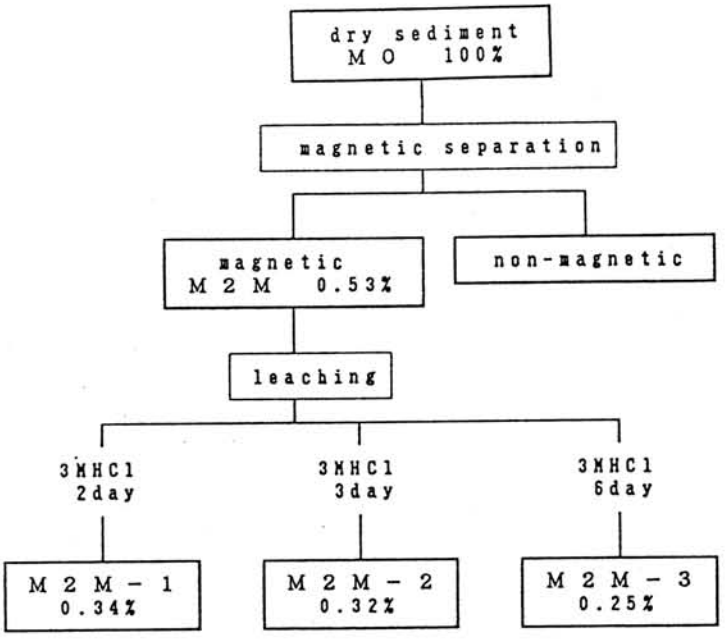

Fig. 1

at 1200°C. These result may reflect the difference of the diffusion coefficients of He and Ne in the magnetic grains.

References (1) Merrihue, C. (1964) Ann. N.Y. Acad. Sci., 119, 351. (2) Ozima, M., Takayanagi, M., Zashu, S. and Amari, S. (1984) Nature, 311, 448. (3) Takayanagi, M. and Ozima, M. (1987) J. Geophy. Res., 92, 12531. (4) Fukumot, H., Nagao, K. and Matsuda, J. (1986) Geochim Cosmochim Acta, 50, 2245. (5) Amari, S. and Ozima, M. (1988) Geochim Cosmochim Acta, 52, 1087. (6) Amari, S. and Ozima, M. (1985) Nature, 317, 520. (7) Krylov, A. Ya., Mamyrin, B. A., Silin, Yu. I. and Khabarin, L. V. (1973) Geochem. Int., 10, 202. (8) Matsuda, J. and Nagao, K. (1986) Geochem. J., 20, 71. (9) Matsubara, K., Matsuda, J., Nagao, K., Kita, I. and Taguchi, S. (1988) Geophys. Res. Rett., 15, 657.

Table 1. Light noble gases in a magnetic fraction and leached samples from deep-sea sediments at 14°29.61'S and 158°52.98'W.

Sample	Weight (g)	Temp. (°C)	^4He*	$^3He/^4He$ ($\times10^{-4}$)	^{20}Ne*	$^{20}Ne/^{22}Ne$	$^{21}Ne/^{22}Ne$
M0	0.3190	800	42.2	0.773±0.098	0.238	11.1±0.6	0.0296±0.0036
		1000	13.1	2.83 ±0.29	0.0336	10.0±0.7	0.0407±0.0086
		1200	3.90	1.99 ±0.29	0.0280	10.9±0.8	0.0565±0.0194
		1400	<0.36	-	0.0326	12.0±0.8	0.0306±0.0097
		1600	<0.15	-	<0.0096	-	-
		Total	59.2	1.30 ±0.09	0.332	11.0±0.4	0.0332±0.0033
M2M	0.0432	800	390	2.75 ±0.24	0.633	11.8±0.4	0.0318±0.0070
		1000	499	2.54 ±0.21	0.861	12.4±0.6	0.0318±0.0066
		1200	220	2.51 ±0.21	1.80	13.1±0.6	0.0302±0.0070
		1400	<3.6	2.79 ±1.00	0.650	11.7±0.4	0.0205±0.0157
		1600	<1.0	-	<0.040	-	-
		Total	1109	2.60 ±0.13	3.94	12.4±0.3	0.0291±0.0045
M2M-1	0.0355	800	182	2.15 ±0.20	0.151	12.6±1.1	0.0457±0.0170
		1000	248	2.49 ±0.22	0.544	14.2±0.8	0.0414±0.0064
		1200	65.5	2.18 ±0.19	0.662	13.3±0.7	0.0339±0.0046
		1400	<2.11	-	0.409	13.5±0.7	0.0311±0.0118
		1600	<1.31	-	<0.072	6.9±2.9	-
		Total	495	2.32 ±0.13	1.76	13.5±0.4	0.0365±0.0040
M2M-3	0.0268	800	214	1.96 ±0.17	0.261	12.4±0.9	0.0458±0.0137
		1000	235	2.42 ±0.22	0.365	12.2±0.6	0.0382±0.0085
		1200	58.7	2.55 ±0.24	0.781	14.4±0.7	0.0413±0.0065
		1400	<2.1	-	0.407	14.2±0.9	0.0399±0.0085
		1600	<1.9	-	<0.10	11.9±1.0	-
		Total	507	2.24 ±0.12	1.81	13.5±0.3	0.0410±0.0043

*Gas concentrations are in units of $10^{-8}cm^3STP/g$. If blank contribution was larger than 30%, we list the data as upper limits without blank correction. As for isotopic ratios, blank correction was applied to all data and the error covers the ratio before blank correction. Total gas amount and its isotopic ratios were calculated only from the data for whuch blank correction was applied for the concentration.

CHEMICAL CHARACTERISTICS OF MAGNETIC, STONY SPHERULES FROM DEEP-SEA SEDIMENTS

K. MISAWA[1], K. YAMAKOSHI[1], K. NOGAMI[2], K. YAMAMOTO[3] and N. NAKAMURA[3]
(1) Institute for Cosmic Ray Research, University of Tokyo, Tanashi 188, JAPAN
(2) Dept. of Physics, Dokkyo University School of Medicine
(3) Dept. of Earth Sciences, Kobe University

Magnetic, stony spherules extracted from deep-sea sediments have been studied chemically and petrographically (see ref. [1]). It is considered that they are extraterrestrial materials [2] and related to carbonaceous chondrites [3]. Minor element signature of olivines showed that olivines in deep-sea particles match poorly those of the CI and CV meteorites but are well matched with olivines from CM meteorites [4]. Moreover, several particles containing CAI-like inclusions were found [5]. In order to study more about the relationship of magnetic, stony spherules to chondritic meteorites, especially carbonaceous chondrites, we have determined abundances of trace and major elements in individual spherules by mass spectrometric isotope dilution (MSID) technique (REE, Mg, Ca, Sr, Ba, Rb, K) as well as instrumental neutron activation analysis (INAA) (Fe, Ni, Co, Au, Sc, Cr, Ti, Al, Mn, V).

More than 30 spherules extracted from red clay were selected for chemical analyses. Most of spherules show brickworklike structures [1]. Spherule #K is more nonspherical than the others. Under SEM-BEI observations, spherules #A, #D and #F show dendritic textures (Fig. 1a). In spherule #K (Fig. 1b), Fe-Ti rich phases are embedded in feldspar ($Ab_{62}An_{28}Or_{10}$).

Alkali elements, K and Rb, are strongly depleted: *e.g.*, in spherules #A and #F, enrichment factors of these elements relative to CI-chondrite are 0.0192-0.580. In Fig. 2, lithophile element abundances of individual spherules determined by MSID are normalized to CI-chondrite. Spherules #A, #D and #E show LREE-enriched patterns with large negative Ce anomalies ($Ce/Ce^*=0.11$) and minor negative Eu anomalies (although La data did not obtained in #D). Negative Ce anomaly was also observed in glassy silicate spherules [6]. In addition, spherules #A and #D show strong depletion of Ca in comparison with chondritic levels and other refractory lithophiles. Spherule #K also shows a LREE-enriched pattern with gradual decrease from La to Lu superimposed a positive Eu anomaly. On the other hand, spherule #F has a nearly flat REE pattern (1.8 x CI-chondrite) with no specific anomaly. Enrichment factors of Al, Ti, V and Mn vary from 0.8 to 50 (Mg=1.0). Generally, siderophile element abundance pattern of spherules is in good agreement with previous results [7,8].

Moderately volatile lithophiles, K and Rb, are depleted relative to chondritic values. These elements may have been lost from the melt droplet when meteoroids enter the Earth's atmosphere. In spherule #E and composite samples #P and #Q, however, volatile siderophile element Au is rather enriched relative to other siderophile elements. Au/Ni ratio of composite sample #P is 3.3×10^{-3} which is two order of magnitude larger than those of **metal phases** of chondritic meteorites ($Au/Ni=1.2 \times 10^{-5}$ [9]). One possible explanation is that Au did not lost from the spherules but concentrated in metal phases during heating and melting event. Another possibility is that the parent meteoroid of these spherules originally enriched in Au. If this is the case, siderophile element fractionation took place in the parent meteoroid. Relatively large LREE/HREE fractionation and negative Ce anomalies are observed in several spherules. LREE/HREE fractionations can be produced by the solid/liquid partitioning of REE. If these fractionations are pre-terrestrial origin, their parent meteoroids may be differentiated materials. However, differentiated meteorites so far reported do not show such a large negative

anomaly of Ce. It is suggested that the depletion of Ce may have been produced under oxidizing conditions [10-12]. These anomalies can be produced when the samples entered the Earth's atmosphere, however, LREE enrichment relative to refractory HREE appears to conflict with the elemental volatilities. It is shown that stony spherules observed in deep-sea sediments have been affected by alteration [1,13]. Under marine environment, it is also suggested that Ce can dissolved selectively by sea-water, and that LREE abundances can be affected by glass/sea-water interaction [14]. Thus we suggest that LREE enrichment observed in spherules is not original feature but secondary, terrestrial contamination and alteration. However, we can not rule out the possibility that the negative Ce anomalies observed in several spherules are extraterrestrial origin.

During the course of this study, we found a tiny Pt-group nugget from the composite sample of #Q. In Fig. 3, X-ray spectra of the nugget is shown. The nugget is mainly composed of Fe, Ni, Ru, Rh, Os, Ir and Pt. Abundance ratios of Os/Ir and Pt/Ir are approximately 1.2 and 2.2, respectively. These ratios are comparable to that of CI chondrite.

REFERENCES:

[1] D.E. Brownlee, *The Sea Vol. 7*, 733-762 (1981) [2] T.H. Millard & R.B. Finkelman, *JGR 75*, 2125-2133 (1970) [3] M.B. Blanchard *et al., EPSL 46*, 178-190 (1980) [4] I.M. Steel *et al., Nature 313*, 297-299 (1985) [5] D.E. Brownlee *et al., LPS XI*, 109-111 (1980) [6] H. Nagasawa *et al,. GCA 43*, 267-272 (1979); H. Nagasawa *et al., LPS XI*, 780-782 (1980) [7] K. Yamakoshi, *Geochem. J. 18*, 147-152 (1984) [8] Ph. Bonte *et al., Proc. 17th LPSC* in *JGR 92*, E642-E648 (1987) [9] E. Rambaldi, *EPSL 31*, 224-238 (1976) [10] W.V. Boynton, *LPS IX*, 1120-1122 (1978) [11] H. Nagasawa & N. Onuma, *LPS X*, 884-886 (1979) [12] A.M. Davis & L. Grossman, *GCA 43*, 1611-1632 (1979) [13] D.W. Parkin *et al., Nature 266*, 515-517 (1977) [14] N.J. Ludden & G. Thompson, *EPSL 43*, 85-92 (1979)

Fig. 1

SEM-BEI images of spherules #A (a) and #K (b).

Fig. 2

CI-chondrite normalized elemental abundances of magnetic, stony spherules from deep-sea sediments.

Fig. 3

X-ray spectra of a Pt-group nugget from the composite sample #Q. Enlarged view is Lα spectrum region of Os, Ir and Pt.

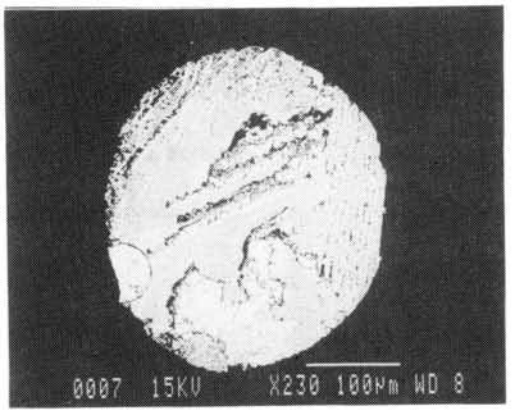

Fig. 1(a)

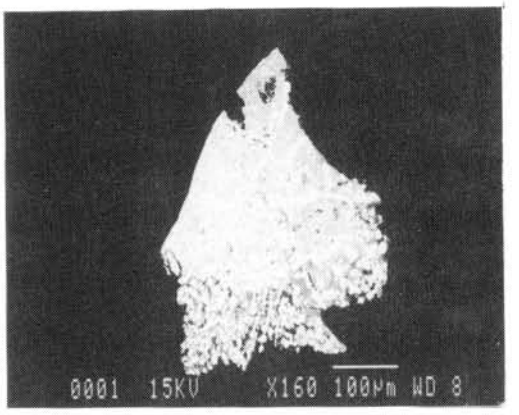

Fig. 1(b)

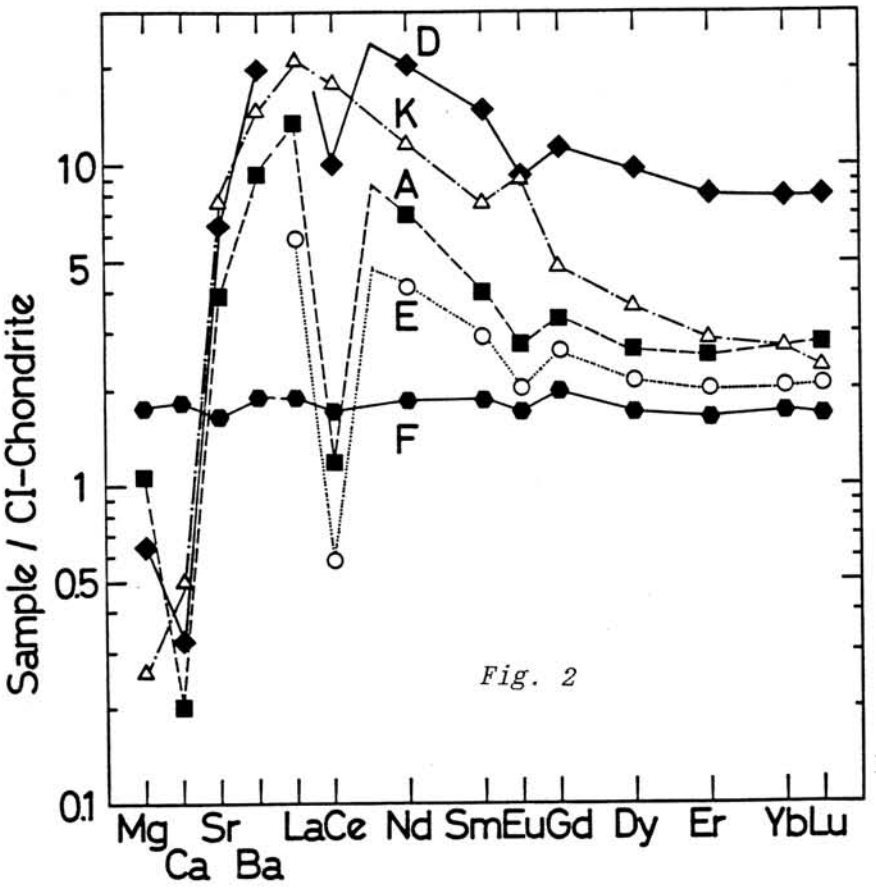

Fig. 2

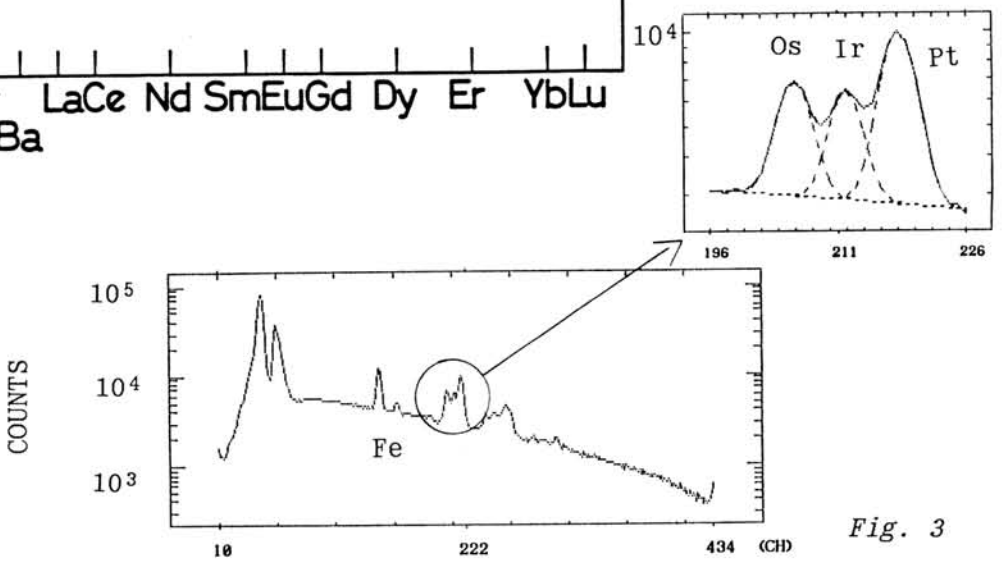

Fig. 3

Nuclear Explosion Glasses and Tektite

Lin Wenzhu
Institute of Geochemistry, Academia, Sinica, Guiyang, Guizhou Province, China

Around crater of nuclear explosion largely distributed splash glasses. They are shaped like drops, pearls, buttons, bar and dumbbells, or calabashs etc.. The glasses surface was smooth to differ from the tektite. Large numbers of samples show that inclusions, bubbles. In reflected light they are usually black-green or brown. Glassy graininess is greater than 1 cm to less than 0.1 cm with distance decreas. Outset 10 km distance can see glassy graininess less than 0.1 cm.yet. The splash-form glasses strewn field consist with range of micro-particle fall-off in the mushroom cloud for the nuclear explosion.

Whether the various sample of glasses and melts differ from colour, shape, scale or distance from burst crater. However, their chemical composition and trace element have deviated from average value a little. Specifically, the rare earth element abundance pattern are very similar to basement rock (sand-shale): rich LREE abundance and Eu negative anomaly (Fig.). The powerful said that glasses and melts until kep the abundance pattern of petrologies under high temperature-pressure melting condition. Result from glasses or melts consists of some kind of rocks was mixed melting according to percenage weight of rock. According as oxide (SiO_2, TiO_2, Al_2O_3, FeO, CaO, MgO, Na_2O, and K_2O) concentration of variant rock type calculation fit oxide abundance of the glasses by variant proportion. The proportion was in accort with in situ geological section estimation.

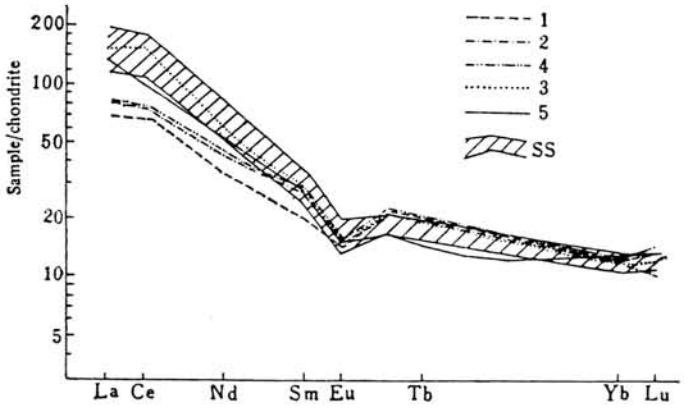

Fig. 2. Chondrite normalized REE patterns of glass, melt rock (SS), Silurian shale (5) and basement rocks (1—4).

The origin of tektite is being in dispute, but

most workers in the field favor already a terrestrial origin. The planetesimal hypervelocity impact on earth's surface has caused vaporte, melting of rocks to form glasses after cooling and condensating. The appearance and construction of the tektite comparison with that nuclear explosion glasses was very similarity. Another, most workers noted significant homogeneous chemical composition in the strewnfield. This is similar to the properties of element geochemistry of the glasses by the nuclear explosion too. So, we can said that formation of tektite very similar to that of cratering nuclear explosion. We may have considered same strewnfield tektite characterized with common target rock by high-Al and lower alkaline. Similarly, the mixed melting has been calculted to fit tektite. It is appear that the result has been present to find parent rocks and source crater of the tektite. The Australasian strewnfield covered about a tenth of the total surface of the earth. The Al_2O_3/SiO_2, K_2O/SiO_2 and $\frac{Na_2O}{SiO_2}$ ratio in the Australasian strewnfield from the South China Sea to the Australian territory has had appearent difference. Another intersting thing is that Muong Nong tektite and philippinites show a layered structure. The splash-form tektite has formed , then rock melts of Muong-Nong type tektites is undisturbed by high tempearture turbulent flow. That is, the Muong-Nong type tektite characterized by massive block and stratification. Thus, in the Australasian strewnfield least present four impact crater at different place. They are situated the Thailand-Laos boundary, the Philippine, the Java and the Australian territory. The petrologies of crater are a set schist and clay rocks (lower primary schist); shallow sea facies settling mudstone, sandstone and claystone; high-Ca,Al argillaceous sandstone parting in schist; high-silica graywacke and high-Fe, Mg sand-shale separately. Even prabably, source crater of the Lei-Gong-Mo tektite (China) lies to Guangxi-Guangdong boundary area.

References:(1)Lin Wenzhu(1989) Chinese Science Bulletin 34,422-425. (2)Koeberl,C. (1986) Ann. Rev. Earth Plamet. Sci. 14, 323-350. (3) Mason, B. (1979) Smithson. Contrib. Earth Sci. 22, 14-26.

END-CRETACEOUS EVENT–IS IT DUE TO AN ENCOUTER WITH A GIANT MOLECULAR CLOUD?

Yabushita, S.
Dept. of Applied Mathematics and Physics, Kyoto University, Kyoto 606

A menber of hypotheses have been presented to account for the well-known end-Cretaceous event. Of these, the most discussed is the one due to Alvarez et al. [1] which ascribes the event to an impact of an asteroid. This hypothesis was put foward to explain the K/T boundary layer which is enriched in Iridium. This hypothesis meets a number of difficulties. One is the thikness of the layer. According to Kyte and Wasson [2], the Ir rich layer in the core of the Pacific ocean bottom corresponds to at least a quarter of a million years, whereas dust grains injected in to the stratosphere by an impact induced explosion falls to the ground within a few years.

A more serious dificulty is that the end-Cretaceous event was not random in extinguishing fauna. Although large reptiles such as dinasaurs became extinct, smaller ones such as snakes, crocodiles and lizards survived. Again, although large insects died out, smaller ones survived. The most interesting feature is that the mammals survived and then became the dominant species in the Teartiary and afterwards. Thus, the end-Cretaceous mass extinction was far from being random. Here I explore the possibility that the event was due to an encouter with a giant molecular cloud. As I show here, this process is more selective regarding the extinction.

A giant molecular cloud is an aggregate of gas molecules which consist mainly of H_2 and He is also included. Estimated number of GMC's in our galaxy is 3000. The linear extent is $10 \sim 20$ parsecs and there are core regions with linear dimension of about 1 persec, where the number density n_{H_2} may be as large as $10^4 \sim 10^5$ cc^{-1}. As in ordinary interestellar clouds, they contain dust grains which amount to a few percent in mass. Here I take 2 % as the canonical value.

The overall scheme of the gas flow as the sun encouters a GMC is shown in Fig. 1. The position of the stagnation point S is 9 astronomical units away from the sun, when the relative velosity at great distance is 10 km s^{-1}. The flow is nearly symmetric about the sun and the earth is immersed in the accretion flow. The flux of gas accreting to the earth is given by

$$\phi = nv_{flow} = 1.3 \times 10^7 n_{H_2} [v_\infty / 20\text{km s}^{-1}]^{-3} \text{cm}^{-2}\text{s}^{-1}$$

Part of the gas escapes from the earth Fig. 2 gives the flux of H_2 which

flows down the atmosphere as H_2O. The flux is estimated by the model of Mckay et al. [3]. It is seen that if $n_{H_2} = 10^4$ cc^{-1}, the loss is negligbly small. This leads to the effective loss of oxygen in the atmosphere.

Next, I consider the effect of dust grains accreted to the earth. Fig. 3 gives the optical depth of the grains suspended in the atmosphere when $n_{H_2} = 10^4$; C is the case for organic grains, while S denotes the case where grains are mainly silicates.

It can be seen that the major effects of a GMC encounter are the loss of O_2 in the atomosphere and the shielding of the solar radiation due to grains shich contain Iridium. On the presumption that GMC grains contain as much Ir as carbonaceous chondrites (0.6 μg / g; [4]), the amount of Ir deposited can be estimated. The time required for the sun to traverse a distance L is

$$t = 10^5(\mathrm{L}/1\mathrm{PC})(10\mathrm{km\ s^{-1}}/v_\infty)\mathrm{year}.$$

The excess Ir deposition rate at the K/T boundary over the mean is 7×10^{-5} ng m^{-2} yr^{-1}, which corresponds to the grain accretion rate of 1.2×10^{-7} g cm^{-2} yr^{-1}. Hence, the K/T boundary corresponds to an encouter with a GMC core of density $n_{H_2} = 2 \times 10^4$ cc^{-1}. The overoll measured Ir deposition corresponds to the accretion of 9×10^{42} H_2 molecules and this could remove 20 % of the oxygen in the atmosphere. If the grain content in the GMC is smaller, say, 1 %, the amount of lost O_2 would be even greater. To summaryze, the effects of accrete GMC gas and dust are three fold;

1. Loss of oxygen in the atmosphere.
2. Shielding of the solar radiation by the grains suspended in the atmosphere, the duration of the event being 10^5 yr or so.
3. Deposition of Ir comparable to the one actually measured in the oceanic cores.

Berner and Landis [6] reported that O_2 content of the air contained in an amber before the K/T event is significantly higher than the present-day value (20 %).

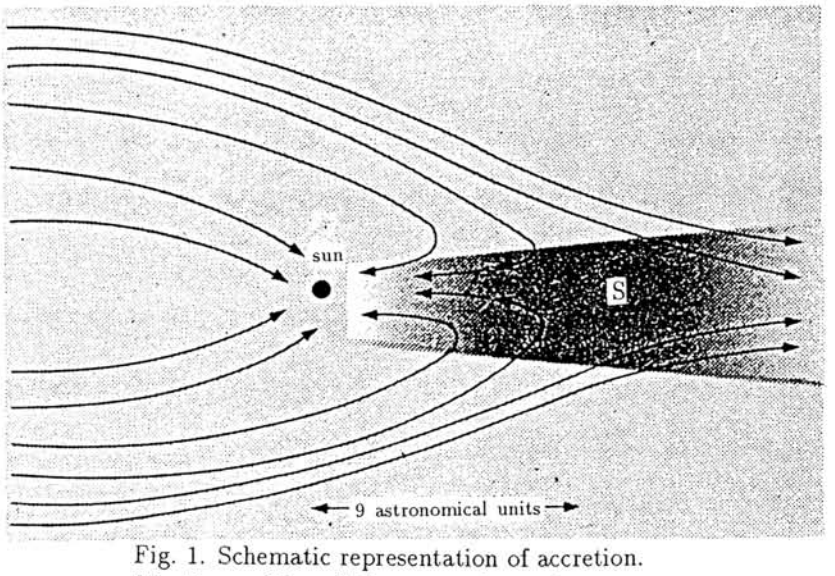

Fig. 1. Schematic representation of accretion.
S is the position of the stagnation point.

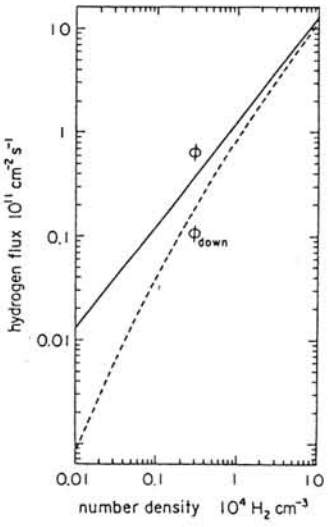

Fig. 2. ϕ is the accretion flux of H_2.
ϕ_{down} is the downward flux of H_2O.

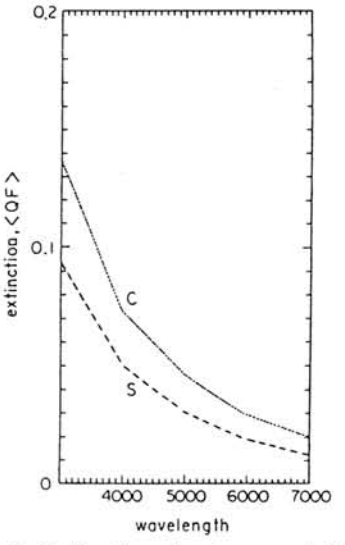

Fig. 3. Extinction due to accreted grains.
n_{H_2} 10^4 cc^{-1}.

References

1. Alvarez, L.W., Alvarez, W., Asaro, F. and Michel, H.V., 1980. Science 208, 1095.
2. Kyte, F.T. and Wasson, J.T., 1986. Science, 232, 1225.
3. Mckay, C.P. and Thomas, G.E., 1978. Geophys. Res. Lett., 5, 215.
4. Kallemeyn, G.W. and Wasson, J.T., 1981. Geochim. Cosmochim Acta, 45, 1217.
5. Yabushita, S. and Allen, A.J., 1989. Mon. Not. R. astr. Soc. in the press.
6. Berner, R.A. and Landis, G., 1987. Report at the annual meeting of the U.S. Geological Society, Pheniy, Arizona.

62—1

Small crater and impactite found in Toyama Prefecture, Japan

AKai J* and Kanno, T.#
* Dept. Geol. & Min. Faculty of Science, Niigata University, Ikarashi 2, Niigata 950-21 ; # Dept. Earth Sci. Faculty of Science, Ehime University, Bunkyo 2, Matsuyama 790

One of the authors (TK) found a glassy rock sample (Fig. 1) which contains fragments of gneiss and many small mineral fragments in the Hida metamorphic complex region. Furthere examinations revealed that this rock sample is impactite with clear evidence of shock effects. Small (~10m) and relatively deep (>12m) hole existing in the neibouring region has been known recently. The authors describe this impactite and this 'small crater' .

Among collected aerial photographs of this area taken at 1947 , 1968, 1971, 1977 , 1987 this 'small crater' was found in the photographs of 1968, 1971, 1977, 1987 but the ' crater' was not observed in that of 1947 . The aerial photograph taken at 1968 (Fig. 2) shows this ' crater' clearly with thinly covered snow . Observing this photograph in detail, it was found that minute reliefs around this 'crater ' exist. It is interpreted that the relief was formed as the result of shock effect from north direction (private communication by T. Uda) . This interpretation is consistent with the characteristic topographic features of the bottom of the ' crater' . Diameter -depth ratio of this crater is a little diffrent from the generall case ; the ratio of this carater is ~1 and general case is 1/ 4 ~1/5 . This high ratio can be explainable by taking acount the softness of the basement rock by weatering and geological fracture zone into consideration (suggested by H Mizutani) .

Examining the samples taken from the wall part of the crater no special evidence other than minerals of basement rocks was detected.
Speciaal gravity of the impactite is 2.01 It is slightly porous but its net density may be really small . Many mineral grains, feldspars, quartz , biotite and hornblendes of various sizes are dispersed in the black opaque matrix. Wood fragment burnt to charcoal is also contained in this impactite and so it is apparently peculiar material. Rock fragments are also contained.

Under the microscope, specimen is composed mostly of black opaque fine matrix . Minerals dispersed in the matrix are mostly feldspars and quartz, and small amounts of biotite and hornblende. These minerals are very similar to the minerlas consiting the basement rocks of gneiss and granite. Both plagioclase and alkali feldspars are , in many cases, changed to brown ~black coloured materials partly, often along cleavages , almost vertical to them or irregularly. Furthere examinations yielded that they are glasses ~ almost amorphous minerals. Optically they are similar to matrix. Quartz often shows wavy extinction and also shows formation of brown coloured materials along

cracks. Biotite and hornblende also have black ~brown materials formed along cleavages or irregularly .

All these minerals often have black ~brown coloured materials in various degrees. Some mineral grains are wholly replaced by the balck materials and others only partly . These black altered materials do not differ from the matrix materials themselves.

So, it is concluded that the matrix materials originated directly from these minerals and they might be produced by shock event, probably in solid states. This solid state reaction may be major process, but matrix materials may have experienced melting process partially, because the surfaces of the impac tite clearly suggest melting of the sample. Two processes might be superimposed.

The result of bulk chemical analysis of the impactite specimen is shown in Table 1. Major and minor elements are contained in the table. The analyses of the probable basement rocks, Granite and Gneiss are also added in the table as reference. Enrichment of Fe and Ni is found although other elements also show small differences . The order of Fe and Ni enrichment is similar for example , to the relation between glasses and basement rocks at Mistastin crater. Other elements are almost consistent with mixture of the Granite and the Gneiss. These results show that the impactite originated from this area , most probably from this crater site and compositional enrichment of Fe and Ni is suggesting that parent meteorite may be iron meteorite though more analyses are necessary .

Examining various parts of this impactite by EM and AEM it was found that almost all of the matrix is composed of glasses or nearly amorphous minerals decomposed in various degrees . Fig. 3 shows varieties of glasses and partially decomposing minerals. Fig. 4 shows a series of ED of decomposing process from perfect crystal to nearly amorphous crystals. Glass compositions in the matrix was examined by AEM. The compositions are heterogeneos probably depending on the parent minerals .

From all these data given it is concluded that this rock found is really impactite with clear shock evidence .

Fig. 1 The impactite found .

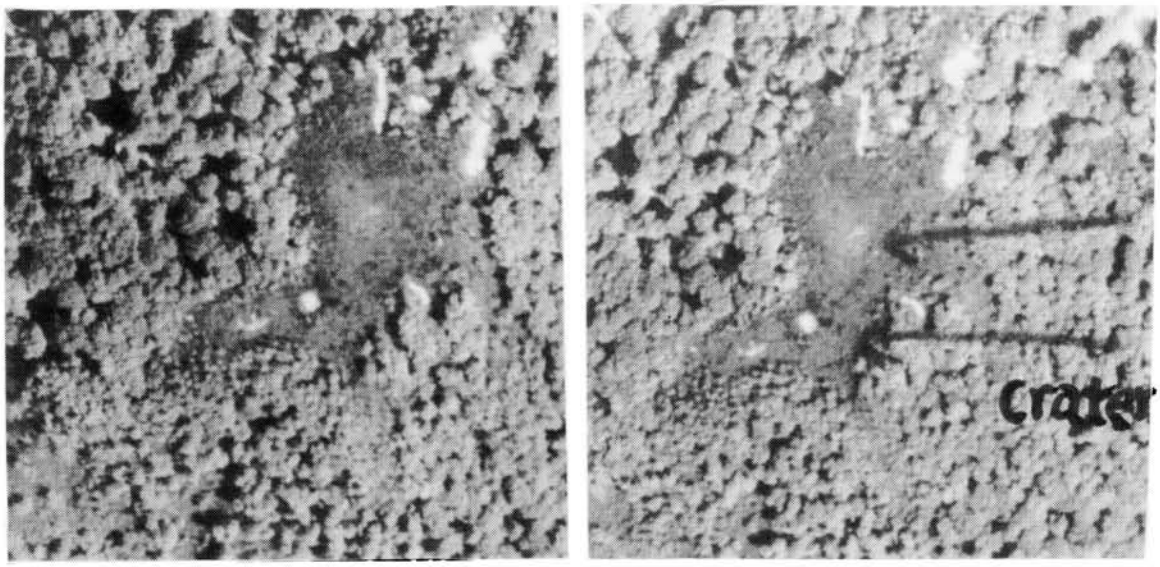

Fig. 2 Stereographic aerial photograph of the 'small crater'

Table 1 Chemical Analysis of Impactite & basement rocks (Gn, Gr)

	Impactite	Impactite ⊛	Gr	Gr	Gn
SiO2	54.00	66.32	73.22	77.84	67.38
TiO2	0.51	0.63	0.13	0.07	0.21
Al2O3	13.95	17.13	14.47	11.80	12.08
Fe2O3*	4.59	5.64	0.06	0.31	0.77
FeO			0.28	0.38	3.39
MnO	0.12	0.14	0.01	0.01	0.23
MgO	1.50	1.84	0.08	0.15	1.00
CaO	1.85	2.28	2.09	0.22	9.23
Na2O	2.48	3.05	2.59	2.79	0.55
K2O	2.10	2.58	5.74	5.73	1.48
Ign. loss	18.53	H2O+	0.16	0.34	1.46
		H2O−	0.08	0.24	0.12
Total	99.74	99.74	98.92	99.88	98.00
Ni	27.8 ppm		−	−	1.7
Rb	74.4		113.8	126.9	64.6
Sr	283.9		273.2	155.0	276.9
Zr	114.4		115.4	115.6	172.2

* total Fe as Fe2O3 ⊛ Ignit. loss → 0 recalculated

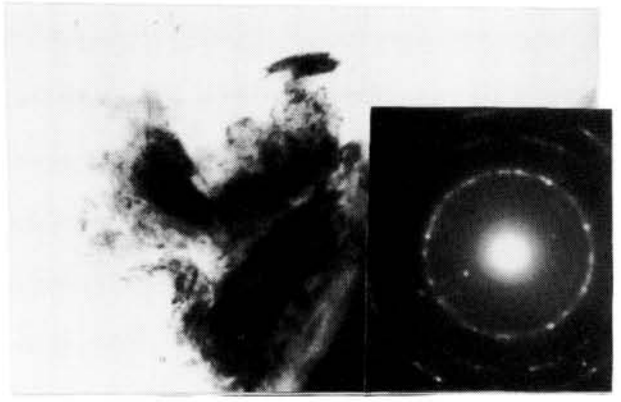

Fig. 3 Ni & Fe bearing glass in the matrix.

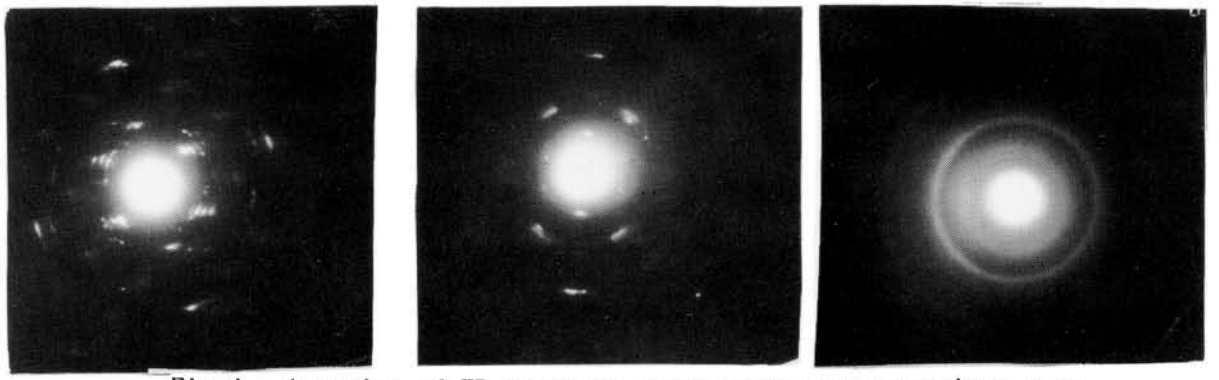

Fig. 4 A series of ED patterns representing decomposition from crystalline state to nealy amorphous state.

CARBONATES IN SOME ANTARCTIC METEORITES: INFRARED SPECTROSCOPY

Miyamoto, M.

Dept. of Pure and Applied Sci., University of Tokyo, Komaba, Tokyo 153

We studied carbonates in some Antarctic meteorites on the basis of absorption bands near 7 μm of infrared diffuse reflectances, because carbonates typically show absorption bands near 7 μm. Infrared spectra of the Murchison meteorite (CM2)(1) and interplanetary dust particle (2) show the 1450 cm^{-1} (6.8 μm) band, which is due to primary carbonates. Antarctic ordinary chondrites usually show weak absorption bands near 1350 cm^{-1} (7.4 μm). We carried out chemical dissolution experiments on some Antarctic meteorites to determine whether the 7 μm band could be caused by carbonates. Etched samples were exposed to 0.5M HCl at 25°C for 15 minutes. Infrared diffuse reflectance measurements were made with a JASCO FT/IR-3 Fourier transform infrared spectrophotometer. Details of measurements are described in Miyamoto (3). Samples of Antarctic meteorites we used were supplied by the National Institute of Polar Research.

Antarctic ordinary chondrites: While studying the degree of weathering of Antarctic meteorites on the basis absorption bands near 3 μm (3), we found weak absorption bands near 1350 cm^{-1} (7.4 μm)(Fig. 1). The 7.4 μm band disappears from the spectrum of the sample etched by a chemical dissolution experiment. We conclude that the 7.4 μm band of Antarctic ordinary chondrites is probably caused by carbonates (4). This result is consistent with the presence of hydrated Mg-carbonates (nesquehonite and hydromagnesite) in some Antarctic meteorites (5-7). In fact, the spectrum of artinite shows the wavelength position of the 7.4 μm band similar to those of Antarctic chondrites. Non-Antarctic meteorites which are falls do not show the 7.4 μm band, although non-Antarctic chondrites which are finds show faint absorption bands near 7.4 μm (Fig. 1). Therefore, the hydrated carbonates are probably formed by terrestrial weathering (5-7). Because infrared spectra of all the Antarctic ordinary chondrites we measured show weak absorption bands near 7.4 μm, hydrated carbonates produced by terrestrial weathering seem to be ubiquitous in Antarctic ordinary chondrites. We need to pay much attention to the presence of hydrated carbonates produced by terrestrial weathering when we study Antarctic chondrites. We can easily detect the presence (or absence) of the hydrated carbonates, using absorption bands near 7.4 μm of infrared diffuse reflectances of meteorites.

Enstatite chondrite: The spectra of both Yamato-691 (enstatite chondrite) and Norton County (E achondrite) show absorption bands near 6.8 μm, whose wavelength position is similar to that of Murchison but is different from that of weathering-produced hydrated carbonates in Antarctic ordinary chondrites (Figs. 1 and 2). The 6.8 μm band of Y-691 disappears from the spectrum of treated residue with water, that is, the material that causes the 6.8 μm band of Y-691 is water soluble. The 6.8 μm band may be due to weathering-produced $NaHCO_3$, because the spectrum of $NaHCO_3$ which is soluble in water shows absorption bands near 6.8 μm. Okada et al. (8) reported the presence of schöllhornite which is a terrestrial weathering product of caswellsilverite in Norton County. $NaHCO_3$ in enstatite chondrites may be a product of this reaction.

Other meteorites: The spectrum of the ALH-77257 ureilite shows no absorption bands near 6.8 μm but shows weak 7.4 μm band (Fig. 2).
The ALH-765 eucrite shows no absorption bands near 6.8 μm (Fig.2). Although the ALH-765 eucrite is severely weathered on the basis of the integrated intensity of absorption bands near 3 μm, the 7.4 μm band is very weak. This apparent discrepancy may be explained by the fact that polymict eucrites do not contain a large amount of olivine, because Jull et al. (9) proposed that the hydrated carbonates are produced by decomposition of olivine.

References: (1) Miyamoto, M. (1987) Icarus 70, 146-152. (2) Sandford, S. A. (1986) Science 231, 1540-1541. (3) Miyamoto, M. (1988) Earth Planet. Sci. Lett. 89, 398-402. (4) Miyamoto, M. (1988) Meteoritics 23, 291. (5) Marvin, U. B. and Motylewski, K. (1980) Lunar Planet. Sci. XI, 669-670. (6) Gooding, J. L., Jull, A. T. J., Cheng, S. and Velbel, M. A. (1988) Lunar Planet. Sci. XIX, 397-398. (7) Velbel, M. A. (1988) Meteoritics 23, 151-159. (8) Okada, A., Keil. K., Leonard, B. F., and Hutcheon, I. D. (1985) Amer. Mineral. 70, 638-643. (9) Jull, A. J. T., Cheng, S., Gooding, J. L., and Velbel, M. A. (1988) Science 242, 417-419.

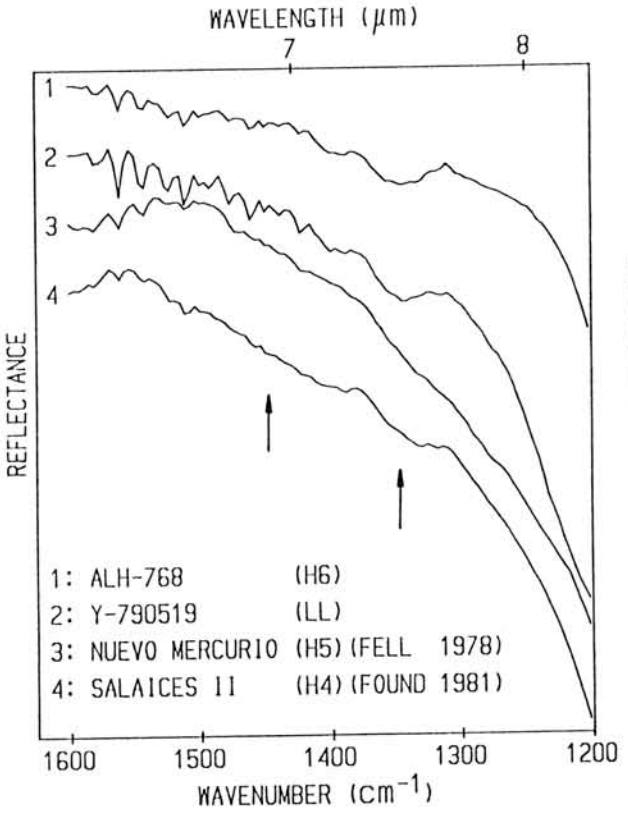

Fig. 1 Infrared diffuse reflectances of some ordinary chondrites. Arrows show the 1450 and 1350 cm^{-1} bands.

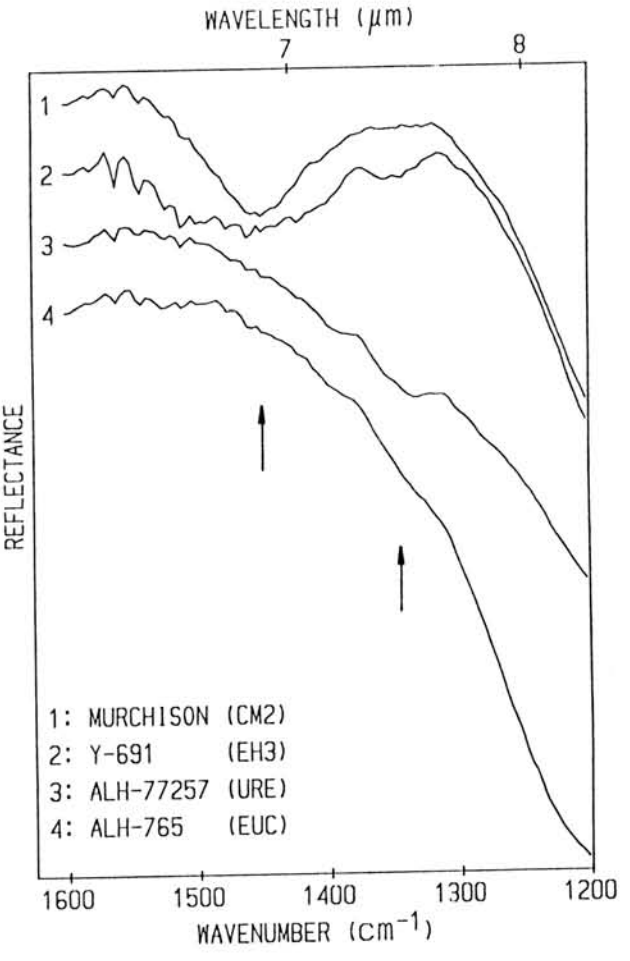

Fig. 2 Infrared diffuse reflectances of some meteorites.

MICROMORPHOMETRY OF SEVERAL YAMATO METEORITES

Żbik Marek

SPACE RESEARCH CENTRE, ul Bartycka 18, 00-716 Warsaw POLAND

Seven samples of antarctic Yamato meteorites were covered by micromorphometric image analyser Hitachi S-800/Iskra 226 and JEOL JSM-T200 scanning electron microscope equipped with an energy dispersive X-ray detector.

Primitive chondrites of the type L3 are represented by meteorites Y-82056 and Y-82095. They are characterized by relatively compact texture, locally with porous fragments similar to those described in /1/. Porosity calculated for such aggregates under magnification x 500 is varying from 13% in less porous Y-82056 to 22% in more porous Y-82095. Pore space in porous fine-grained aggregates of the meteorite Y-82095 /photo 1/ is of the intergranular type /2/. Individual pores are partly infilled with glassy material. Their specific surface /see Tabte/, expressed as totat circumference of individual pores, are fairly high because of their ultra-small dimensions /below 1 um/. Y-82095 displays numerous nonporous troilite grains over 100 um in size whereas sulfides in Y-82056 are present in the form porous of fluffy aggregates. Meteorites of the type L4 are represented by Y-81070 and Y-81075. The former is characterized by low porosity, up to 13.8% in some fragments and presence of not numerous pores of the vug type/photo 3/, up to 100 um in diameter.

Primitive chondrites of the type H3 are represented by Y-82038. It is strongly porous and displays numerous fragments with ultrafine-grained texture and porosity measured under magnification x 500, around 24.5%. The total circumference of pores is relatively high because of very small size of grains. The pore form coefficient is also high, which is typical for inergranular pores. Photo 2 and 5 shows pore space in this meteorite.

Meteorites of the type H4 are represented by Y-81058 and Y-82061. Both of them appear markedly porous, with porosity ranging from 16% to 23%. Microphotographs /see photo 6/ show brecciated texture, with pore space between large mineral grains infilled with fine-grained matrix. Intergranular pores are common here and may be found between large grains as well as grains of the fine-grained matrix. Specific surface of pores is very high as shown by total circumference values much higher than in all the above mentioned meteorites, ranging from 12994 to 18472 um.

The analyses failed to show porosity and morphological type of pores to be dependent on petrological type of meteorite, as it was stated in/ 3/.

1. S. Watanabe, M. Kitamura, N. Mirimoto
Earth and Planetary Science Letters, 86 205-213 /1987/.

2. M. Żbik
Bulletin de L'Academie Polonaise Des Sciences, Vol.XXX,No.1-2 59-65 /1983/

3. K. Yomogida, T. Matsui
Journal of Geophysical Research, 88, No. B11, 9513-9533 /1983/

Name of meteorite	Petrological type	Porosity in %	Total circumference of pores in um	mean radius of pores in um
Y-82095	L3	21.9	11882.75	2.23
Y-82056	L3	13.0	7859.50	1.63
Y-81075	L4	20.3	10089.75	2.60
Y-81070	L4	13.8	8742.25	2.84
Y-82038	H3	24.5	10895.50	3.20
Y-81058	H4	22.7	12993.75	2.18
Y-82061	H4	15.6	18472.14	1.75

Intergranular pores in meteorites

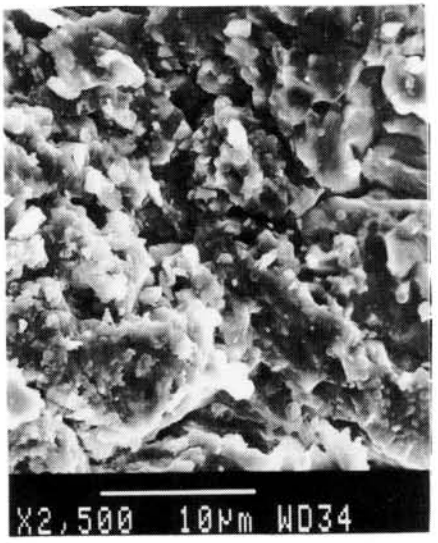

photo 1
Y-82095

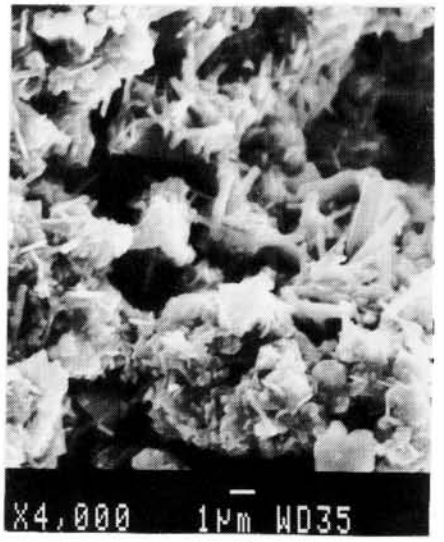

photo 2
Y-82038

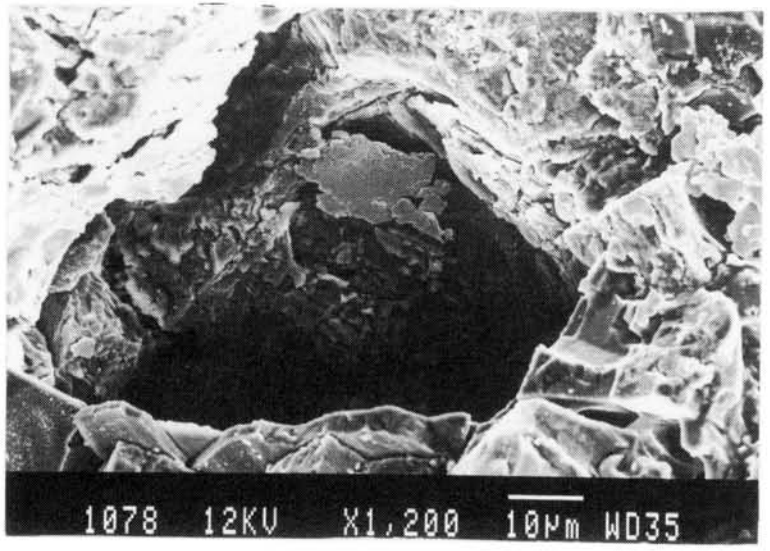

photo 3 Vugs in Y-81075

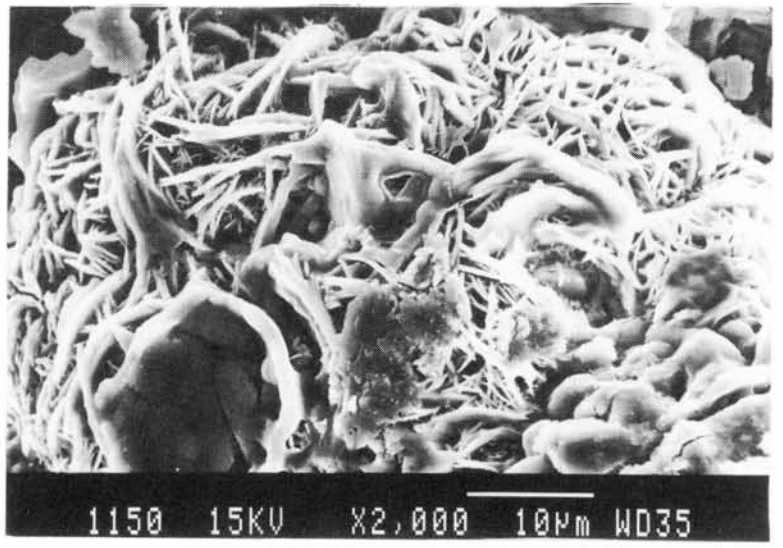

photo 4 fluffy agregates in Y-82056

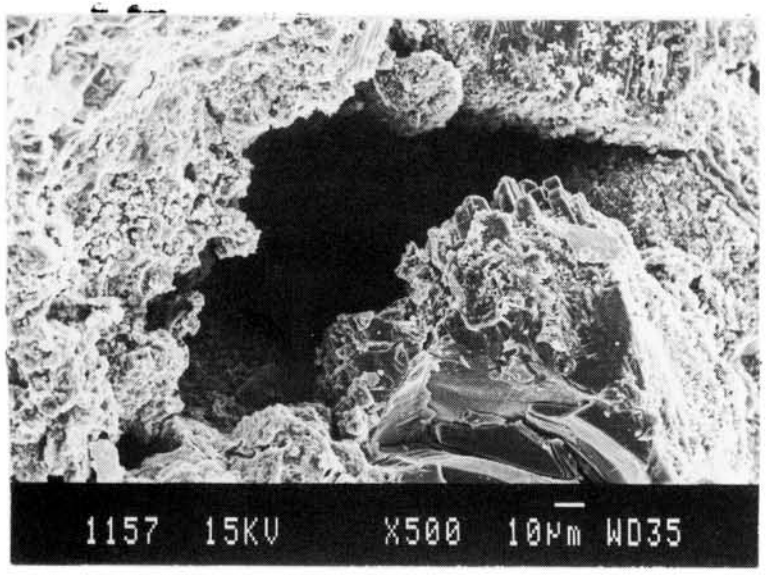

photo 5 Vugs in Y-82038

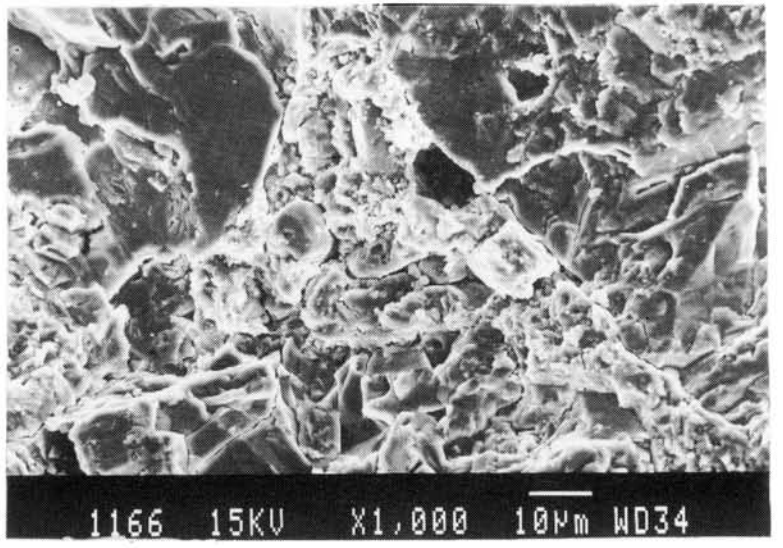

photo 6 brecciated texture in Y-81058

Observation of Allende and Antarctic Meteorites by Monochromatic X-ray CT Based on Synchrotron Radiation

Tatsumi Hirano, Minoru Funaki*, Takeshi Nagata*, Isamu Taguchi**, Hiroki Hamada***, Katsuhisa Usami and Kazunobu Hayakawa****

Hitachi Research Lab., Hitachi, Ltd., Hitachi, Ibaraki 319-12
**National Institute of Polar Research, Tokyo 173*
***National Museum of Japanese History, Sakura, Chiba 285*
****R&D Lab., Analysis Research Lab., Nippon Steel Corporation, Kawasaki, Kanagawa 211*
*****Advanced Research Lab., Hitachi, Ltd., Kokubunji, Tokyo 185*

X-ray computed tomography (X-ray CT) is a method to observe internal structures of objects, nondestructively. The images are obtained as two-dimensional distributions of X-ray linear absorption coefficients which depend on the X-ray energy used. A high resolution, tunably monochromatic X-ray CT based on synchrotron radiation (SR) have been developed and applied to observe internal structures of Allende and Antarctic meteorites.

The schematic diagram of the developed CT scanner[1] is shown in Fig. 1. It is installed to BL-8C experimental station in the KEK Photon Factory 2.5 GeV electron storage ring. SR is monochromatized through a Si(400) channel cut monochrometor. The energy range is varied from 15 to 40 keV. A high resolution X-ray pickup tube is used to detect a two-dimensional projection image corresponding to an intensity distribution of the X-rays transmitted through a sample. The two-dimensional projection images are measured by rotating the sample and are reconstructed as CT images with up to the forty slice planes. The reconstructed image is displayed as a gray-scale image on a 512 x 512 pixel video display. The limiting spatial resolution is about 10 μm[2].

The advantage of using monochromatic X-rays is the ability to reconstruct a specific element image based on the difference between two CT images just above and below the absorption edge. However, this subtraction method could not be applied to the meteorites because many metallic components in them strongly attenuated the low energy X-rays. We measured Allende and Antarctic meteorites at the photon energy of 30 keV.

Fig.2 displays six CT images of Allende meteorite at the fourth to ninth slice planes from among twenty slice planes measured. The slice thickness was 37 μm and the slice planes were spaced at 110 μm intervals. In the CT images, brighter pixels reflect the higher X-ray attenuated region. Heavy elements attenuate the X-ray beam more than light elements. The spherical dark region is thought to correspond to chondrule because of containing a small amount of metal. The X-ray absorption coefficient of the matrix (gray region) is larger than that of SiO_2 so that there is much metal in the matrix. The brightest regions in the boundary between the matrix and the chondrule are many times more opaque than the matrix. Presumably those highly attenuating regions are rich in iron or nickel, which are known to be present in Allende meteorite. In order to observe the distribution of several elements, we evaluated Allende meteorite by a chemical analysis method, after cutting out it near the

seventh slice plane. The regions rich in iron and nickel agreed with the brightest regions in the CT image. These metal-rich regions spherically surround the chondrules.

This work has been performed under the approval of the National Laboratory for High Energy Physics (Accepted No. 88-U033).

References

1) Y.Suzuki et al.: Jpn. J. Appl. Phys. **27** (1988) L461.

2) T.Hirano and K.Usami: Jpn. J. Appl. Phys. **28** (1989) 263.

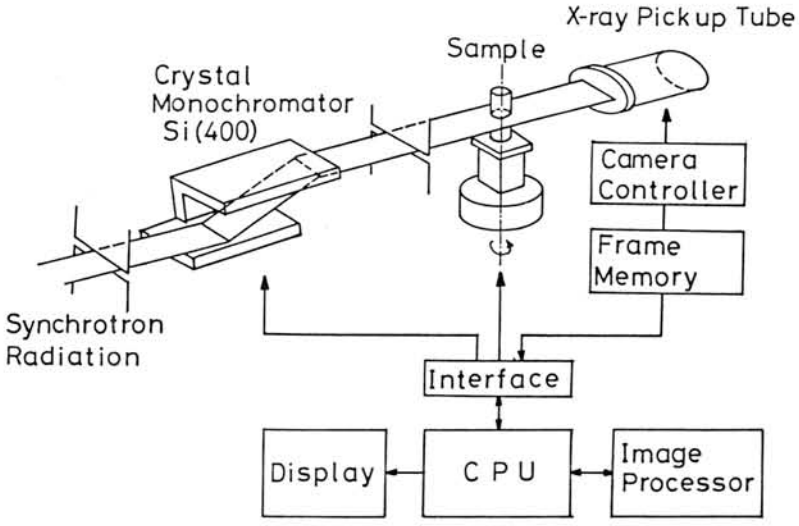

Fig.1 Schematic diagram of the monochromatic X-ray CT

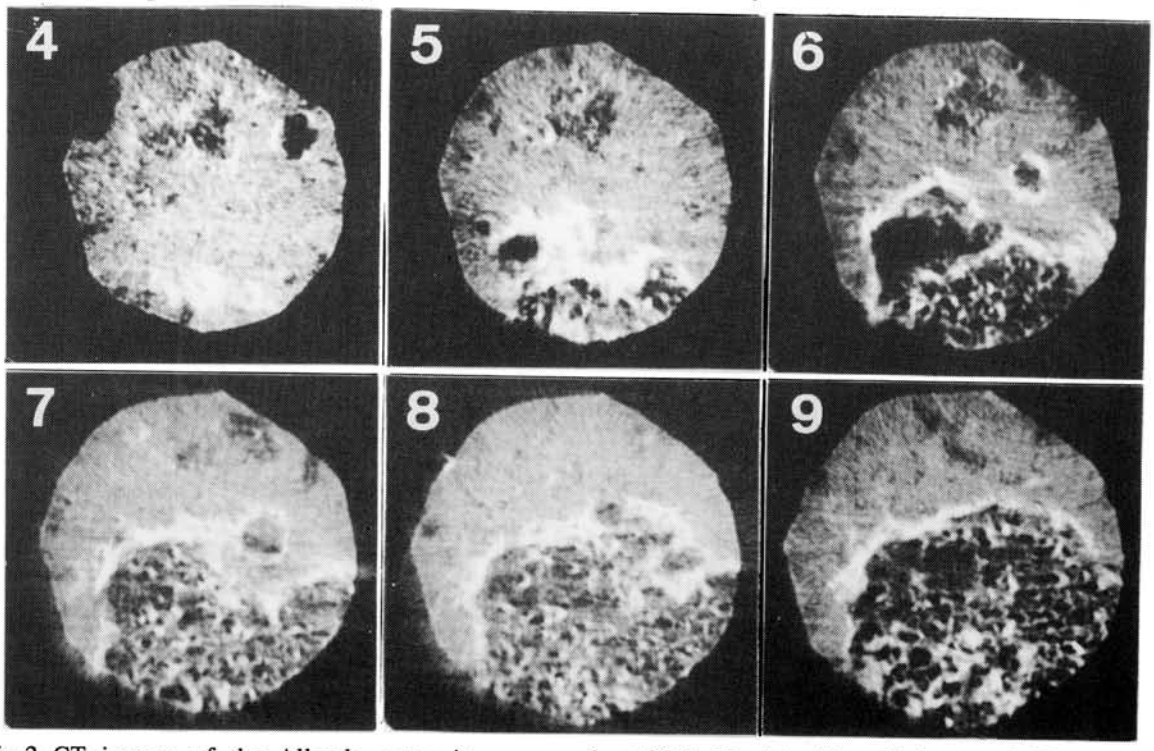

Fig.2 CT images of the Allende meteorite measured at 30 keV with slice thickness of 37 μm and slice plane interval of 110 μm. Bright localized features are regions probably rich in highly attenuating iron or nickel.

Paleomagnetic Intensity Studies on Carbonaceous Chondrites

Takesi NAGATA and Minoru FUNAKI
National Institute of Polar Research

Natural remanent magnetization (NRM) of three carbonaceous chondrites, Y-74662 (C_4), Y-81020(C_3) and Allende(C_3), are critically examined for the purpose of their paleomagnetic intensity determination. Petrographical and chemical compositions of these chondrites have already been reported. In particular, magnetic properties and NRM characteristics of the Allende were studied in detail, (1)(2). Table 1 summarizes the intensity of NRM(I_n), remanence coercive force (H_{RC}), magnetic minerals detected by EMPA, temperature range for dominant acquisition of TRM and paleomagnetic intensity (F_p) obtained on the basis of TRM acquisition assumption for the three C-chondrites, where magnetic minerals are classified into a low temperature phase(L*) and a high temperature phase(H*) in accordance with their dominant TRM acquisition ranges.

Table 1

	Y-74662(C_4)		Y-81020(C_3)		ALLENDE(C_3)	
I_n(emu/g)	5.9×10^{-4}		8.6×10^{-4}		$(1.8\sim2.5)\times10^{-4}$	
H_{RC}(Oe)	860		570		530～590	
	(L*)	(H*)	(L*)	(H*)	(L*)	(H*)
Temp.Range(°C)	25-300	300-650	25-320	320-530	25-320	320-600
Mag. Minerals	FeS_{1+x}	α Fe-Ni (4.4-6.3%Ni)	FeS_{1+x}	α Fe-Ni (4.6-6.0%Ni) + Fe_3O_4	FeS_{1+x}	γ Fe-Ni (65%Ni) + Fe_3O_4
F_p(Oe)	0.78	0.011	1.2	0.09-0.01	0.8-3.2	<0.01

Fig.1 illustrates, for example, a diagram of NRM thermally lost versus PTRM acquired for L* and H* phases of Y-74662. As shown in the table, F_p values evaluated from L* phase of the three chondrites are around 1 Oe or larger, while F_p values derived from H* phase are around 0.1 Oe or smaller. The observed difference of F_p between L* and H* phases was well noted for the Allende, (1)(2). We see here the same tendency in Y-74662

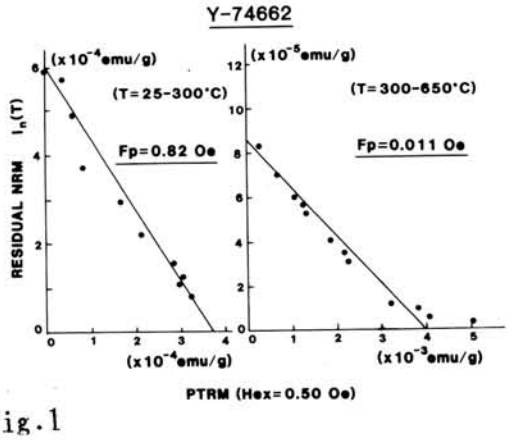

Fig.1

and Y-81020 as well. As far as the TRM acquisition assumption is accepted for the origin of NRM of the chondrites, either inference of (i) that F_p was 0.1 Oe or smaller until the ambient temperature was cooled down to about 300℃ and then F_p became 1 Oe or more at temperatures below 300℃, or (ii) that F_p was 0.1 Oe or less throughout the first cooling but the C-chondrites were reheated later up to about 300℃ in presence of a magnetic field of 1 Oe or more, (1)(2).

It is ascertained that the L*-phase NRM component of these C chondrites is possessed by pyrrhotite particles. Complicated phase structures of Fe-S system around 50% Fe 50% S (at.%) in chemical composition have been understood to a certain extent, though not completely yet, (3). According to the result, ferrimagnetic pyrrhotite phase forms below 260℃ with chemical composition of $F_{7\pm x}S_8$, and its Curie temperature is around 309℃ (4). Therefore, the hexagonal crystal grains of pyrrhotite form at temperatures below 260℃ and their grain size grows with time provided that temperature is kept adequately.

If the formation of nuclii and their growth take place in presence of a magnetic field F_p, crystallization remanent magnetization (CRM) ought to be acquired by the ensemble of pyrrhotite as already been generally reported, (5) (6).

As generally discussed and experimentally confirmed, general characteristics of CRM are substantially same as those of TRM, provided that the grownup magnettic particles possessing CRM have already reached their practically stable state. In order to examine the above-mentioned key point of stability of pyrrhotite particles in the carbonaceous chondrites, the thermal stability of NRM and PTRM acquisition rate was experimentally examined by repeated thermal demagnetizations of NRM and repeated measurements of PTRM acquisition rate for L*-phase of Allende samples.

Fig.2 shows the experimental procedures for the first and second steps of measurements with elevating temperature. As shown in the diagram, 3 readings of NRM thermal demagnetization and 2 readings of PTRM acquisition are obtained for each step of measurement. Fig.3 illustrates an example of 3 measured values of NRM thermal demagnetization for

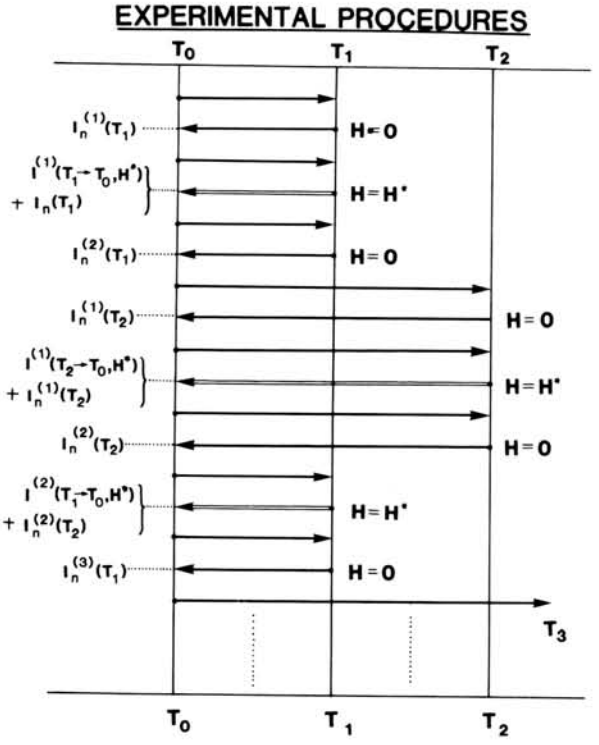

Fig.2

each step and 2 measured values of each step for PTRM acquisition process. Figures 4 and 5 show respectively correlations between 2nd and 1st readings and between 3rd and 1st readings of NRM thermal demagnetization process for 5 specimens of the Allende. Fig.6 is a similar diagram to show a correlation between 1st and 2nd readings of PTRM acquisition. Observed plots in Fig.6 are rather scattering, but the correlation coefficient is still larger than 0.8. Fig.7 shows a linear dependence of TRM intensity acquired within L* temperature range upon applied magnetic field intensity for 3 specimens of the Allende. The heating-cooling cycle between 28℃ and 360℃ was repeated 6 times for each sample to obtain the results in Fig.7, where a linear relation still approximately holds for each sample.

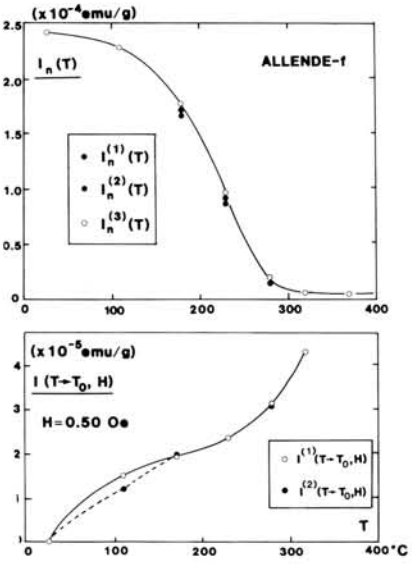

Fig.3

These experimental results suggest that pyrrhotite particles in Allende chondrite are approximately unchanged during repeated heat treatments which are necessary for experimentally evaluating F_p values based on either assumption of NRM origin, TRM or CRM. We may conclude therefore that the estimated paleomagnetic intensity F_p, $F_p \gtrsim 1$ Oe, derived from L* phase NRM of the three chondrites is acceptable as far as their order of magnitude is concerned, regardless whether the acquisition process of the NRM is due to TRM or CRM.

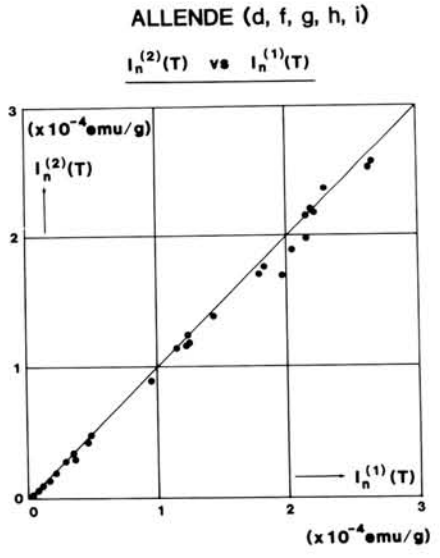

Fig.4

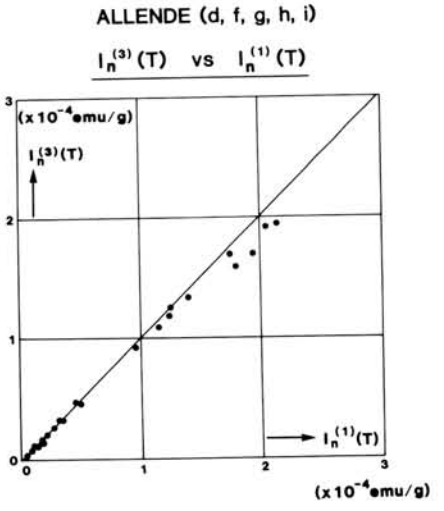

Fig.5

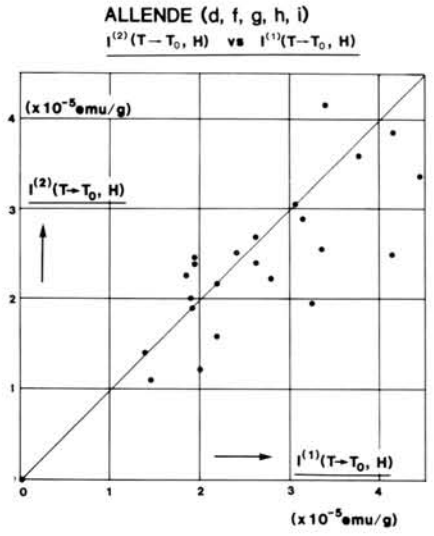

Fig.6

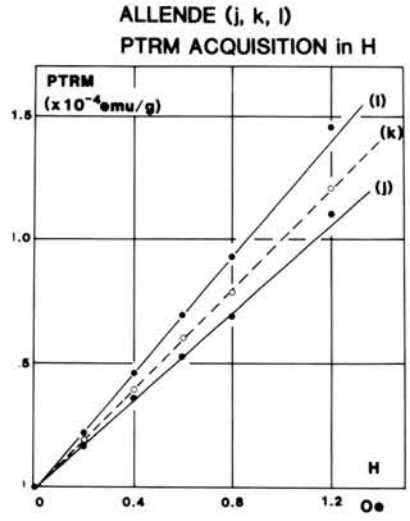

Fig.7

References

(1) Sugiura N., Lanoix M. and Strangway D.W., 1979, Phys. Earth Planet Inter., 20. 342-349.
(2) Nagata T. and Funaki M., 1983, Proc. 8th Sympo. Antar. Meteor. NIPR, 403-434.
(3) Craig J.R. and Scott S.D., 1976, "Sulfide Phase. Equiblia" in Sulfide Minerals. Minor. Soc. America, CS1-104.
(4) Tebble R.S. and Crack D.J., 1969, Magnetic Materials. 167-170.
(5) Nagata T. and Kobayashi K., 1958, Proc. Japan Acad., 34. 269-273.
(6) Kobayashi K., 1959, J. Geomag. Geoele., 10. 99-117.

MAGNETIC PROPERTIES OF THE ALLOY MIXTURES SIMULATED TO Y-74115 AND DRPA78007

Nagai, H.[1], Momose, K.[2] and Funaki, M.[3]

1) Department of Physics, Faculty of Science, Shinshu University, Matsumoto 390
2) Department of Geology, Faculty of Science, Shinshu University, Matsumoto 390
3) National Institute of Polar Research, Tokyo 173.

In order to study magnetic properties of meteorites, we have investigated the thermo-magnetic behaviours of Fe-Ni alloys [1]. The present work aims to study the magnetic properties of the mixtures of Fe-Ni alloys simulated to Y-74115 and DRPA78007.

The alloys were prepared by melting constituent elements of 99.99% purity in an induction furnace under argon atmosphere. The alloy mixture simulated to Y-74115 was produced in accordance with the EPMA analysis by Nagahara [2] and that of DRPA78007 was made of 7.3%Ni-Fe alloy which is the main magnetic substance in DRPA78007.

The Mössbauer spectra of the alloy mixtures are shown in Fig.1, where the spectra (A) and (B) show those of the mixture simulated to Y-74115 and DRPA78007, respectively. The spectra (A) containing near 30%Ni-Fe alloys show the co-existence of non-magnetic phase, while the spectra (B) of Fe-rich alloy show no existence of non-magnetic phase. The non-magnetic phase (marked by arrow) is fcc-phase with Curie temperature (T_c) below room temperature (T_0) and decreases by the martensitic transformation (fcc → bcc) after cooling at 77K, because T_c of bcc-phase is higher than T_0. The magnetic properties will be discussed in detail, comparing with the results of meteorites.

References;

[1] Momose,K. and Nagai,H.(1983) Mem. Natl. Inst. Polar Res., Spec. Issue 30 447

Momose,K., Nagai,H. and Muraoka,Y. (1984) Mem. Natl. Inst. Polar Res., Spec. Issue 35 298

Momose,K. and Nagai,H.(1985) J. Geomag. Geoelectr., 37 817

Momose,K. and Nagai,H.(1986) J. Geomag. Geoelectr., 38 721

Nagai,H. Momose,K. and Funaki,M.(1987) J. Geomag. Geoelectr., 39 431

[2] Nagahara,H.(1979) Mem. Natl. Inst. Polar Res. Spec. Issue 15 77

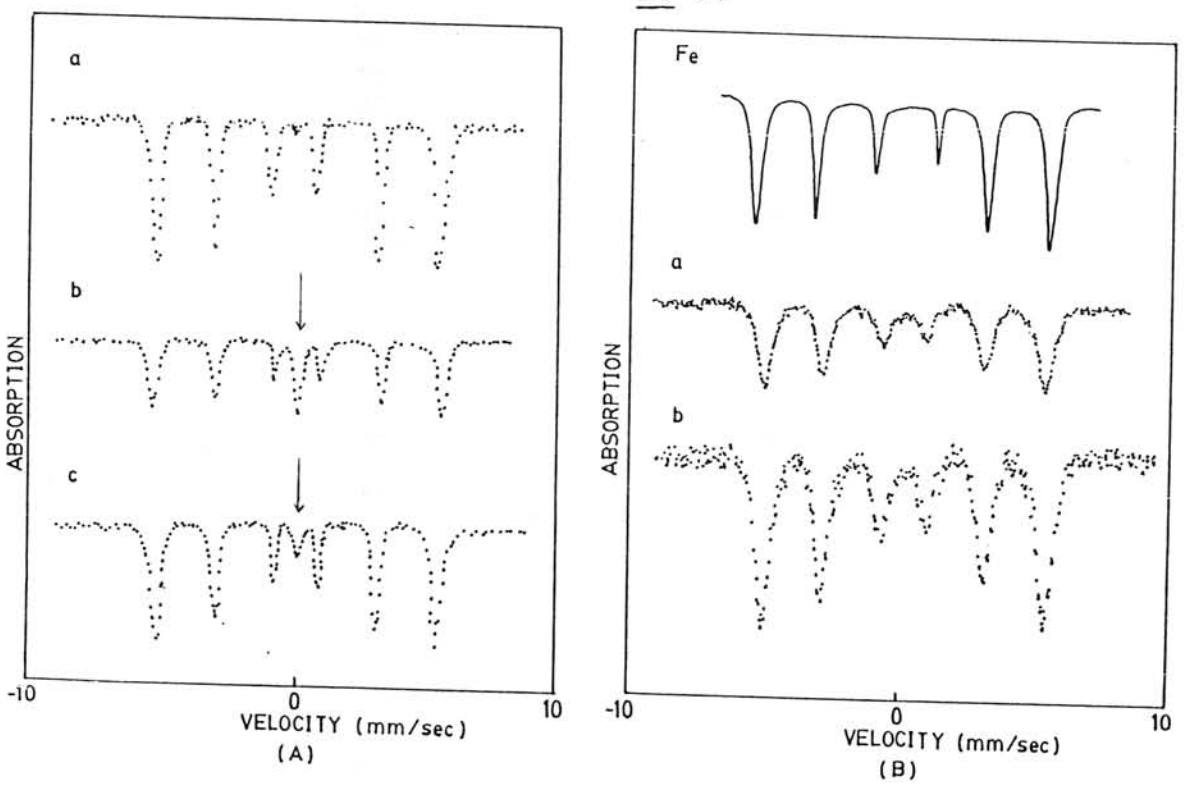

Fig.1 The Mössbauer spectra of the alloy mixtures simulated to Y-74115(A) and DRPA78007(B).
(A): spectrum(a) is in the case of original one at T_0.
spectrum(b) is measured at T_0 after heating at 850°C for 1hr
spectrum(c) is at 77K after heating at 850°C.
(B): the spectrum plotted by the solid line is due to natural iron at T_0.
Spectrum (a) is in the case of original one at T_0.
Spectrum (b) is measured at T_0 after heating at 850°C for 1hr.

MAGNETIC AND MÖSSBAUER PROPERTIES OF CHEROKEE SPRING LL6 CHONDRITE

J. Danon (1), M. Funaki (2), T. Nagata (2) and I. Taguchi (3)

1) National Observatory, Rio de Janeiro, Brazil
2) National Institute of Polar Research, Tokyo 173
3) National Museum of Japan History, Sakura, Chiba 285

Cherokee Spring is an LL6 chondrite having large chondrules some of them up to several millimeters in diameter in its groudmass which is a granular aggregate of olivine and pyroxene with interstitial plagioclase; nickel-iron and troilite are usually present (1).

Cherokee Spring is one of the rather rare unbrecciated LL chondrites. Detailed mineralogical analysis (2) shows that the meteorite has supported a slight shock event and as a consequence the iron-nickel phases have been modified according to the mechanism described by Grokhovsky and Bevan (3).

The composition of the nickel-iron pases have been analysed by magnetic methods.

Thermomagnetic curves of extracted FeNi grains from the meteorite showed at least 3 types of FeNi phases: kamacite with up to 6% Ni, taenite of about 50% Ni and tetrataenite in the original sample. In the cooling curve martensitic transformation at 60 C was observed, with the disappearance of the tetrataenite curve.

Magnetic hysteresis curves of the original sample indicated a very large coercive force (7.3 mT) and remanent coercive force (42.3 mT). These values decreased to 0.2 mT and 4.2 mT respectively by heat treatment up to 850 C. This variation of coercive forces is explained by the presence of tetrataenite in the metal phases.

The presence of tetrataenite has been confirmed both qualitatively by the magnetic colloidal method (4) and quantitatively by Mossbauer spectroscopy (5) which indicates about 36% of tetrataenite in the metal phase of Cherokee Spring.

(1) Jarosewich and Mason 1969
(2) M. Christophe Michel-Levi and J. Danon, submited to 52nd annual meeting of the Meteoritical Society.
(3) V.J. Grokhovsky and A.W.R. Bevan, Nature, 301, 323 (1983).
(4) M. Funaki, I. Taguchi, J. Danon, T. Nagata, Y. Kondo, Proc. NIPR Symp. 1, 231 (1988)
(5) J. Danon, I. Souza-Azevzdo and R.B. Scorzelli- to be published.

Special Lecture

Professor Michael E. Lipschutz

COMPARISON BETWEEN ANTARCTIC AND NON ANTARCTIC METEORITE POPULATIONS

M. E. Lipschutz

Dept. of Chemistry, Purdue University, W. Lafayette, IN 47907 USA.

In comparing Antarctic and non-Antarctic meteorite populations, three questions are important.

1. Do the properties of the populations differ significantly?

2. If so, are the differences due to terrestrial processes?

3. If not, what preterrestrial processes do the differences reflect?

To answer the first question, we review in detail those properties that have been compared in various meteorite groups of the Antarctic and non-Antarctic populations. Since Dennison et al. (1986) first made such a comparison, nearly all of the substantial data that have accumulated indicate significant differences between the two populations.

Most of the differences observed cannot reflect terrestrial processes such as Antarctic weathering. Trivial causes, such as pairing of Antarctic specimens, statistical modeling, chance, etc. also can be eliminated. Only a preterrestrial cause can account for the differences.

The nature of the observed differences indicates that meteorite groups found in Antarctica have different average thermal histories - hence, genesis - than do similar groups falling elsewhere on Earth today. It is not necessary that all members of an Antarctic meteorite group have a different origin from the non-Antarctic group: each might be composed of the same two components with different genetic histories, but in different proportions.

At present, we favor the idea that the population-differences arise from the Earth's having encountered and sampled a different extraterrestrial flux $\geq 10^5$ years ago, when the majority of Antarctic meteorites fell, than is being encountered and sampled by contemporary falls. Less-likely alternatives include a higher proportion of debris in Antarctica from parent objects with highly-inclined orbits, or a size-dependent variation. All possibilities are problematical (Dennison et al., 1986). The principal drawback to the notion of a time-dependent change of extraterrestrial material, the requirement for the existence of meteorite streams (Wetherill, 1986), may not be serious. Halliday et al. (1989) report direct observations of such streams in the Prairie Network and Meteorite Observation and Recovery Project camera networks, reenforcing indirect arguments and observations by others.

References

J. E. Dennison, D. W. Lingner and M. E. Lipschutz (1986) *Nature* **319**, 390-393.

I. Halliday, A. T. Blackwell and A. A. Griffin (1989) *Meteoritics*, submitted.

G. W. Wetherill (1986) *Nature* **319**, 357-358.

Abstract Only

Y 86032 AND ALHA 81005 - CARBON AND NITROGEN STABLE ISOTOPE ANALYSES OF TWO LUNAR METEORITES.

Grady, Monica M. and Pillinger, C. T.
Planetary Sciences Unit, Dept. of Earth Sciences, The Open University, Walton Hall, Milton Keynes MK7 6AA, U.K.

Lunar meteorites were first recognized in 1982, with the description of Allan Hills A81005 (ALHA 81005) (1); since then, five other specimens have been recovered from the Yamato Mountains by the Japanese Antarctic meteorite programme (2). Three of these Japanese samples are believed to be paired, hence we now have representatives of at least four separate meteorites from the moon. Geochemical criteria (3-5) show that these four samples are derived from separate (at least three) craters, *i.e.* they are the result of several discrete impact events, and are not simply the products of a single impact, subsequently breaking up during Earth-Moon transit into several meteorites. The lunar meteorites are most similar in terms of major, minor and trace element composition to anorthositic highland material, and hence are most frequently compared with the regolith breccias returned from the Apollo 16 landing site (6), particularly those collected from Station 10, half-way between the North Ray and South Ray craters (7).

Carbon and nitrogen stable isotope analyses of lunar samples have shown that there is a variety of different components in lunar materials. The soils contain the highest concentrations of these elements, an over-abundance which is mainly purported to emanate from the solar wind (8). Lunar highland breccias contain intermediate amounts of nitrogen and carbon, from a mixture of sources: ancient solar wind, modern solar wind, possibly meteoritic debris, plus indigenous nitrogen and carbon, reflecting the depth and extent of surface exposure and subsequent lithification. However, the moon has had a complex history, and unfortunately the returned lunar samples (Apollo and Luna) were all located in a relatively restricted area from the near-side of the moon. Lunar meteorites have extended the types of material available for analysis, and comparison with the returned lunar rocks has been able to elucidate several problems. It was hoped that stable carbon and nitrogen analysis of lunar meteorites would extend this facility to the stable isotope geochemistry of lunar materials.

Two samples have been made available for analysis: ALHA 81005 (30 mg) and Y 86032 (160 mg). This latter sample is paired with Y 82192 and Y 82193 (2). Each meteorite was analyzed by stepped combustion from room temperature to 1200°C, generally in 50°C increments. Separate aliquots of crushed powder were taken for the carbon and nitrogen analyses. Results are tabulated below. The total carbon contents of the two meteorites (429 and 320 ppm, excluding data below 450°C as due to terrestrial organic contamination) are much higher than comparable lunar regolith breccias (12-198 ppm; 9, 10), or indeed soils. Summed carbon isotopic compositions (–21.9 and –25.2‰) are within the range of $\delta^{13}C$ exhibited by lunar breccias

(–30.1 to +9.2‰; 9,10), however it must be stated that the majority of mature regolith samples tend toward positive $\delta^{13}C$ values. Carbon data from stepped combustion of the two samples are shown in the top half of the figure. It is apparent from the yield histogram that there are three components present, identified as (i) terrestrial organic contamination (T ~ 200-450°C; $\delta^{13}C$ *ca.* –28 to –26‰); (ii) a moderately resistant form of carbon (T ~ 550-700°C; $\delta^{13}C$ *ca.* –23‰) and (iii) a component requiring high temperatures for release (T ~ 900-1100°C; $\delta^{13}C$ *ca.* –28 to –26‰). A fourth component occurring in minor abundance is indicated in the isotope trace, presumably spallogenic carbon (T > 1150°C; $\delta^{13}C$ > 0‰). ALHA 81005 is richer in this component than Y 86032, in keeping with the observation that ALHA 81005 has been exposed to cosmic rays (and the solar wind), whereas Y 86032 has not (5,11,12). By far the most conspicuous aspect of the stepped combustion profile is the resolution of components (ii) and (iii); such a clear-cut picture has never been observed during analyses of Apollo samples. Also important is the fact that most of the excess carbon is in the highly resistant component (iii), precluding any chance of its being contamination.

Total nitrogen data for the two specimens are given in the table. Both nitrogen abundances (31 ppm in Y 86032 and 53 ppm in ALHA 81005) and $\delta^{15}N$ (+7.7, +29.1 respectively) are within the range reported for lunar breccias (4 - 70 ppm; $\delta^{15}N$ *ca.* –65 to +74‰; refs. 13 - 15). Nitrogen stepped combustion data are pictured in the lower half of the figure; they are less straightforward to interpret than the corresponding carbon data, partly a result of higher temperature increments taken to compensate for the low quantities of nitrogen released. However, it can readily be appreciated that, as for carbon, there are several nitrogen-bearing components present, with variable isotopic composition. ALHA 81005 again evinces the greater influence of spallogenic nitrogen (as indicated by a higher $\delta^{15}N$ value) in the 1200°C step than does Y 86032, but the amount of nitrogen released in the single 800-1200°C increment is mainly due to another component, since spallogenic nitrogen does not contribute substantially to the total nitrogen abundance. Ignoring the complicated structure at temperatures below 450°C, which may be, to some extent, a feature of terrestrial contamination, the $\delta^{15}N$ profiles show the characteristic heavy-light-heavy pattern of lunar materials (16).

Both samples are sufficiently different from lunar counterparts, particularly in carbon systematics, to warrant the question has some component of meteoritic material been added from the projectile during the impact which excavated the samples and sent them on their long journey to Earth?

References: (1) Mason, B. (1982). *Ant. Met. Newsletter*, **5** (4); (2) Takeda *et al.* (1988). *13th Symp. on Ant. Met.* (abstract) 9-11; (3) Dennison, J.E. (1987). *Proc. 11th Ant. Met. Symp. Natl. Inst. Polar Res.* **Special Issue 46**, 89-95; (4) Warren, P.H. (1989). *Earth Planet. Sci. Lett.* **91**, 245-260; (5) Eugster, O. & Niedermann, S. (1988). *Earth Planet. Sci. Lett.* **89**, 15-27; (6) Warren, P.H. *et al.* (1983). *Geophys. Res. Lett.* **10**, 779-782; (7) Takeda, H. *et al.* (1986). *Proc. 10th Ant. Met. Symp. Natl. Inst. Polar Res.* **Special Issue 41**, 45-57; (8)

Kerridge *et al.* (1975) *Geochimica cosmochimica Acta* **39** 137-162; (9) Kaplan, I.R. *et al.* (1970). *Proc. Apollo 11 Conf.* 1317-1329; (10) Petrowski, C. *et al.* (1974). *Proc. 5th Lunar Conf.* 1939-1948; (11) Bogard, D.D. & Johnson, P. (1983). *Geophys. Res. Lett.* **10**, 801-803; (12) Eugster, O. *et al.* (1986). *Earth Planet. Sci. Lett.* **78**, 139-147; (13) Becker, R.H. & Clayton, R.N. (1975). *PLSC6th.* 2131-2149; (14) Fourcade, S. & Clayton, R.N. (1984) *Earth Planet. Sci. Lett.* **68**, 7-18; (15) Kaplan, I.R. *et al.* (1976). *PLSC7th.* 481-492; Carr, L.P *et al.* (1985). *LPSC.* **XVI**, 115-116.

Sample	[C] ppm	$\delta^{13}C$ ‰	wt mg	[N] ppm	$\delta^{15}N$ ‰	wt mg
ALHA 81005	1055	–23.9	2.667	53	+29.1	3.557
	479*	–21.9*				
Y 86032	612	–26.7	1.929	31	+ 7.7	2.351
	320*	–25.2*				

* Excluding data below 450°C as being due to terrestrial contamination.

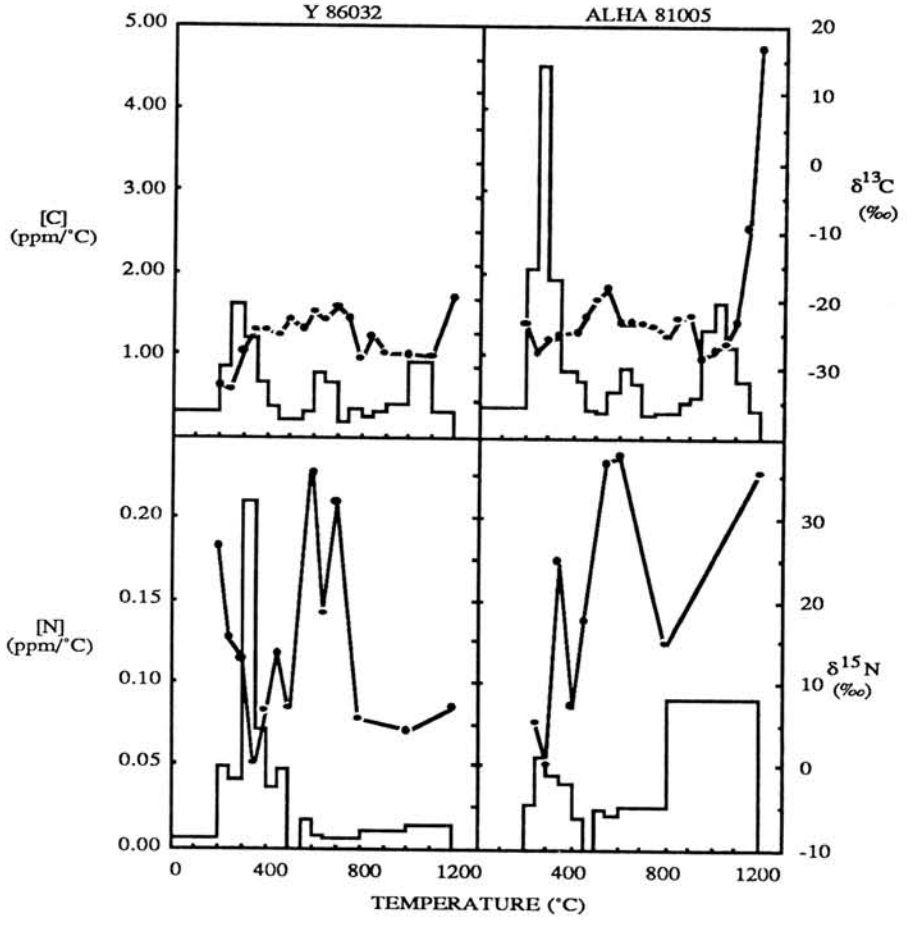

OXYGEN ISOTOPIC COMPOSITIONS OF UNIQUE ANTARCTIC METEORITES; Toshiko K. Mayeda and Robert N. Clayton, Enrico Fermi Institute, University of Chicago, Chicago, IL 60637, USA.

Oxygen isotope analyses have been determined for seven Antarctic meteorites as an aid in their classification and a search for new meteorite types. Samples were all analyzed as whole-rocks without acid washing, following procedures of Clayton and Mayeda (1963, 1983). Results are presented in Table 1. Data on apparently related samples are discussed together.

Y 74359, Y 74360

These two small stones have isotopic compositions typical of equilibrated H chondrites. This assignment is consistent with the published olivine composition.

Y 75261, Y 75300

The isotopic compositions of these meteorites fall in the field of winonaites (e.g., Winona, Pontlyfni) and IAB iron meteorites.

ALH 78230, Y8002

A possible mixing line has been recognized extending from enstatite chondrites, through IAB irons, Acapulco, Sombrerete, Lea County 002 to Kakangari. This line is formed by a diverse assortment of meteorites, including irons, achondrites and chondrites.

ALH 78230 and Y 8002 have isotopic compositions similar to Acapulco and Sombrerete, respectively. Genetic relations, if any, among meteorites in this "group" are obscure.

Y 75305

This meteorite is close isotopically to the howardite-eucrite-diogenite field, but chemical compositions of its minerals are incompatible with such an association (Meteorite News, 1985).

Table 1
Oxygen Isotopic Compositions of Small Unique Antarctic Meteorites

Sample No.	Catalog Class	$\delta^{18}O$	$\delta^{17}O$	$\Delta^{17}O$	Isotopic Class
ALH 78230	Unique	+3.97	+1.07	-1.00	Like Acapulco
Y 74359	Unique	+3.81	+2.73	+0.75	H
Y 74360	Unique	+4.12	+2.86	+0.72	H
Y 75261	Unique	+5.76	+2.73	-0.27	Winonaite?
Y 75300	Unique	+5.20	+2.22	-0.48	Winonaite?
Y 75305	Unique	+3.26	+1.15	-0.55	Unique
Y 8002	Lodranite	+3.36	+0.35	-1.40	Like Sombrerete

MINERAL CHEMISTRY, TRACE ELEMENTS AND OXYGEN ISOTOPES OF COARSE-GRAINED REFRACTORY INCLUSIONS FROM THE GROZNAIJ CARBONACEOUS CHONDRITE

Ulyanov A.A., Kononkova N.N., Ustinov V.I., Kolesov G.M.
V.I.Vernadsky Institute of Geochemistry and Analytical chemistry of the USSR Academy of Sciences, Moscow, USSR

INTRODUCTION. Carbonaceous meteorite Groznaij is a typical C3V chondrite, and like Allende and Efremovka,contains numerous Ca-, Al-rich inclusions (CAI's). Unlike Allende and Efremovka, however the Groznaij inclusions have been little studied. Detail geochemical,mineralogical and isotopic data for them are nessesary because Groznaija CAI's are more altered than those in Allende and Efremovka (1) and they are potentially very informative for understanding of the high temperature processes, which probably took place in the Solar nebula. In this paper we report the results of detail mineralogical, geochemical and isotopic studies of six Groznaij coarse-grained inclusions. The results of the similar investigation of one of the fine-grained inclusions from Groznaij reported in (1).

METHODS. All inclusions were first studied by optical microscopy. The mineral chemistry of CAI's in Groznaij meteorite was studied by electoron probe microanalysis. Mineral analyses were performed using CAMECA MICROBEAM operated at 15 kV and 30 nA. The INAA was used for determination of REE abundances in several refractory objects from Groznaij. The oxygen isotope composition was measured by standard BrF_5-method using VARIAN MAT-250.

PETROGRAPHY AND CLASSIFICATION. The most abundant type of inclusions consists mainly of melilite, Ti-Al-rich pyroxen,spinel and anorthite. These correspond mineralogucally to the Type B Allende and Efremovka inclusions. However two of these CAI's (Gr-6 and Gr-8) are anorthite-rich inclusions and it is possible that they represent intermedium type between Type B and Type C. Less abundant than Type B (and Type B/C) inclusions are refractory objects that correspond to Type A and Type C inclusions (the last was found in Allende (2)). The Type A inclusion Gr-4 is the melilite-rich object containing spinel (Ti-Al-pyroxen is very rare). The Type C inclusion Gr-2 composed mainly of plagioclase, spinel, Ti-Al-pyroxene and garnet (melilite is absent).

MINERAL CHEMISTRY. Melilite is the most abundant mineral in the inclusions of Type A and Type B. It encloses pyroxene, spinel, and sometimes plagioclase grains. Some melilite crystals of Type B CAI's in Groznaij contain tiny (< 5 μm) grains of garnets. Melilites in Type B inclusions have similar average compositions (Ak 50-70) and compositional ranges. Melilites in Gr-4 (Type A) is essentually enriched in the gehlenite component; moreover the content of this gehlenite component is progressively increase from core of inclusion to its periphery (mantle is more refractory than core!). Average composition of melilite in CAI Gr-4 (Type A) is Ak 30. In all melilites of Groznaij refractory inclusions, there is a broad positive correlation between the Na_2O and MgO concentrations. Many melilite grains exibit composition concentric zonning: the content of Ak-component in melilite gradually increase (or decrease) from core of individual grain to its periphery.

Pyroxenes in Groznaij CAI's are Ti-Al-rich fassaites. Ti-Al-pyroxenes in Type B and Type B/C inclusions have similar compositions: they contain relatively high amounts of Al_2O_3(15-20 wt%) and TiO_2 (3-5 wt%). Unlike Allende and Efremovka pyroxenes, there is no correlation between atomic content of Ti and sum of cations in formula (per 6 atoms of O). One of a possible explanation for the absence of this correlation is origin Groznaij pyroxenes in more oxidizing environment than Efremovka and Allende pyroxenes. Ti-Al-fassaites from core of CAI Gr-2 (Type C) contain more TiO_2 (5-6.5 wt%) and Al_2O_3 (14-20 wt%) than mantle pyroxenes (average: TiO_2 = 2.5 wt%, Al_2O_3 = 9.7 wt%) of this inclusion. The highest contents of titanium and aluminium were found in rare Ti-Al-fassaites in the Type A inclusion Gr-4 (9.6 wt% TiO_2 and 21.6 wt% Al_2O_3).

Plagioclases. The primary plagioclase occurs in two Type B inclusions. (Gr-3, Gr-5), two intermedium Type B/C inclusions (Gr-6, Gr-8) and one Type C inclusion (Gr-2). Average analyses of these plagioclases from each inclusions are very similar. All of the plagioclases contain appreciable amount of MgO ($\sim$.05 -.3 wt%). Plagioclase consists largely of the anorthite component ($CaAl_2Si_2O_8$) and also contains small amount TiO_2, Cr_2O_3, V_2O_3, FeO, and Na_2O ($<$.1 wt% each). The range of average compositions of primary plagioclases in inclusions from Groznaij is An 98.5 - An 99.6 (Ab$<$1.5, Or$\leq$.1). The average composition of secondary plagioclase in coarse-grained Groznaij CAI's is An 93.5. Secondary anorthite consists largely of $CaAl_2Si_2O_8$-component also, but it contains more Na_2O and FeO (up to 3 wt% each) than primary anorthite from Groznaij CAI's.

Spinel. Tiny grains of spinel occured enclosed in melilites and pyroxens in all varieties of coarse-grained Groznaij CAI's. Spinels in Type A and Type B refractory inclusions have similar average composition; spinel in Type C inclusion is slightly enriched in Cr_2O_3 (up to .8 wt%). Spinels typically contain 98 mol% of $MgAl_2O_4$. Small amounts of minor elements Si, Ti, Cr, V, Mn and Zn occur in most spinels in all varieties of Groznaij inclusions.

Other minerals in refractory Groznaij inclusions that were analyzed include grossular, andradite and calcite. Grossulares typically contained 2 - 2.5 wt% MgO and 1 - 2.5 wt% FeO. Andradites consist largely of the $Ca_3Fe_2Si_3O_{12}$component, but also contain small amount Al_2O_3(generally .1 wt%) and MgO (generally .2 wt%). Calcite contains .2 wt% FeO, .1 wt% MgO and MnO, which are present at the $FeCO_3$, $MgCO_3$,and $MnCO_3$ components.

RARE EARTH ELEMENT CONCENTRATIONS. The measured REE patterns in Type B and Type B/C Groznaij CAI's are either flat with positive Eu-anomaly or demonstrate HREE enrichment (Gr-5) with small negative Eu- and Yb-anomalies. For Type B/C inclusions we found small positive Yb-anomaly also. CAI Gr-4 (Type A) has highly fractionated REE pattern with the light rare earth enriched and small negative Yb-anomaly. Like Efremovka CAI's (3) there is no correlation between REE patterns and petrological types of Groznaij CAI's. Our INAA results demonstrate the heterogeneity of the condensed material in the early solar nebula on mm-scale.

OXYGEN ISOTOPE ANALYSES. CAI's from Groznaij (Type B and TypeB/C) give $\delta^{17}O$ = -12.1 and -11.5, $\delta^{18}O$ = -6.6 and -7.5 ‰

(relative SMOW), respectively, which plot on non-mass fractionation line at the centre of the cluster of other Groznaij CAI's (4) on the three oxygen isotope diagram. Majority of inclusions from Allende and Efremovka are riched by ^{16}O relative Groznaij CAI's. These isotope data suggest that the major solid reservoir (from which the CAI's were formed) was heterogenous on the isotope level.

CONCLUSION. The mineral chemistry of the Groznaij inclusions suggests that they formed under more oxidizing conditions than redox conditions for Allende and Efremovka CAI's. Evidences for oxidizing conditions at high temperature are coming from chemistry of Ti-Al- pyroxenes and absence of metalic phases (taenite, kamasite) in Groznaij CAI's. Inclusions from Groznaij are much more altered than Allende and Efremovka CAI's. Degree of second alteration of refractory inclusions increases in sequence: Efremovka-Allende-Groznaij. Moreover degree of the methasomatic alteration does not influence on oxygen isotope compositions of CAI's. Primitive solar nebula was macro- and micro-heterogenous. These suggest the complex and multi- stage process of the formation of the primary solid mater in the solar nebula.

REFERENCES: (1) Ulyanov, A. A., et al. (1987) Meteoritika (in Russian). (2) Wark, D. A. (1984) Ph. D. Thesis, Melbourne University. (3) Ulyanov, A.A., Kolesov, G.M. (1984) LPSC XV, p.974. (4) Ulyanov, A.A., et al. (1987) Geochimij, 8, p.1075 (in Russian).

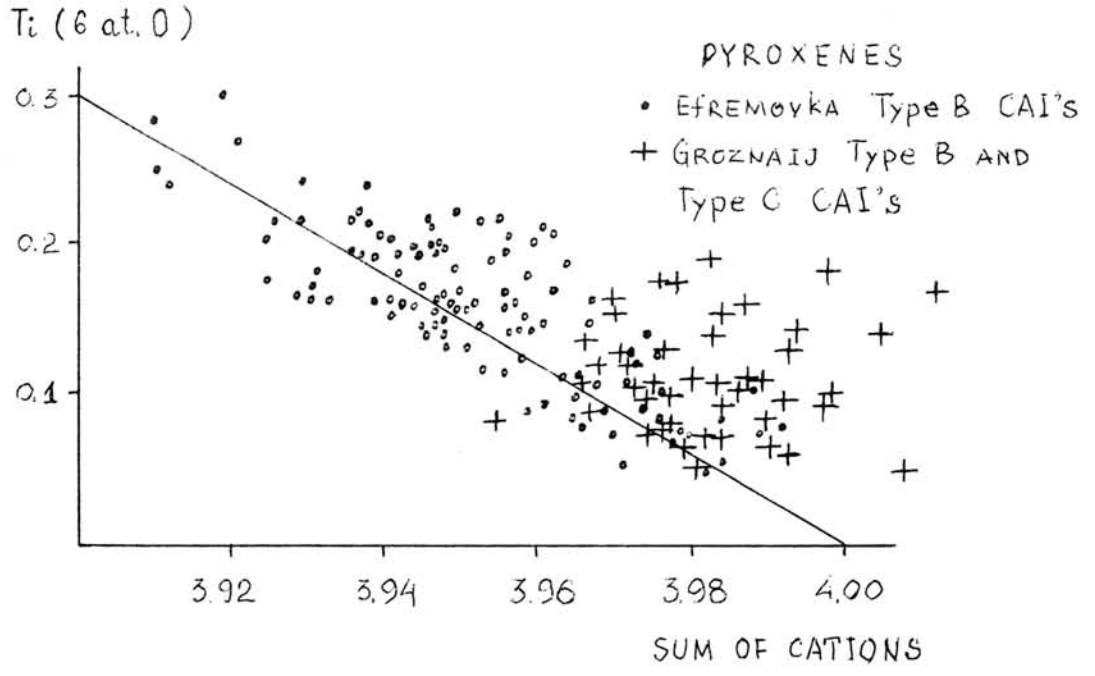

METECRITE BREAKUP AT ATMOSPHERIC ENTRY : WHAT CAN WE LEARN FROM FRAGMENTS ?

Bruno Lang and Krzysztof Franaszczuk, Warsaw University, Department of Chemistry, Żwirki i Wigury 101, 02-089 Warsaw

Meteorite breakup at atmospheric entry is a peculiar type of fragmentation of solids. Some portion of information about such an event is carried by the fragments. However, two different aspects of this information can be conceived: the first of them would make allowance for the phenomena as occurring inside a body while accompanying generation of fragments. Linking usually the statistical data with the mechanics of fracture based on initiation, propagation and coalescence of cracks and flaws this approach is treating rather marginally the disruptive forces acting from outside. From the viewpoint of atmospheric breakage such an approach does not much differ from standard terrestrial practice of rock mechanics. Thus it would be unspecific and of limited value. More useful would be exploration of the other aspect involving the destructive regime responsible for disintegration of a body. The observed independence of the mass/size distribution of fragments from the meteoritic material - stony, stony-iron, iron - argues for the importance of the destructive regime when compared with the material properties.

The fundamental for such a search has been elaborated by ReVelle [1979] who proficiently summarized the documented observation of fall of Přibram, Lost City and Innisfree meteorites.

To retrieve the concerned information we applied some simplifying assumptions: for unavailability of the required data we replaced the unknown natural geometry of fragments by a conventional one based on the cubic root of the mass-to-density ratio m/o adopted as the size of a fragment. Further we assumed the set of fragments ordered according to decreasing sizes to represent the sequence of comminution of the original pre-atmospheric body. The statistical self-similarity of fragments was considered in terms of the fractal geometry of Mandelbrot [1983] while the concept of a fracture cascade used as developed by Matsushita [1985]. Numerical estimates for fractal exponents x and y are essential for this concept. They are obtained in log-log plots as slopes of the regression straight lines for cumulative numbers $N(r)$ and cumulative masses $N_m(r)$ in equations

$$N(r) = r^{-x} \quad \text{and} \quad N_m(r) = r^{-y},$$

where r is the size of a fragment. The idea of our approach is the supposed close correspondence between the fractal geometry of fragments and the generating them destructive regime of flight. The invariance of the fractal dimension $D = x - y$ i.e. the difference of the slopes over the same mass/size range of fragments was interpreted as the invariance of the destructive regime which produced these fragments. The distinct ranges of invariance of the slopes were found to be distinct stages of the involved fracture cascade see Lang and Franaszczuk, 1989 .

To visualize our procedure we used the Chico Hills ordinary chondrite of type H 4, with its 37 fragments ranging from 3 g up to 400 g and with bulk meteorite density adopted as 3.7 $g \cdot cm^{-3}$ [Hutchison, 1987]. The results of our procedure are shown in Fig.1. In Fig. 1a are shown the plots for the cumulative number

while in Fig. 1b for the cumulative mass of fragments. The influence of ablation on the self-similarity of fragments was neglected: it was assumed to precede the fragmentation. Regression straight lines with two distinct - strongly differing - slopes are seen extended over the same two mass ranges of fragments. The numerical data underlying Fig.1 are given in Table 1.

Table 1.
Fractal parameters for fragments of the Chico Hills chondrite H 4.

Stage of the fracture cascade	Fragments covered	x	y	D
I	1 - 20	9.90	8.16	1.74
II	20 - 37	0.32	0.04	0.28

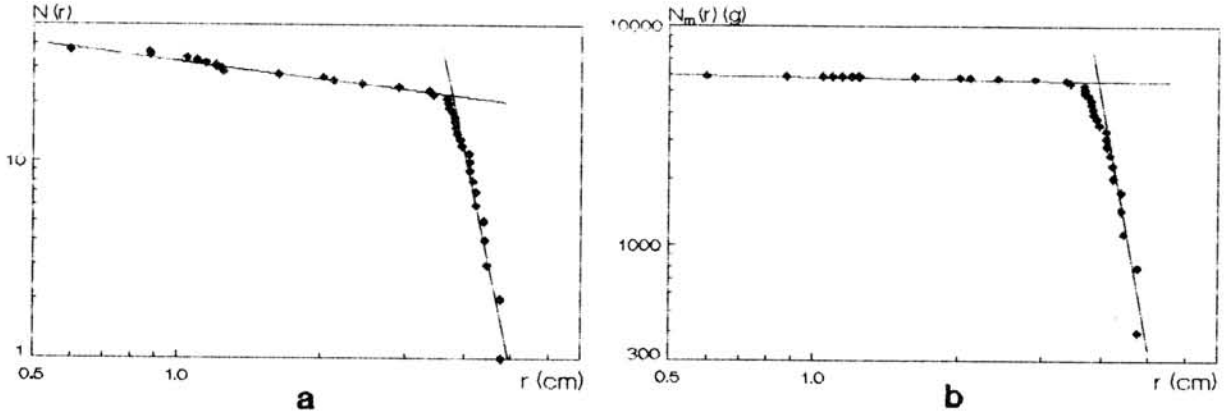

Fig.1
Fractal analysis of fragments of the Chico Hills chondrite.
(a) The cumulative number (b) the cumulative mass in g
r - the size of a fragment (in cm)

Fragmentation of a meteoritic body during its atmospheric passage is subordinated to the rate of conversion of the kinetic energy of the body into disruptive factors: aerodynamic heating and pressure. Velocity and angle at atmospheric entry apart from its size, shape and cohesion pre-determine the outcome of the interaction of the decelerating body with the atmosphere. Formation of a shock wave /air cap/ releases a violent heat attack on the body followed by aerodynamic pressure rising along the trajectory. Heat is transferred to the body by convection and radiation. Resembling some outburst the radiative heating stimulates the onset of fragmentation as subsequent to earlier episodic ablative mass losses. Thermomechanical fracturing is evolved from stress pulses produced by thermal shocks on the surface while penetrating the interior of a body to lead eventually to its spallation. So the first stage of a fracture cascade is carried out. The transition to the next one - transient or final - is due to the advanced exhaustion of the original kinetic energy. The destructive regime becomes milder, presumably the convective heating

coincides with gradually rising in importance aerodynamic pressure. It is likely that cracks, flaws and voids evolved earlier in the body or in the larger fragments under the impact of the heavy thermal attack are propagating, branching and coalescing to yield at this stage smaller and smallest fragments. The interference of the time factor can be expected: the smaller the fragment - the more time is needed to detach it, to break down its bonds and make free its boundary surfaces.

Prior to discussing the obtained results let us comment the formalism of our procedure. The slopes x and y are obtained for regression straight lines extended over r-values representing each an ordered subset of fragments. To arrive at a real invariance we eliminated from fitting those exterior points and only exterior ones which make the percent relative standard deviation of a slope larger than 20%. Fragments eliminated or disregarded by fitting are believed to be transient produced by a transient destructive regime.

For the Chico Hills chondrite we received two stages of the fracture cascade and no transients. These stages are characterized by the values for the fractal dimension D being 1.74 and 0.28 respectively. Very close to them are the values obtained for the Tsarev ordinary chondrite L 5 1.79 and 0.25. For the Canyon Diablo iron we received 2.93 and 0.55 respectively. From a high velocity experimental impact the value of 2.56 was obtained for a terrestrial basalt.

Two stages of a fracture cascade are likely to be a minimum. For the Odessa iron and the Łowicz mesosiderite three stages were received, while for the Wolf Creek iron even four. The incomplete recovery of fragments from meteorite breakages in the atmosphere is leading to uncertain identification of particular stages of fracture cascades.

Against all importance of the destructive regime meteorite breakup at atmospheric entry as recorded in fragments is nothing but the response of the body to the action of the destructive forces. This aspect should not be overlookedwhile the contribution accounted of the material properties including mineral composition, texture, compaction, porosity, bulk strength etc., apart from size and shape. Material data are complementary to the features of the destructive regime.

References: (1) Hutchison, R. (1987) Personal communication. (2) Lang B. and Franaszczuk, K. (1989) Proc.Lunar Planet.Sci.Conf. 19th, 683 - 689. (3) Mandelbrot, B. (1983) The fractal geometry of Nature, 2nd ed., Freeman, S.Francisco. (4) Matsushita, M. (1985) J.Phys.Soc.Japan, 54, 857 - 860. (5) ReVelle, D. (1979) J.Atmos. Terr.Phys., 41, 453 - 473.

GEOSCIENTIFIC SIGNIFICANCE OF THE LONAR IMPACT EVENT, INDIA

V. K. NAYAK
Department of Applied Geology, Indian School of Mines, Dhanbad, India

Historically, J. E. Alexander (1824) was perhaps the first person who in August 1823, accidently came across this remarkable feature and described vividly its morphology and scenery. G. K. Gilbert (1896) the famous American geologist while proposing the meteoritic origin of the Moon's craters, strongly argued in favour of volcanic origin for the well known Arizona crater and surprisingly compared it with the Indian Lonar crater. The origin of the Indian crater has been a debated subject for more than a century and various hypotheses suggested from time to time are reviewed. Over the past two decades, several institutions in India, U.S.A., and Russia, have been involved in the investigation of the Indian crater which provides a natural laboratory to resolve cratering process and understand cosmo-terrestrial relations.

Lonar crater ($19^{\circ}58'N : 76^{\circ}31'E$), Buldana District, Maharashtra State, India, located in the Deccan Traps basalt flows of the Cretaceous-Eocene age, is a magnificient authentic impact event (Nayak, 1972; Fredriksson et al. 1973) which in recent years has awaken a world-wide interest. It is nearly a circular depression with a breach in the north-east, 1830 m in diameter and is about 150 m deep, with a saline lake in the crater floor which is filled up with sediments. It has provided the closest analog for comparison with the Apollo material and the processes at the lunar surface. Recently, the Indian crater has been compared with the so-called 'fluidized craters' of Mars (Fudali et al. 1980). Another smaller circular structure also in basalt, 300 m in diameter, is located 700 m north of the main crater and this is thought to be a second crater which is designated as 'Little Lonar' (Fredriksson et al. 1979), and deserves close attention.

The target rocks are basalts of tholeiitic type and occur as flows exposed within the inner slope of the crater. There

are five flows and some flows have a weathered top with sometimes red boles and vesiclse filled with zeolite and secondary minerals. The ejecta debris consists of shocked, unshocked and unusual rocks with pulverized material and all this has helped to understand the style and degrees of shock metamorphism, impact generated basalt melt (impactite glasses), vitrification of plagioclase into maskelynite, and above all to interpret the history of transient pressure-temperature regime in a shock environment (Kieffer at al. 1976; Nayak, 1988).

Lonar is a very young crater with an age between 30,000 and 56,000 years (Fredriksson et al. 1979; Sengupta et al. 1984) and this youthfulness strongly supports the impact origin of the crater because there is no evidence of any volcanic activity in the Deccan basalt province during this time. Bhandari (1984) conjectured that a large meteorite perhaps a stony one, 60 m in diameter with a velocity of 18 km per second hit the target basalts at an angle from the north-east direction and is suspected to lie buried in the south-west.

From all considerations, therefore, the study of the Lonar Impact Event has certainly helped to resolve many significant geoscientific problems, and hopefully will continue to provide insight into several other questions and generate new ideas to solve mysteries of nature.

References

Alexander, C. J. E. (1824) Edin. Phil. Jour., XI, 308-311.

Bhandari, N. (1984) Science Age, India, 2 (3), 24-26.

Fredriksson, K., Dube, A., Milton, D. J., and Balasundaram, M.S.(1973) Science, 180, 862-864.

Fredriksson, K., Brenner, P., Dube, A., Milton, D.J., Mooring, C., and Nelen, J. A. (1979) Smithsonian Contrib. Earth Science, No. 22, 1-13.

Fudali, R.F., Milton, D.J., Fredriksson, K. and Dube, A. (1980) The Moon and the Planets, 23, 493-515.

Gilbert, G. K. (1896) Science, New Series, 3, pt. 1, 1-13.

Kieffer, S. W., Schaal, R. B., Gibbons, R., Horz, F., Milton, D. J. and Dube, A. (1976) Proc. 7th Lunar Sci. Conf. 1391-1412.

Nayak, V. K. (1972) Earth & Planet. Sci. Letts., 14 (1), 1-6.

Nayak, V. K. (1988) 13th Symposium on Antarctic Meteorites, National Institute of Polar Research, Tokyo, Japan, 68.

FORMATION PROCESSES OF THE K-T BOUNDARY SAMPLES FROM DENSITY VARIATION OF QUARTZ MINERALS

Yasunori MIURA and Masashi IMAI
Faculty of Science, Yamaguchi University, Yamaguchi, 753.

1. Introduction

The Cretaceous-Tertiary (K-T) boundary samples have been discussed from archaeological, mineralogical and geochemical evidences by many scientists. Mineralogical data of shocked quartz and stishovite are considered to be direct evidences of impact events at the K-T boundary, though various geochemical data are sometimes difficult to be direct evidence of impact events. The purposes of the present study are (1) investigation of the K-T boundary samples (Japan, Italy, Denmark and Tunisia) from density variation of the quartz mineral, compared with those of the terrestrial impact craters and various terrestrial metamorphic, volcanic and plutonic rocks, and tectonic complex, and (2) discussion of the probable formation processes from the silica mineral data.

2. Calculated density of silica minerals

Quartz minerals from different 4 K-T boundary samples, 2 terrestrial impact craters (Barringer and Manicouagan), and 5 terrestrial rocks (Sangun high-pressure type metamorphic, Rhyoke high-temperature type metamorphic rocks, Nagato tectonic complex, volcanic tuff-breccias sedimentary rocks, and igneous ganitic rocks from Japan) are used in this study, compared with the calculated density from X-ray and EPMA data on the basis of standard α-quartz of rock-crystal.

Deviations of the calculated density (Δd) from the standard quartz are summarized as follows:

1) As the higher-density silica minerals of coesite and stishovite are easily changed to glass by higher impact processes, the progressive changes of quartz mineral are considered to be one of the best indicator of the formation process of the host rocks.

2) **Negative values** of the deviation (i.e. lower density of quartz) indicate the **higher-temperature type** silica minerals of β-type quartz (-5.0%) and tridymite (-14.7%).

3) **Positive values** of the deviation (i.e. higher density of quartz) indicate the **higher-pressure type** silica minerals of coesite (+9.7%) and stishovite (+61.9%).

4) Quartz minerals of the terrestrial metamorphic rocks show the positive Δd values (+0.03 to +0.09%), though volcanic sedimentary rocks show various data from -0.06 to 0.22 (%).

5) Quartz minerals from the Barringer crater have larger positive values (+0.09 to +0.49%), though quartz from the melt rocks of the Manicouagan impact crater shows negative values (-0.11 to +0.01%).

6) The K-T boundary samples show various Δd values; that is, mixed data of Japan (-0.18 to -0.12%; +0.23 to +0.59%), positive data of Tunisia (+0.63%), negative value of Italy (-0.06%), and positive value of Denmark (+0.12%).

3. Formation processes of the K-T boundary samples

Probable formation processes can be discussed from the density variation from the silica minerals, as listed in Table 1.

Table 1. Probable formation processes of the K-T boundary samples.

Sample	Δd (%)	P/T Type	Remarks
1) Pressure-dependent type:			
·Denmark	+0.12	(High) pressure	Typical standard K-T type showing direct impact event.
·Tunisia	+0.63	(High) pressure	The largest positive type of all the K-T samples.
2) Temperature-dependent type:			
·Italy	-0.06	(High) temperature	Temperature-dependent value caused by (1) impact melt, or (2) valcanic melt.
3) Mixed P/T type:			
·Japan	-0.18 to -0.12	(High) T	Temperature-dependent value caused by (1) impact melt, or (2) tectonic complex melt.
	+0.23 to +0.59	(High) P	Pressure-dependent value caused by impact process.

Typical quartz minerals formed by impact process are found in Tunisia sample (and also in Denmark sample), though the quartz from the Italy K-T boundary sample shows temperature-dependent effect caused by impact melt and/or valcanic melt. The Japanese K/T boundary samples are mixed samples of temperature- and pressure-dependent events.

The above probable formation processes from the density variation of quartz minerals are nearly consistent with the previous reported data of geological, geochemical and mineralogical data.

Although there are two major explanations of the various K-T boundary events in the world (i.e. extraterrestrial impact and terrestrial volcanic event)s, it is important to find the **real simple K-T** boundary samples which include relict or memory of the first events without major terrestrial products and mixtures.

References:

Alvarez L. W. et al. (1980): Science, 208, 1095-1107.
Bohor B. F. et al. (1986): Science, 224, 867-869.
Miura Y.(1986): LPSC XVII, 555-556.
Miura Y. et al. (1985): ESR Dating and Dosimetry (Ionics, Tokyo), 1, 469-476.
Miura Y., et al. (1988): Global Catastrophes in Earth History, 124-125.
Miura Y. and Imai M. (1986): 13th Symp. Antarctic Meteorites, 99-100.
Takaoka N. and Miura Y. (1988): Ibid., 96-98.